This is to certify that the
dissertation entitled

ULTRAVIOLET RADIATION SURFACE TREATMENT OF
POLYMERS

presented by

ALEKH S. BHURKE

has been accepted towards fulfillment
of the requirements for the

Ph.D. degree in Chemical Engineering

Lawrence T. Drzal
Major Professor's Signature

November 26, 2003

Date

ULTRAV

D

ULTRAVIOLET RADIATION SURFACE TREATMENT OF POLYMERS

By

Alekh S. Bhurke

A DISSERTATION

Submitted to
Michigan State University
in partial fulfillment of the requirements
for the degree of

DOCTOR OF PHILOSOPHY

Department of Chemical Engineering and Materials Science

2003

ULTRAVI

Ultraviolet

polymer surfaces

production of ozo

functional groups

force required for g

UV treatme

and polydiene rub

chemistry (determ

found to depend p

effect of temperat

proposed to char

used to describe

parameters are re

can be extended

polymer surfaces

Keywords: UV,

ABSTRACT

ULTRAVIOLET RADIATION SURFACE TREATMENT OF POLYMERS

By

Alekh S. Bhurke

Ultraviolet (UV) radiation in the 185 nm – 280 nm (UVC) band can oxidize polymer surfaces by a combined effect of UV activation of the polymer and the production of ozone and atomic oxygen from air. UV photo-oxidation creates polar functional groups that increase surface energy and provide the thermodynamic driving force required for good wettability and adhesive performance of the polymer.

UV treatment of polycarbonate (PC), polyethylene terephthalate (PET), epoxy, and polydiene rubber was studied in detail. The changes in wettability and surface chemistry (determined by XPS) were related to the UV treatment process variables and found to depend primarily on the net irradiation. In the case of low Tg polymers, a strong effect of temperature on the surface properties was also observed. A process model is proposed to characterize the UV modification of these polymers. Sensitivity functions are used to describe the evolution of surface properties as a function of irradiation, and model parameters are related to physical and chemical properties of the polymers. The model can be extended to other polymers and ultimately used to predict the properties of polymer surfaces after irradiation by xenon arc UV lamps.

Keywords: UV, surface modification, surface energy, XPS, polycarbonate.

DEDICATION

To my parents who have always

encouraged and supported me.

I would

whose tutelage I

Bruening, Naray

appreciate the va

Center, whose fr

Lastly, my since

throughout the d

ACKNOWLEDGEMENTS

I would like to express my gratitude towards Prof. Lawrence T. Drzal under whose tutelage I have learnt so much over the years. I would also like to thank Professors Bruening, Narayan, and Jayaraman for their comments and input on this work. I appreciate the various students, staff, and faculty at the Composite Materials & Structures Center, whose friendship I have enjoyed during my stay at Michigan State University. Lastly, my sincere thanks to Dr. Per Askeland who has been a friend, guide, and mentor throughout the duration of this work.

TABLE OF CONTENTS

LIST OF TABLES

Table C.2 Re
co

Table C.3 Re

Table C.4 Re
fro

Figure 1.1 T

Figure 1.2 S

Figure 1.3 T

Figure 1.4 S

Figure 1.5 T
f
v
v

Figure 1.6 E
d

Figure 1.7 A
P
e

Figure 1.8 I
a

Figure 1.9 I
a

Figure 1.10 M

Figure 1.11 V

Figure 1.12 P

Figure 1.13 P
F

Figure 1.14 P

Figure 1.15 N

Figure 1.16 N
c

LIST OF FIGURES

Surf

years. In th

surfaces of

commerciall

including e

industries. W

these materia

carbon based

and inks. The

surface treatme

the modificatio

friendly method

1.1 Surface Tr

Adhesiv

structural fabri

superior mech

CHAPTER ONE

INTRODUCTION

"God made solids, but surfaces were the work of the Devil."

– Wolfgang Pauli (1900-1958)

Surfaces of solids have been the subject of many scientific investigations over the years. In the last century, the growing use of polymers has focussed attention on the surfaces of polymeric materials. Today, hundreds of different types of polymers are commercially available and find use in almost all conceivable areas of applications including engineering, medical, transportation, packaging, and commodity goods industries. With such widespread use arises the need for painting and adhesive bonding of these materials. Many of the commercially important polymers are low surface energy carbon based materials with inadequate adhesion and wettability with adhesives, paints, and inks. The modification of these properties by physical or chemical means is termed surface treatment. Various methods of surface treatment are available commercially for the modification of polymers and metals. This work investigates an environmentally friendly method for the surface modification of polymers with ultraviolet (UV) radiation.

1.1 Surface Treatments

Adhesive bonding of metals, polymers, and polymer composites is an attractive structural fabrication method. Adhesive bonding can create strong, stable joints with superior mechanical properties and durability compared to mechanically fastened

structures.

important r

pre-preparat

composites.

or limit adhe

painting, req

addition of ch

Surfac

as the adhesiv

between two d

dimensional in

two bulk phase

Drzal [1] whe

proposed to

microstructure,

adhering phases

interfacial phen

as the effect of

Various

overcome the

such as abrasi

Organic solver

problems and

structures. The application of protective coatings and paints to surfaces is also an important manufacturing process in the durable goods industry. In such processes, the pre-preparation of the surface is an important step. Processed polymer, polymer composites, and metallic surfaces contain undesirable compounds or additives that reduce or limit adhesion. Surface preparation of the adherend, whether for adhesive bonding or painting, requires the removal of labile organic compounds and contamination, as well as addition of chemical functionalities that can interact strongly with the adhesive or paint.

Surface treatments are designed to alter the interface between two materials such as the adhesive and the adherend. The idea of a two dimensional, well-defined interface between two different materials is necessarily an idealistic one. In most materials, a three dimensional interphase with unique properties is formed and the boundary between the two bulk phases is blurred. A model of an adhesive bond interphase was proposed by Drzal [1] where the interphase between a viscoelastic adhesive and solid substrate is proposed to be dependent on the surface chemistry, morphology, topography, microstructure, local chemical composition as well as the bulk properties of the two adhering phases. Figure 1.1 shows a schematic of such an interphase. The study of any interfacial phenomenon must take into account the contribution from these factors as well as the effect of the thermal, chemical and mechanical environments of the interphase.

Various mechanical and chemical surface treatments have been developed to overcome the problem of weak adhesion in polymers. Mechanical surface treatments such as abrasion are time consuming, labor intensive and can damage the substrate. Organic solvents are often used for cleaning surfaces but present various environmental problems and are being eliminated in order to reduce volatile organic compound (VOC)

emissions.

discharge ha

and used wi

operating co

shapes. The

environmenta

the manufactu

1.2 Overview

emissions. Other surface treatment techniques such as flame, plasma, and corona discharge have also been developed [2-10]. While these surface treatments are efficient and used widely in industry, they suffer from drawbacks such as high cost, hazardous operating conditions and by-products, and the inability to treat complex geometric shapes. There is a growing need in industry for a fast, simple, efficient, and environmentally friendly surface treatment process that can be easily incorporated into the manufacturing environment [11].

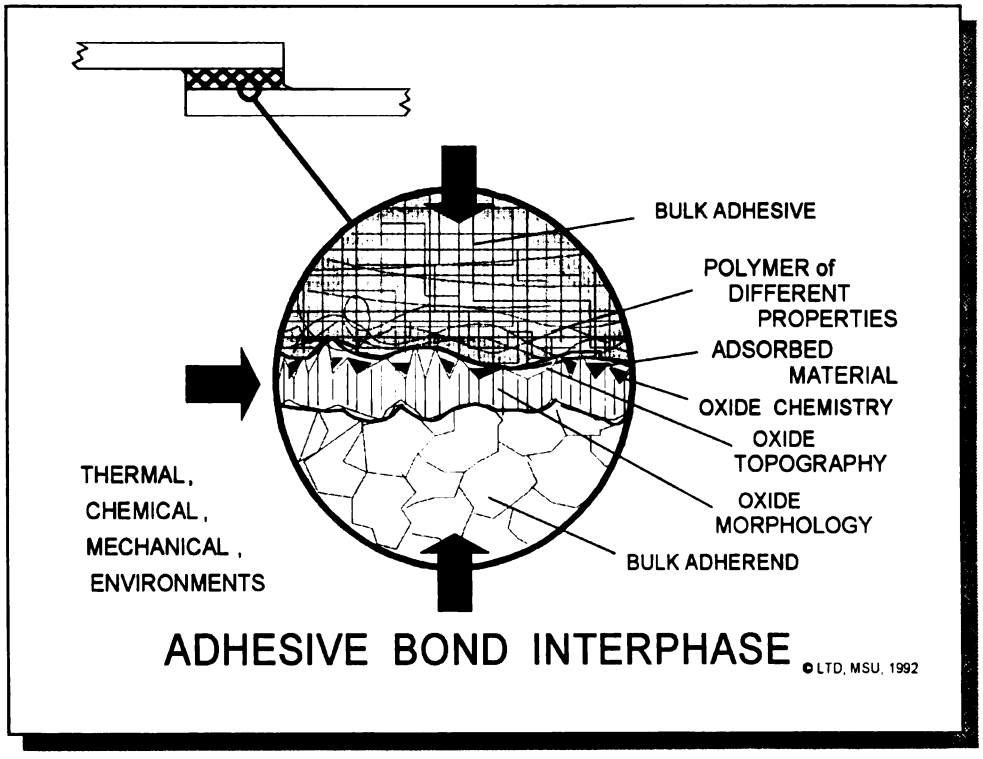

Figure 1.1 The adhesive bond interphase [1].

1.2 Overview of the UV Surface Treatment

Sin

combinatio

This pheno

oxygen crea

like carbon c

nm) UV rad

oxygen and c

effectively re

phenomenon

ablation by hi

exposure to U

be rapidly bro

are exposed to

surface group

wettability and

(UVC radiatio

vapor lamps is

receptive mate

can yield a su

UV surface tre

of-sight nature

be small mole

solvents and

Since the early 1970's it has been known that Ultraviolet (UV) light in combination with atmospheric oxygen can clean organic contaminants from surfaces. This phenomenon occurs when low wavelength UV light interacts with atmospheric oxygen creating ozone, which oxidizes surface organic compounds to small molecules like carbon dioxide and water. This reaction occurs in the presence of high-energy (< 185 nm) UV radiation [12, 13]. Ozone absorbs UV radiation at 254nm and dissociates into oxygen and oxygen radicals creating a very aggressive oxidizing environment which can effectively remove low molecular weight organic contaminants from the surface. Another phenomenon that is responsible for cleaning the surface, especially in polymers, is that of ablation by high energy UV radiation, which can etch and activate surfaces [14-18]. On exposure to UV light of sufficiently high energy, organic bonds in the surface layer can be rapidly broken depending on the absorbance of the substrate. When activated surfaces are exposed to the atmosphere, oxidation takes place with the formation of highly polar surface groups such as hydroxyl, carbonyl and carboxylic acids that can improve wettability and adhesion [8,10,13,19-30]. UV light with wavelengths from 184-365nm (UVC radiation) produced by commercially available xenon and low-pressure mercury vapor lamps is ideal for the process of surface activation and oxidation. Exposure of a receptive material to UVC radiation for short times in the presence of oxygen or ozone can yield a surface with high surface energy, wettability and adhesive strength [31,32]. UV surface treatment also has the ability to treat 3-dimensional surfaces due to the line-of-sight nature of the process. The by-products of such processes are largely expected to be small molecules like water and oxides of carbon. The process does not utilize any solvents and the ozone is dynamically created and dissociated in the treatment

environmen

phase proc

chemicals n

1.3 Compa

Ther

polymers. T

treatment, c

techniques w

Flame

or organic fue

oxygen radica

The adhesive

an increase in

weak boundar

(0.25 inch) to t

of tens of inch

Flame treatme

treatment is s

combustion o

consequences

typically used

environment. The process is considered environmentally friendly because the dry, gas phase process does not create VOC emissions and does not use any hazardous wet chemicals needing elaborate handling and disposal.

1.3 Comparison With Other Surface Treatment Techniques

There are several commercially available techniques for surface modification of polymers. The most widely accepted techniques today include flame treatment, plasma treatment, corona treatment, and chemical modification. A brief comparison of these techniques with the UV treatment process is presented in this section.

Flame treatment involves the rapid oxidation of the polymer surface by hydrogen or organic fuel flames which can achieve temperatures of 2000 K [33]. The flame creates oxygen radicals in the air which attack the polymer and form polar groups on the surface. The adhesive characteristics of the surface are enhanced by a combination of two factors: an increase in surface energy by oxidation and the physical oxidative degradation of weak boundary layers and contaminants. The flame head is typically placed very close (0.25 inch) to the product surface which allows very high treatment speeds on the order of tens of inches per second. The treated surfaces can remain stable for several weeks. Flame treatment is not particularly suitable for three-dimensional objects because the treatment is strongly dependent on the position of the surface within the flame. The combustion of fuel as the primary source of energy has obvious environmental consequences and safety considerations are very important. The process is low cost and typically used for high speed processing of polymer webs.

Pla

or any oth

created in a

discharge)

can be cho

range from

electrons, i

chemical, m

the flame tre

contaminants

that the surfa

controlled at

processing. Ar

to the extrem

expensive beca

Corona

technique for t

formed by the

positioned a sh

and the ionize

oxidizes the p

treatments are

does not util

Plasma treatment involves the exposure of a material to oxygen, nitrogen, argon, or any other gas that can be energized to a plasma state [34]. The plasma is usually created in a partial vacuum. The plasma can be high temperature (energized by electrical discharge) or cold (energized by radio frequency). The components of the gas mixture can be chosen to seed required functional groups on the surface and typical exposures range from a few seconds to tens of minutes [2-3,7-10]. The plasma contains energetic electrons, ions, and UV radiation, which aggressively attack the surface, causing chemical, morphological, and topographical changes that can improve adhesion. As with the flame treatment, the surface is also cleaned in the process and organic compounds or contaminants are removed efficiently. An advantage of plasma over flame treatment is that the surface of three-dimensional objects can be treated, but the requirement of a controlled atmosphere and vacuum are disadvantages as they inhibit continuous processing. Another disadvantage is that the polymer surface can be easily damaged due to the extremely aggressive environment in the plasma. The process is generally expensive because of the need for vacuum and batch processing.

Corona treatment, sometimes called 'non-vacuum plasma', is a very popular technique for treatment of polymers in web type applications [3-6,8-10]. The corona is formed by the application of high voltage (on the order of 10,000 Volts) to an electrode positioned a short distance from the substrate. The air gap is ionized by the electric field and the ionized oxygen in the air forms high levels of ozone. The corona and ozone oxidizes the polymer, resulting in a high energy suitable for printing and bonding. Corona treatments are less likely to damage treated surfaces than flame or plasma treatments and does not utilize volatile solvents. The technique is well suited to fast continuous

manufactu

disadvanta

voltages. s

which can

Ch

These inclu

acid and a

other applic

typically inc

which can c

issues.

Table

processes. It

conventional

use of UV tr

reductions in

comparing the

treatment proce

manufacturing but generally unsuitable for treatment of convoluted surfaces. The disadvantages of corona treatment include safety concerns because of the use of high voltages, static buildup, and the extremely efficient production of high levels of ozone, which can cause environmental problems.

Chemical treatments are the most widely used processes for surface modification. These include organic solvent cleaning of surfaces, primer coatings for paint applications, acid and alkaline baths for metals, detergent washes, surface coatings, and numerous other applications. These processes are well suited for continuous manufacturing and typically inexpensive. The disadvantages include the use of solvents and wet chemicals which can cause VOC emissions, human hazards, effluents, and other waste disposal issues.

Table 1.1 compares the UV treatment process with the above mentioned processes. It is observed that UV treatment can address many of the disadvantages of conventional surface treatment techniques without posing risks to the environment. The use of UV treatment to replace flame or chemical treatments can result in significant reductions in VOC and greenhouse gas emissions. Chapter 7 includes an analysis comparing the economical benefits of these processes and the results indicate that the UV treatment process is cost competitive with existing processes.

Tab

Current Statu
Environmenta Impact
Ability to Treat Comple Geometries
Treatment Time
Hazards
Cost
Suitability i Manufacturi Environmen

Table 1.1 Comparison of various surface treatment techniques.

	Conventional Treatments (Flame, Corona, Plasma, and Chemical Modification)	UV Surface Treatment
Current Status	Flame, Corona and Chemical – Mainstream technologies. Plasma - Limited acceptance.	Developing technology - Equipment manufacturing base exists.
Environmental Impact	Chemical – VOC emission, waste disposal. Corona – High levels of ozone produced. Flame – Greenhouse gases, organic fuels consumed.	Low levels of ozone produced in contained environment.
Ability to Treat Complex Geometries	Flame, Corona and Plasma – Treatments have severe limitations in treating convoluted surfaces.	Line-of-sight treatment. Potential to treat convoluted surfaces is excellent.
Treatment Time	Corona, Flame – Very fast. Chemical, Plasma – Moderate treatment times.	Fast treatment times.
Hazards	Chemical – Human exposure, waste disposal. Corona – High levels of ozone production.	UV protection for humans. Low levels of ozone produced.
Cost	Corona, Flame, Chemical – Inexpensive Plasma – Expensive.	Inexpensive.
Suitability in Manufacturing Environment	Corona, Flame – Web treatment applications only. Removal of process gases is required. Chemical – Environmental concerns, hazardous. Plasma – Unsuitable for large scale continuous processing.	Excellent suitability for all applications – batch and continuous processing of flat, convoluted, and large scale surfaces. Minimal hazards – UV protection and removal of low levels of ozone required.

1.4 Litera

Ex

the surface

phenomen

rapidly [1-

degradatio

emission la

In

understandi

wettability a

in the prese

mechanism c

ozone is show

UV at 1

nm to form si

reactions are v

occurring are

topography of

1.4 Literature Review

Exposure of polymers to UV radiation causes chemical and physical changes on the surface, and depending on the nature, intensity and duration of the radiation, different phenomenon are observed. High intensity UV lasers can be used to ablate surfaces rapidly [14,15,17] while long term exposure to low intensity UV radiation leads to photo-degradation [35-38]. Various types of UV sources such as pulsed and continuous emission lasers and lamps can be used for these purposes [39].

In recent years, a significant amount of study has been devoted to the understanding of UV photo-oxidation as a surface treatment process to enhance wettability and adhesion [19-30]. Deep UV radiation, of wavelengths 185-280 nm (UVC) in the presence of oxygen oxidizes surfaces and creates polar functional groups. The mechanism of oxidation with UV radiation in the presence of atmospheric oxygen and/or ozone is shown below [12,13,40-43]:

$$O_2 \xrightarrow{h\nu} O^* + O^* \tag{1.1}$$

$$O^* + O_2 \rightarrow O_3 \tag{1.2}$$

$$O_3 \xrightarrow{h\nu} O_2 + O^* \tag{1.3}$$

UV at 184.9 nm interacts with oxygen to form ozone. Ozone decomposes at 253.7 nm to form singlet molecular oxygen and atomic oxygen. All products of the above reactions are very reactive and capable of oxidizing the surface. The chemical changes occurring are often accompanied by changes in the wettability, morphology and topography of the surface [44-46].

In addit

surface also oc

cause dissociat

chain scission.

The presence o

subsequent rea

Due to t

the photo-activ

more suitable t

The production

lamp and com

Exposure to o

often very lon

oxidation proc

uptake in the

treatment in a

UV treatment b

UV tre

exposed subst

polymers. Th

temperature g

changes [18,4

provide a con

In addition to the thermal oxidation by ozone [47], UV initiated photolysis of the surface also occurs simultaneously [48-49]. UV photons of sufficiently high energies can cause dissociation of chemical bonds on the surface. Such bond dissociations can lead to chain scission, molecular rearrangement and creation of free radicals in the polymer [50]. The presence of oxidizing gases near the activated surfaces leads to a wide variety of subsequent reactions that can form high-energy surface functional groups.

Due to the different wavelengths required for the photo-dissociation of ozone and the photo-activation of different polymers, UV lamps with a broad spectral output are more suitable for surface modification than monochromatic UV lasers or excimer lamps. The production and dissociation of ozone is a cyclic process that occurs under the UV lamp and combined with the photo-degradation of the surface leads to rapid oxidation. Exposure to ozone alone can cause significant uptake of oxygen in a polymer surface but often very long exposure times on the order of hours are required [20,51-53]. The oxidation process is accelerated in the presence of UV radiation and the levels of oxygen uptake in the surface achieved by ozonation can be achieved by UV-Ozone (UVO) treatment in a matter of a few minutes [13, 32]. Increasing the ozone concentration during UV treatment by using an external ozone generator enhances the rate of reaction.

UV treatment can also cause morphological and topographical changes in the exposed substrate. Clear evidence is available from UV laser irradiation studies on polymers. These changes are brought about by ablation and etching, or very high temperature gradients in the surface regions which can lead to local microstructural changes [18,44-46]. These physical and chemical changes occur simultaneously and provide a complex set of variables which must be analyzed in order to understand the

process. The c

wettability and

The con

exposure deper

conditions has

there is a large

surfaces, a sys

universal surfac

UV oxi

robust method

enhanced adhe

activation proc

adaptable to tre

for optimum m

Figure

with provision

factors that car

pulse repetitio

composition, r

kinetics. These

UV Ir

studied with t

shown that a

process. The effects of these surface changes are realized in terms of changes in wettability and adhesion.

The complex physical and chemical changes occurring on the surface due to UV exposure depend on the treatment conditions used and the proper manipulation of these conditions has the potential to yield tailored surfaces for various applications. Although there is a large amount of phenomenological data regarding the effect of UV radiation on surfaces, a systematic understanding of this process can lead to the formulation of universal surface treatment strategies that can be used for a wide variety of materials.

UV oxidation and surface activation has the potential for creating a low-cost, fast, robust method for surface preparation of polymer and polymer composite surfaces for enhanced adhesive bonding. With the right process conditions, UV oxidation and surface activation process can be: *i)* capable of cleaning/treating any polymer surface; *ii)* adaptable to treat flat or convoluted surfaces; *iii)* environmentally benign; and i*v)* tailored for optimum mechanical performance of adhesive joints and coatings.

Figure 1.2 shows a schematic representation of a typical UV treatment process with provision of supplemental ozone to accelerate the surface treatment process. Several factors that can affect the surface treatment process have been identified: UV irradiance, pulse repetition rate, ozone concentration, temperature, exposure time, chemical composition, microstructure and morphology of the substrate, mass transfer, and reaction kinetics. These process variables are discussed briefly.

UV Irradiance. The effect of very strong UV radiation on polymers has been studied with the use of UV lasers. Many of these studies relate to ablation and it has been shown that ablation and photo-oxidation are related processes [39]. Ablation of the

surface occurs

material and c

the surface mo

processes resp

rates of these

radiation is thu

model.

Po
Su

The pu

spectrum and

various materi

filled UV lam

radiation in th

surface occurs when the UV radiation fluence exceeds the ablation threshold of the material and causes gross degradation of the surface. This manifests itself as a change in the surface morphology and topography. Moreover, the ozone formation and dissociation processes responsible for the bulk of the surface oxidation are photo-initiated and the rates of these reactions depend on the photon flux available. The intensity of UV radiation is thus one of the most important variables to consider in any chemical process model.

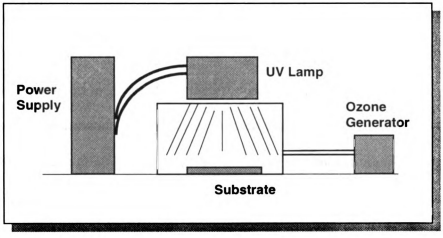

Figure 1.2 Schematic of the UV treatment process

The pulsed xenon arc lamps used in this work have a continuous radiation spectrum and the identification of key wavelengths and their characteristic effect on various materials is an important variable. Figure 1.3 shows the typical output of a xenon filled UV lamp. Preliminary experiments with quartz and Pyrex® filters have shown that radiation in the 185nm - 280 nm region is necessary for efficient UVO treatment.

Pulse r

flexibility in c

UV lamps hav

120 Hz. Figure

operating at 1

variable, espec

can be seen th

relatively long

surrounding ga

for a given tot

pulses to allow

Ozone c

was found by V

in the treatme

polymers like

Walzak et al. u

treatment env

approach has

generator to F

guarantees tha

to vary the oz

to study the ef

Pulse repetition rate. One of the advantages of using pulsed UV lamps is the flexibility in controlling the exposure time and intensity of the radiation. Typical pulsed UV lamps have pulse widths of 100-200 μs and pulse frequencies ranging from 3 Hz to 120 Hz. Figure 1.4 shows a schematic representation of the output of a pulsed UV lamp operating at 120 Hz. The pulse frequency of lamps is expected to be a significant variable, especially in the treatment of polymers which are sensitive to temperature. It can be seen that the emission of UV radiation is accomplished in short bursts with relatively long dark periods during which heat transfer from the polymer to the surrounding gas can occur. As the operating frequency is decreased, the energy per pulse for a given total output can be increased along with a larger cooling period between pulses to allow dissipation of heat from the irradiated surface.

Ozone concentration. The rate of surface modification by UV photo-oxidation was found by Walzak et al. [19] to be proportional to the concentration of atomic oxygen in the treatment of UV transparent polymers like polypropylene. In the case of other polymers like poly-ethyleneterephthalate (PET) this dependence was not observed. Walzak et al. used an external ozone generator to provide a stable source of ozone in the treatment environment that was independent of the irradiance at 185 nm. A similar approach has been followed in this study. The motivation for using an external ozone generator to provide supplemental ozone in the treatment environment is two fold: it guarantees that the UV treatment occurs at steady state conditions, and it gives the ability to vary the ozone concentration independently of the UV lamp output which is necessary to study the effect of ozone concentration on the rate of surface oxidation.

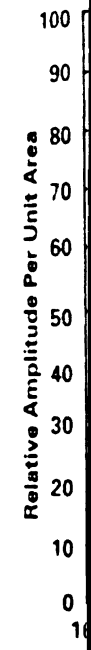
Relative Amplitude Per Unit Area
100
90
80
70
60
50
40
30
20
10
0

Figure 1.

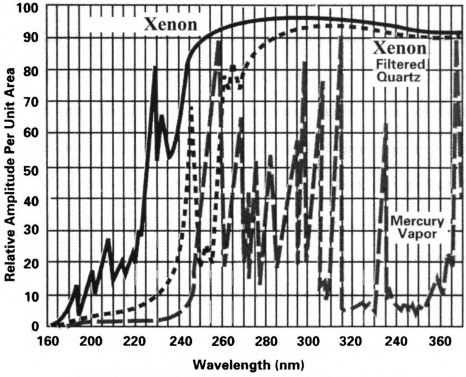

Figure 1.3 Typical outputs of pulsed xenon UV lamps. [Source Xenon Corp., Woburn, MA, USA]

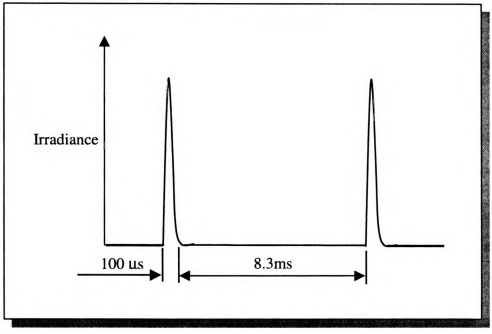

Figure 1.4 Schematic representation of pulsed UV lamp operation at 120Hz.

temperature.

the UV lamps

IR radiation

relaxation fro

energy in the

heating becau

higher vibrati

Franck-Condo

states that due

transitions occ

electronic tran

the excited ele

vibrational sta

Moreover, the

compared to s

steep temperat

present and the

the glass trans

surfaces due

rates of reacti

optimum rang

between the ra

Temperature. One of the important parameters in UV treatment is the substrate temperature. Substrate temperatures can increase rapidly during UV treatment because the UV lamps used have a broad spectral output ranging from UVC to the infrared region. IR radiation is very effective at causing vibrational transitions in polymers and the relaxation from excited vibrational states is generally accompanied by the release of energy in the form of heat. In addition, UV radiation can also contribute to surface heating because the electronic transitions caused by UV radiation often excite bonds to higher vibrational levels of the excited state (vibronic excitations) according to the Franck-Condon principle [54]. Figure 1.5 describes the Franck-Condon principle, which states that due to the mass difference between an electron and the nuclei, electronic transitions occur at much faster rates than those of nuclear vibrations, and a vertical electronic transition results in the excitation of the bond to a higher vibrational state of the excited electronic state. Relaxation from the excited vibrational states to the ground vibrational state by internal conversion results in the release of thermal energy. Moreover, the rates of relaxation of vibrational and vibronic excited states are very high compared to slow thermal diffusion (heat conductivity) in polymers. This can lead to steep temperature gradients in the surface region even when no infrared radiation is present and the transient surface temperatures can be very high. Temperatures higher than the glass transition (Tg) in polymers can have adverse effects on the properties of treated surfaces due to the higher mobility of the polymer. However, at low temperatures, the rates of reactions, which are generally temperature dependent, are also slower. Thus, an optimum range of temperatures may exist for a material where a balance is achieved between the rates of reactions and adverse effects of high surface temperatures.

Figure 1.
from the g
excited m

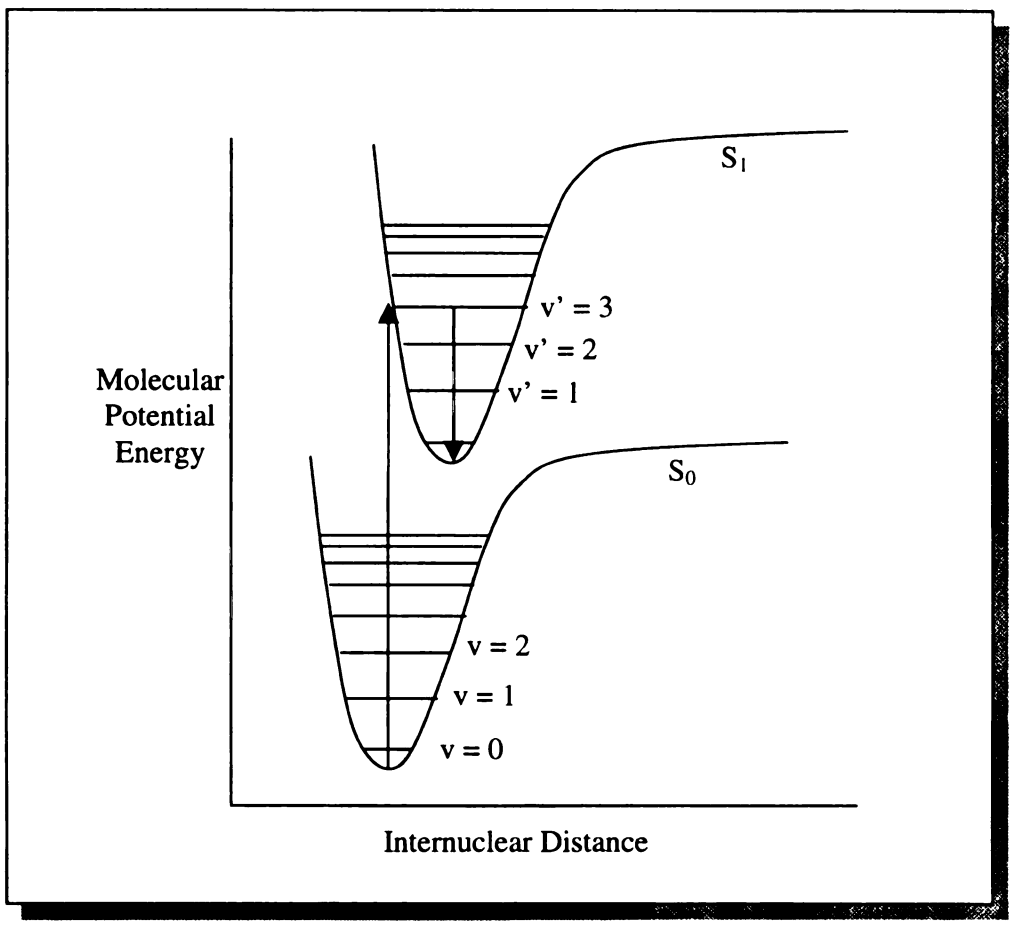

Figure 1.5 The Franck-Condon Principle showing excitation of an electron from the ground state of the molecule (S_0) to a higher vibrational state of the excited molecule (S_1) followed by vibrational relaxation of the excited state.

Chemic

physical and c

modification p

of the incident

transitions in th

the ground stat

photon. The I

ionization. Ele

shown in Figu

repulsive disso

enough to diss

Chemical structure, microstructure and morphology of the substrate. The physical and chemical characteristics of the substrate play a key role in any surface modification process. The chemical structure of the substrate determines the absorption of the incident radiation. Absorption of radiation in the ultraviolet region occurs due to transitions in the electronic structure of the molecule. The excited electrons can return to the ground state or escape depending on the energy transferred by the incident exciting photon. The latter case, where electrons are emitted from the molecule, leads to ionization. Electronic transitions can also cause bond dissociation in the molecule as shown in Figure 1.6 if the transition excites the molecule from the ground state to a repulsive dissociative state. At very low UV wavelengths, the photon energy can be high enough to dissociate many organic bonds.

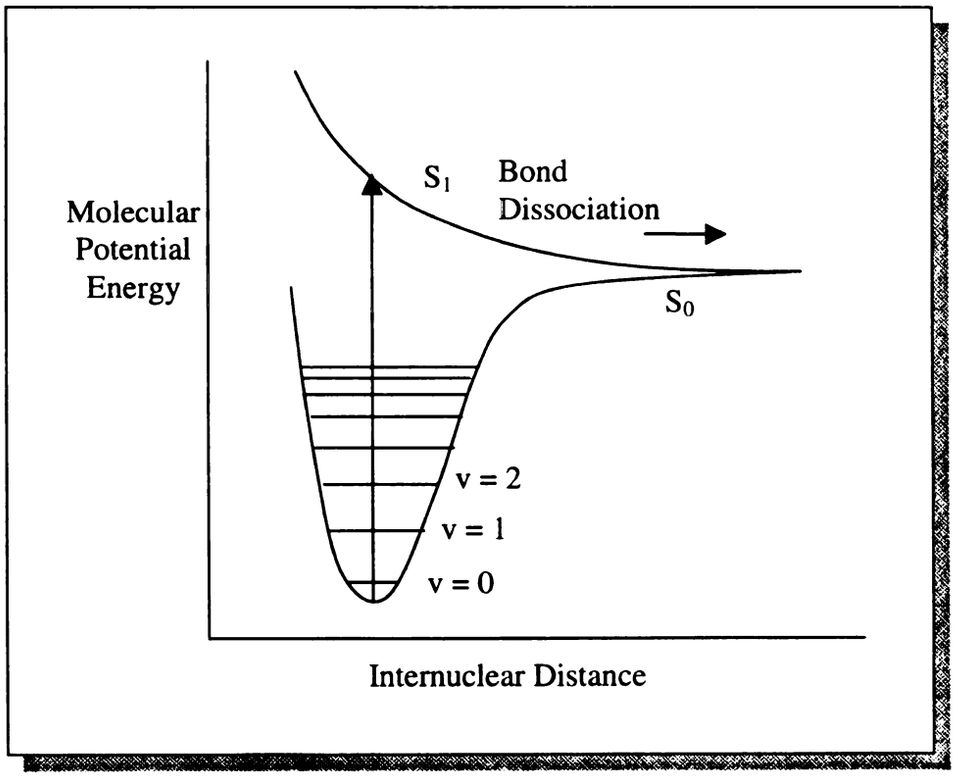

Figure 1.6 Electronic transition in a molecule from the ground state (S_0) to a dissociative state (S_1).

The ab

structure (chr

dependent on

bonds. Table

[55].

Ta

The ab

Weakly abso

absorption co

absorbing po

more difficul

microstructure

properties of

The absorption of radiation by a molecule is a characteristic of the molecular structure (chromophore) and the photochemical reactions occurring in the material are dependent on the wavelength of incident radiation and the absorbance of the constituent bonds. Table 1.2 shows the typical absorption wavelengths for different organic bonds [55].

Table 1.2 Absorption bands for some common organic bonds.

Chromophore	λ_{max} (nm)
Ether (–O-)	185
Ketone (C=O)	195
Ester (COOR)	205
Aldehyde (CHO)	210
Carboxyl (COOH)	200-210
Hydroxyl (O-H)	230

The absorption coefficient of a few common polymers is shown in Figure 1.7. Weakly absorbing polymers such as polypropylene (PP) and polyethylene (PE) have absorption coefficients about two to three orders of magnitude lower than strongly absorbing polymers like polyethylene terephthalate (PET) [14] and are consequently more difficult to modify by photo-oxidative processes. The surface morphology and microstructure may also play a critical role in UV treatment due to the different physical properties of amorphous, crystalline and transcrystalline regions in the polymer. In a

study on UV-

reactivity and

polyethylene

ozonated LDP

Absorption coefficient [cm⁻¹]

Figu

po

(PTFE

study on UV-ozone treatment of polyolefins, Peeling and Clark [20] found that the reactivity and oxygen uptake of high density polyethylene (HDPE) and low density polyethylene (LDPE) varied considerably. Figure 1.8 shows the XPS C1s/O1s ratio of ozonated LDPE and HDPE measured by Peeling and Clark.

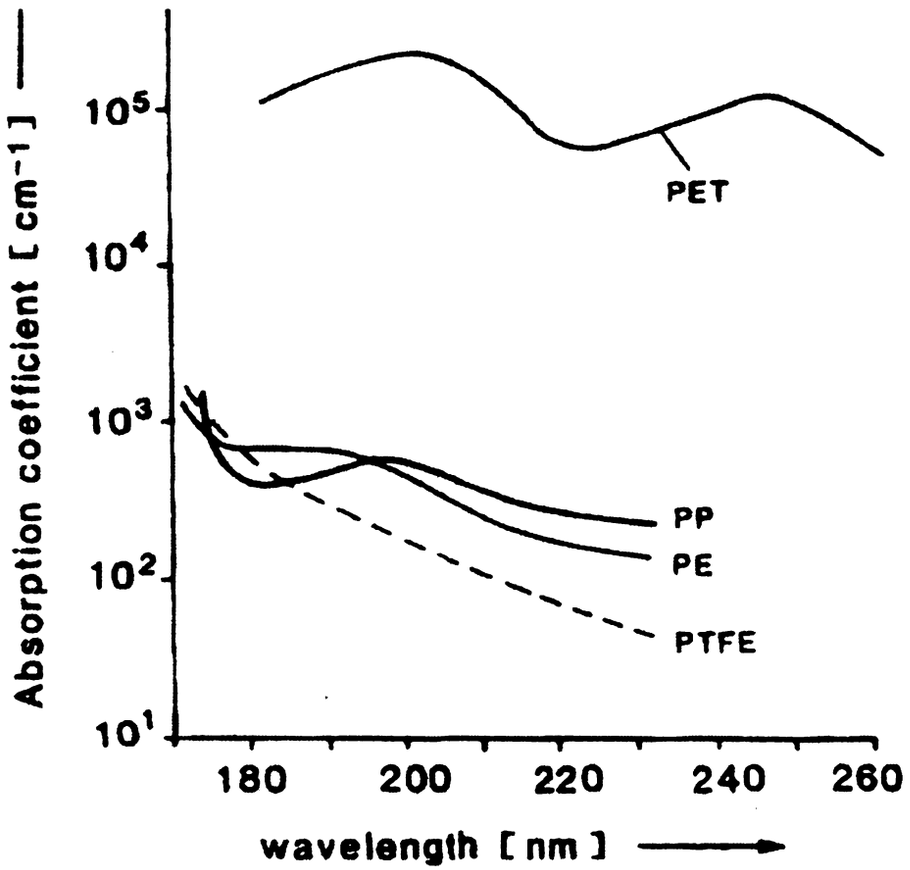

Figure 1.7 Absorption coefficient as a function of wavelength for poly(ethylene terephthalate) (PET), poly(tetrafluoro ethylene) (PTFE), polypropylene (PP) and polyethylene (PE) (Kesting et al.[14]).

Figure

The hi

attributed to t

LDPE leading

HDPE has a

crystallites, it

measured by

in UVO treat

ratios when t

the higher rat

The behavior

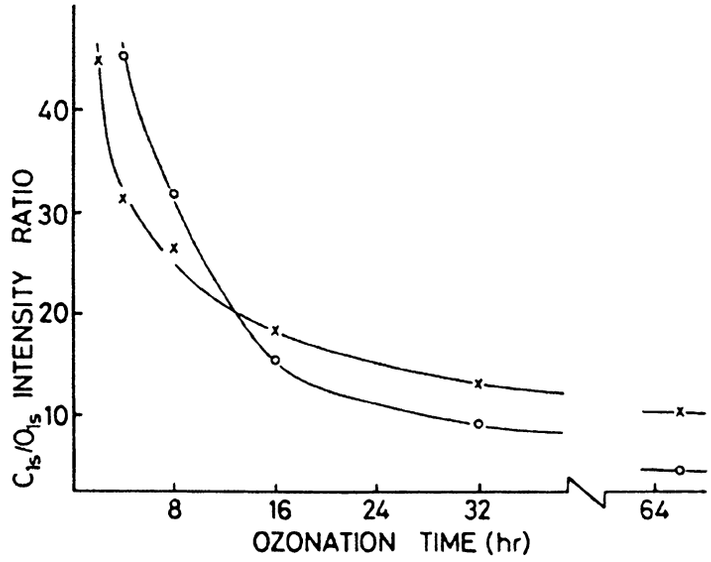

Figure 1.8 Intensity ratio of C_{1S}/O_{1S} bands for LDPE (x) and HDPE (o) as a function of ozonation time. (Peeling & Clark [20]).

The higher initial oxidation and uptake of ozone in LDPE compared to HDPE is attributed to the lower crystallinity of LDPE. Diffusion is faster in the more amorphous LDPE leading to a higher uptake of ozone/oxygen in the bulk while the highly crystalline HDPE has a very slow uptake of ozone, but due to the low diffusion through the crystallites, it is confined to the surface. This accounts for the higher C/O ratios in HDPE measured by Peeling and Clark at longer exposures. Similar behavior has been reported in UVO treated LDPE and HDPE. Figure 1.9 shows the corresponding XPS C_{1S}/O_{1S} ratios when the polymers were exposed to 254 nm UV radiation and ozone. Apart from the higher rate of oxidation, HDPE has a higher oxygen content at long exposure times. The behavior of such systems at short exposure times will be of interest.

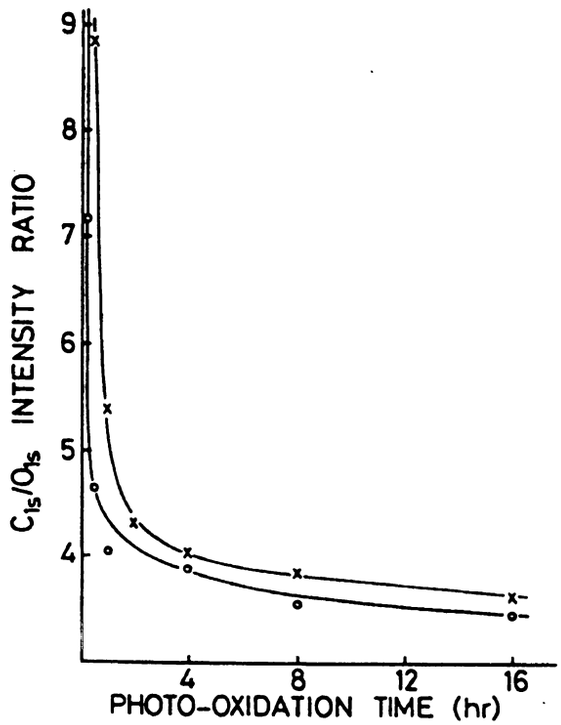

Figure 1.9 Intensity ratio of C_{1S}/O_{1S} bands for LDPE (x) and HDPE (o) as a function of photo-oxidation time. (Peeling & Clark [20]).

Besides the influence of crystallinity, other factors may influence the adhesive performance of UV treated polymers. Crosslinking has been widely reported in the surface layers of UV irradiated polymers [56-59]. Crosslinking of the polymer chains can increase the modulus of the surface and increase the adhesive bond strength. Conversely, excessive surface degradation can lead to formation of weak boundary layers and low adhesive performance.

Topographical changes in the polymer can occur due to ablation, photo-degradation, incubation, and other diffusive processes and lead to changes in the surface roughness. Surface roughness is known to have a strong effect on the wettability and adhesive properties of solids. Knittel et al. [44-46] report the formation of intricate ring

like morphology in UV laser irradiated cold-drawn PET fibers, which they attribute to the internal stresses present in the fibers. With increasing exposure, the fine rippled surface of the fibers became coarser. An empirical model has been proposed to relate the formation of these features to the UV laser exposure. Breuer et. al also report the formation of rippled surfaces in UV laser irradiated PP films [49]. The appearance of the surface features was found to be dependent on the surrounding atmosphere. In oxygen atmosphere, the laser induced surface structures had a lower frequency than in helium. This may be due to differences in the surface temperature in the two environments. The release of crystalline or residual stresses at elevated temperatures during UV treatment can also lead to changes in topography which are important from the point of view of adhesive performance. Another form of topographical change reported by Walzak et al. in UVO treated PP is the formation of mound-like structures detected by AFM measurements [19]. These mounds of polymer are low molecular weight oxidized fragments which can be removed by water. Similar morphology was observed in corona treated PP by Strobel et. al [60] and they concluded that the formation of low molecular weight fragments on the surface did not necessarily lead to the formation of a weak boundary layer if the fragments could be displaced into a polar solvent such as inks or adhesives.

Reaction and Transport. Apart from the above factors relating to the chemistry, microstructure and morphology of the substrate, there are other variables relating to the transport of the reactive species in the reaction environment that determine the efficiency of the UV/ozone treatment. The reaction of ozone with the surface is a gas-solid reaction and the rate of reaction depends on the relative rates of the surface chemical reaction and

the mass transfer of reactive species to the surface. The typical gas-solid interphase consists of the bulk fluid, the boundary layer and the solid surface. The reactive gas species must diffuse through the boundary layer to adsorb on the surface before the reaction can occur as illustrated in Figure 1.10.

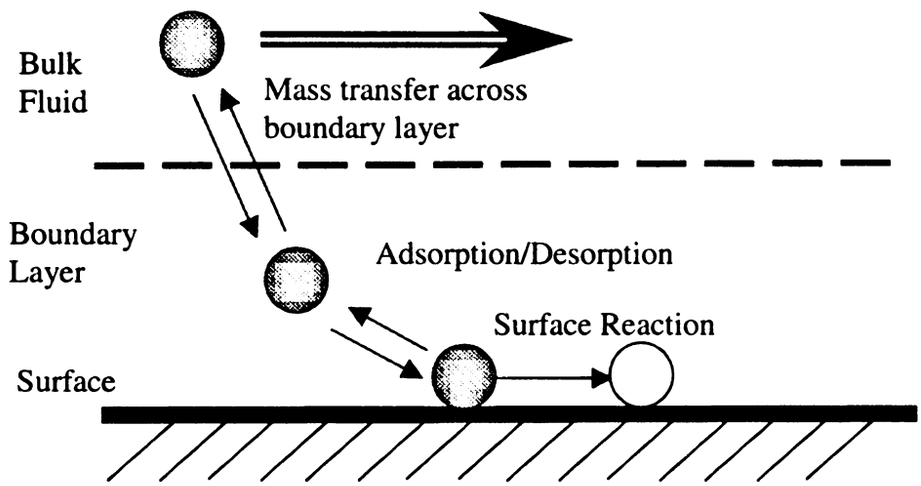

Figure 1.10 Mass transport in gas-solid surface reaction.

The chemical reactions occurring in the UV treatment environment can be classified as gas phase reactions and surface reactions. The gas phase reactions involve the formation of reactive species, O* and O_3, and photolysis of O_3 as described earlier (Equations 1-3). The mechanisms of these reactions as well as the quantum yield (ϕ, moles of product formed per mole of photons consumed), rate and equilibrium constant data are reported in literature [19]. Photochemical reaction rates are expressed in terms of quantum yields of the reaction and the photon flux. For the reactions involving dissociation of oxygen and ozone at 185 nm and 254 nm respectively, the quantum yield for the dissociation of

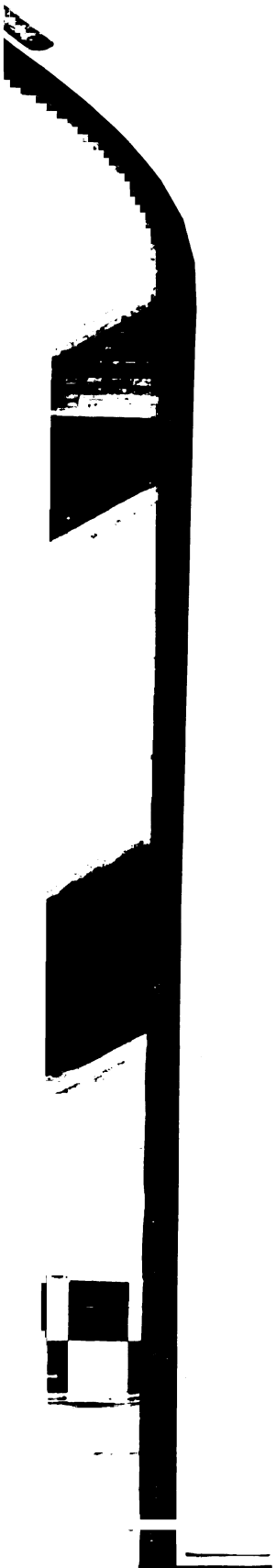

oxygen is 2 and that for dissociation of ozone is 0.9. The overall reaction kinetics are, however, dependent on the actual surface reactions that occur during treatment.

Photo-degradation mechanisms of common polymers. UV treatment of polymers can be considered to be analogous to controlled photo-degradation. A lot of work has been done in the field of polymer degradation to study the weathering behavior of these materials. Many of the photo-oxidation and photolysis mechanisms observed in long term photodegradation are expected to be the initial steps in the UV oxidation process. The reactions with ozone can yield other products which are not described by these mechanisms, but they can provide a good reference for the analysis of UVO treated surfaces.

Reaction mechanisms for various polymers have been proposed in literature. Figure 1.11 shows one of the proposed reaction schemes for polyethylene (PE) and polypropylene (PP) under VUV (< 185 nm) irradiation [48,61]. Polyolefins should in theory be photo-oxidatively stable to radiation above 185 nm because of the lack of chromophores that absorb strongly at longer wavelengths, yet PE and PP polymers can be oxidized with mercury as well as xenon lamps. This is believed to be a result of sensitizing impurities in the polymers. Rabek, in his excellent treatise on photochemical reactions in polymers [50] identifies vinyl and vinylidene impurities in polyethylene as the starting points for photo-oxidation. The mechanisms of UV photo-oxidation of HDPE are shown in Figure 1.12. The vinyl impurity in the polyethylene chain leads to the formation of hydro-peroxy radicals and ultimately aldehydes, ketones and crosslinked polymer.

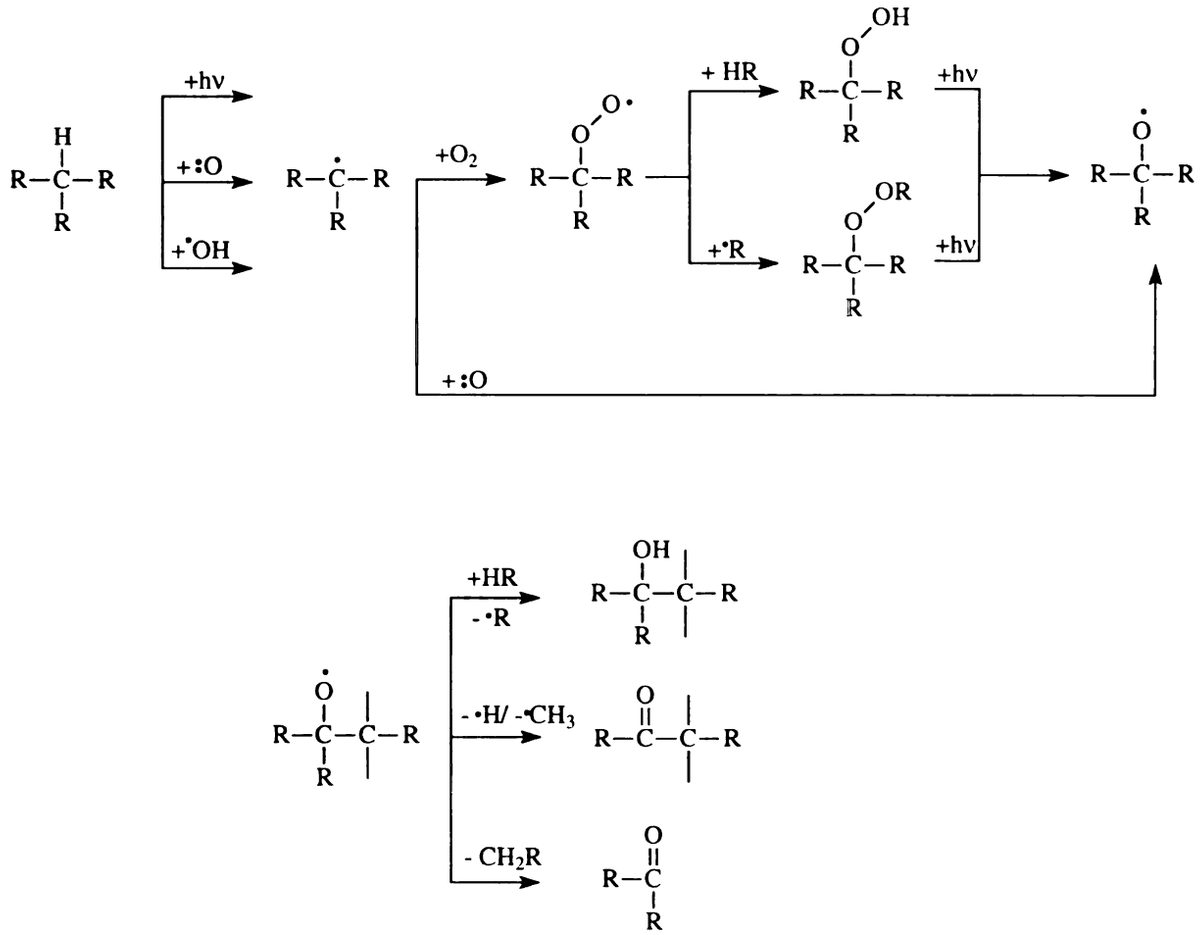

Figure 1.11 VUV photo-oxidation reaction scheme for PE and PP [48].

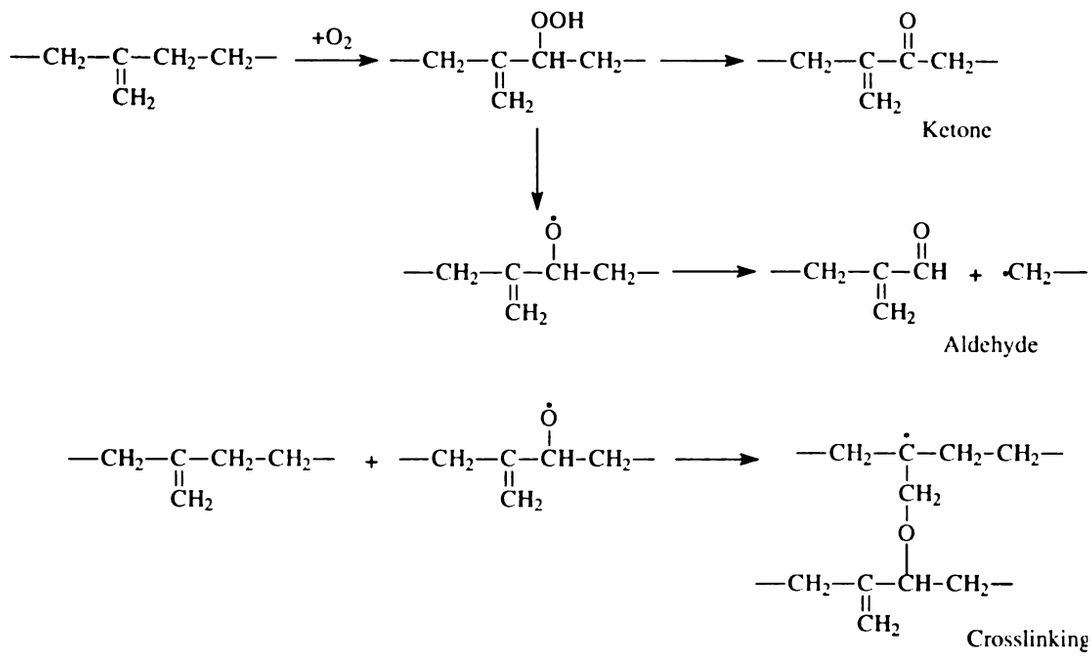

Figure 1.12 Photo-oxidation reaction scheme for PE.

The degradation mechanisms of polycarbonate have been the focus of many studies [35-38]. Figure 1.13 shows the typical photo induced reactions in bisphenol-A polycarbonate [50]. The most important reaction is the photo-Fries rearrangement of the carbonate linkage under UV irradiation to form phenyl salicylate, and ultimately, o-hydroxybenzophenone. Both compounds are UV stabilizers and give polycarbonate an auto-stabilizing capability. The photo-Fries rearrangement occurs independently of chain scission mechanisms that cleave the carbonate linkage to liberate CO_2 and the phenoxy radical formed can abstract a hydrogen or the methyl group in the bisphenol-A structure. These products of these basic reactions undergo crosslinking reactions or further oxidation with ozone to yield a wide range of products.

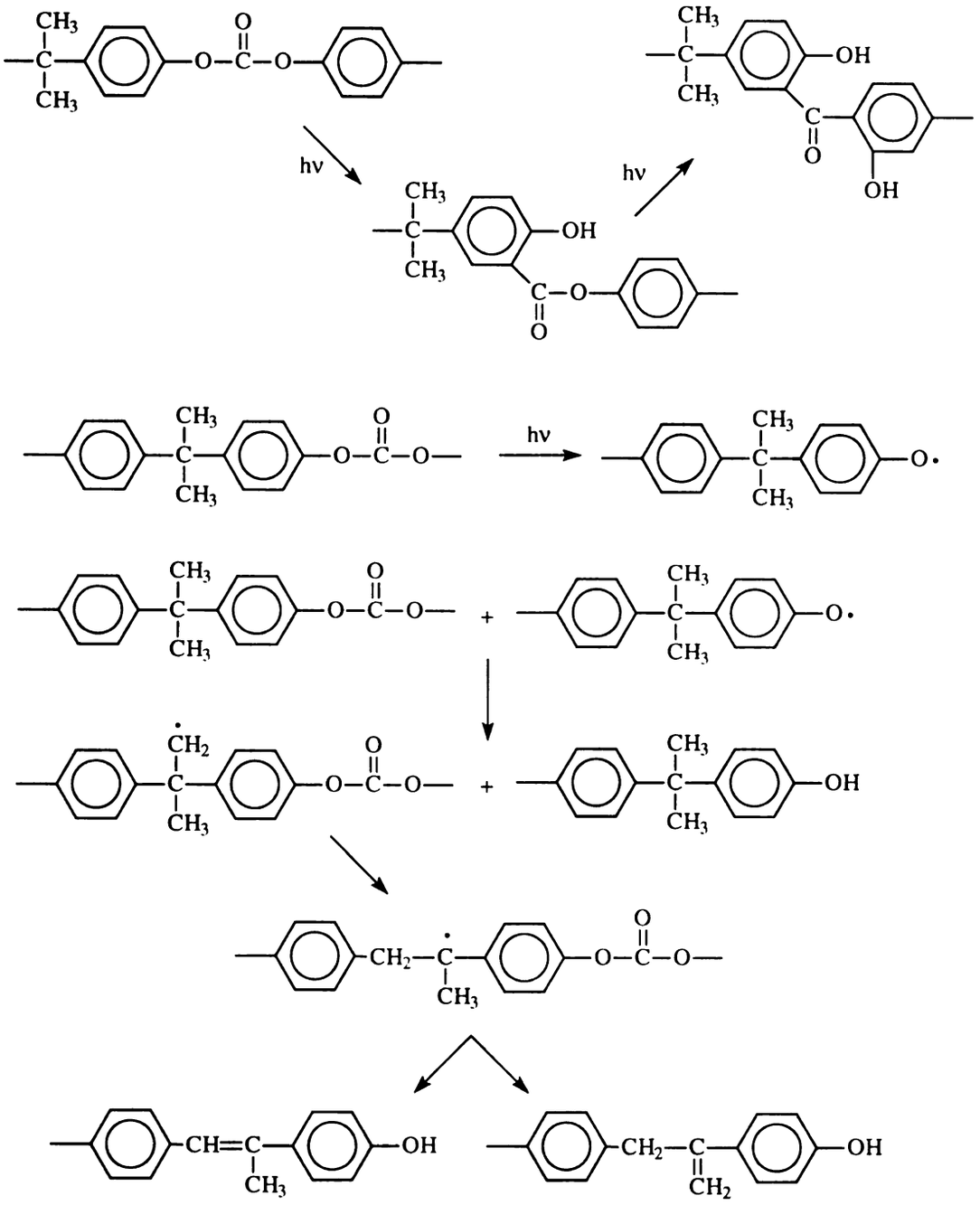

Figure 1.13 Photo-Fries rearrangement and photolysis reaction scheme for polycarbonate.

Polye

susceptibility

chromophore

direct scissi

mechanism o

with the loss

peroxy (P-O(

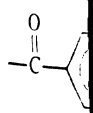

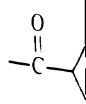

Figu

There

which are co

general mech

mechanisms

mechanism

Polyethylene terephthalate (PET) is an aromatic polyester known for its susceptibility to UV degradation. The aromatic esters are strongly absorbing chromophores with high absorptivities below 315 nm. The degradation of PET occurs by direct scission of the ester bonds in the backbone. Figure 1.14 shows the basic mechanism of chain scission in PET [50]. The radicals formed under decarboxylation with the loss of CO or CO_2 and are then oxidized by oxygen or ozone to form reactive peroxy (P-OO*), alkyloxy (P-O*) or hydro-peroxy (P-OOH) groups.

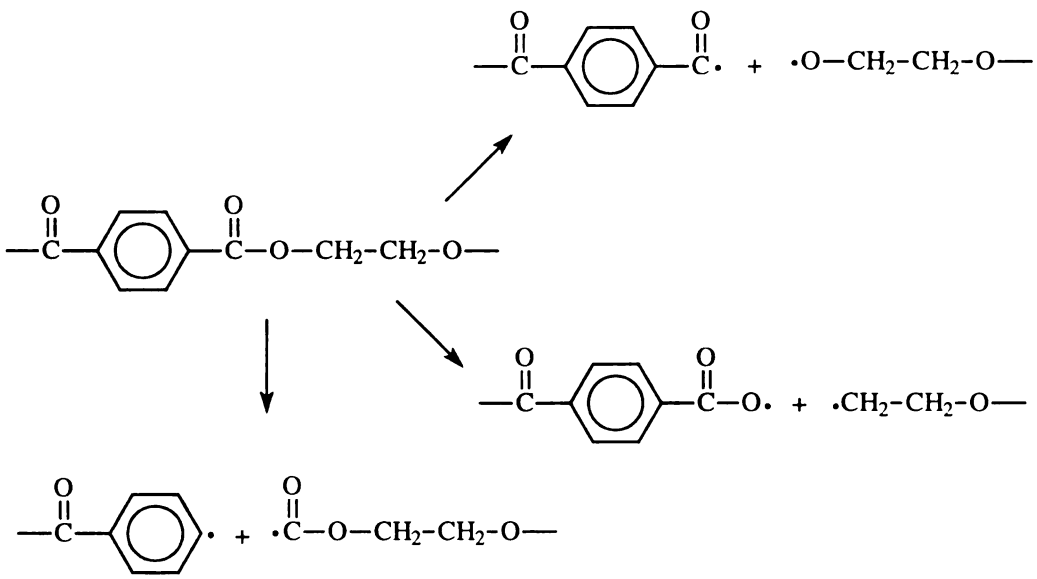

Figure 1.14 Photo-oxidation scheme for polyethylene terephthalate.

There are several other important photo and oxidative degradation mechanisms which are commonly observed in organic molecules. The most important class of these general mechanisms for polymers are the Norrish Type I and Type II photodegradation mechanisms in polymers containing carbonyl groups [50,62]. The Norrish Type I mechanism describes the photo-cleavage of a bond at α position in relation to the

carbonyl gro

containing k

decarbonylat

RCH$_2$CH

RCH

Figure

The N

atom on a γ

the γ carbon

carbon to fo

Norrish mec

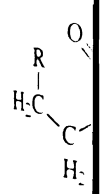

carbonyl group. This type of reaction is responsible for chain scission in polymers containing ketone and aldehyde groups. At elevated temperatures the acyl radical decarbonylates with the evolution of carbon monoxide as illustrated in Figure 1.15.

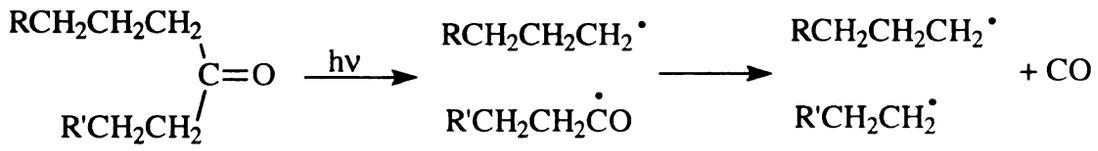

Figure 1.15 Norrish Type I mechanism for α-cleavage of carbonyl groups.

The Norrish Type II mechanism is observed in ketones possessing a hydrogen atom on a γ carbon atom. The oxygen on the carbonyl group abstracts a hydrogen from the γ carbon to form a six membered cyclic intermediate which causes cleavage at the β carbon to form end groups with unsaturation as illustrated in Figure 1.16. Both types of Norrish mechanisms are important in photodegradation of polymers.

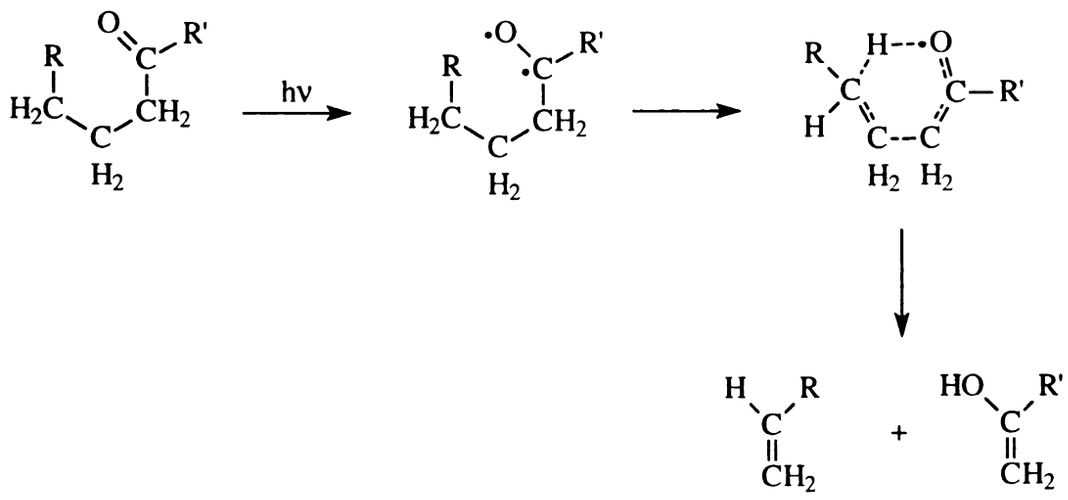

Figure 1.16 Norrish Type II photo-elimination mechanism in polymers containing carbonyl groups.

The

proposed by

attacks the

peroxy radic

subsequent

elastomers a

Criegee mec

R

H

Figur

It ca

organic mo

irradiation a

undergo oz

determinati

UV and ozo

The oxidative attack of ozone on unsaturated bonds in organic molecules was proposed by Criegee and is known as the Criegee mechanism [63]. The ozone molecule attacks the π bond and forms an ozonide ring. The ozonide ring dissociates to form a peroxy radical ion and a ketone. The peroxy radical ion which can undergo a variety of subsequent reactions including chain cleavage in the polymer. The susceptibility of elastomers and other unsaturated polymers to ozone attack is primarily explained by the Criegee mechanism.

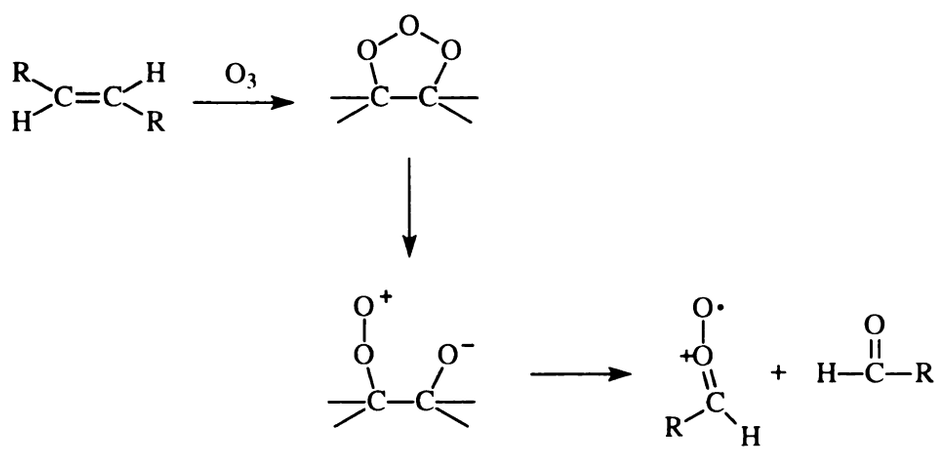

Figure 1.17 Criegee mechanism for ozone attack on unsaturated bonds.

It can be seen from this brief review of the literature that the photochemistry of organic molecules, especially polymers, can be very complicated when the effects of UV irradiation and ozonation are combined. The products of UV photolysis of a molecule can undergo ozonation, and the products of ozonation can themselves be photoactive. The determination of the precise reactions occurring in various polymers under conditions of UV and ozone oxidation is not trivial and beyond the scope of this study.

1.5 Goals

The c

surface treatr

different pol

manufacturin

commercial

stabilization

in the compo

be useful in

This work w

most, if not a

This

four differen

(PC), and c

these materi

must be con

The

changes occ

steps which

can be don

change in s

conditions a

the surface

1.5 Goals

The objective of this study is to obtain a predictive engineering model for the UV surface treatment process. The determination of precise mechanisms of UV oxidation for different polymers is a fascinating field of study, but it has limited use in the manufacturing environment where pure, repeatable surfaces are rarely available. Most commercial polymers are processed to various extents and have additives to aid stabilization and processing. Moreover, there can be considerable batch to batch variation in the composition and surface quality of commercial polymers. Any model that hopes to be useful in such environments must be adaptable to these, sometimes large, variations. This work will focus on developing a model for UV treatment which can be applicable to most, if not all, polymers.

This will be accomplished by studying the properties of polymers belonging to four different classes: thermosets (epoxy), elastomers (rubber), amorphous thermoplastics (PC), and crystalline thermoplastics (PET). The similarities and differences between these materials will be used to determine the key UV treatment process parameters which must be controlled to achieve the required level of surface modification in a material.

The approach will involve the consideration of the sum total of all chemical changes occurring on the surface during UV treatment instead of modeling the individual steps which can be different for each polymer. The characterization of surface treatment can be done with surface energy measurements and surface chemical analysis. The change in surface functional groups can be analyzed as a function of various treatment conditions and empirical relationships can be developed between the functionalization of the surface and process parameters. This macroscopic approach to the problem can

provide pro

effect of su

correlated to

ultimate eng

The g

can account

predictive p

estimated fr

provide process optimization guidelines, which can be easily applied in practice. The effect of surface modification on the adhesive properties of the material can also be correlated to the functionalization of the surface, providing relationships between the ultimate engineering properties and treatment process parameters.

The generalization of these observations will be used to develop relationships that can account for the differences between polymers. This will ultimately lead to a predictive process model where the effect of UV treatment on the polymers can be estimated from a minimal set of data and information about the structure of the material.

1. Drzal L.

2. Mahlber
Adhesion

3. Gutowsk

4. Sohn, S.
2003.

5. Martinez
Torregro
47-65, 2

6. Strobel,

7. Sako, N.;
415, 199

8. Strobel,
Adhesion

9. Kruse,
Modifica

10. Lane, J.
1993.

11. Bhurke,
Surface
Engineer

12. Hashem,
48, 199

13. Macman
Polymer

14. Kesting,
54, pp. 3

References

1. Drzal L.T. *SAMPE Journal*, Vol. 19, No. 5, pp. 7-13, 1983.

2. Mahlberg, R.; Nieme, H.E.M., Denes, F.,; Rowell, R.M. *International Journal of Adhesion & Adhesives*, Vol. 18, pp. 283-297, 1998.

3. Gutowski, W.S.; Wu, D.Y.; LI, S. *J. Adhesion*, Vol. 43, pp. 139-155, 1993.

4. Sohn, S.; Chang, S.; Hwang, I. *J. Adhesion Sci. Technol.*, Vol. 17, No. 3, pp. 453-469, 2003.

5. Martinez-Garcia, A.; Sanchez-Reche, A.; Gisbert-Soler, S.; Cepeda-Jiminez, C.M.; Torregrosa-Macia, R.; Martin-Martinez, *J. Adhesion Sci. Technol.*, Vol. 17, No. 1, pp. 47-65, 2003.

6. Strobel, M.; Lyons, C.S. , *J. Adhesion Sci. Technol.*, Vol. 17, No. 1, pp. 15-23, 2003.

7. Sako, N.; Matsuoka, T.; Sakaguchi, K.; *Composite Interfaces*, Vol. 4, No. 6, pp. 401-415, 1997.

8. Strobel, M.; Walzak, M.J.; Hill, J.M.; Lin, A.; Karbashewski, E.; Lyons, C.S. *J. Adhesion Sci. Technol.*, Vol 9, No 3, pp. 365-383, 1995.

9. Kruse, A.; Kruger, G.; Baalmann, A.; Hennemann, O.D. *Polymer Surface Modification: Relevance to Adhesion*, K.L. Mittal (Ed.), pp. 291-301, 1995.

10. Lane, J.M.; Hourston, D.J. *Progress in Organic Coatings*, Vol. 21, pp. 269-284, 1993.

11. Bhurke, A.S.; Jensen, M.; *UV Treatment – A Low Cost, Environmentally Friendly Surface Treatment Technique*, ML890 Report, Case Center for Computer-Aided Engineering and Manufacturing, Michigan State University, USA, 1997.

12. Hashem, T.M.; Zirlewagen, M.; Braun, A.M. *Wat. Sci. Tech.*, Vol. 35, No. 4, pp. 41-48, 1997.

13. Macmanus, L.F.; Walzak, M.J.; Mcintyre, N.S. *Journal of Polymer Science: Part A: Polymer Chemistry*, Vol. 37, pp. 2489-2501, 1999.

14. Kesting, W.; Knittel, D.; Bahmers, T.; Schollmeyer, E. *Applied Surface Science*, Vol. 54, pp. 330-335, 1992.

15. Buchman
Relevanc

16. Sancakta
133, 199

17. Bolle, M

18. Krajnovi

19. Walzak,
M. *Polyn*
272, 199

20. Peeling,
21, pp. 2

21. Charbon
404, 200

22. Praschak

23. Pasternal

24. Minagaw
Sasaki, T

25. Yu, J.R.
XIV, 4,

26. Petit, S.
Adhesio

27. Romero-
Adhesio

28. Ouyang,
Vol. 12,

29. Kave, T
1059, 2

30. Grujicic
Vol. 21

15. Buchman, A.; Dodiuk, H.; Rotel, M.; Zahavi, J. *Polymer Surface Modification: Relevance to Adhesion*, K.L. Mittal (Ed.), pp. 199-212, 1995.

16. Sancaktar, E.; Babu, S.V.; Zhang, E.; D'Couto, G.C. *J. Adhesion*, Vol. 50, pp. 103-133, 1995.

17. Bolle, M.; Lazare, S. *Applied Surface Science*, vol. 54, pp. 471-476, 1992.

18. Krajnovich, D.J. *J. Phys. Chem. A*, Vol. 101, pp. 2033-2039, 1997.

19. Walzak, M.J.; Flynn, S.; Foerch, R.; Hill, J.M.; Karbashewski, E.; Lin, A.; Strobel, M. *Polymer Surface Modification; Relevance to Adhesion*, K.L. Mittal (Ed.), pp. 253-272, 1995.

20. Peeling, J.; Clark, D.T. *Journal of Polymer Science: Polymer Chemistry Edition*, Vol. 21, pp. 2047-2055, 1983.

21. Charbonnier, M.; Romand, M.; Esrom, H.; Seebock, R. *J. Adhesion*, Vol. 75, pp. 381-404, 2001.

22. Praschak, D.; Bahners, T.; Schollmeyer, E. *Appl. Phys. A*, Vol. 66, pp. 69-75, 1998.

23. Pasternak, M. *Journal of Applied Polymer Science*, Vol. 57, pp. 1211-1216, 1995.

24. Minagawa, M.; Saito, T.; Fujikura, Y.; Watanabe, T.; Iwabuchi, H.; Yoshii, F.; Sasaki, T. *J. Appl. Polym. Sci.* Vol. 63, No. 12, pp. 1625-33, 1997.

25. Yu, J.R.; Chen, Z.L.; Zhu, J.; Liu, Z.F.; Wang, Q.R. *Intern. Polymer Processing*, XIV, 4, pp. 331-335, 1999.

26. Petit, S.; Laurens, P.; Barthes-Labrousse, M.G.; Amouroux, J.; Arefi-Khonsari, F. *J. Adhesion Sci. Technol.*, Vol.17, No. 3, pp. 353-368, 2003.

27. Romero-Sanchez, M.D.; Pastor-Blas, M.M.; Martin-Martinez, J.M.; Walzak, M.J. *J. Adhesion Sci. Technol.*, Vol. 17, No. 1, pp. 25-45, 2003.

28. Ouyang, M.; Yuan, C.; Muisener, R.J.; Boulares, A.; Koberstein, J.T. *Chem. Mater.*, Vol. 12, No. 6, pp. 1591-1596, 2000.

29. Kavc, T.; Kern, W.; Ebel, M.; Svagera, R.; Polt, P. *Chem. Mater.*, Vol. 12, pp. 1053-1059, 2000.

30. Grujicic, M.; Cao, G.; Rao, A.M.; Tritt, T.M.; Nayak, S. *Applied Surface Science*, Vol. 214, pp. 289-303, 2003.

31. Dontula,
Society, 1

32. Bhurke,
106-108.

33. Sullivan,
Internati
publicati

34. Liston,
Polymer

35. Webb, J

36. Factor,

37. Ramani,
354, 200

38. Turton,
182, 200

39. Zhang;
Adhesion

40. Ning, X.
1999.

41. O'Keeffe
Chemica

42. Gurol, M

43. Heit, G.;

44. Knittel,
1997.

45. Knittel,
1997.

46. Knittel,
1998.

31. Dontula, N.; Weitzsacker, C.; Drzal, L.T. *Proc. 20th Annual Meeting of the Adhesion Society*, pp. 97, 1997.

32. Bhurke, A.S.; Drzal, L.T. *Proc. 26th Annual Meeting of the Adhesion Society*, pp. 106-108, 2003.

33. Sullivan, N.; Branch, M.C.; Ulsh, M.; Strobel, M. *Proceedings of the 17th International Colloquium on Dynamics of Explosion and Reactive Systems*, electronic publication, http://reaflow.iwr.uni-heidelberg.de/~icders99/icders99.html, 1999.

34. Liston, E.M.; Martinu, L.; Wertheimer, M.R. *Plasma Surface Modification of Polymers*, M. Strobel, C. Lyons, K.L. Mittal (Eds.), pp. 3-39, 1994.

35. Webb, J.D.; Czanderna, A.W.; *Macromolecules*, Vol. 19, pp. 2810-2825, 1986.

36. Factor, A.; Ligon, W.V.; May, R.J. *Macromolecules*, Vol. 20, pp. 2461-2468, 1987.

37. Ramani, R.; Ranganathaiah, C. *Polymer Degradation and Stability*, Vol. 69, pp. 347-354, 2000.

38. Turton, T.J.; White, J.R. *Plastics, Rubber and Composites*, Vol. 30, No.4, pp. 175-182, 2001.

39. Zhang; Esrom; Kogelschatz; Emig *Polymer Surface Modification: Relevance to Adhesion*, K.L.Mittal (Ed.), pp. 153-184, 1995.

40. Ning, X.; Qin, Q. *Journal of Computational Chemistry*, Vol. 20, No. 6, pp. 623-628, 1999.

41. O'Keeffe, P.; Ridley, T.; Lawley, K.P.; Maier, R.R.J.; Donovan, R.J. *Journal of Chemical Physics*, Vol. 110, No. 22, pp. 10803-10809, 1999.

42. Gurol, M.D.; Akata, A. *AICHE Journal*, Vol. 42, No. 11, pp.3283-3292, 1999.

43. Heit, G.; Braun, A.M. *Wat. Sci. Tech.*, Vol. 35, No. 4, pp. 25-30, 1997.

44. Knittel, D.; Kesting, W.; Schollmeyer E. *Polymer International*, Vol 43, pp. 231-239, 1997.

45. Knittel, D.; Kesting, W.; Schollmeyer E. *Polymer International*, vol 43, pp. 240-250, 1997.

46. Knittel, D.; Kesting, W.; Schollmeyer E. *Polymer International*, vol 45, pp. 103-109, 1998.

47. Watanab
323-331.

48. Hollando
Polymer

49. Breuer:
Mittal (E

50. Rabek. J
Polymer

51. Fu. X.; I

52. Cheng. H

53. Dasgupt

54. Atkins.
Univers

55. Lothian.

56. Qu. B.
1993.

57. Ranby, I

58. Ranby, I
pp. 303-

59. Shi. W.
1994.

60. Strobel.
Plasma

61. Wilken.
1998.

62. Horspo
Society

63. Criegee.
pp.133-

47. Watanabe, F.; Shimomura, O.; *Journal of Hygienic Chemistry*, Vol. 37, No. 5, pp. 323-331, 1991.

48. Hollander, A.; Klemberg-Sapieha, J.; Wertheimer, M.; *J. Polymer Science Part A: Polymer Chemistry*, Vol. 23, pp. 2013-2025, 1995.

49. Breuer; Metev; Sepold; *Polymer Surface Modification: Relevance to Adhesion*, K.L. Mittal (Ed.), pp. 185-197, 1995.

50. Rabek, J.F. *Mechanisms of Photophysical Processes and Photochemical Reactions in Polymers*, John Wiley, New York, 1987.

51. Fu, X.; Lu, W.; Chung, D.D.L. *Carbon*, Vol. 36, No.9, pp.1337-1345, 1998.

52. Cheng, F.; Hong, S.; Ho, C. *J. Adhesion*, Vol. 67, pp. 123-137, 1998.

53. Dasgupta, S. *Journal of Applied Polymer Science*, Vol. 41, pp. 233-248, 1990.

54. Atkins, P.W.; Friedman, R.S. *Molecular Quantum Mechanics*, Third Ed., Oxford University Press, Oxford, 1997.

55. Lothian, G. *Absorption Spectrophotometry*, 3rd ed., pp. 101, Hilger, London, 1969.

56. Qu, B.; Ranby, B. *Journal of Applied Polymer Science*, Vol. 49, pp. 1799-1807, 1993.

57. Ranby, B. *Polymer Engineering and Science*, Vol. 38, No. 8, pp. 1229 –1243, 1998.

58. Ranby, B. *Polymer Surface Modification: Relevance to Adhesion*, K.L. Mittal (ed.), pp. 303-317, 1995.

59. Shi, W.; Ranby, B. *Journal of Applied Polymer Science*, Vol. 51, pp. 1129-1139, 1994.

60. Strobel, M.; Jones, V.; Lyons, C.S.; Ulsh, M.; Kushner, M.J.; Dorai, R.; Branch, M.C. *Plasmas and Polymers*, Vol. 8, No. 1, pp. 61-95, 2003.

61. Wilken, R.; Hollander, A.; Behnisch, J. *Macromolecules*, Vol. 31, pp. 7613-7617, 1998.

62. Horspool, W.M.; *Photolysis of Carbonyl Compounds*, Photochemistry, Vol. 30, Royal Society of Chemistry, Cambridge, UK, 1999.

63. Criegee, R. in: *Ozone Chemistry and Technology*, American Chemical Society, pp.133-135, Washington, 1959.

The equipm

of the treat

Woburn, M

output in th

built alumin

analytical ch

UV spectros

treated surfa

2.1 UV Lam

Three Xeno

used. The n

2.1. The lam

provide opti

and all emit

the heat gen

outer surfac

determinati

distance be

RC 747, RC

CHAPTER TWO

EXPERIMENTAL METHODS

The equipment and experimental techniques used for UV surface treatment and analysis of the treated surfaces are described in this chapter. Xenon UV lamps (Xenon Corp., Woburn, MA) were used in this study because of their pulsed operation and enhanced output in the low wavelength UV-C region. Various polymers were treated in a custom built aluminum chamber, and treated surfaces were characterized by different surface analytical characterization techniques including X-ray photoelectron spectroscopy (XPS), UV spectroscopy, and surface energy measurements. Mechanical characterization of the treated surfaces was accomplished with nano-indentation and adhesion measurements.

2.1 UV Lamps and Filters

Three Xenon flashlamps operating at frequencies ranging from 3 Hz to 120 Hz were used. The nominal power, frequency, and shape of the lamps are summarized in Table 2.1. The lamps are equipped with aluminum reflectors and fused quartz windows to provide optimum transmission of UV radiation. The lamp housings are made of metal and all emitted radiation is transmitted through the fused quartz windows. A portion of the heat generated by the bulb is removed from the housing by forced air convection. The outer surface of the lamp window is considered the area source of UV radiation for all determinations of irradiant energy and is the reference plane for measurement of the distance between the lamp and sample surface. Figure 2.1 shows the Xenon UV lamps (RC 747, RC 740, and RC 500) used in this work. Samples were UV treated in a chamber

made fr

x 1 inc

provide

Dynasil®

equipped

schematic

material f

various gl

quartz gla

UV radiati

but the tra

10% transm

to determin

process.

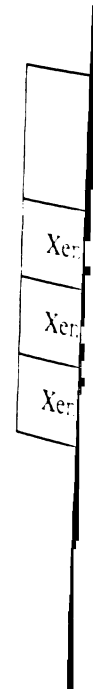

made from 1/4 inch aluminum plates having exterior dimensions of 8 inch (l) x 8 inch (w) x 1 inch (h). A 4 inch x 4 inch opening was machined in the top of the chamber to provide a path for illuminating radiation. The opening was closed with either Suprasil®, Dynasil®2000, Quartz, or Pyrex® glass plates during treatment. The chamber was equipped with an inlet and outlet for process gases. The UV treatment chamber and a schematic of the experimental setup are shown in Figures 2.2 and 2.3. The selection of material for the treatment chamber window or filter was based on the transmission of the various glasses as shown in Figure 2.4. Suprasil® and Dynasil® are high purity fused quartz glasses with very low hydroxyl concentrations, which enhances transmission of UV radiation below 200 nm. Ordinary quartz has very high transmittance above 230 nm but the transmittance drops sharply below 200 nm. Pyrex® windows have a cut-off of ca. 10% transmittance at 290 nm. The Pyrex® window was used as a 280 nm high pass filter to determine the effect of exclusion of low wavelength UV-C radiation on the treatment process.

Table 2.1 Description of UV lamps

Lamp	Power (W)	Frequency (Hz)	Bulb Shape
Xenon RC 500	300	120	5 inches, linear
Xenon RC 740	1500	10	3.5 inches, coil
Xenon RC 747	1500	3, 120	16 inches, linear

Figure 2.1 Xenon pulsed UV lamps (from left) RC 747, RC 500, and RC 740.

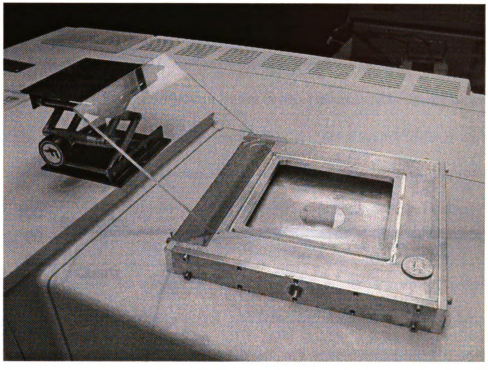

Figure 2.2 Aluminum UV treatment chamber with Suprasil® cover.

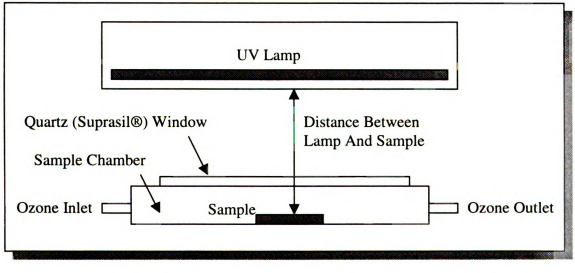

Figure 2.3 Schematic of the experimental setup for UV surface treatment.

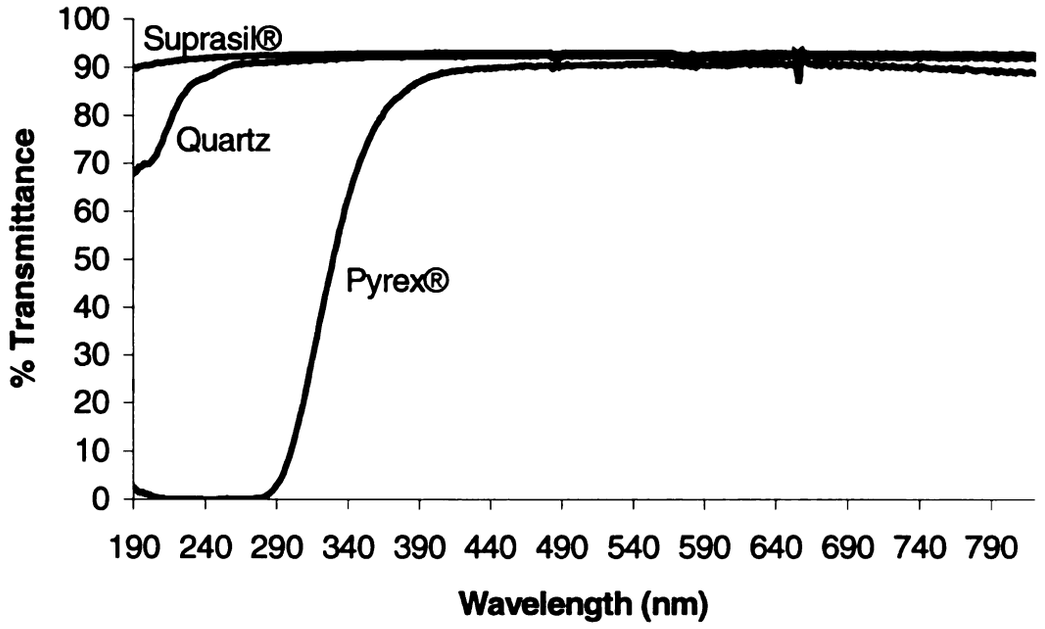

Figure 2.4 UV transmittance of Suprasil®, Quartz, and Pyrex® filters

2.2 Measurement of UV Radiation

The measurement of radiation is broadly classified into two categories: radiometry and photometry [1]. Radiometry is the measurement of energy emitted in a range of wavelengths by a source of radiation while photometry is the measurement of visible light, more commonly concerned with the effect and response of the human eye to light. Radiometric measurement at specific wavelengths of the spectrum or spectral bands is called spectral radiometry. In terms of chemical applications of radiation, spectral radiometry is widely used since chemical reactions often occur at particular wavelengths and the measurement of the amount of radiation emitted at those wavelengths can be used to quantify the processes. The concepts, symbols, and definitions used to describe the quantitative measurement of radiation are varied and some of the widely used concepts and symbols are listed in Table 2.2.

Table 2.2 Radiometric units and descriptions.

Radiometric Unit	Symbol	Units	Description
Radiant Energy	Q	J	Energy transported in the form of electromagnetic waves.
Radiant Flux (Radiant Power)	ϕ	W	Radiant energy transmitted by radiation in unit time.
Radiant Emittance	M	W/m^2	Radiant flux emitted from a unit surface.
Radiant Intensity	I	W/sr	Radiant flux leaving the radiation source per solid angle (steradian, sr).
Radiance	L	$W/sr.m^2$	Radiant intensity passing through a unit area.
Irradiance	E	W/m^2	Radiant flux received by a unit area.
Irradiation	H	J/m^2	Integrated irradiance over the exposure time.

Due to the variety of radiometric units available to quantify radiation, it is important to choose the right unit to describe the system. In an application such as UV surface treatment, the amount of radiation reaching the surface is the quantity of interest and both intensity and irradiance can be used to quantify the radiation. However, it is important to note that the two units differ in concept: intensity is a unit related to the source of the radiation while irradiance is a unit related to the receiving surface. Thus, intensity is more useful in describing the amount of UV radiation emitted by the UV lamp while irradiance is more useful in describing the amount of emitted radiation received by a surface exposed to it. Therefore, irradiance will be used to quantify radiation in this study.

During treatment, the UV lamp is placed above the aluminum treatment chamber with a UV transparent fused quartz (Suprasil® 300) window sealing the chamber. The UV radiation emitted by the lamp passes through air, a quartz window, and a layer of ozone, before reaching the sample. All of these materials absorb radiation to varying extents, causing attenuation of the UV radiation emitted from the lamp. Another factor to consider in the measurement of irradiance is the geometric arrangement and nature of the receiving surface. Lambert's cosine law [1] states that the irradiance incident on a surface varies as the cosine of the incident angle, θ, such that $E_\theta = E \cos(\theta)$. As seen in Figure 2.5, the projected area of the receiving surface orthogonal to the incident radiation decreases as the incident angle increases. Most real surfaces are Lambertian in nature and the dependence of the incident irradiance on the angle of incidence must be taken into account especially since most commercially available lamps are not point sources of light.

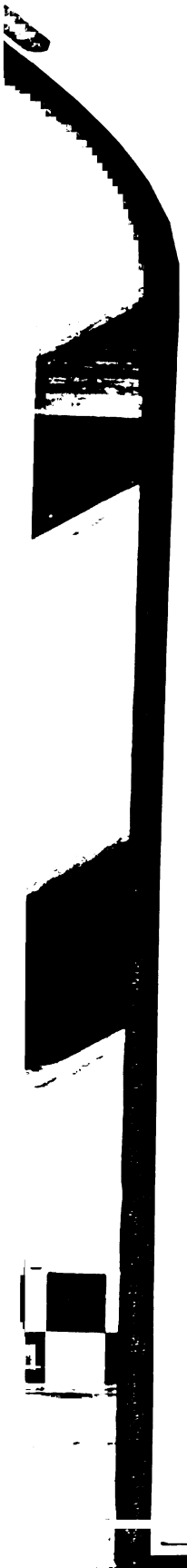

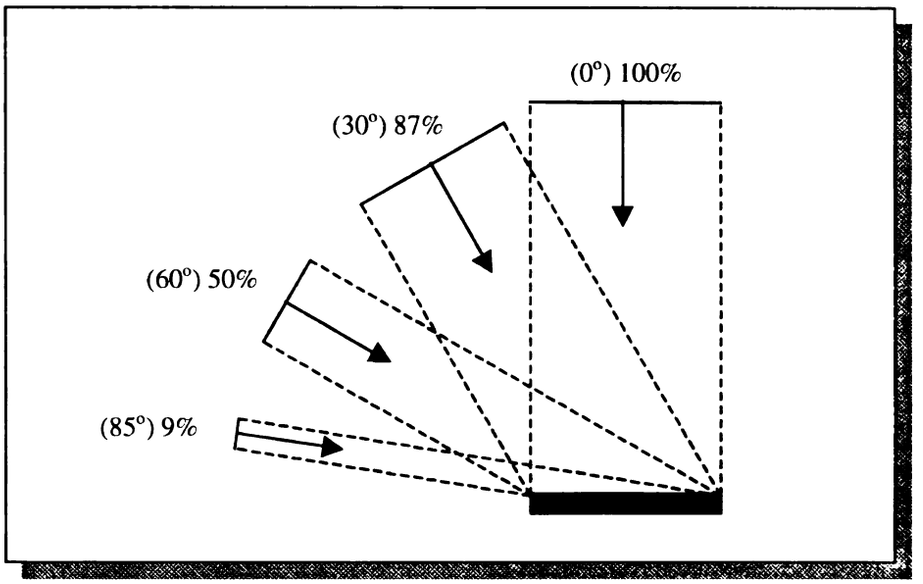

Figure 2.5 Lambert's cosine law showing decrease in irradiance with increasing angle of incidence.

The irradiance at 254 nm wavelength incident on the sample was measured using a radiometer (International Light, IL1700 Research Radiometer) coupled with a solar blind photodiode detector (International Light, SED 220), a 254 nm narrow-band filter (International Light, NS 254), and a quartz cosine-response filter. The setup was calibrated with NIST traceable standards. The photodetector used has a narrow (8-10°) viewing angle, hence a quartz cosine-response filter was installed over the detector to allow collection of radiation incident at oblique angles. To obtain an accurate measure of the amount of radiant energy reaching the sample surface during UV treatment, the entire detector assembly was mounted inside the chamber at the location where samples were mounted for treatment. Irradiance was measured with ozone (approximately 750 ppm) and oxygen gases flowing through the chamber at 30 scfh. Irradiation was measured in time-integral mode and the irradiance calculated as the average energy reaching the detector per unit time. Irradiance for RC500 and RC747 lamps was measured as a

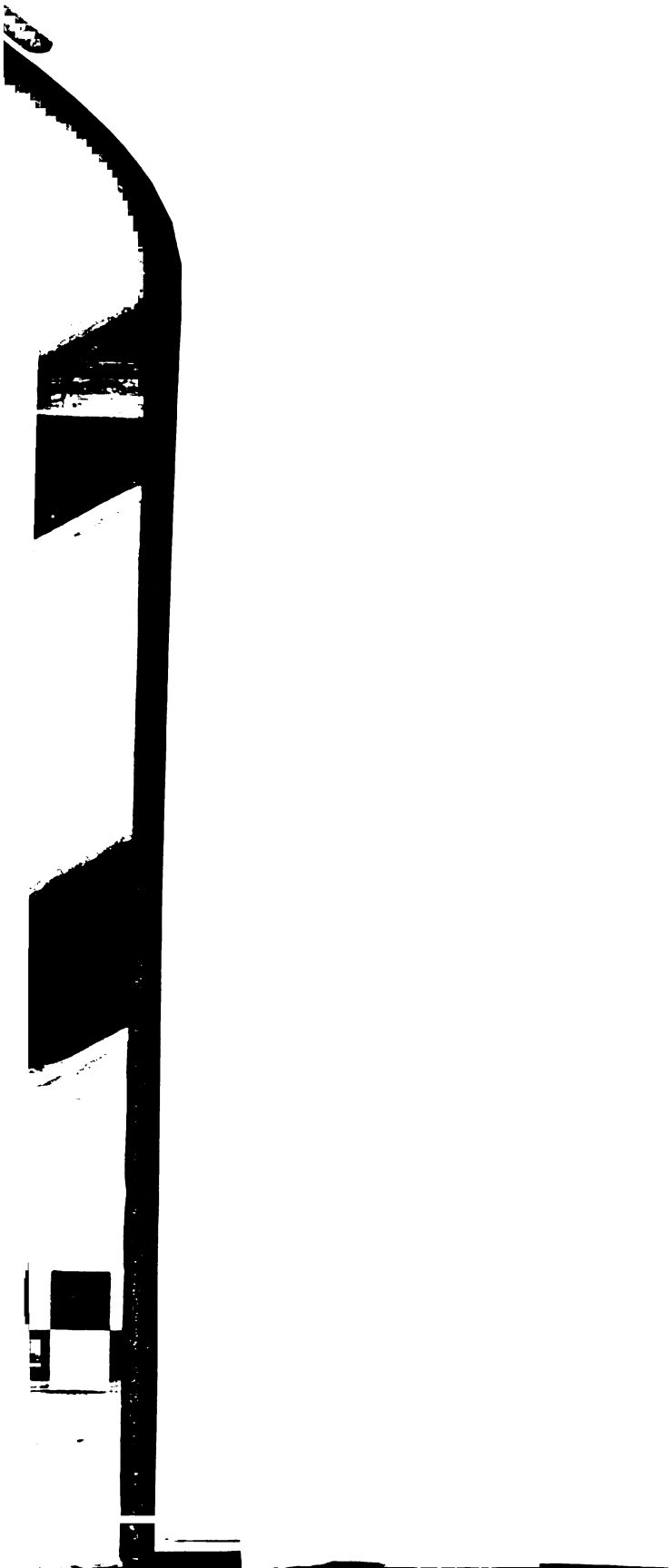

function of varying distance from the treatment chamber. The relationship between irradiance and distance from a point source is defined by the Inverse Square law which states that the irradiance decreases as the square of the distance between the detector and the source [1]. The results of the irradiance measurements for the two lamps are shown in Figures 2.6 and 2.7. The irradiance increases as the distance from the lamp decreases. However, the change in irradiance does not follow the Inverse Square law exactly because the lamps, far from being point sources, are high aspect ratio cylindrical tubes. Additional deviation is caused by the presence of the chamber and window which limits the angle of view of the detector assembly. This alleviates the effect of increasing distance as a greater length of the UV lamp is brought into the limited angle of view of the detector as the lamp is moved farther away. The irradiance values obtained also take into account the radiation absorbed by the gas layer (oxygen and ozone) and any reflection and refraction effects from the quartz window and aluminum chamber. The data obtained is a measure of the actual irradiance received by a sample placed in the UV treatment chamber under these specific conditions. Since the irradiance is invariant for a given set of physical conditions, values from the irradiance-distance calibration curves were used for calculating the total irradiation (irradiant energy) received by a sample during treatment such that:

$$H = \int_0^t E dt = Et \tag{2.1}$$

where H is the irradiant energy or irradiation (J/cm^2), E is the irradiant power or irradiance (W/cm^2), and t is the total UV exposure time (seconds).

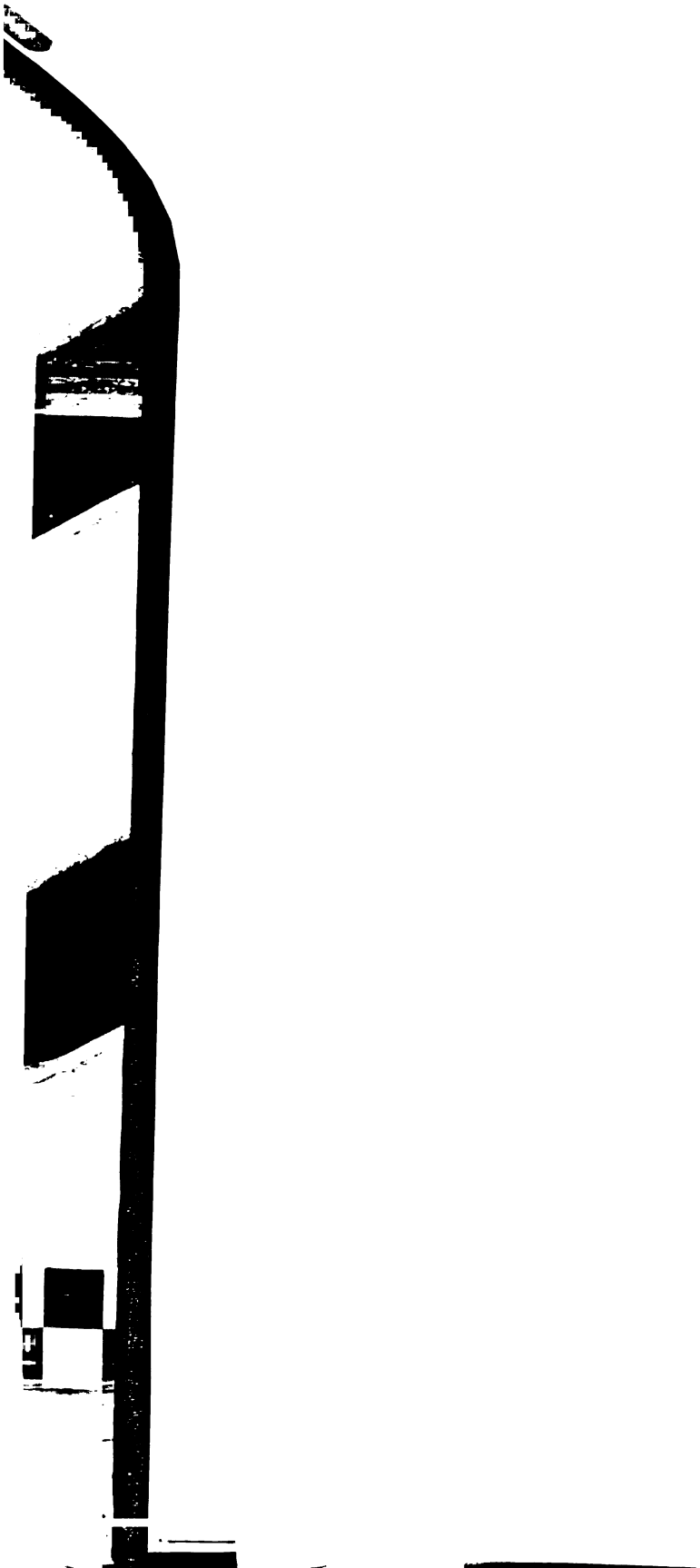

The effect of the gas flowing through the chamber has a marked effect on the irradiance. Ozone has a very strong absorption peak at 254 nm and the incident UV radiation is absorbed by the layer of gas present between the sample and the quartz window. This decrease is absent in the case of oxygen (or air), which has no significant absorption at 254 nm, and consequently higher levels of irradiance were obtained.

2.3 Measurement of Ozone Concentration

The UV surface treatment process involves the oxidation of the material surface with ozone in the presence of UV radiation. Ozone is produced by the interaction of 185 nm wavelength photons with molecular oxygen and the amount of ozone formed depends on the output of 185 nm radiation [2]. Xenon lamps have significant output at 185 nm and with appropriate selection of the equipment, the required ozone can be produced *in-situ* during UV treatment. However, reliance on *in-situ* production of ozone can present problems during short batch operations such as laboratory experiments because the ozone produced under the lamp may not reach steady state concentrations immediately on startup. To avoid this problem, an external ozone generator (Ozotech Inc., OZ6BTU) was used in experiments requiring ozone to ensure steady-state conditions. Another advantage of using an external ozone generator is the ability to vary the ozone concentration and flow rate, independently, to study their effect on the process. The measurement of ozone concentration can be accomplished in different ways. Iodometric titration and spectrometric absorption measurement are the two most widely used methods. Quantitative methods based on absorption measurement are more attractive because of their simplicity, speed, and the adaptability to continuous sampling.

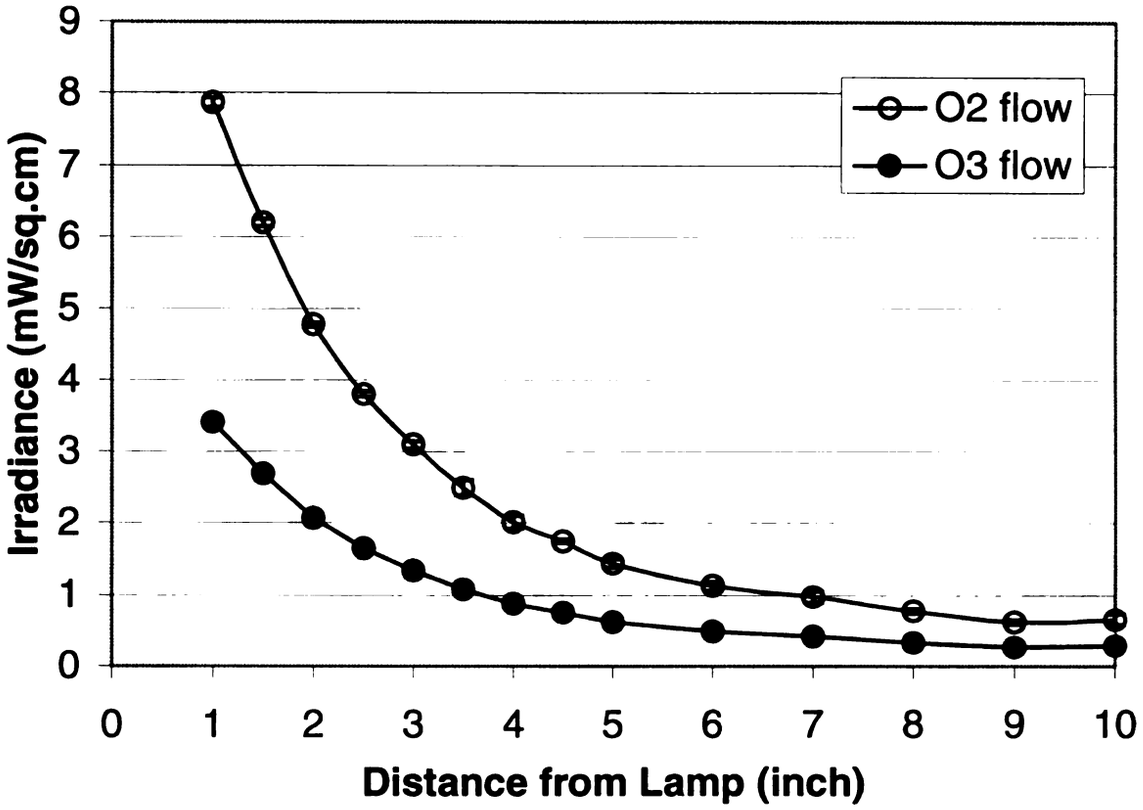

Figure 2.6 Irradiance measurements for RC500 lamp with ozone and oxygen flow.

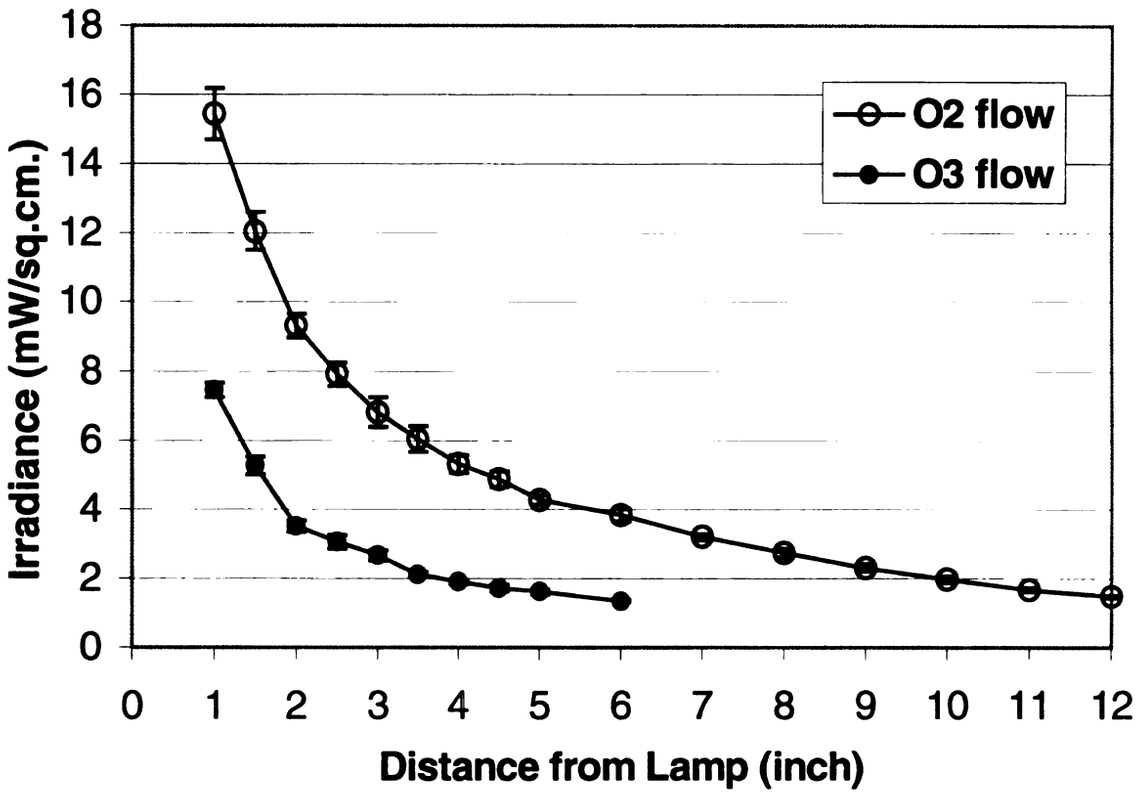

Figure 2.7 Irradiance measurements for RC747 lamp with ozone and oxygen flow.

Beer-Bouguer-Lambert Laws

The principle laws of light absorption of interest in quantitative UV spectroscopy are the Bouguer-Lambert law and Beer's law. Bouguer (1729) stated that the proportion of radiation absorbed by a substance was independent of the intensity of the incident radiation [3]. This was later formalized by Lambert. The Lambert-Bouguer law states:

$$\ln\left(\frac{I_o}{I}\right) = \alpha b \tag{2.2}$$

where I_0 is the intensity of the incident light, I is the intensity of transmitted light, b is the thickness of the transmitting medium, and α is the absorption coefficient characteristic of the medium. The absorption coefficient α contains no concentration factor and is applicable only to pure materials. When the natural log in Equation 2.2 is converted to base 10 log, α is converted to the Bunsen and Roscoe extinction coefficient, K [4].

Beer (1852) related the Bouguer-Lambert law to the concentration of the transmitting medium by stating that a photon can only be absorbed by a molecule if it collides with that molecule. Accordingly, the absorption of light through a solution is also proportional to the concentration of absorbing molecules present in the transparent medium. The proportionality to concentration can be incorporated in Equation 2.2 to give Beer's law [3]:

$$\log\left(\frac{I_o}{I}\right) = A = \varepsilon bc \tag{2.3}$$

where ε is the molar absorptivity, or molar extinction coefficient, c is the concentration, b is the path length, and A is the absorbance of the medium.

The absorbance can be measured with spectrophotometers and with known values of the extinction coefficient and path length, the concentration can be calculated. Ozone has a strong absorption maximum at 253.7 nm, as shown in Figure 2.8, with a molar extinction coefficient of 0.000308 $ppm^{-1}cm^{-1}$ at 0°C and 1 atm pressure [5].

A commercially available ozone generator was used to produce supplemental ozone. The generator produces ozone by corona discharge through a stream of oxygen source gas. The concentration of ozone generated can be controlled by adjusting the voltage applied to the corona tubes. The flow rate of gas through the generator can also be varied. Typical flow rates used in the ozone generator range from 10 to 30 scfh (std. cubic feet per hour). As the flow rate of the gas is decreased, the residence time in the corona tubes increases, leading to higher conversion of oxygen to ozone, and consequently, higher ozone concentration in the stream.

A Perkin Elmer Lambda 900 UV-VIS-NIR dual beam spectrometer was used to measure the concentration of ozone. The outlet from the ozone generator was connected to the UV treatment chamber and gas samples from the treatment chamber were transferred via a glass nozzle and ozone resistant silicone tubing to a 1mm path length quartz flow cell mounted in the spectrometer. Continuous flow of the sample gas through the flow cell was achieved by connecting the outlet of the cell to a small vacuum pump. The spectrometer and sampling setup is shown in Figure 2.9.

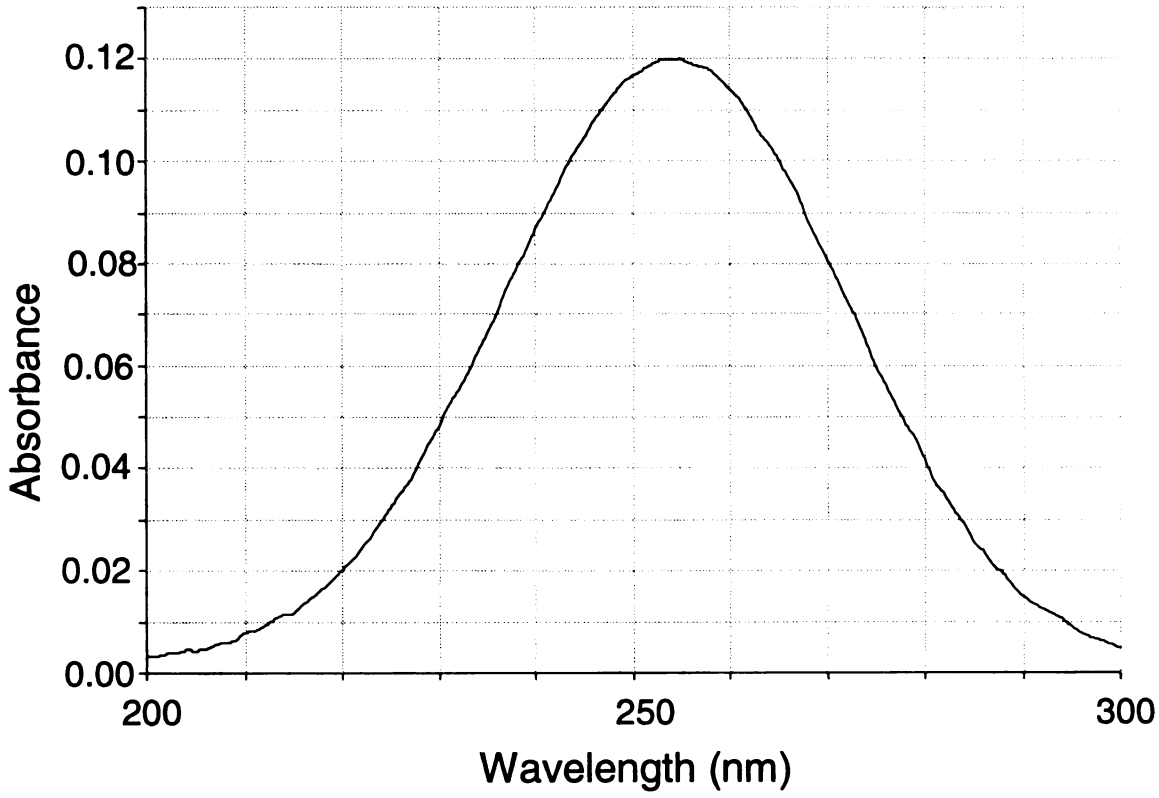

Figure 2.8 Absorption spectrum of ozone.

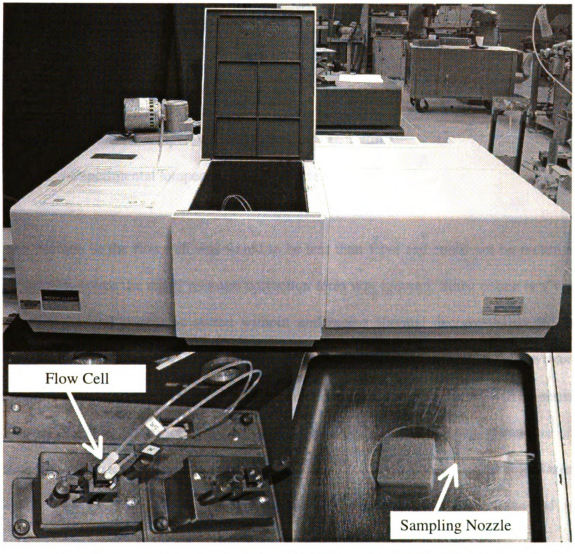

Figure 2.9 Perkin Elmer Lambda 900 UV-VIS-NIR Spectrometer with quartz flow cell and sampling nozzle for continuous ozone measurement.

Ozo

corr

atm.

whe

T_0 a

T ar

The

acc

reac

exte

con

in l

thus

con

flow

Ozone concentrations were measured at room temperature. The concentration can be corrected for deviation of temperature and pressure from the standard conditions (0°C, 1 atm. pressure) such that :

$$c = \frac{A}{\varepsilon\, b}\left(\frac{T}{T_0} \times \frac{P_0}{P}\right) \tag{2.4}$$

where

T_0 and P_0 = standard temperature and pressure (0°C, 1 atm.)

T and P = experimental temperature and pressure.

The vacuum in the flow cell was found to be less than 1 psi and could not be measured accurately, hence the small pressure correction term was ignored. Since ozone is a very reactive gas and cannot be stored without undergoing thermal decomposition [6], no external ozone standard was available for experimental calibration. Therefore, the ozone concentrations reported here should be considered approximate values. As will be shown in later chapters, the exact ozone concentration is not a critical process parameter and thus the approximate concentrations obtained were considered to be acceptable. Ozone concentration was measured at different combinations of the generator voltage and gas flow rates as shown in Figure 2.10.

Ozone Concentration (ppm)

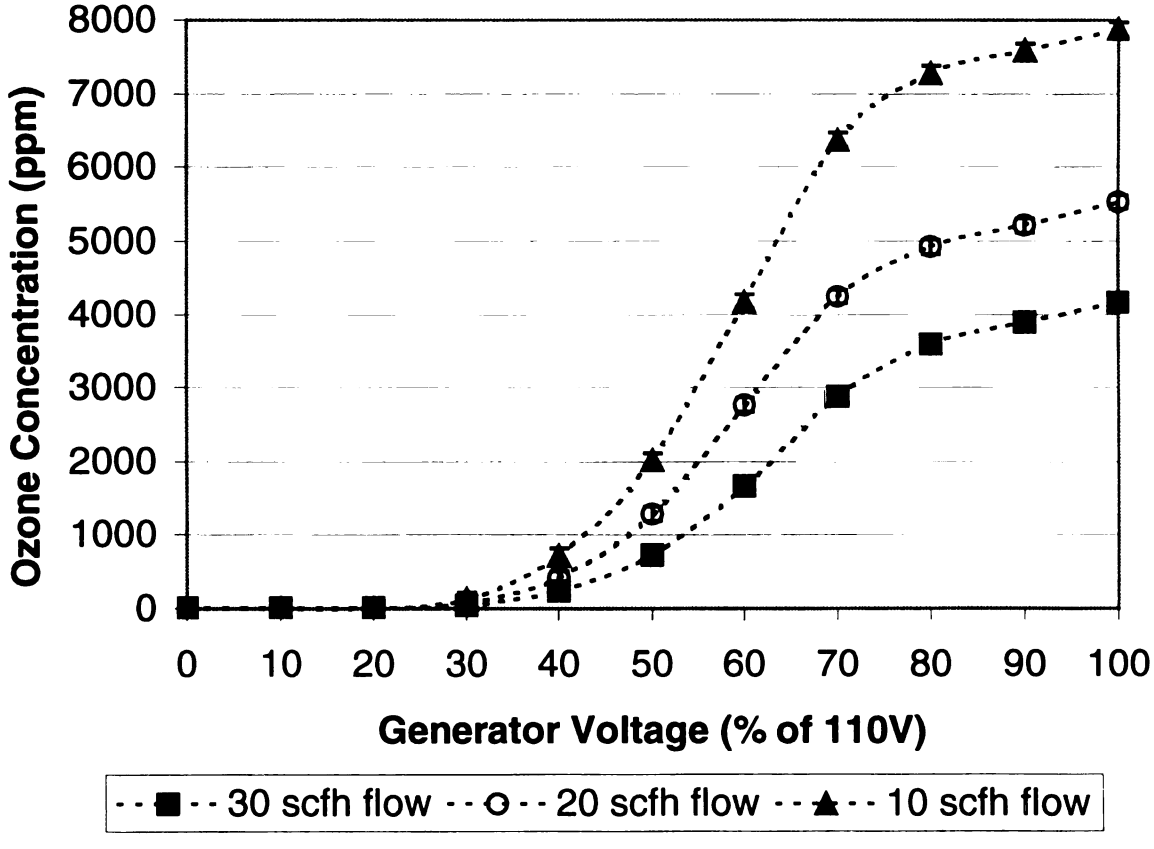

Figure 2.10 Ozone concentration in the UV treatment chamber at different voltages and gas flow rates.

2.4 Surface

Contact ang

When a ses

contracts an

drop makes

angle (θ) as

The contact

Young's Eq

where

γ_{sv} = s

γ_{sl} = i

γ_{lv} = s

θ =

The quant

solid surfa

a solid su

of the so

thermodyn

2.4 Surface Energy Measurement

Contact angles are a thermodynamic measure of the wettability of a solid-liquid system. When a sessile drop of liquid is placed on a solid surface, the drop of liquid spreads or contracts and eventually the solid-liquid-vapor system reaches equilibrium. The angle the drop makes with the solid at the point of contact at equilibrium is termed the contact angle (θ) as shown in Figure 2.11.

The contact angle is related to the surface and interfacial energy of the solid and liquid by Young's Equation [7]:

$$\cos\theta = \frac{\gamma_{SV} - \gamma_{SL}}{\gamma_{LV}} \tag{2.5}$$

where

γ_{SV} = surface tension of the solid in equilibrium with vapor

γ_{SL} = interfacial tension of the solid in equilibrium with liquid

γ_{LV} = surface tension of the liquid in equilibrium with vapor

θ = contact angle in degrees

The quantity (γ_{SV}-γ_{SL}) is the difference in energy between the free solid surface and the solid surface wetted by the liquid. This provides the driving force for the liquid to cover a solid surface. The total energy gained by the system when the liquid covers a unit area of the solid surface is given by the term $\{\gamma_{LV} + (\gamma_{SV}-\gamma_{SL})\}$ which is termed the thermodynamic work of adhesion (W_{SLV}) [7].

adhe

Thus

for a

of 0

liqui

angle

prob

from

to lo

Fig

Young's equation can be expressed in terms of the thermodynamic work of adhesion to give the Young-Dupré equation :

$$w_{SLV} = \gamma_{LV}(1+\cos\theta) \tag{2.6}$$

Thus, contact angles can be used as a measure of the thermodynamic work of adhesion for a given solid-liquid pair. Contact angles can vary from 0° to 180°. For a contact angle of 0°, the liquid is said to spread on the solid. This represents the ideal state where a liquid has complete affinity for the solid surface and covers it spontaneously. For contact angles higher than 90°, the liquid is said to be non-wetting and presents practical problems for adhesion due to incomplete contact between the two phases. It can be seen from Young's equation that an increase in the surface free energy of the solid (γ_{SV}) leads to lower contact angles with the liquid.

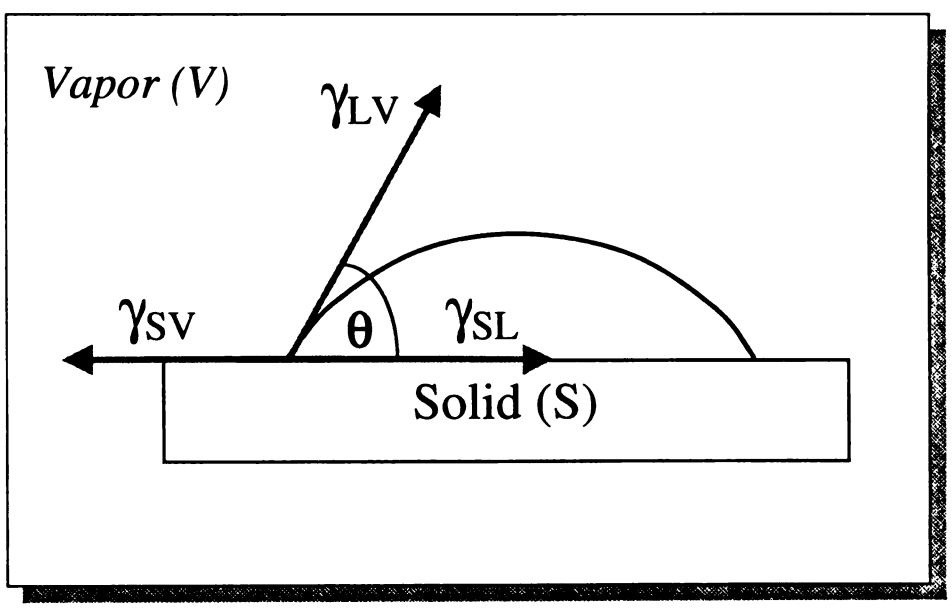

Figure 2.11 Contact angle (θ) at the solid-liquid interface and surface tension.

The surf

interacti

compon

respecti

The inte

two phas

The abov

to the ad

The polar

contact a

This equa

character

componen

polar and

suggested

The surface tension (or surface energy) can be expressed in terms of polar and dispersive interactions. The total surface tension is expressed in terms of dispersive and polar components where superscripts d and p refer to dispersive and polar components respectively :

$$\gamma = \gamma^d + \gamma^p \tag{2.7}$$

The interfacial tension between two phases can be related to the surface tension of the two phases by a geometric mean model [8] :

$$\gamma_{SL} = \gamma_{SV} + \gamma_{LV} - 2\left(\gamma_S^d \gamma_L^d\right)^{1/2} - 2\left(\gamma_S^p \gamma_L^p\right)^{1/2} \tag{2.8}$$

The above relationship can also be expressed in terms of the work of adhesion according to the additive model suggested by Fowkes [9],

$$W_{SL} = \gamma_{LV}(1 + \cos\theta) = W_{SL}^d + W_{SL}^p + \ldots \tag{2.9}$$

The polar-dispersive model in terms of Young's equation gives a relationship between the contact angle and polar-dispersive components of surface tension [24]:

$$\cos\theta = -1 + \frac{2\left(\gamma_S^d \gamma_L^d\right)^{1/2} + 2\left(\gamma_S^p \gamma_L^p\right)^{1/2}}{\gamma_{LV}} \tag{2.10}$$

This equation is significant as it allows the measurement of the polar and dispersive character of the surface. With two or more liquids of known polar and dispersive components of surface tension, contact angle measurements can be used to determine the polar and dispersive interactions of the solid surface. Good and van Oss [10] further suggested that the polar term (γ^p) was not a physically relevant property and the major

co

W

in

Su

the

cor

use

Tab

vari

(App

estim

for a

meth

comb

averag

(Kruss

digitiz

softwa

measur

components of surface energy can be separated into two categories: i) Lifshitz-van der Waals forces (γ^{LW}) and ii) forces from Lewis acid (γ^{+}) and Lewis base (γ^{-}) pair-wise interactions (electron donor and electron acceptor components) [11] such that:

$$W_{SL} = \gamma_{LV}(1+\cos\theta) = W_{SL}^{LW} + W_{SL}^{AB} = 2\left(\sqrt{\gamma_S^{LW}\gamma_L^{LW}} + \sqrt{\gamma_S^{+}\gamma_L^{-}} + \sqrt{\gamma_S^{-}\gamma_L^{+}}\right) \qquad (2.11)$$

Surface treatment of polymers leads to the formation of polar surface functionalities, and the changes in the polar, dispersive, and acid-base interactions can be determined with contact angle measurements with three or more liquids. In this study five liquids were used for surface energy analysis. The liquids used and their surface energies are given in Table 2.3. The use of five liquids provides five simultaneous equations with three variables. The parameters were calculated using a sum of least squares approach (Appendix A), a method analogous to the graphical or linear regression analysis used to estimate polar and dispersive parameters. This has the advantage of finding the best fit for all data in three dimensions. This method is recommended by Good [11] over the method of data reduction involving the calculation of acid-base parameters for multiple combinations of data for three liquids from the set of five liquids and reporting the average of all combinations.

Contact angles were measured on a Kruss Drop Shape Analysis System 10 Mk.2 (Kruss, Germany) shown in Figure 2.12. The instrument has video capture capability to digitize drop shapes. Image analysis was performed using the Drop Shape Analysis software provided with the system. A manual goniometer (Rame-Hart) was also used to measure contact angles.

Table 2.3 Surface energies of liquids used for contact angle measurement.

Liquid	γ_L^{Total}	γ_L^{LW}	$\gamma_L^{(+)}$	$\gamma_L^{(-)}$	γ_L^{D}	γ_L^{P}
Water	72.80	21.80	25.50	25.50	21.80	51.00
Glycerol	64.00	34.00	3.92	57.40	34.00	30.00
Ethylene Glycol	48.00	29.00	1.92	47.00	29.00	19.00
Formamide	58.00	39.00	2.28	39.60	39.00	19.00
Diiodomethane	50.80	50.80	0.00	0.00	50.80	0.00

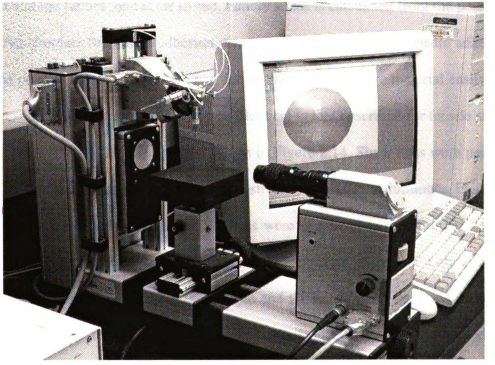

Figure 2.12 Kruss Drop Shape Analysis System.

2.5

Stub-

Pneu

used

surfa

repre

samp

testin

bendi

the a

pressu

very t

tensil

tests b

on a U

and st

failure

cases

failure

strengt

determ

2.5 Adhesion Measurements

Stub-pull tensile tests (ASTM D4541) were used to measure adhesive bond strength. A Pneumatic Adhesion Tensile Testing Instrument (PATTI, M.E. Taylor Engineering) was used to measure the pull-off strength of an aluminum stub adhesively bonded to treated surfaces with a structural epoxy (Araldite 2015, Vantico). Figure 2.13 is a schematic representation of the PATTI test configuration. In the case of thin film or flexible samples, the entire sample is first mounted on a rigid metallic or wooden base prior to testing to prevent sample bending during tensile testing. This is necessary because any bending deformation in the sample can lead to the generation of strong peeling forces at the adhesive interface. Tensile pull-off strength is measured by applying pneumatic pressure and the failure load is measured. Failure stress is calculated from the peak load.

An alternate stub-shear adhesion test was also developed to measure adhesion on very thin polycarbonate films which can detach from the stiff base material easily during tensile testing. The sample configuration is identical to that described for tensile stub-pull tests but the loading is in pure shear as shown in Figure 2.14. Shear tests were performed on a UTS mechanical testing machine with a strain rate of 0.05 inch/minute. Failure load and stress were measured. The tested surfaces were examined to determine the locus of failure. The failure mode can be either interfacial or substrate. Interfacial failure is seen in cases where the interface between the sample and the adhesive is weak, while substrate failure is generally seen when the interfacial adhesion is very high compared to the strength of the bulk substrate. Examination of the failure surfaces by XPS was used to determine the locus of failure.

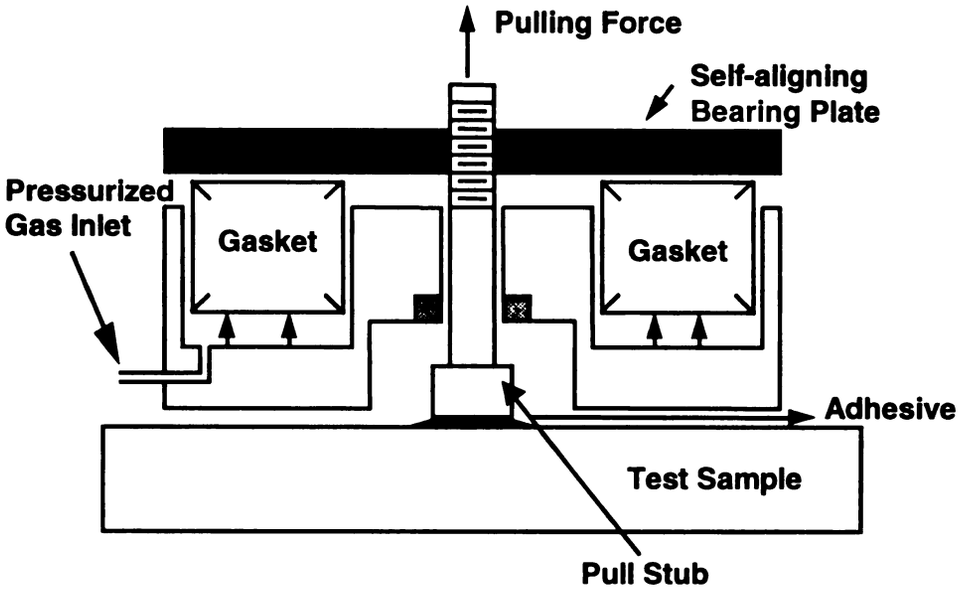

Figure 2.13 Schematic representation of the tensile stub-pull (PATTI) test

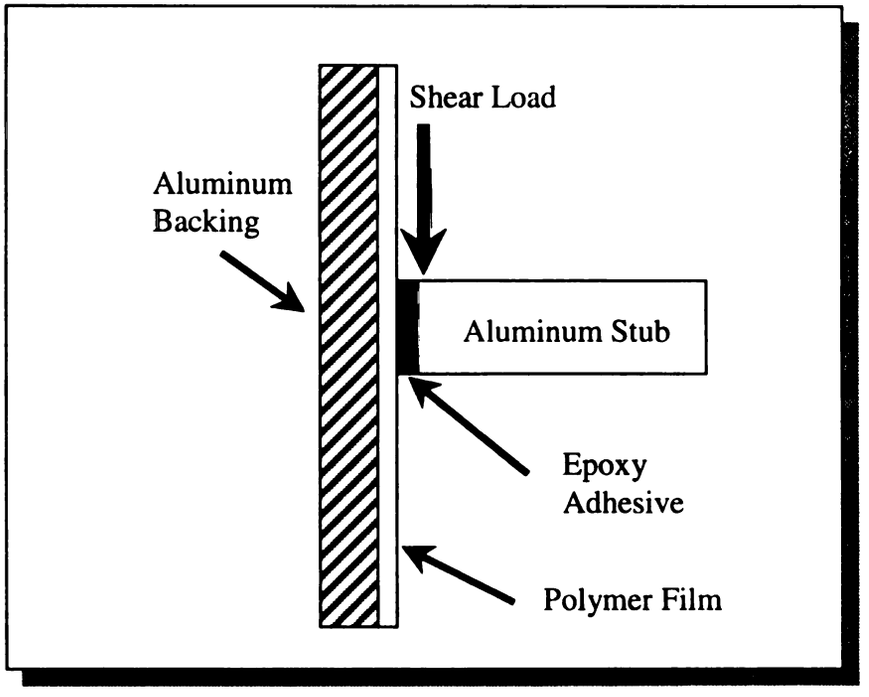

Figure 2.14 Schematic representation of the stub-shear adhesion test

2.6 X-ray Photoelectron Spectroscopy (XPS) Surface Analysis

XPS surface analysis is based on the principle of photoemission of electrons to obtain quantitative and qualitative information about the atomic composition and chemical structure of the surface of a material [12]. Photons from an X-ray source are bombarded onto a surface in an ultra high vacuum environment, causing emission of core and valence photoelectrons which are measured by an analyzer. The process is very surface sensitive because although the absorption depth of the incident X-rays is large, the emitted photoelectrons have a short mean free path and the photoelectrons emitted from the bulk of the material quickly lose their kinetic energy due to inelastic scattering and cannot escape the material. Only electrons near the surface of the material are able to escape and reach the detector. The mean free path of emitted photoelectrons in a solid is given by Equation 2.12.

$$\lambda = \frac{E}{a(\ln E + b)} \tag{2.12}$$

where E is the energy of the incident photon, a and b are parameters related to the concentrations of valence and core electrons in the material. Ninety five percent of the emitted photoelectrons reaching the detector emerge from within a depth of 3λ from the surface. Typically this results in limiting the maximum sampling depth of XPS to 75-100 Å from the surface.

The binding energy (E_B) of a photoemitted electron is given by the following equation.

$$E_B = h\nu - E_K - \phi_{spec} \tag{2.13}$$

where E_K is t

photon, and

emitted elec

energy of th

with variou

composition

spectrum o

The area ur

intensity of

where

I_0 = X-ray fl

η_i = concent

σ_i = photoio

$D(\varepsilon_i)$ = trans

$\lambda_a(\varepsilon_i)$ = mea

It i

concentratio

of two elem

flux is elimi

where E_K is the kinetic energy of the emitted electron, $h\nu$ is the energy of the incident photon, and ϕ_{spec} is the work function of the spectrometer. The kinetic energy of the emitted electron is measured by the analyzer allowing the determination of the binding energy of the electrons. Each element has a unique set of binding energies associated with various electron orbitals which allows accurate determination of the elemental composition of a surface from its XPS spectrum. Figure 2.15 shows the typical XPS spectrum of a polycarbonate film. Peaks for carbon (C1s) and oxygen (O1s) are labeled. The area under the peak is proportional to the atomic concentration of the element. The intensity of the signal for an element *i* (I_i) is given by

$$I_i = I_o \eta_i \sigma_i D(\varepsilon_i) \lambda_i(\varepsilon_i) \tag{2.14}$$

where

I_o = X-ray flux,

η_i = concentration of element *i*,

σ_i = photoionization cross-section of element *i*,

$D(\varepsilon_i)$ = transmission function of the analyzer, and

$\lambda_i(\varepsilon_i)$ = mean free path of the emitted electron.

It is difficult to measure I_o and $D(\varepsilon_i)$ directly hence absolute atomic concentrations are seldom measured by XPS. However, if the relative concentration, C, of two elements (A and B) is calculated using Equation 2.15, the dependence on x-ray flux is eliminated and only the kinetic energy dependence of $D(\varepsilon_i)$ is retained.

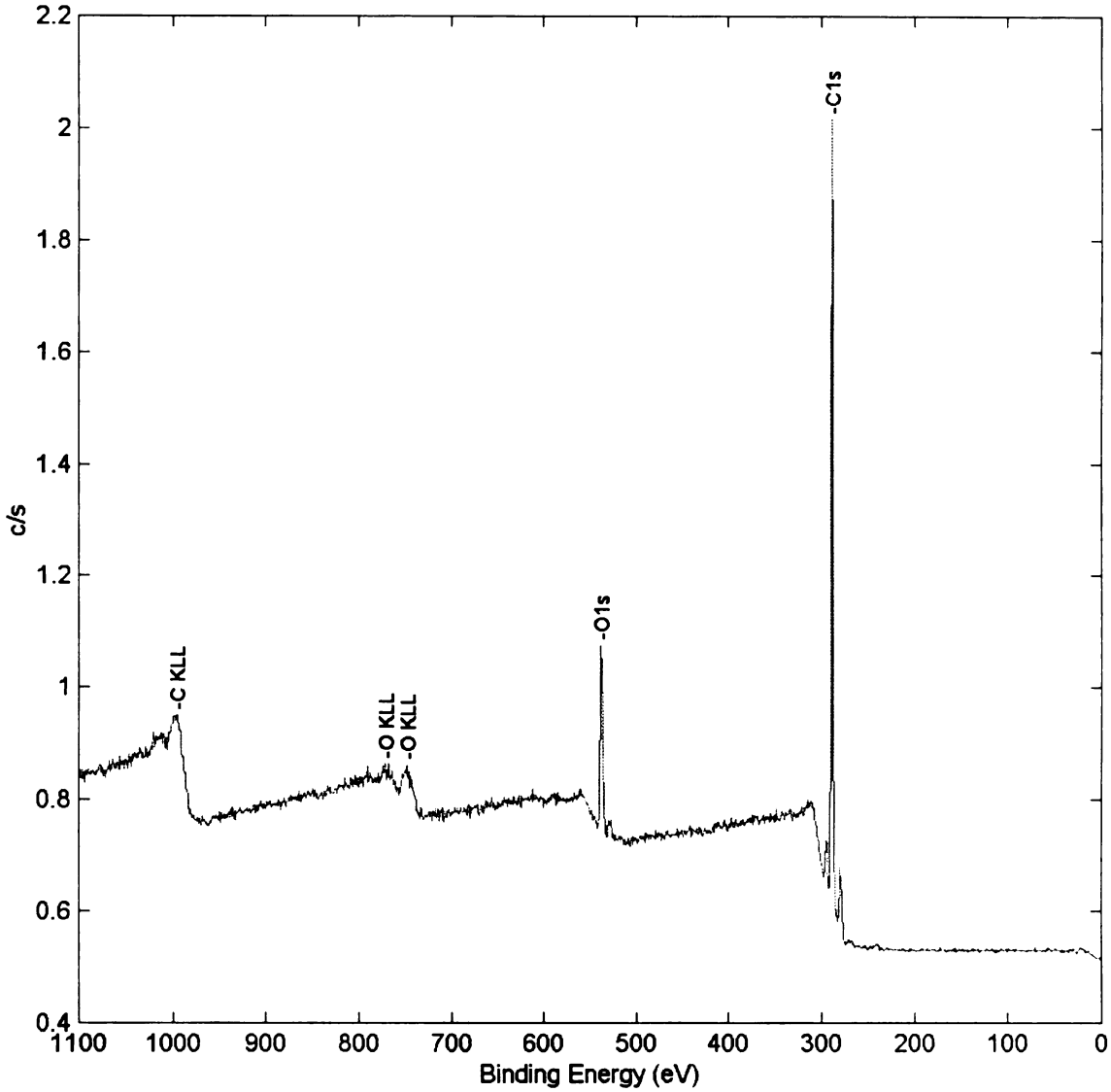

Figure 2.15 XPS survey scan showing elemental carbon and oxygen peaks in polycarbonate.

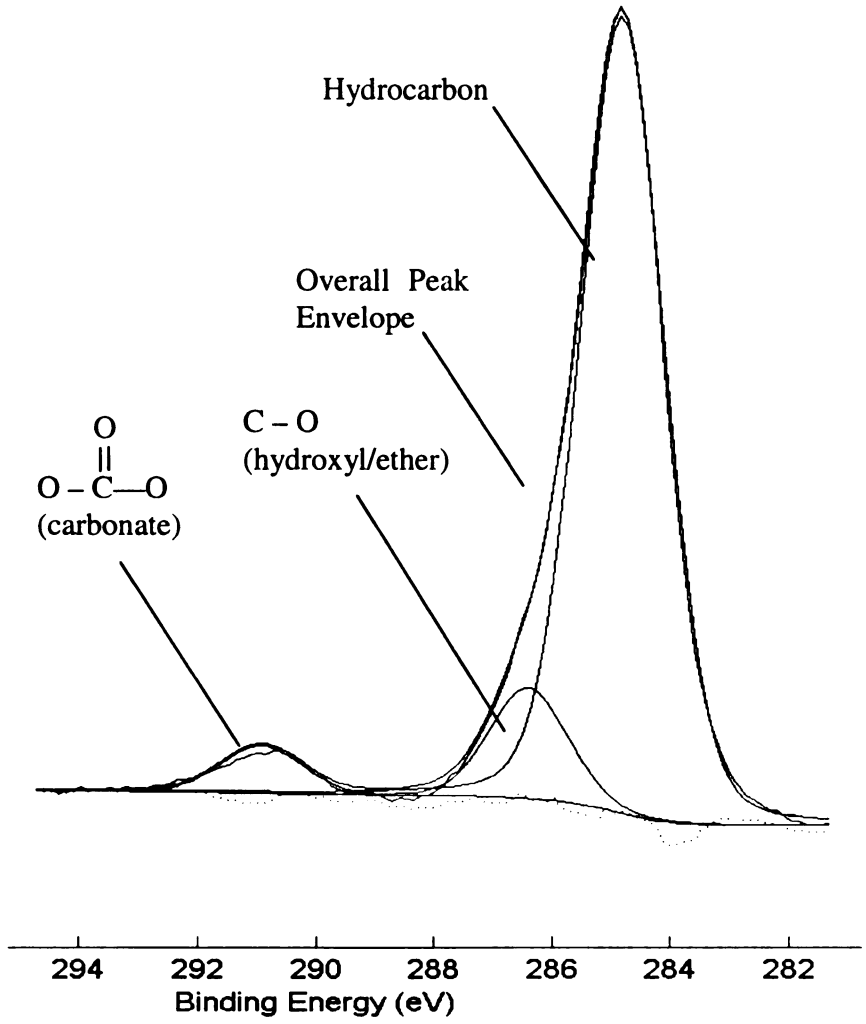

Figure 2.16 Deconvolution of the C1s peak envelope in polycarbonate showing multiple peaks corresponding to carbon atoms with increasing number of bonds with oxygen.

$$\left(\frac{C_A}{C_B}\right) = \frac{I_A}{I_B}\left(\frac{\sigma_B \lambda_B \varepsilon_B^{-0.5}}{\sigma_A \lambda_A \varepsilon_A^{-0.5}}\right) \tag{2.15}$$

The term in the right bracket in Equation 2.15 is called the sensitivity factor of the element. Sensitivity factors can be calculated theoretically using cross-sections determined by Schofield [13] and the mean free paths [14]. The mean free paths are dependent on the material and the ε_i term depends on the instrument. Sensitivity factors can also be determined experimentally by using standard analytical specimen of known compositions. Thus the relative atomic concentrations and atomic ratios can be easily calculated for a given specimen.

Information about the chemical environment of the atom can also be determined by XPS. As the electronegativity of the neighbouring atoms increases, electrons in the analyzed orbital are more tightly bound and the binding energy increases. This is seen as a shift in the peak position in the XPS spectra. In most materials, where various chemical states of the same element exist, a series of peaks are obtained for an orbital. Figure 2.16 shows the peak for the carbon 1s orbital (C1s) for polycarbonate. Polycarbonate has carbon atoms in three different bonding states with carbon-carbon bonds (C-C, C=C), carbon bonded to a single oxygen atom (C-O), and the carbon atom in the carbonate linkage with four bonds with oxygen atoms (O-CO-O). As the number of electrons shared with oxygen increases, the binding energy of the C1s orbital increases by ca. 1.5 eV per bond [15]. Figure 2.16 shows the overall C1s peak envelope and the deconvoluted Gaussian-Lorentzian statistical fit showing the constituent peaks. The areas of these

peaks are proportional to the number of atoms in that particular bonding state. This allows indirect determination of the chemical structure of the material surface.

A Perkin Elmer Phi 5400 ESCA system was used for experimentation with a Magnesium Kα x-ray source. Samples were analyzed at pressures between 10^{-9} and 10^{-8} torr with a pass energy of 29.35 eV and 45° take-off angle unless stated otherwise.

2.7 Nanoindentation Tests

Nanoindentation tests were developed for the purpose of probing the mechanical properties of very small volumes of materials. It is an ideal technique for the characterization of thin films, coatings, and surface layers. The advantage of nanoindentation tests is that material properties in the top 1-2 μm of the substrate can be measured as a function of depth. A MTS Nanoindenter (MTS Systems Corp.) was used to probe the elastic modulus (E) and hardness (H) of UV treated surfaces.

A nanoindentation test consists of three main steps. An indenter is pushed into the material surface causing elastic and plastic deformation in the material up to a pre-determined contact depth, h_c. The indenter is held at the indentation depth for a period of time with a constant indenter load. The indenter is subsequently withdrawn and the elastic deformation in the material is recovered. It is the elastic recovery which allows the determination of the elastic properties of the surface layers.

Figure 2.17 shows a typical loading and unloading cycle in the nanoindenter. The important quantities are the peak load and displacement (P_{max} and h_{max}), the residual depth after unloading (h_f), and the slope of the initial portion of the unloading curve (S)

also known as the elastic stiffness of contact. The hardness of the test surface (H) is determined by equation 2.16 [16].

$$H = \frac{P}{A} \tag{2.16}$$

where P is the applied load and A is the projected contact area at that load. The elastic modulus of the surface is determined from the reduced modulus (E_r):

$$E_r = \frac{\left(\sqrt{\pi} \bullet S\right)}{2\beta\sqrt{A}} \tag{2.17}$$

where b is a constant depending on the geometry of the indenter. The elastic modulus of the material surface (E_S) is calculated using the expression:

$$\frac{1}{E_r} = \frac{\left(1-\nu_s^2\right)}{E_s} + \frac{\left(1-\nu_i^2\right)}{E_i} \tag{2.18}$$

where E_i and ν_i are the elastic modulus and Poisson's ratio of the indenter and ν_S is the Poisson's ratio of the test material. The indenter used for testing was a diamond Berkovich pyramidal tip with β = 1.034, E_i = 1141 GPa, and Poisson's ratio = 0.07. Poisson's ratios for most polymers range between 0.25 and 0.35.

For testing of polymers, which can exhibit large plastic deformations, a series of 36 indents were made in a 6 x 6 matrix with horizontal and vertical spacing of 50 μm between indents. Indents were made to a depth of 2 μm. For UV treated polycarbonate, significant changes in modulus were observed in the first 500 nm of the surface.

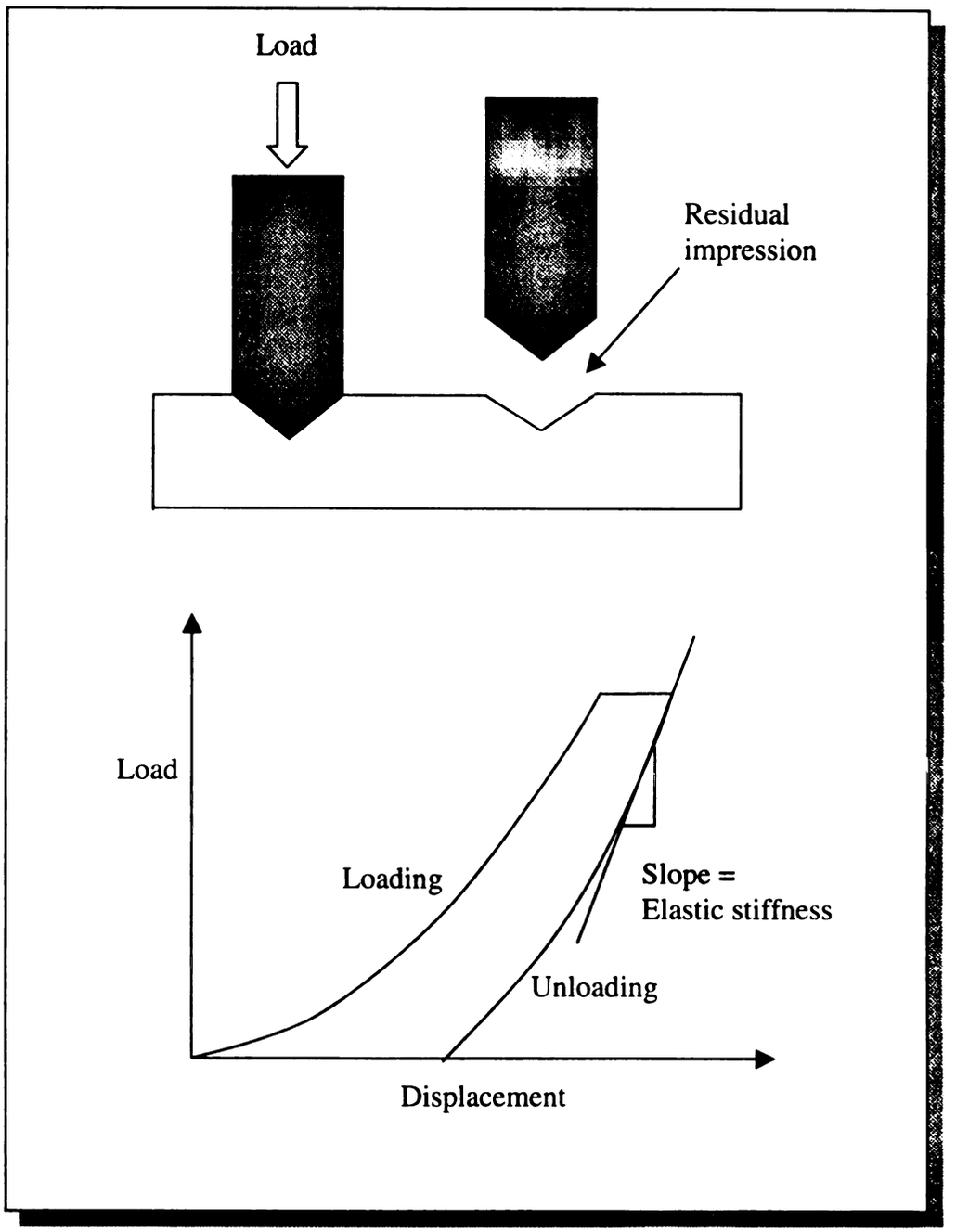

Figure 2.17 Typical nanoindentation load displacement curve showing loading and unloading behavior.

2.8 Summary

The UV lamps used for surface treatment of polymers in this study and the measurement of their output has been discussed in this chapter. Insufficient characterization of the lamp outputs in many published works in the area of UV surface treatment has limited a thorough characterization of the process in the past. The biggest advantage of UV surface treatment is that the process can be run under ambient conditions. However, ambient conditions present severe problems for measurement of lamp output, especially in the UV-C region, because of the absorption of radiation by air. The use of vacuum or noble gas purges during radiation measurement is also not ideal because the measured irradiances can be very different from the irradiance received by samples under treatment conditions where oxygen and ozone are both present in relatively high local concentrations. The difference in irradiance under oxygen and ozone purge in the sample chamber for identical lamp configurations is significant. Using the output at a single wavelength (254 nm) to draw conclusions about the entire spectral output of the lamp is a simplification, but in the absence of a full spectrum NIST calibration standard UV lamp, it is a reasonable strategy which can be used to make relative comparisons between different process conditions.

In addition to the experimental methods described in this chapter, UV treated polycarbonate was also characterized by attenuated total reflection Fourier transform infrared spectroscopy (ATR-FTIR), UV spectroscopy, and electron paramagnetic resonance spectroscopy (EPR) to examine the changes occurring on the surface due to UV oxidation. These techniques will be discussed briefly in later chapters.

References

1. Rabek, J.F. *Experimental Methods in Photochemistry and Photophysics Part 1*, Wiley-Interscience, New York, 1982.

2. Walzak, M.J.; Flynn, S.; Foerch, R.; Hill, J.M.; Karbashewski, E.; Lin, A.; Strobel, M. *Polymer Surface Modification; Relevance to Adhesion*, K.L. Mittal (Ed.), pp. 253-272, 1995.

3. Lothian G., *Absorption Spectrophotometry*, 3rd Ed., pp. 101, Hilger, London, 1969.

4. Jaffe H. and Orchin M., *Theory and Applications of Ultraviolet Spectroscopy*, pp.8-10, Wiley, New York, 1962.

5. ASTM D5110-94.

6. Watanabe, F.; Shimomura, O.; *Journal of Hygienic Chemistry*, Vol. 37, No. 5, pp. 323-331, 1991.

7. Adamson, A.W. *Physical Chemistry of Surfaces*, 5th ed., Wiley Interscience, New York, 1990.

8. Kaelble, D.H.; Uy, K.C. *J. Adhesion*, Vol.2, p.50, 1970.

9. Fowkes, F.M.; McCarthy, D.C.; Mostafa, M.A. *J. Colloid Interface Sci.*, Vol. 78, p. 200, 1980.

10. VanOss, C.J.; Good, R.J.; Chaudhury, M.K. *J. Colloid Interface Sci.*, Vol. 111, p. 378, 1986.

11. Good, R.J. *J. Adhesion Sci. Technol.*, Vol. 6, No. 12, pp. 1269-1302, 1992.

12. Vickerman, J.C. *Surface Analysis – The Principal Techniques*, Wiley, UK, 2000.

13. Scofield, J.H. *J. Electron Spect.:Relat. Phenom.*, Vol. 8, p. 129, 1979.

14. Seah, M.P.; Dench, W.A. *Surf. Interface Anal.*, Vol. 1, p. 2, 1979.

15. Briggs D.; Seah, M.P. *Practical Surface Analysis*, Wiley, New York, 1983.

16. MTS Systems Corp, *Nanoindenter XP user guide*.

CHAPTER THREE

SURFACE MODIFICATION OF POLYCARBONATE

3.1 Description of Polycarbonate

The polymer chosen for this study was a commercial grade bisphenol-A based polycarbonate (GE Plastics, GE8040). The material is available as an extruded film of 175 μm thickness and is packaged with a protective polymer (polyolefinic) film on both sides. One of the protective films adheres to the polycarbonate (PC) film by electrostatic attraction while the film on the other side of the polycarbonate adheres with a pressure sensitive adhesive. Although XPS analysis of the side protected by pressure sensitive adhesive film did not show any evidence of transfer of the adhesive to the polycarbonate film, only the side protected by the electrostatically attached film was used in all experiments to avoid the possibility of artifacts. Figure 3.1 shows the chemical structure of bisphenol-A polycarbonate [1]. The molecular weight of the polycarbonate used is ca. 20,000 Dalton. This chapter describes the changes occurring on the polycarbonate surface as a result of UV induced oxidation.

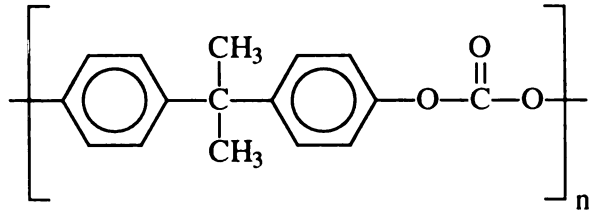

Figure 3.1 Chemical structure of polycarbonate

3.2 Process Parameters

UV/Ozone (UVO) surface treatment depends on a variety of process variables including: irradiance, exposure time, ozone concentration, temperature, and humidity. In addition, the changes occurring on the surface are strongly dependent on external mass transfer, nature and surface chemistry of the substrate, and surface chemical reactions on the surface. Understanding the process involves a systematic study of these process parameters. In this section, results of studies on the effects of mass transfer, ozone concentration, irradiance, and exposure time will be presented. The effect of various process variables was determined by contact angle measurements which are known to be sensitive to monolayer level changes in surface chemistry and topography and are relatable to adhesion.

3.2.1 Flow Rate

The reaction of ozone with the UV irradiated surfaces is a gas-solid reaction and the overall rate of reaction depends on the relative rates of the surface chemical reaction, and the mass transfer of reactive species to the surface. The slowest step in the process is the rate determining step and for a given chemical reaction, the rate constants cannot be changed easily. The external mass transfer in a gas-solid surface reaction, a measure of the ability to transport reactants to the reaction sites on the surface, is a more easily modified parameter. If the system is mass transfer limited then the overall rate of the reaction is dependent on the mass transfer coefficient and an increase in mass transfer results in an increase in the total reaction rate to the limit allowed by the reaction kinetics. To determine if mass transfer limitations existed in the experimental setup, contact angles

were measured on samples treated at different flow rates. Flow rates of 10, 20 and 30 scfh (standard cubic feet per hour) were used while keeping the ozone concentration and UV treatment time constant. When the flow rate is decreased, the gas velocity decreases and the mass transfer coefficient decreases. Any mass transfer limitation in this case would be seen as a reduction in the treatment efficiency and higher than normal contact angles for a set of given treatment conditions as the transport of ozone to the surface is hindered by the slow flow rate.

Figure 3.2 shows the variation of contact angles as the flow rate is changed by a factor of three for treatment times ranging from 0 to 90 seconds UV exposure. The contact angles for untreated polycarbonate were found to be approximately 90°. After UVO oxidation, the contact angles decrease sharply for treatments as short as 10 seconds. As the treatment time is increased, the rate of change of contact angles decreases and angles of less than 20° are obtained after treatments of 90 to 120 seconds. Further changes in contact angles are difficult to measure accurately. Contact angles measured for treatments at all three flow rates were found to be identical within the limits of experimental error and leads to the conclusion that no mass transfer limitation is present when flow rates on the order of 10-30 scfh are used. All further experiments in this chapter were performed at a flow rate of 30 scfh to ensure no external mass transfer limitations were present.

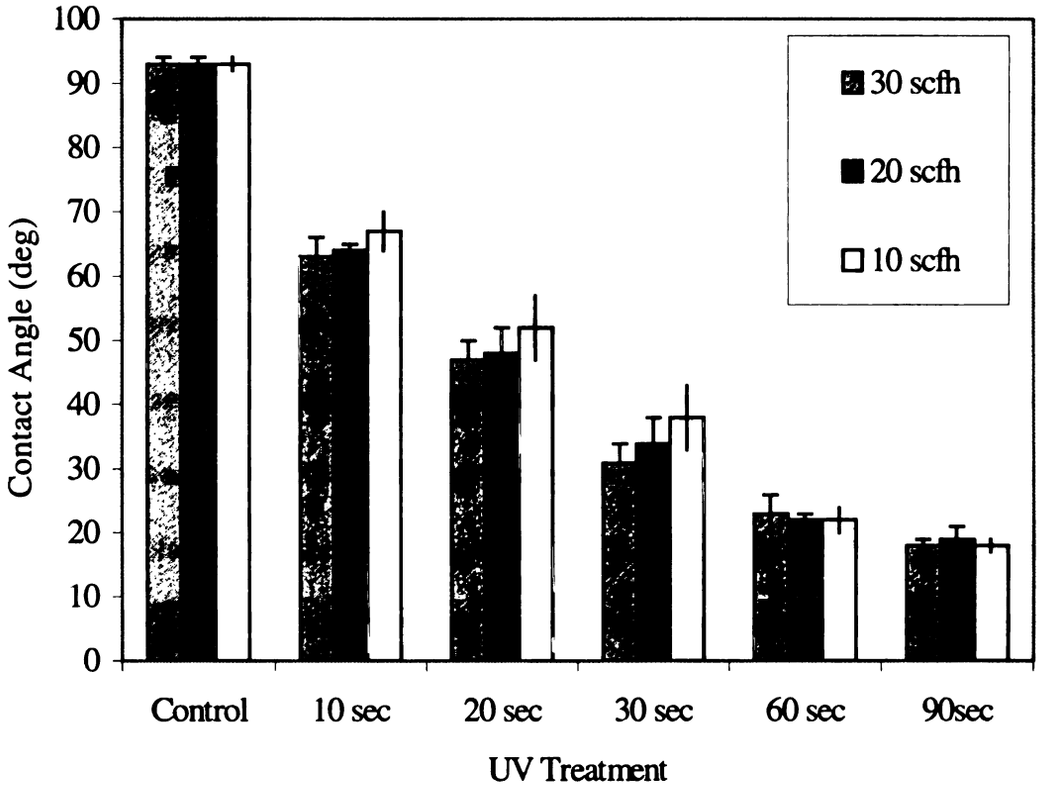

Figure 3.2 Contact angles of UV treated PC for ozone flow rates of 10, 20, and 30 scfh indicating no mass transfer limitations

3.2.2 Ozone Concentration

The Ozone concentration is a potentially important process variable. Depending on the kinetics of the surface reaction between ozone and the UV treated surface, the reaction can be strongly dependent on the concentration of ozone on the surface. To determine the influence of ozone concentration on the UV treatment process, polycarbonate samples were treated at various ozone concentrations at identical operating conditions of irradiance and exposure time. Sessile drop equilibrium contact angles were measured at various locations on multiple samples as shown in Figure 3.3.

It was found that ozone was necessary for UV treatment, but the concentration of ozone did not have any effect on the quality of treatment achieved. Without additional ozone, contact angles between 70-80° were measured for most samples after a 30 second UV exposure. With 400 to 800 ppm ozone in the treatment chamber, contact angles of 30° were obtained for the same exposure. With decreasing ozone concentration, the data shows a large amount of scatter in the individual measurements. However, the lowest value of contact angles measured (shown by horizontal line) was ca. 30° for all samples irrespective of the ozone concentration. This was observed to be true even at the lower limit (ca. 10 ppm) of our capability to measure ozone concentration accurately. In terms of process parameters, UV treatment of PC can be considered to be independent of ozone concentration because, for a surface reaction, ideally only a small amount of ozone is needed to form a monolayer and obtain full surface coverage. The scatter in data at low ozone concentrations is suggested to be a result of poor sample coverage, starvation of ozone near some parts of the sample due to inadequate mixing of ozone in the treatment chamber, or non-uniform air flow patterns and channeling in the UV treatment chamber.

At high concentrations, the mixing and diffusion rate of ozone inside the UV treatment chamber is increased and the scatter decreases. This is likely an artifact of the treatment chamber design and not the process itself. To avoid data scatter, ozone concentrations in the range of 700-800 ppm were used for all experimentation and generally very low errors in measured contact angles were observed at this concentration.

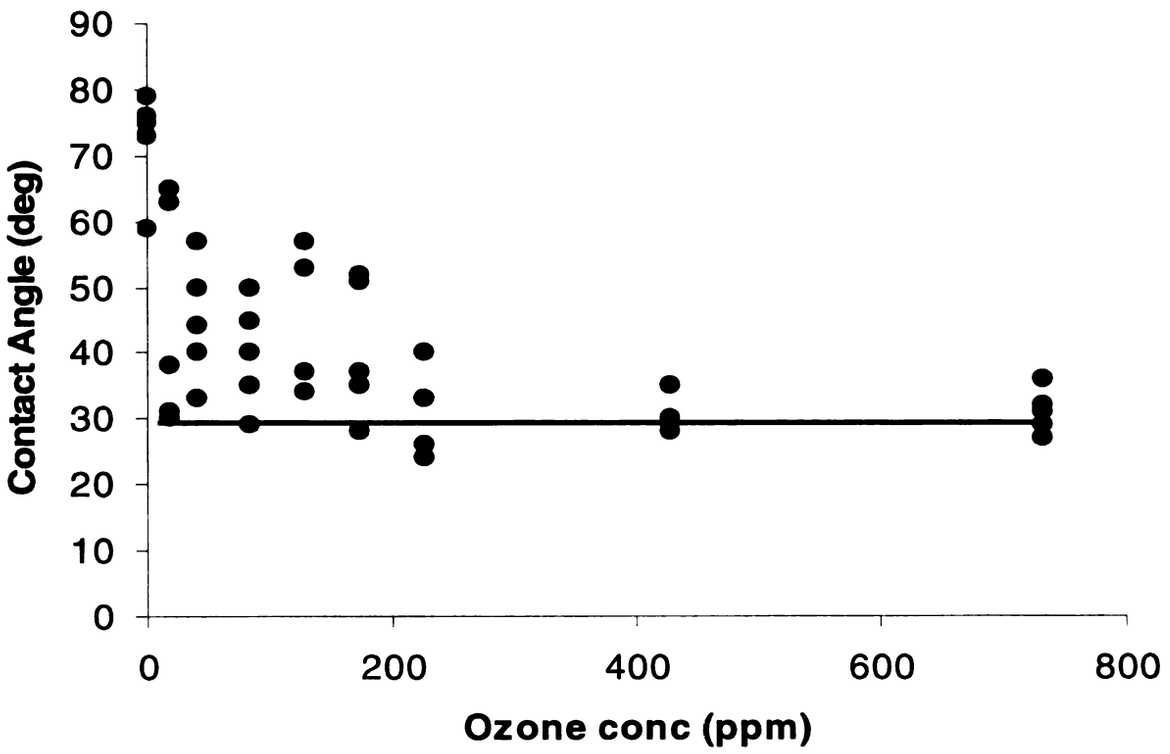

Figure 3.3 Contact angles of PC after 30 sec UVO treatment as a function of ozone concentration. Horizontal line indicates the lowest angles measured at the lower limit of measured ozone concentrations.

3.2.3 Irradiance

Irradiance is the most important variable in the UV treatment process. The irradiance received by the sample determines the extent of modification possible on the surface. As described in the previous chapter, irradiance levels were measured and varied by controlling the distance between the lamp and sample (however, the path length of ozone the radiation travels through remains constant). Polycarbonate film was exposed to UV radiation from the RC-747 lamp at distances ranging from 1 to 5 inches in the presence of approximately 700 to 800 ppm supplemental ozone concentration and a flow rate of 30 scfh. Contact angles of the UV modified surfaces with deionized water are shown in Figure 3.4.

As the treatment time is increased, a reduction in contact angles is observed till the contact angles reach 20° and further reduction in contact angles is difficult to measure accurately as the liquid spreads on the surface. At treatment distances over 3 inches (irradiance < 2.6 mJ/m^2) the rate of change of contact angles is almost linear. As the treatment distance is decreased, the increase in irradiance causes the rate of change to be increasingly non-linear. It is of particular interest to relate the rate of change of contact angles with an absolute process parameter such as UV irradiance. From observations of the trends in contact angles, it was found that it is possible to super-position the work of adhesion curves for different combinations of irradiance and exposure time. This is similar to the concept of time-temperature super-positioning in polymer creep properties [2]. The time-irradiance superpositioning of the thermodynamic work of adhesion (proportional to the cosine of the contact angle) can be expressed as a function of the total irradiation incident on the surface. Figure 3.4 shows the work of adhesion for deionized

water on UV treated polycarbonate treated at various combinations of distances and UV exposure times. The irradiance was varied by a factor of five and exposure times of 20 to 150 seconds were used to generate work of adhesion data. All of the data in Figure 3.4 can be reduced to a universal curve shown in Figure 3.5. To test the robustness of this assumption, work of adhesion data was also collected using the low power RC-500 lamp to create irradiance levels differing by almost an order of magnitude compared to the RC-747 lamp. The data from both lamps follow the universal wettability curve for polycarbonate shown in Figure 3.5. This trend was seen to exist in other polymers as well and will be discussed in Chapter 5.

The construction of a universal curve for the change in wettability as a function of irradiation is significant in terms of developing a process model. One of the implications is that time ceases to be a controlling variable in the UV treatment process and a specific targetted level of wettability can be achieved by a variety of combinations of irradiance and time. Short treatments at high irradiances, and long treatments at low irradiances can yield the same work of adhesion. However, there can be qualitative differences between treatments at high and low irradiances. Surface modification by UV depends on the ability of chromophores in the material to absorb radiation, which is necessary to start a chain of complex reactions. Absorption in the material follows Beer's law [3] and the intensity of radiation at any point in the thickness of the material depends on the intensity of the incident radiation. Consequently, as irrandiance levels are increased to reduce exposure times, the depth at which chemical changes occur in the material can potentially increase and vice-versa. The penetration depth of radiation can thus become an important consideration in choosing combinations of irradiance and time to suit a given application.

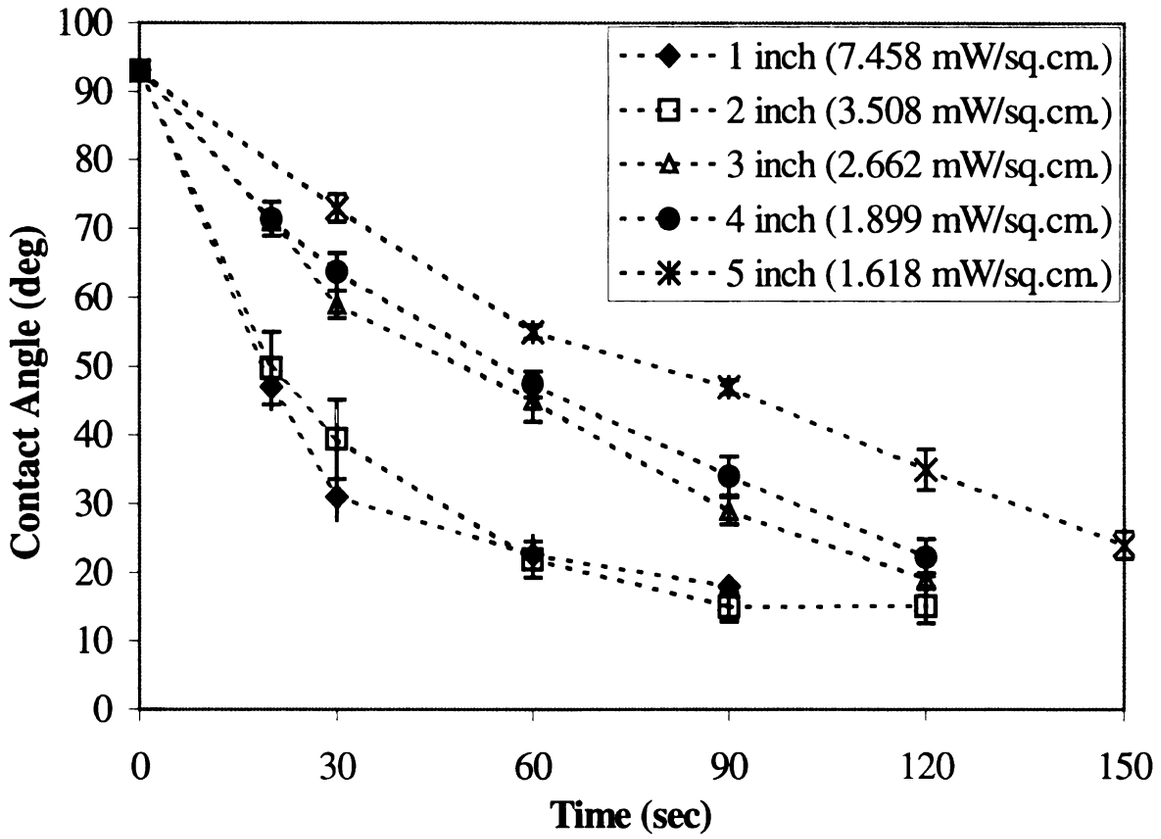

Figure 3.4 Equilibrium contact angles of deionized water on UV treated polycarbonate as a function of time at 1 to 5 inches from the UV source.

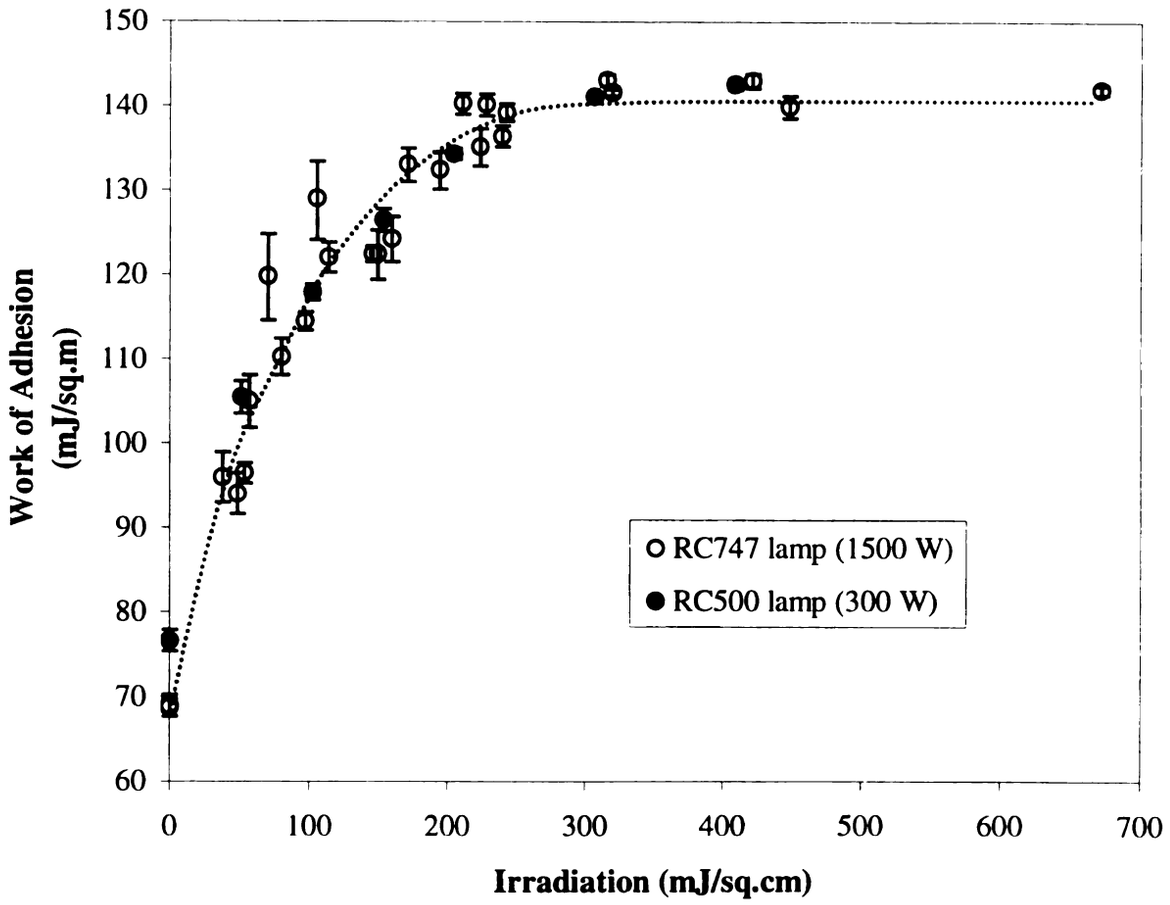

Figure 3.5 Work of adhesion of UV treated polycarbonate with deionized water as a function of irradiation for data obtained at various combinations of irradiant powers and exposure times for multiple lamps.

3.3 Wettability and Surface Energy

Contact angles were measured with five liquids of varying acid-base and polar-dispersive character to calculate the surface energy of modified polycarbonate using acid-base and polar-dispersive models [4]. As polar oxygen containing functional groups are incorporated on the polymer surface, the wettability and surface energy increases. The previous section showed the dependence of the change in wettability on the irradiation received by the polymer. The surface energy after UV treatment also exhibits an identical trend. Samples exposed to the same levels of irradiation had the same surface energy and polarity regardless of the level of irradiance and exposure time.

The change in the polar-dispersive components of surface energy for UVO treated polycarbonate is shown in Figure 3.6. The untreated polycarbonate has a total surface energy of 38.6 mJ/m^2. Most of the surface energy is due to dispersive interactions and only a small polar component of 0.2 mJ/m^2 was measured. After UVO treatment the dispersive van der Waals interactions remain almost constant while a sharp, linear increase in the polar component is observed as a function of irradiation. The total surface energy increases to over 60 mJ/m^2 after irradiation of 300 mJ/cm^2 in ozone.

Similar trends are seen from results of the acid-base analysis shown in Figure 3.7. The surface energy increases from approximately 38 mJ/m^2 to approximately 55 mJ/m^2 after UVO treatment. The Lifshitz-van der Waals (39-41 mJ/m^2) and acid (0.5-1 mJ/m^2) contributions remain constant and most of the increase in surface energy is from a sharp increase in the basic component from 2 mJ/m^2 to 60 mJ/m^2. The increase in the basic character is due to the addition of hydroxyl, carbonyl, and carboxylate functional groups on the surface.

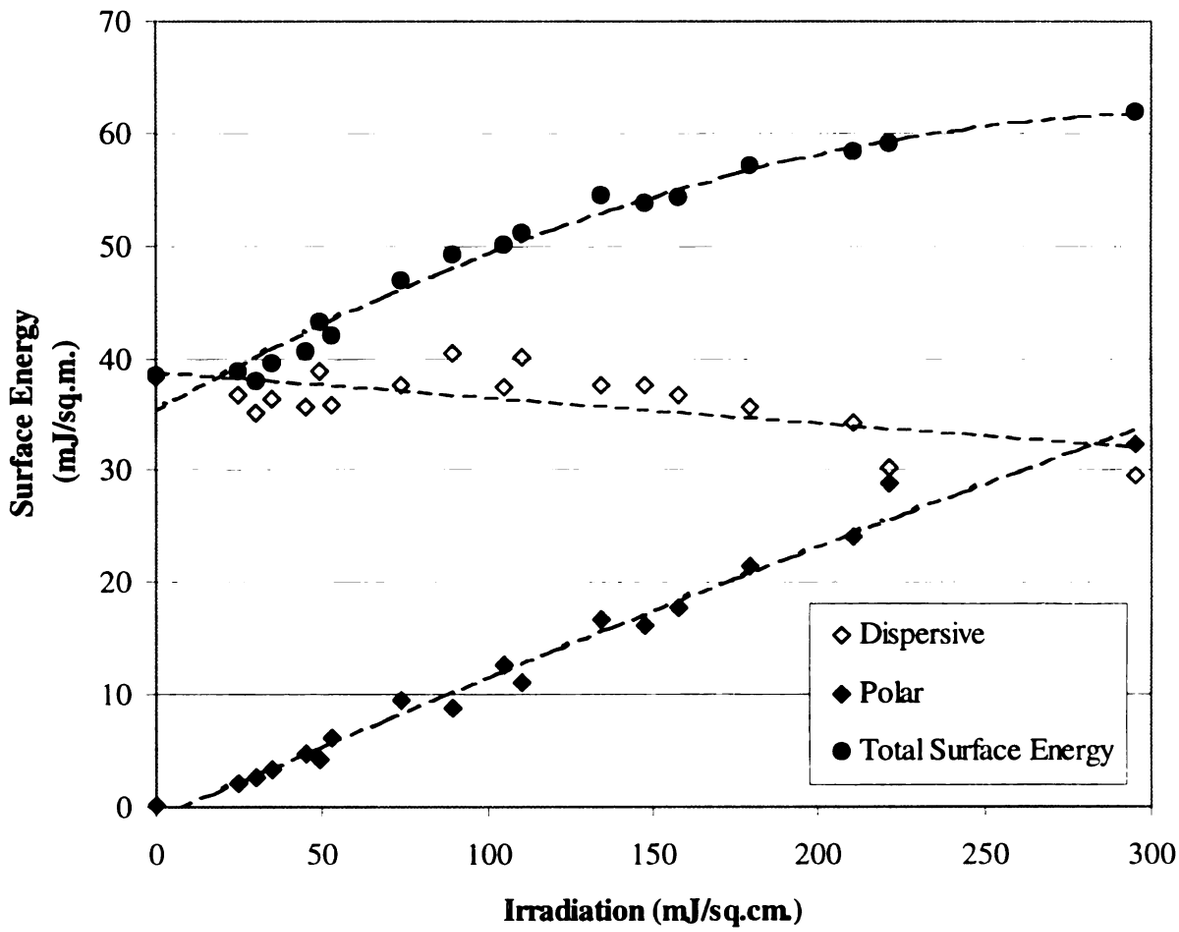

Figure 3.6 Polar-Dispersive surface energy of UV treated polycarbonate for various combinations of irradiance and exposure time.

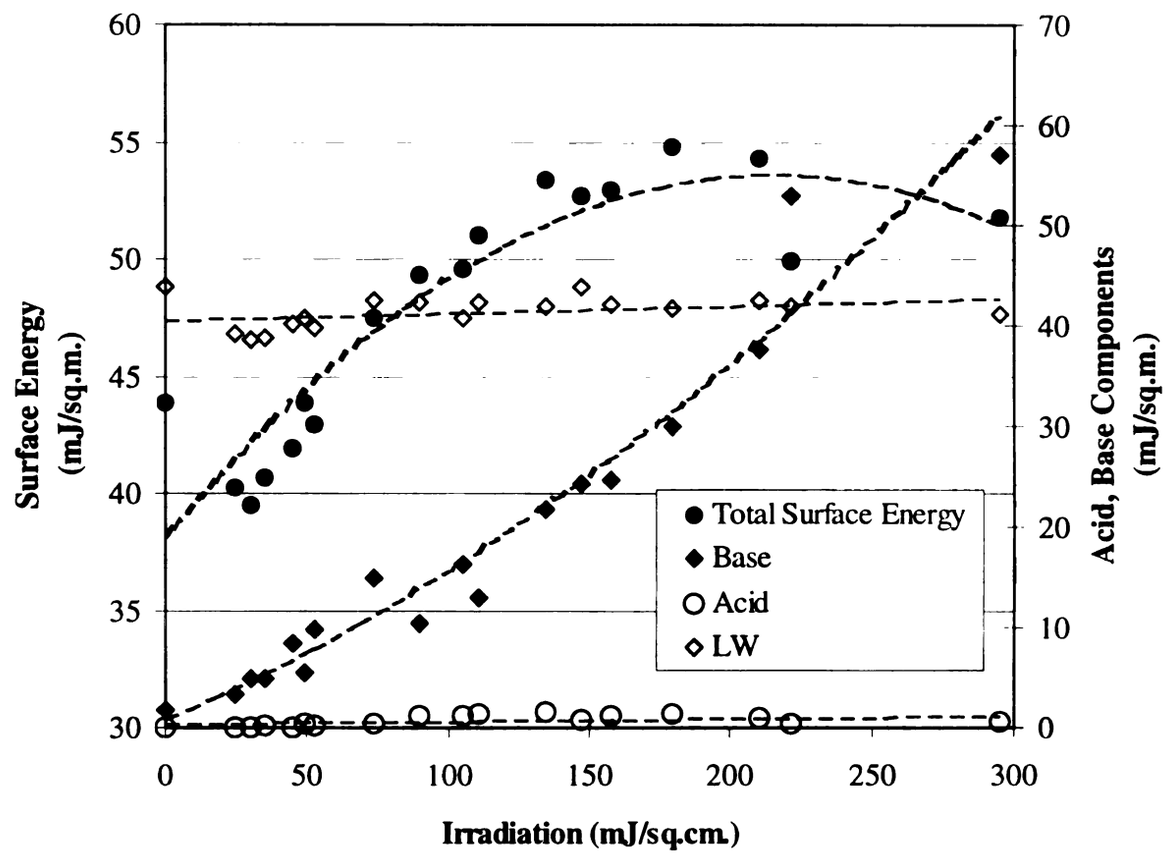

Figure 3.7 Acid-Base surface energy of UV treated polycarbonate for various combinations of irradiance and exposure time.

3.4 Molecular Spectroscopy

Chemical changes occurring in polycarbonate because of UV oxidation were investigated by ATR-FTIR and UV spectroscopy. The two techniques are capable of providing molecular information [5,6], but suffer from a lack of surface selectivity. ATR-FTIR is more surface selective than transmission FTIR, but the sampling depth is on the order of several hundred nanometers and resembles a bulk spectroscopic method in the context of probing changes in surface properties which may be limited to the top few hundred Angstroms of the material. However, changes in chemistry were observed and are presented here.

3.4.1 ATR-FTIR Spectroscopy

Polycarbonate films were UV treated and analyzed by ATR-FTIR. Thin film samples of PC spin-coated on KBr pellets were also evaluated for use in transmission FTIR, but it was observed that UVO treatment of the films caused changes in the KBr baseline, invalidating any further analysis. ATR-FTIR spectrum of PC is characterized by characteristic absorption peaks at 1770 cm^{-1} (C=O, carbonate stretch), 1620 cm^{-1} and 1500 cm^{-1} (C=C, benzene ring stretch), 1250 cm^{-1} (O-C-O carbonate asymmetrical stretch), and 830 cm^{-1} (C-H, benzene out of plane bending) [7]. Figure 3.8 shows the ATR-FTIR spectra for untreated, 90 sec UVO, and 180 sec UVO treated PC. The spectra could not be normalized with respect to each other because of the lack of a stable reference peak. The structural changes caused by UV oxidation are broad and it is suggested that both bisphenol-A and carbonate linkages in PC are subject to UV oxidative attack. The major features observed after surface modification include the

appearance of a broad hydroxyl peak between 3500 cm^{-1} and 3100 cm^{-1} after UV exposure and the broadening of the carbonate peak at 1700 cm^{-1}. The broadening of the carbonate peak and the appearance of a shoulder at 1690 cm^{-1} are indicative of scission of the carbonate group and the addition of substituents to the aromatic structures, including rearrangement to form phenyl salicylates according to the mechanisms proposed in literature for photo-Fries rearrangement of PC and the associated oxidative pathways previously described in Chapter 1 [8]. Evidence is obtained from the relative intensities of the carbonate peak at 1770 cm-1 and the aromatic peak at 1500 cm^{-1} shown in Table 3.1 where the intensity of the carbonate peak decreases and the intensity of the broad hydroxyl peak increases compared to the aromatic phenyl peak.

Table 3.1 ATR-FTIR peak ratios of carbonate, hydroxyl, and aromatic structures in PC after UVO treatment.

Treatment	Ratio of peak intensities at 1770 cm^{-1} and 1500 cm^{-1} (Carbonate/Aromatic)	Ratio of peak intensities at 3460 cm^{-1} and 1500 cm^{-1} (Hydroxyl/Aromatic)
Untreated	1.64	0.04
90 sec UVO	1.40	0.13
180 sec UVO	1.36	0.15

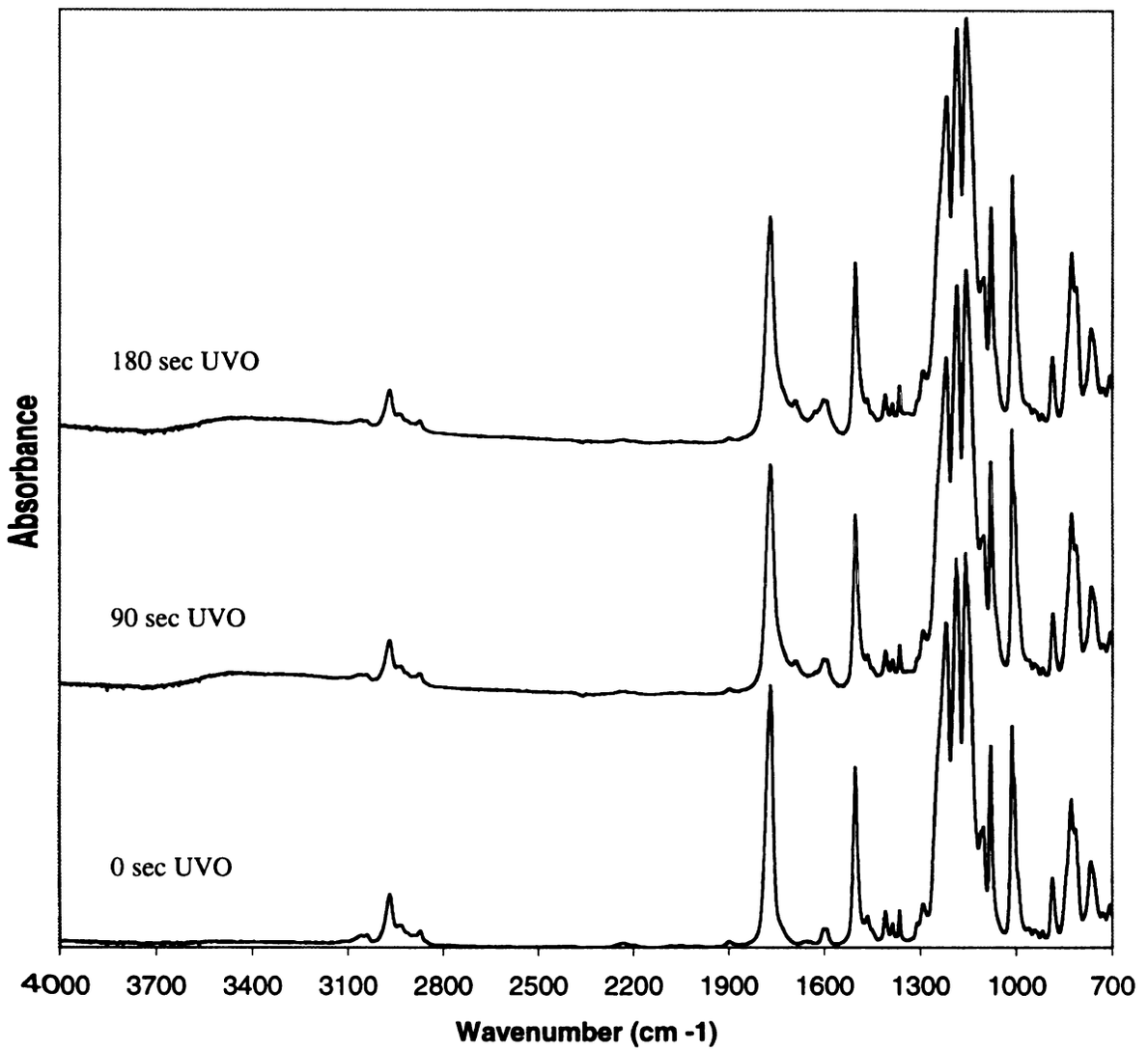

Figure 3.8 ATR-FTIR spectra of PC after UV treatment at 2.662 mJ/m^2 irradiance and 700 ppm ozone

3.4.2 UV Spectroscopy

Polycarbonate samples were spincoated on quartz slides using tetrahydrofuran (THF) as solvent and analyzed by transmission UV spectroscopy. Figure 3.9 shows the UV spectra for untreated, UVA and UVO modified PC. The untreated samples have a flat absorption profile till 280 nm and peaks characteristic of phenyl groups in the bisphenol-A structure are seen in the 260-280 nm range. After exposure to UV in air and ozone, broad peaks are formed in the 280-380 nm region and peaks in the 260-280 nm region increase in intensity. The spectra of UV treated PC are similar to those reported in literature for the degradation of polycarbonate by photo-Fries rearrangement and chain scission [9-12]. The increase in intensity at 245 nm and 315 nm is attributed to the formation of phenyl salicylate while the set of peaks between 260 – 280 nm indicate the formation of phenols as the carbonate linkages are cleaved by UV radiation. The higher amount of ozone present in UVO treatment compared to UVA treatment results in a slight reduction in the intensity of peaks of the degradation products indicating further oxidation of the phenolic end-products of UV degradation. It must, however, be remembered that the spectra obtained are essentially bulk spectra of spincoated films several microns thick and are not surface selective. Subtle changes in the surface chemistry can easily be masked by stronger changes occurring in the bulk polymer. Figure 3.10 shows the evolution of the UV absorbance profiles as a function of UV exposure. The spectra obtained at 30 second UV exposure intervals show the rate of formation of products of photo-Fries rearrangement and degradation is maximum at the start of the UV exposure cycle and gradually decreases up to 120 seconds exposure, after which no significant changes are observed.

Absorbance

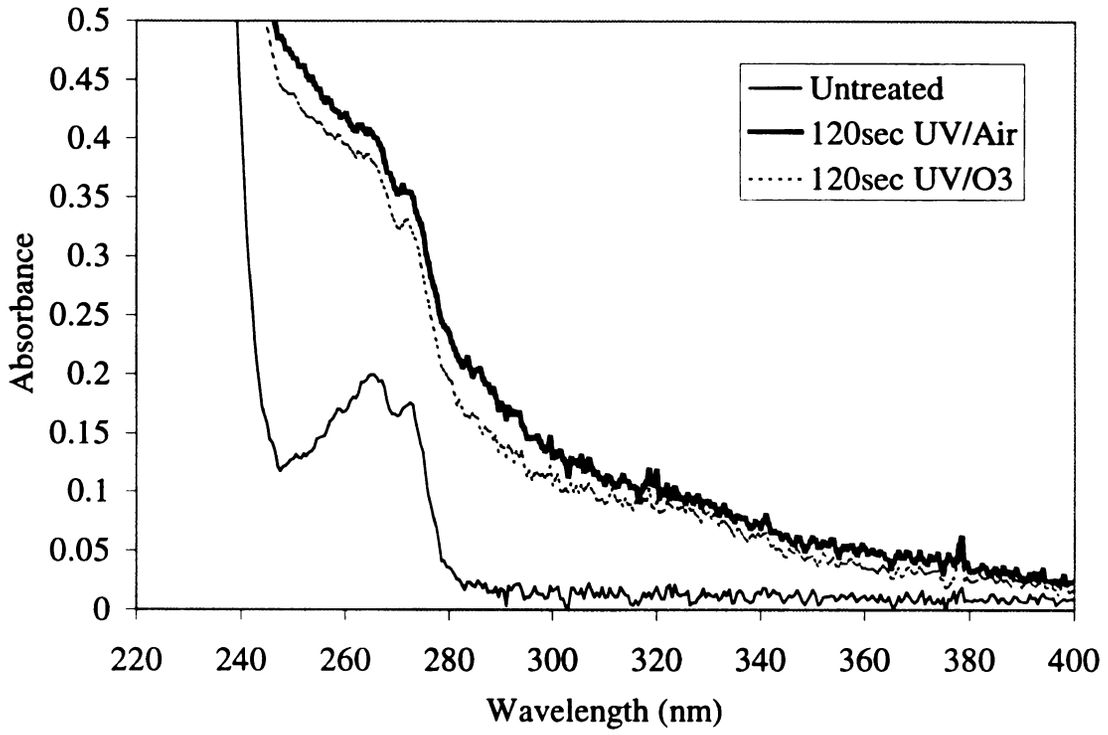

Figure 3.9 UV spectra of UVO, UVA, and untreated PC showing UV induced chain scission and the formation of phenolic groups (260-278 nm) and phenyl salicylates (245 nm and 315 nm) in the polymer because of photofries rearrangement.

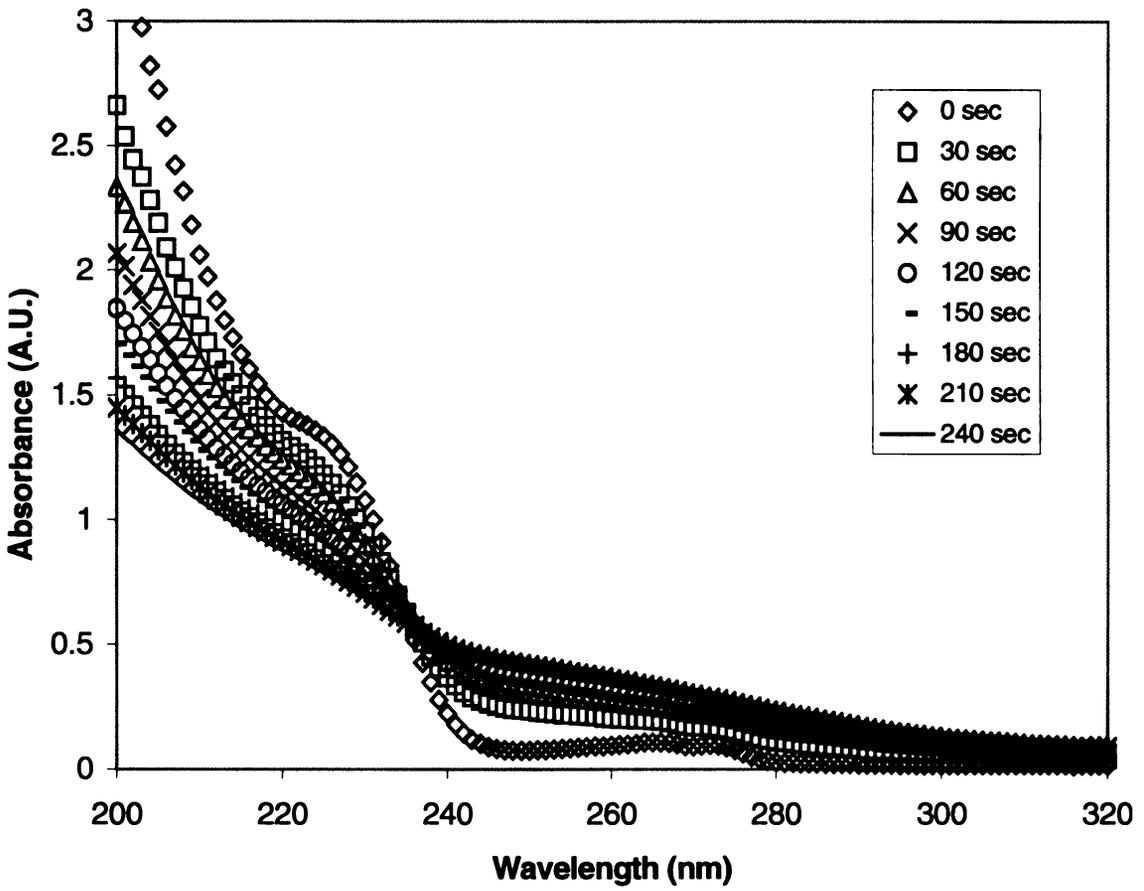

Figure 3.10 UV spectra of PC spincoated on quartz after UV Treatment at 2.662 mJ/m^2 irradiance and 700 ppm ozone.

3.5 EPR Spectroscopy

Electron Paramagnetic Resonance (EPR) spectroscopy is used to detect the presence of free radicals or any electron with an unpaired spin. The UV activation and subsequent reaction with oxygen (itself a paramagnetic molecule) leads to a high concentration of unpaired spins in the polycarbonate. These unpaired electrons may serve as further reaction sites. The presence of unpaired spins was detected and quantified using room temperature EPR spectroscopy at a magnetic field of 3364 Gauss and a microwave frequency of 9.46 GHz. Torikai et al. [13-14] have reported similar spectra in PC irradiated in vacuum and air and assigned the signal to phenoxy and phenyl radicals; both products of chain scission in polycarbonate. EPR is not a very robust quantitative technique for direct measurement of spin concentrations. Quantitative EPR requires the use of a constant amount of sample with identical surface areas which is difficult to achieve with solid samples. Although the amount of sample used for each spectra was kept as uniform as possible, slight changes in sample location, alignment, and weight can cause changes in the results obtained. All samples were analyzed at the same receiver gain in order to make some quantitative comparisons between samples possible. The data provided here is only intended to compare changes in spin concentrations differing by large values.

Figure 3.11 shows the spectra of polycarbonate film exposed to ozone, 120 sec UVA, and 120 sec UVO treatments. The y-axis shows the amplitude of the integrated signal in the material. Spin concentrations are usually calculated by measuring the area under the absorbance peak or by the product of the amplitude and FWHM (full width at half maximum) of the peak, but here only the amplitudes will be compared directly as a

measure of the approximate spin concentrations because all analyzed samples had similar peak widths.

PC exposed to ozone does not show any peaks and only a low background is observed with a peak amplitude of less than 4000. After UV treatment the amplitude increases to ca. 70,000 for UVA and 110,000 for UVO samples indicating either the presence of free radicals or paramagnetic oxygen in the material bulk or surface.

In addition to increasing the surface energy, UV treatment also creates free radicals on the surface that can react with applied paints and adhesives, forming chemical bonds and improving adhesion. Thus it is of interest to determine if the free radicals formed during UV treatment, and seen in the EPR spectra, are on the surface or in the bulk. Free radicals in the bulk can neither react with the adhesive nor contribute to surface energy and may be detrimental to the bulk properties of the material in much the same way as long term weathering. An indication of the amount of free radicals on the UV treated polymer surface which can react further was obtained by analyzing samples of UV treated PC immersed in an epoxy resin. The resin used was a DGEBA based epoxy (Shell, Epon 828) cured with triethylene tetramine (Jeffamine T403). UV treated samples were immersed in the epoxy resin and allowed to cure for 24 hours before EPR spectra was obtained. Baseline spectra of the epoxy and the treated polymer were also obtained.

Figure 3.12 shows the EPR spectra of the cured epoxy, UVO treated PC and UVO treated PC cured in epoxy resin. The neat epoxy does not show any paramagnetic response. The background is very low and on the amplitude is approximately 2000. The UVO treated polycarbonate film has an amplitude of ca. 110,000 and the treated film

cured in epoxy shows a much reduced amplitude of ca. 20,000. These changes are significant despite the approximate nature of the comparison, and indicates that the radicals which do not react with the ozone during treatment, or indeed the radicals or ions which may be formed due to the reaction with ozone during treatment, are largely located on the surface and are capable of reacting with an adhesive or paint applied to the surface.

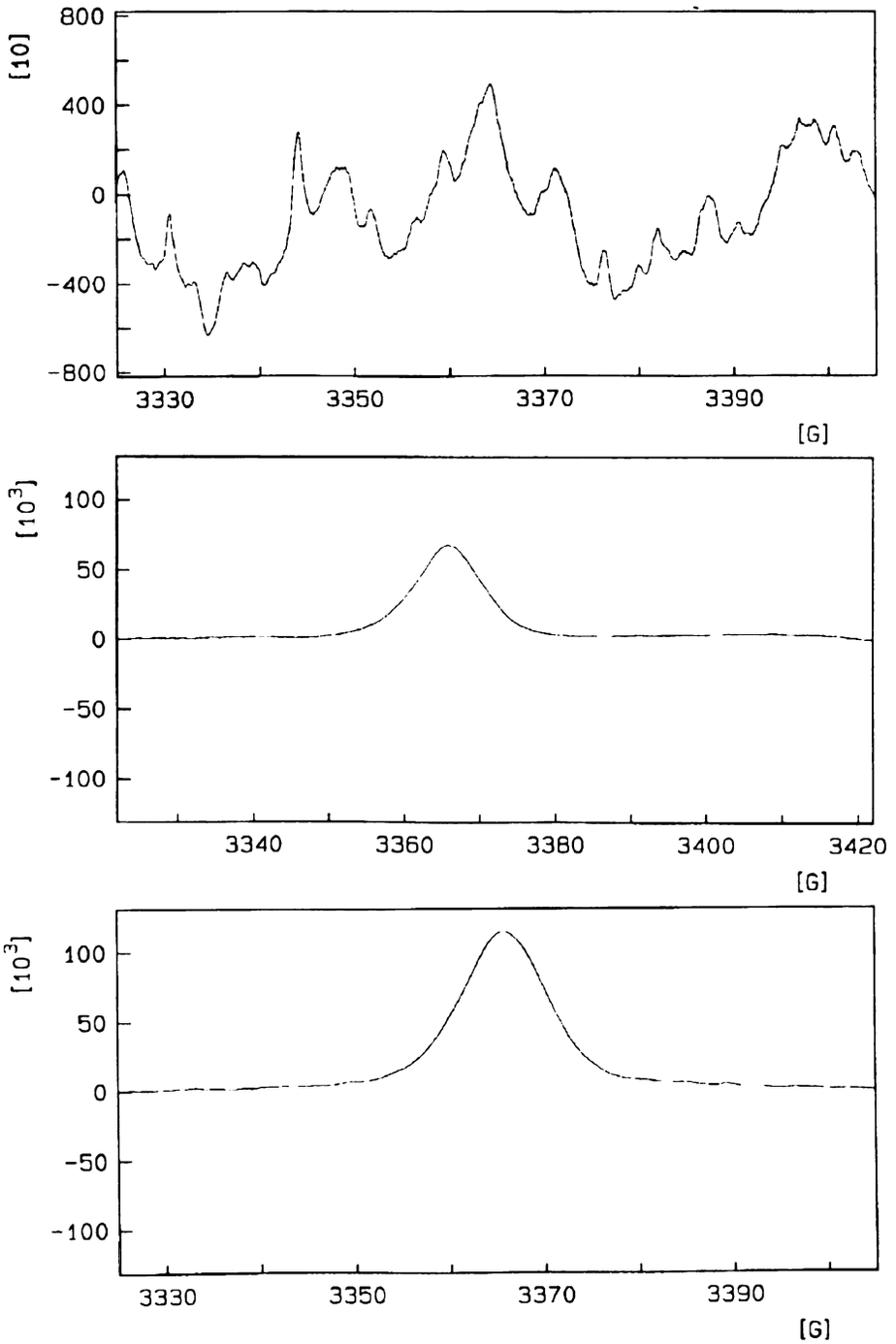

Figure 3.11 EPR spectra of PC exposed to ozone (top), 120 sec UVA treatment (middle), and 120 sec UVO treatment (bottom).

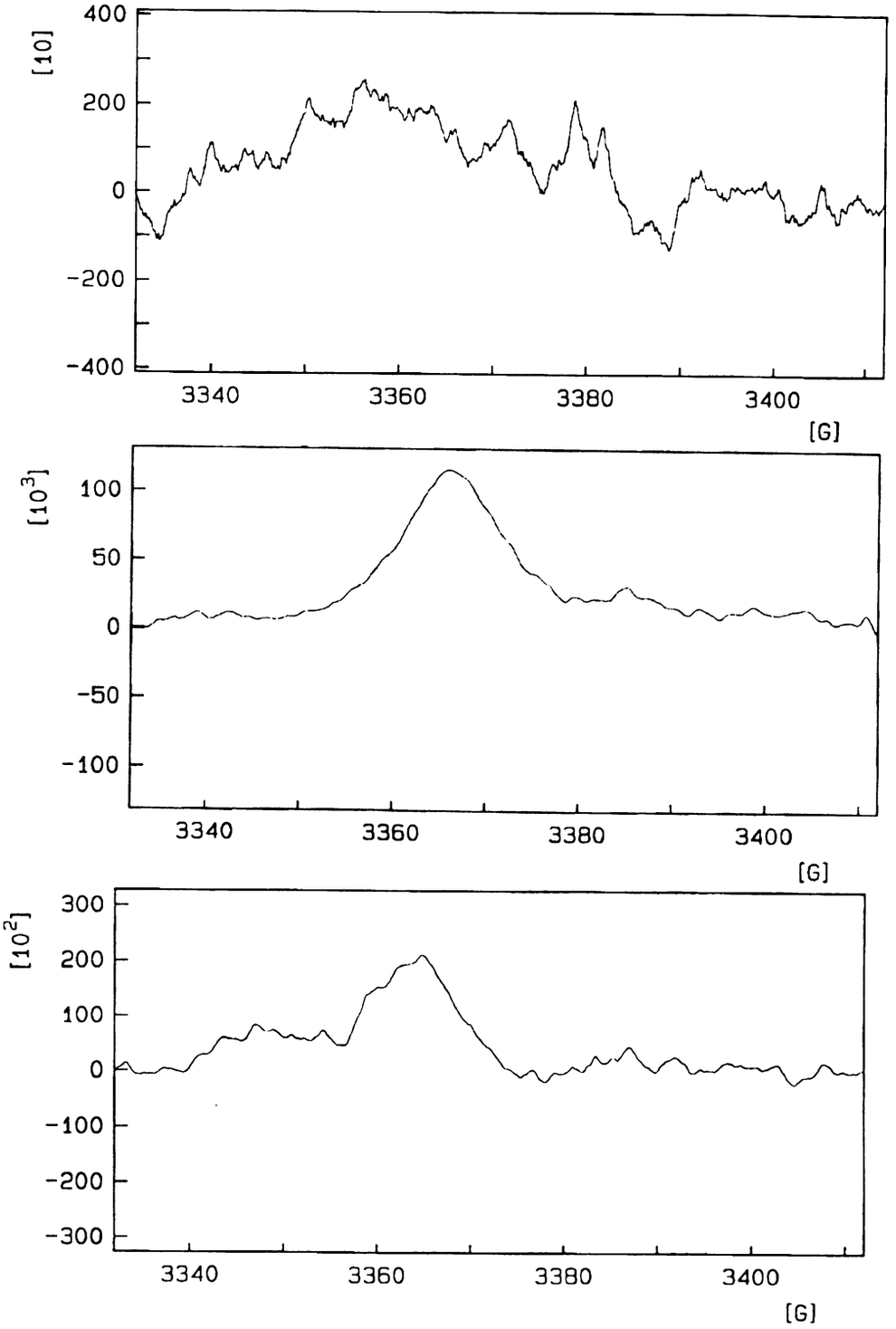

Figure 3.12 EPR spectra of epoxy (top), 120 sec UVO treated PC (middle), and 120 sec UVO treated PC cured in epoxy (bottom).

3.6 Nanoindentation

Nanoindentation tests on UVO treated polycarbonate films were performed using a Berkovich pyramidal tip to make 36 indents in the sample surface to a depth of 2000 nm. The spacing between indents was 50 μm, and Poisson's ratio of 0.35 was used for the polycarbonate. Three samples were tested for each treatment condition and the data for the each sample (36 indents) was averaged separately. Nanoindentation uses the load displacement data obtained by pushing the diamond tip into the sample surface to calculate surface modulus and hardness. On soft polymer samples this analysis is complicated by the difficulty experienced by the tip in determining the topmost layer of the surface. The surface is found by the instrument by increasing displacement till a pre-determined load is experienced. Due to the arbitrary nature of the surface find segment, properties measured very near the surface have large standard errors. Thus data obtained in the top 20-25 nm of the surface is not reliable and should be considered as machine noise. Figure 3.13 shows the surface modulus of UVO treated PC as a function of depth up to 500 nm. In spite of the large standard deviations in the top 100 nm of the surface, definite trends in modulus can be observed as a function of UVO treatment. The untreated material has a modulus between 2.7-2.8 GPa in the top 100 nm which increases to 2.9-3.0 GPa after UV treatment. The trend is clearer and becomes statistically significant as the probe depth increases beyond 100 nm. The increase in modulus of the polymer can be due to cross-linking of the surface layers under UV oxidation conditions. Similar increases in modulus and hardness of physically aged polycarbonate have been recently reported and attributed to changes in free volume and chain scission induced crosslinking [15].

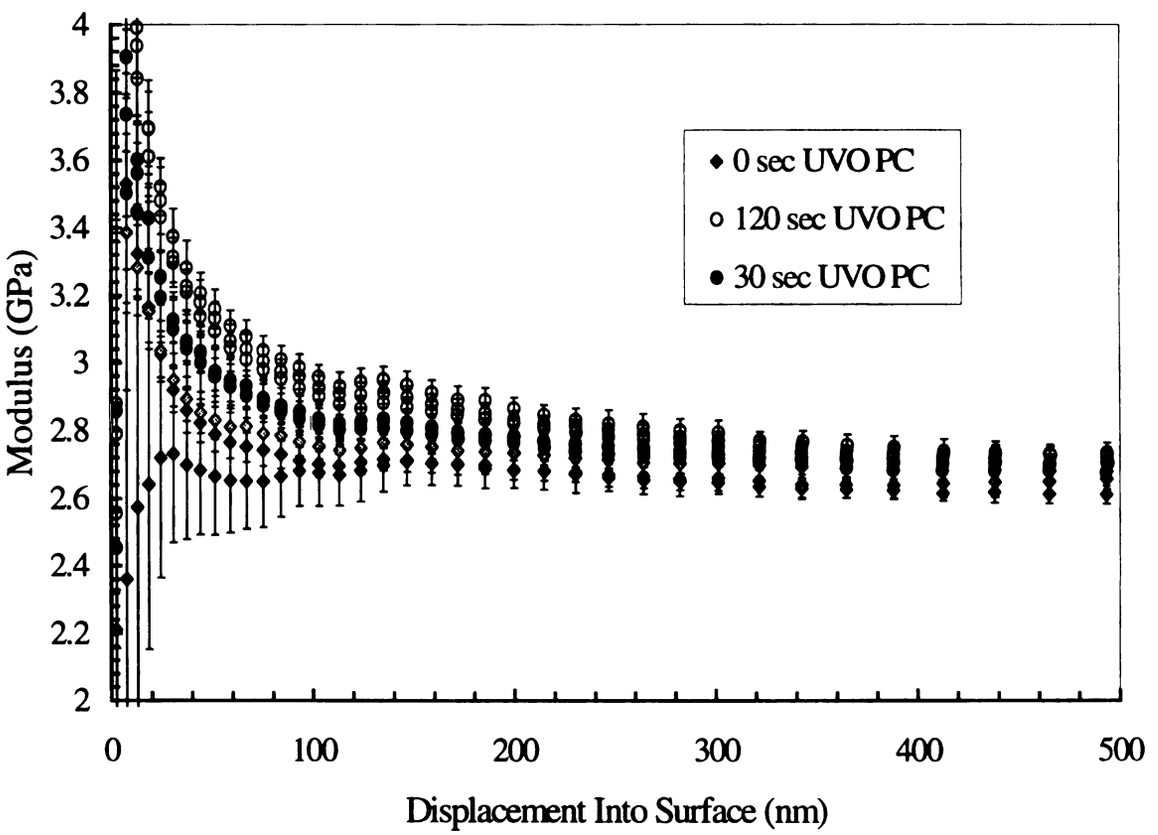

Figure 3.13 Modulus vs depth profiles of UVO treated polycarbonate measured by nanoindentation tests. Higher modulus in the surface layers is observed with increasing UVO exposure.

3.7 Adhesion

The adhesive performance of UV treated polycarbonate was measured using two adhesion tests: tensile stub-pull and stub shear. Tensile tests used a pneumatic piston to pull off an aluminum stub bonded to the PC film and the failure load was recorded. Shear tests were performed on similar samples and the shear load-displacement curves were recorded.

3.7.1 Tensile Stub-Pull Tests

UVO and UVA treated polycarbonate was bonded to 0.5 inch diameter aluminum stubs with a two part epoxy adhesive (Vantico, Araldite 2011). Figures 3.14 and 3.15 show the peak adhesive strength for UVO and UVA samples respectively. The untreated polycarbonate has a bond strength of ca. 300 psi. After UV treatment no statistically significant change in the adhesive strength was observed for treatments up to 120 seconds. Increased adhesive bond strengths were expected from UV treated samples because of the increase in work of adhesion and surface energy. The locus of failure appeared to be at the polycarbonate-epoxy interface from visual observations, but detailed fracture surface analysis, described in the following chapter, proved that the failure occurs within the polycarbonate substrate and the adhesive bond strength values reported here are not representative of the strength of the interface between the PC and adhesive. Samples were also prepared using a two part polyurethane adhesive (Vantico, Araldite 2040) in an effort to see if the failure mode changed for a different adhesive chemistry. Figure 3.16 shows the adhesive strength of UV treated PC with polyurethane and similar trends to the epoxy adhesive are observed.

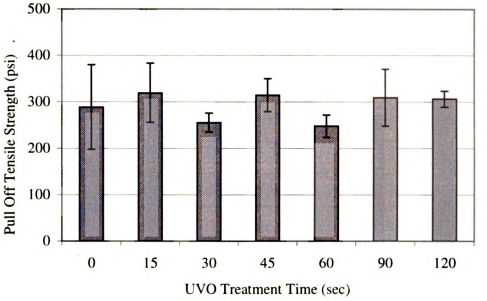

Figure 3.14 Adhesive strength of UVO treated PC with epoxy adhesive.

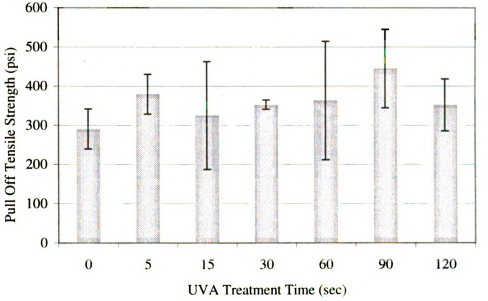

Figure 3.15 Adhesive strength of UVA treated PC with epoxy adhesive.

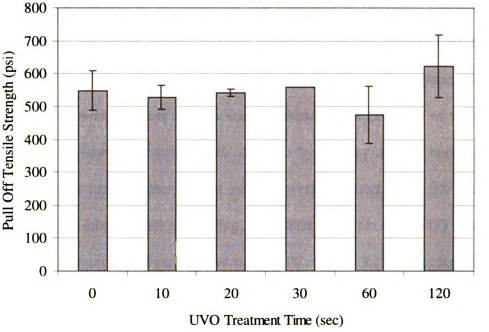

Figure 3.16 Adhesive strength of UVO treated PC with polyurethane adhesive.

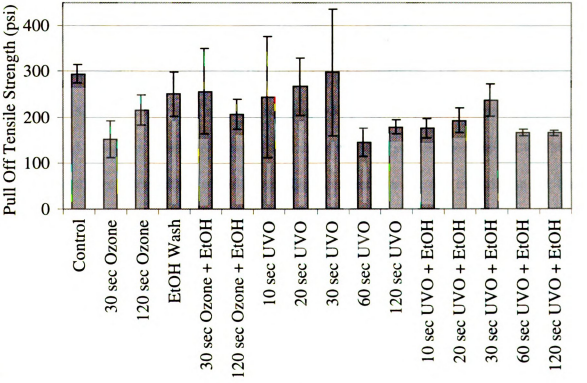

Figure 3.17 Adhesive strength of ozonated and UVO treated polycarbonate before and after ethanol wash to remove low molecular weight material.

It has been reported in literature that UV treatment of polymers can lead to the formation of low molecular weight (LMW) fragments on the surface due to chain scission [16,17]. LMW fragments are typically loosely bonded to the surface and can be washed away with weak solvents such as water or ethanol. The presence of weak LMW material at the interface can interfere with adhesion by creating a weak boundary layer that fails under low loads. Adhesion test samples were prepared using UV treated PC which was rinsed in ethanol prior to bonding. The effect of ozonation (no UV irradiation) was also studied for unwashed and ethanol washed PC. Figure 3.17 shows the results for ozonated and UVO treated samples before and after washing. As in the case of previous results, no significant changes in adhesion were observed.

3.7.2 Stub-Shear Tests

One of the possible drawbacks of the tensile stub pull test for thin film samples is the possibility of debonding between the untreated film surface and the rigid backing to which the PC is attached. This can lead to the development of peeling forces which can reduce bond strengths. Shear tests were performed to address this potential flaw. Shear tests also allowed recording of full load-displacement curves for calculation of the adhesive bond stiffness as well as peak failure loads. Figures 3.18 shows the bond stiffness for UVO and UVA treated samples bonded with epoxy (Vantico, Araldite 2011). As in the case of tensile tests, no statistically significant changes in adhesion bond stiffness and peak failure loads were observed. This is an unexpected result and an explanation will be proposed in the following chapter based on XPS failure analysis of adhesion test fracture surfaces.

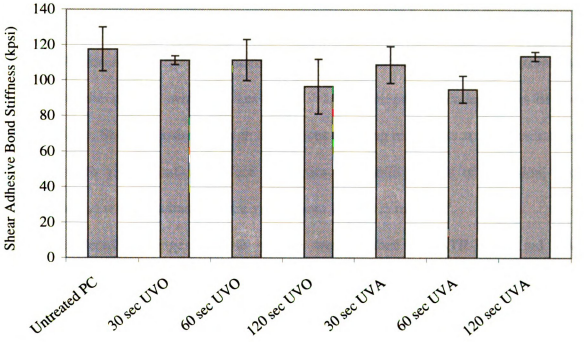

Figure 3.18 Slopes of load displacement curves for stub shear adhesion tests.

3.8 Summary

The surface treatment of polycarbonate by UV oxidation was characterized by wettability and surface energy measurements. UV exposure in ozone and air was found to impart strong hydrophilic nature to the normally hydrophobic PC surface. UV process variables such as the ozone flow rate were carefully chosen to avoid mass transfer limitations and under these conditions, it was found that the UV modification was independent of the ozone concentration in the treatment environment. The most important process parameter was found to be the UV irradiance. The changes occurring in the polymer are strongly dependent on the total irradiant energy, or irradiation, incident on the surface, which makes the UV treatment process independent of the exposure time. Short exposures at high irradiances and long exposures at low irradiances were found to yield identical surface properties (wettability, work of adhesion, and surface energy) when irradiances were varied from 1.6 to 7.5 mW/cm^2.

The molecular changes on the surface were probed by ATR-FTIR and UV spectroscopic techniques. The results show that UV exposure leads to the photo-Fries rearrangement of the bisphenol A carbonate to form phenyl salicylate and di-hydroxy benzophenones. The products of UV degradation on the surface can undergo oxidation by ozone to form hydroxyl, carbonyl, and carboxylate functional groups. The net result of this oxidation is the formation of conjugate bases on the surface which is seen as a strong increase in the base component of the surface energy. This increase in surface polarity is responsible for the enhanced wettability of UV modified surfaces.

EPR spectroscopy of UV exposed PC showed a strong paramagnetic response from the material after UVA and UVO treatments. This is believed to arise from unpaired

spins on oxygen containing functional groups, trapped free radicals, or radical ions in the polymer. The majority of paramagnetic sites were found to be near the surface of the PC as they can be effectively quenched or undergo reactions with an amine cured epoxy.

The mechanical properties of the modified surface were probed by nanoindentation tests. UVO treated PC showed an increase in the modulus in the top 500 nm with increasing UV irradiation. This is expected to be a result of UV irradiation induced crosslinking in the near-surface material. Despite the increase in surface modulus, adhesion tests showed no change in the adhesive bond strength with epoxy and polyurethane adhesives. This is an unexpected result and an explanation will be proposed in the following chapter based on XPS failure analysis of adhesion test fracture surfaces.

References

1. Brydson, J.A.; *Plastics Materials*, 5th ed., London, 1989.

2. Crawford, R.J. *Plastics Engineering*, 2nd ed., Oxford, 1987.

3. Rabek, J.F. *Mechanisms of Photophysical Processes and Photochemical Reactions in Polymers*, John Wiley, New York, 1987.

4. Good, R.J. *J. Adhesion Sci. Technol.*, Vol. 6, No. 12, pp. 1269-1302, 1992.

5. White, R. *Chromatography/Fourier Transform Infrared Spectroscopy and its Applications*, Marcek Dekker, New York, 1990.

6. Jaffe H. and Orchin M., *Theory and Applications of Ultraviolet Spectroscopy*, Wiley, New York, 1962.

7. Ming-Shiu, L.; Chem-Chi M. M.; Jyh-Luen C.; Miaw-Ling L.; Feng-Chih C. *Macromolecules*, Vol. 29, No.2, pp. 499-506, 1996.

8. Rabek, J.F. *Mechanisms of Photophysical Processes and Photochemical Reactions in Polymers*, John Wiley, New York, 1987.

9. Humphrey, J.S.; Shultz, A.R.; Jaquiss, D.B.G. Macromolecules, Vol. 6, No. 3, pp. 305-314, 1973.

10. Pankasem, S.; Kuczynski, J.; Thomas J.K. *Macromolecules*, vol. 27, pp. 3773-3781, 1994.

11. Gupta, A.; Rembaum, A.; Moacanin, J. *Macromolecules*, Vol. 11, No. 6, pp. 1285-1288, 1978.

12. Gupta, A.; Liang, R.; Moacanin, J.; Goldbeck, R.; Kliger, D. *Macromolecules*, Vol. 13, pp. 262-267, 1980.

13. Torikai, A.; Murata, T.; Fueki, K. *Polymer Photochemistry*, vol. 4, p. 255, 1984.

14. Torikai, A.; Suzuki, K.; Fueki, K. *Polymer Photochemistry*, vol. 3, p. 379, 1984.

15. Soloukhin, V.A.; Brokken-Zijp, J.C.; VanAsselen, O.; DeWith, G. *Macromolecules*, vol. 36, pp. 7585-7597, 2003.

16. Strobel, M.; Lyons, C.S. , *J. Adhesion Sci. Technol.*, Vol. 17, No. 1, pp. 15-23, 2003.

17. Walzak, M.J.; Flynn, S.; Foerch, R.; Hill, J.M.; Karbashewski, E.; Lin, A.; Strobel, M. *Polymer Surface Modification; Relevance to Adhesion*, K.L. Mittal (Ed.), pp. 253-272, 1995.

CHAPTER FOUR

SURFACE ANALYSIS OF UV TREATED POLYCARBONATE

UV oxidation induced changes in the atomic composition and chemical bonding state of polycarbonate generally occur in the top few atomic layers of the surface. Qualitative and semi-quantitative characterization of these chemical changes was accomplished using X-ray Photoelectron Spectroscopy (XPS). UV treated polycarbonate samples were analyzed with MgKα x-rays in a Perkin Elmer Phi 5400 ESCA system at pressures between 10^{-9} and 10^{-8} torr, pass energy of 29.35 eV, and a 45° take-off angle unless stated otherwise.

4.1 Surface Chemistry of Polycarbonate

The major change occurring in polycarbonate because of UV oxidation is an increase in the surface oxygen content. Figure 4.1 shows an example of the C1s peak and the deconvoluted fits for polycarbonate samples before and after UV treatment. As explained in Chapter 2, deconvolution of the carbon peak gives indirect information about the chemical environment of the carbon atoms. The untreated polycarbonate shows three distinct peaks in the C1s envelope. The peak at 284.7 eV is assigned to aliphatic and aromatic hydrocarbon bonds. Carbon atoms bonded to more electronegative atoms like oxygen experience an increase in the binding energy and Figure 4.1(a) shows two additional peaks around 286.2 eV and 290.9 eV corresponding to carbon atoms in hydroxyl/ether groups and carbonate groups respectively. The stoichiometric ratio of carbon and oxygen in the polycarbonate repeat unit is 16:3 ($C_{16}H_{14}O_3$) corresponding to a

stoichiometric O/C ratio of 0.187. The atomic compositions of untreated polycarbonate films determined by XPS were generally in good agreement with the stoichiometric composition, however, the material used is a commercial grade engineering polymer and the surface cannot be considered a pure polycarbonate surface. Included and adventitious impurities are expected to be found on the film surface and the state of the material more closely resembles materials likely to be used in industrial applications. Polycarbonate from two different batches was used in this study and small variations in the overall O/C ratio between batches or sheets within batches were observed as shown in Table 4.1. This variation in the baseline material was not considered significant compared to the changes in O/C ratios after UV treatment. From repeatability studies, the standard error in O/C ratios was found to be less than 5% and the error in deconvoluted curve fit data was approximately 10%.

The polycarbonate repeat unit has two ether carbon atoms and one carbonate carbon atom. Table 4.2 compares the stoichiometric and experimentally observed distribution of carbon. The polymer has ca. 11.5% ether groups and 5% carbonate which is in good agreement with the expected distribution. Figure 4.1(b) shows the C1s peak for a typical UV oxidized sample. After UV oxidation of the polycarbonate in air or ozone, the oxygen content increases sharply. Deconvolution of the C1s peak shows an increase in the hydroxyl/ether peak (286.2 eV) and the appearance of two new peaks between the hydroxyl and carbonate (290.9 eV) peaks corresponding to carbonyl (287.5 eV) and carboxylate/ester (289.8 eV) functional groups. A more detailed description of the changes in chemistry of UV/Ozone (UVO), UV/Air (UVA), and UV/Vacuum (UVV) treated polycarbonate is provided in the following sections.

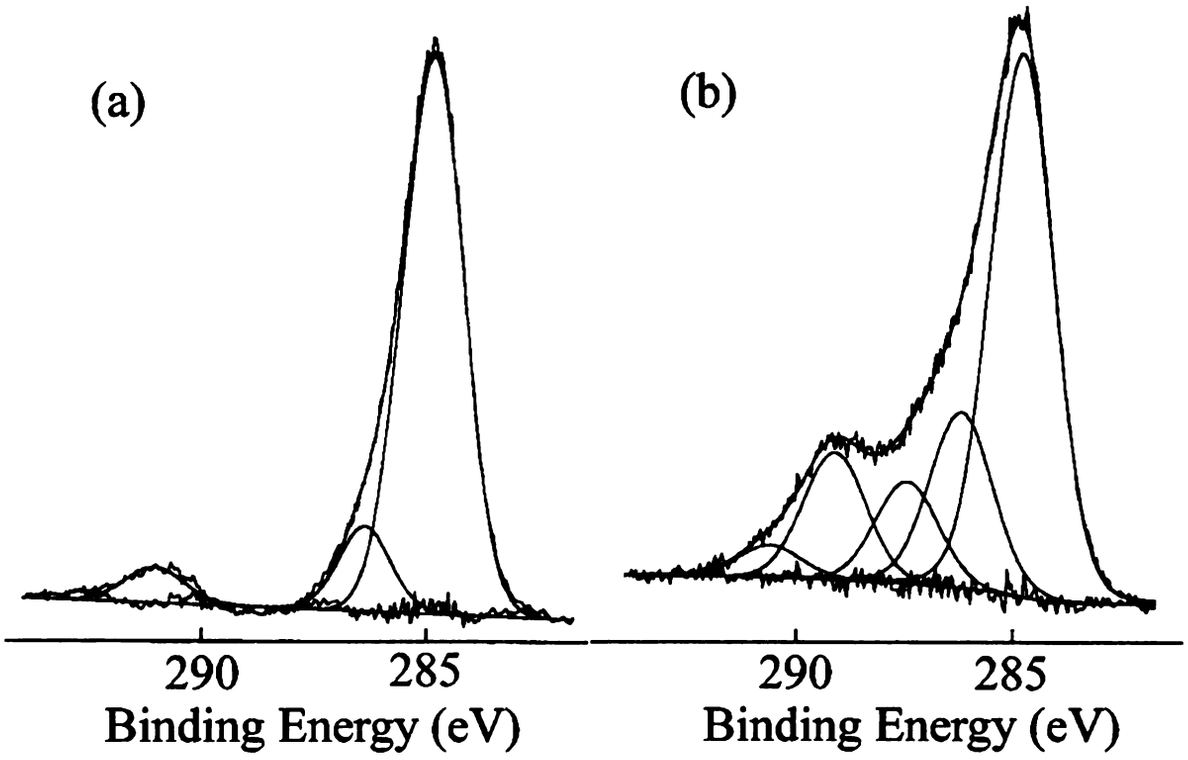

Figure 4.1 C1s peak for polycarbonate (a) before and (b) after UV treatment.

Table 4.1 O/C ratios in untreated polycarbonate.

Polycarbonate	C(%)	O(%)	O/C
Sample 1	85.1	14.9	0.175
Sample 2	86.2	13.5	0.156
Sample 3	84.4	15.6	0.184
Sample 4	87.8	12.2	0.139
Sample 5	84.4	15.6	0.185
Sample 6	84.6	15.4	0.182

Table 4.2 Carbon distribution in untreated polycarbonate.

Carbon distribution	Stoichiometric (%)	Experimental (%)
Hydrocarbon	81.3	83.4
Ether / Hydroxyl	12.5	11.4
Carbonyl	0.0	0.0
Carboxylate / Ester	0.0	0.0
Carbonate	6.3	5.1

*Values expressed as percentage of total carbon.

4.2 Surface Chemistry of UV/Ozone Treated Polycarbonate

There is significant oxygen uptake in the surface after UV treatment and the O/C ratio reaches an asymptotic value of 0.5 after prolonged exposure. Samples were UVO treated at irradiance levels ranging from 1.6 to 3.0 mW/cm^2 for times ranging from 10 to 120 seconds. Figure 4.2 shows the O/C ratio for UVO treated samples. It is apparent that the increase in O/C ratio depends solely on the total irradiation and all data points follow a universal trend for polycarbonate.

A clear correlation can be drawn between the increase in surface energy, work of adhesion, and O/C ratio for UVO treatment. The deconvoluted C1s curve fit data for various treatment conditions is shown in Table 4.3. The detailed C1s spectra provides some information regarding the mechanism of oxidative degradation. The hydrocarbon and carbonate peaks decrease with increasing irradiation suggesting that the UVO treatment attacks multiple sights on the PC chain. The carbonyl and carboxylate peaks increase following a trend similar to the overall O/C ratio. The ether/hydroxyl ratio increases by a small amount initially and remains constant even after extended treatments. The decrease in the carbonate peak is indicative of a chain scission mechanism involving cleavage of almost 50% of the carbonate linkages in the polymer. The number of carbon atoms with C-C and C-H (hydrocarbon) bonds also decreases gradually indicating breaking of bonds in the bisphenol-A structure including the opening of aromatic rings and possible cleavage of the primary carbons (methyl groups). The reduction of carbonate and hydrocarbon peaks by 50% after extended exposures points to extensive chain scission on the surface, possibly followed by further reactions such as oxidation or crosslinking of the chain fragments.

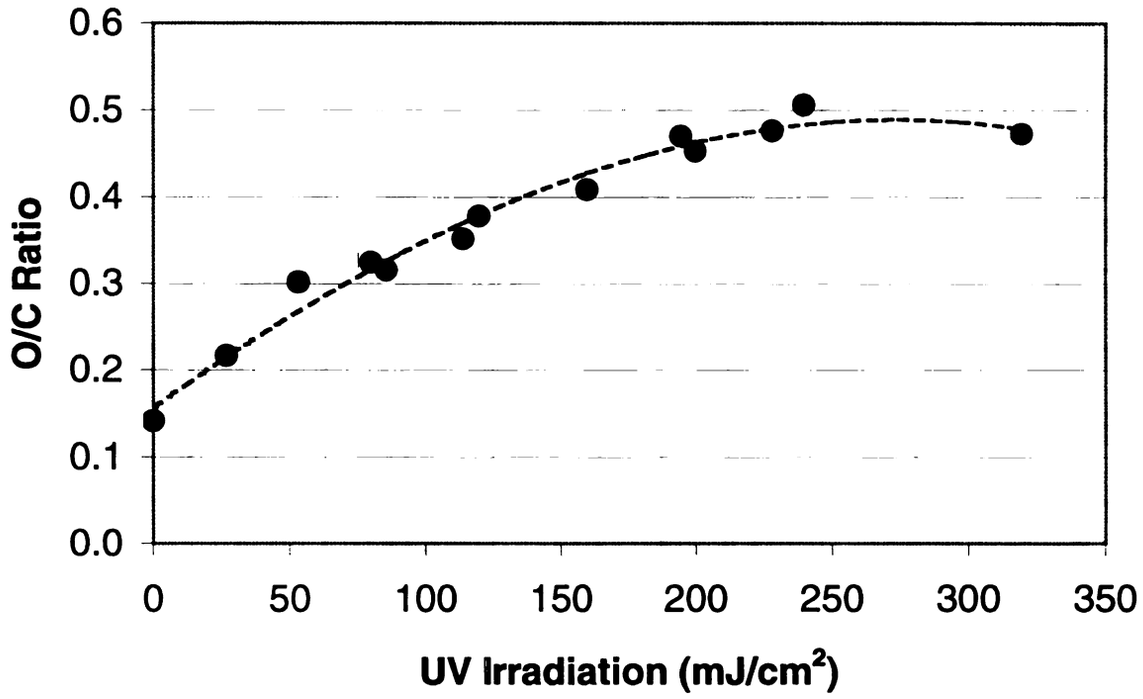

Figure 4.2 O/C ratio of UV treated PC as a function of irradiation.

Table 4.3 XPS surface chemical composition of UV treated polycarbonate showing the O/C ratio and C1s curve fit analysis.

Irradiant Energy (mJ/cm^2)	Total Carbon (%)	Hydro-carbon* (%)	Ether/ Hydroxyl* (%)	Carbonyl* (%)	Carboxyl* (%)	Carbonate* (%)
0	87.6	73.1	10.0	0.0	0.0	4.5
27	82.2	63.9	13.9	0.9	0.9	2.6
53	76.8	55.0	11.6	3.9	3.3	3.1
80	75.5	50.6	12.8	4.6	4.8	2.7
85	76.0	52.2	13.7	3.6	4.6	1.9
114	74.0	44.8	15.3	5.7	5.7	2.5
120	72.6	44.5	12.1	6.3	6.9	2.8
160	71.0	43.4	13.4	5.9	6.4	1.9
194	68.0	38.6	13.1	6.9	8.5	0.9
200	68.8	38.9	13.8	7.1	7.9	1.1
228	67.7	35.9	14.3	6.8	9.1	1.7
240	66.4	36.8	12.5	5.5	10.0	1.7
319	67.9	37.8	12.4	6.9	8.5	2.4

*Values expressed as percentage concentration of total surface.

4.3 UV Treatment in Vacuum

The samples described in previous sections were treated in an external aluminum treatment chamber and subsequently transferred to the XPS for analysis. To avoid sample exposure to ambient conditions between treatment and analysis, a UV treatment pre-chamber was designed to interface with the XPS as shown in Figure 4.3. The XPS pre-chamber has a UV transparent sapphire window and provides the ability to irradiate surfaces in a clean environment, including exposure in vacuum (pressure < 10^{-6} torr) as well as other gases. The UV lamp was mounted over the sapphire window and after treatment, samples were directly introduced into the XPS for analysis. Due to size restrictions, only the RC500 lamp was used with the prechamber. The more restrictive opening for the lamp on the prechamber causes a reduction in irradiance compared to the external chamber, hence irradiances measured for the lamp in Figure 2.4 do not apply to UV exposures in the prechamber. However, irradiance in the prechamber is constant due to the inability to vary the distance between the lamp and sample, and the total irradiation in the prechamber is in direct proportion to the exposure time. The irradiance in the pre-chamber could not be measured directly because of restricted space and large size of the radiometer detector assembly. The dependence of most properties on the irradiation has already been demonstrated, so trends in time in the pre-chamber experiments can be considered to be linearly equivalent to trends in irradiation in the external chamber.

The ability to treat samples in vacuum in the pre-chamber also allows the separation of UV exposure and gas exposure reactions. Experiments were performed to measure the oxygen uptake in samples irradiated in vacuum by introducing ozone and other gases into the pre-chamber after the UV exposure. This will be termed 'post-

treatment' in this text and indicates a consecutive, but separate, operation in the treatment process. Table 4.4 shows the chemical composition of polycarbonate samples treated in vacuum, air, and ozone.

Polycarbonate treated in UV/Vacuum (UVV) did not show any change in the surface chemical composition (O/C), although for very long UVV treatment on the order of 120-180 seconds, a small amount of carboxylate was observed, most likely due to cleavage of some carbonate bonds. The possibility of creating free radicals in the surface with UVV exposure and the reaction of such an activated surface with a gas was investigated. In samples exposed to air (ca. 20% oxygen) for 10 minutes following UVV exposure, there was no noticeable change in the chemical composition from the untreated polymer. However, when activated samples were exposed to ozone for 5 minutes, the surface O/C ratio changed to values expected from direct UVO treatment.

Untreated PC exposed to ozone for such short times does not account for the change in O/C ratios seen in these samples. Figure 4.4 shows the increase in O/C ratio of PC exposed to ozone. The O/C ratio increases initially but reaches a maximum value of ca. 0.23 to 0.24 after 30 seconds of ozone exposure and remains relatively constant thereafter. O/C ratios of UVV treated PC post-treated with ozone ranged between 0.27 to 0.30. This suggests a mechanism which may involve the formation of activated radicals or unsaturated bonds on the surface which are susceptible to selective oxidative attack by ozone and not oxygen. This result also provides confirmation of the necessity of low wavelength (below 200nm) UV light which is capable of producing trace amounts of ozone *in-situ* during UV exposure. The independence of UV activation of the surface and the actual surface modification also opens avenues for the use of different gases to

achieve specific functional groups on the treated surfaces. Activated surfaces can be grafted with different groups once the specific reaction sites are identified.

Activated surfaces also proved to be stable in air and can be post-oxidized with ozone after aging in ambient conditions for long periods. Table 4.5 shows the O/C ratio for samples aged up to 6 days in normal laboratory environment after UVV exposure. Samples were exposed to ozone for 5 minutes immediately before XPS analysis to react any active sites not quenched by storage in ambient conditions. The O/C ratio of aged activated samples remained stable between 0.27 and 0.30 over the period of six days and only a slight decrease was seen up to 139 hours of aging. No increase in oxygen concentration was found in samples stored in air if they were not exposed to ozone prior to analysis. This strongly suggests that the active radical or ionic sites within the XPS sampling depth do not get quenched by exposure to oxygen on time scales spanning tens of hours. This may be a combined effect of the formation of stable ions or trapped radicals under the surface which do not recombine easily.

The amount and rate of uptake of ozone in UVV treated samples is studied in more detail in the following section.

Table 4.4 Surface chemical composition of polycarbonate UV treated in vacuum, air and ozone.

Treatment Conditions	C (%)	O (%)	O/C
Untreated	86.0	14.0	0.16
120 sec UV/Vacuum	86.4	13.6	0.16
120 sec UV/Vacuum + 10 min Air	86.6	13.5	0.16
120 sec UV/Air	81.4	18.6	0.23
120 sec UV/Air + 5 min ozone	78.4	21.6	0.28
120 sec UV/Ozone	77.7	22.3	0.29
120 sec UV/Vacuum + 1 min Ozone	78.8	21.2	0.27
120 sec UV/Vacuum + 5 min Ozone	77.0	23.0	0.30
120 sec UV/Vacuum + 10 min Air + 5 min Ozone	74.6	22.3	0.30

Post-treatment with gas indicated by '+'.

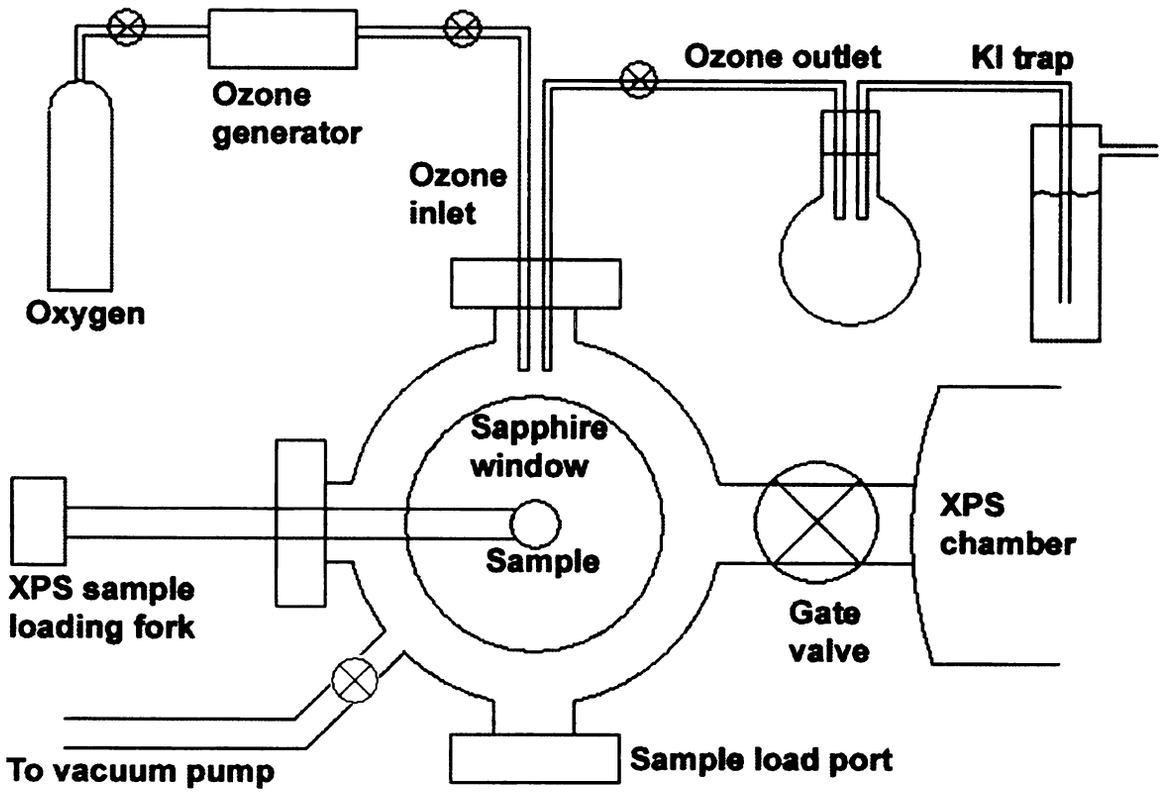

Figure 4.3 Schematic of the XPS pre-chamber for UV treatment

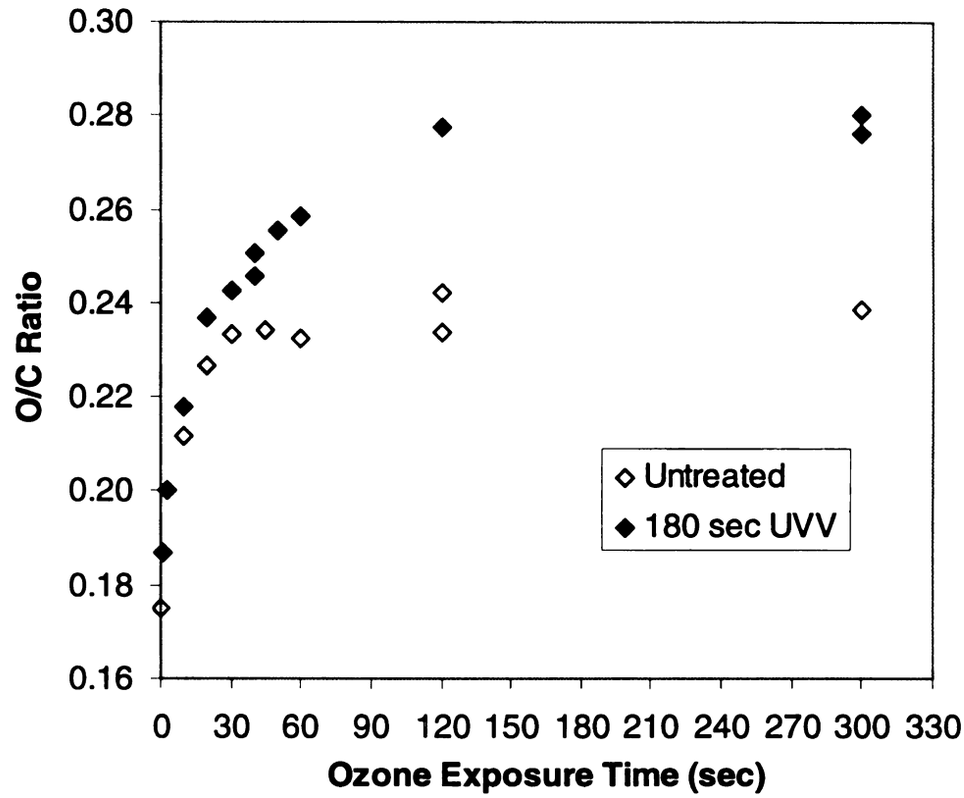

Figure 4.4 O/C ratio of untreated and UVV treated PC exposed to 700 ppm ozone.

Table 4.5 Surface chemical composition of UVV treated PC aged in air. Aged samples oxidized in ozone for 5 minutes prior to analysis.

Aging Conditions	O/C Ratio
0 hrs	0.18
95 hrs	0.18
0 hrs aged + 5 min. Ozone	0.30
22 hrs aged + 5 min. Ozone	0.28
46 hrs aged + 5 min. Ozone	0.29
90 hrs aged + 5 min. Ozone	0.27
95 hrs aged + 5 min. Ozone	0.28
139 hrs aged + 5 min. Ozone	0.27

4.4 Oxygen Uptake in UV/Vacuum Treated PC

As mentioned in the previous section, UVV treated samples post treated with ozone exhibit uptake of oxygen in the surface which is greater than that expected by ozonation of untreated polycarbonate. A detailed study of the kinetics of oxygen uptake was performed by ozonation of samples UVV treated for different times. The UVV activated samples were exposed to ozone for times ranging from 1 to 300 seconds in an external ozonation chamber with 700-800 ppm ozone in oxygen carrier gas flowing at 30 scfh. The high concentration of ozone guarantees availability of enough ozone to the surface. Figure 4.5 shows the rate of ozone uptake in samples UVV treated for 30, 60, and 180 seconds. The data in Figure 4.5 is reported in terms of percent oxygen on the surface instead of the O/C ratio in order to compare the concentration of oxygen with an approximate concentration profile of a first order surface reaction between an active surface site and an ozone molecule. This is valid because only two elements are present on the surface and the percent composition can be converted to O/C ratio. Thus 19% O corresponds to a O/C ratio of 0.23.

The rate of oxygen uptake in Figure 4.5 clearly shows the uptake is proportional to the level of UVV irradiation at long ozone exposure times. However, for short ozone exposures between 1 and 30 seconds, the rate is similar for all three samples. After an exposure of approximately 30 seconds, the curves begin to diverge. A hypothetical first order kinetic model, shown by the dashed line, was used to examine the possibility of the initial part of the curves being indicative of the reaction between ozone and an active site on the surface. Since the precise reaction mechanisms for a complex process such as UV oxidation are as yet undetermined, the elementary reactions and rates are unavailable.

The first order kinetic model is overly simplified and presented for purely illustrative purposes. The assumptions made for this simple model are that a surface active site reacts with one ozone molecule, the reaction adds a single oxygen atom at that site, excess ozone is available for the surface reaction and the reaction is of the first order with a rate expression as shown in Equation 4.1.

$$S^* + O_3 \rightarrow SO + \ldots \qquad r = kS^* \tag{4.1}$$

where, S^* is the active surface site, SO is the site after oxidation, and k is the reaction constant. The first order kinetic solution for the reaction is of the form

$$[S^*] = [S^*]_o \exp(-kt) \tag{4.2}$$

where, $[S^*]_o$ and $[S^*]$ are respectively the initial and final concentrations of active surface sites. For an initial concentration of surface sites bonded to oxygen, $[SO]_o$, and the increase in surface oxygen due to oxidation reactions given by $[S^*]_o$-$[S^*]$, the final amount of oxygen on the surface can be expressed as

$$[SO] = [SO]_o + [S^*]_o \{1 - \exp(-kt)\} \tag{4.3}$$

An arbitrary reaction rate constant of 0.15 and a 3.5% surface concentration of active sites after UVV treatment were assumed to generate an illustrative concentration profile of oxygen for a first order surface reaction in Figure 4.5.

The UVV treated samples exhibit oxygen uptake beyond the initial part of the curves that is dependent on the amount of irradiation received. Since absorption of radiation by the polymer follows Beer's law, it is reasonable to assume that irrespective of the irradiation levels, the surface of the sample receives the maximum dosage and

increasing the dosage progressively activates sub-surface material. In such a scenario, the rate of oxidation of the polymer under the surface must be limited by diffusion of gaseous ozone into the material and the maximum oxygen uptake at any level of irradiation is indicative of the number of active sites created beyond the first few monolayers.

The separation of the oxygen uptake into a surface reaction limited to the top few monolayers and a diffusion limited oxidation of the sub-surface layers was further investigated using surface derivatization experiments described in the following section.

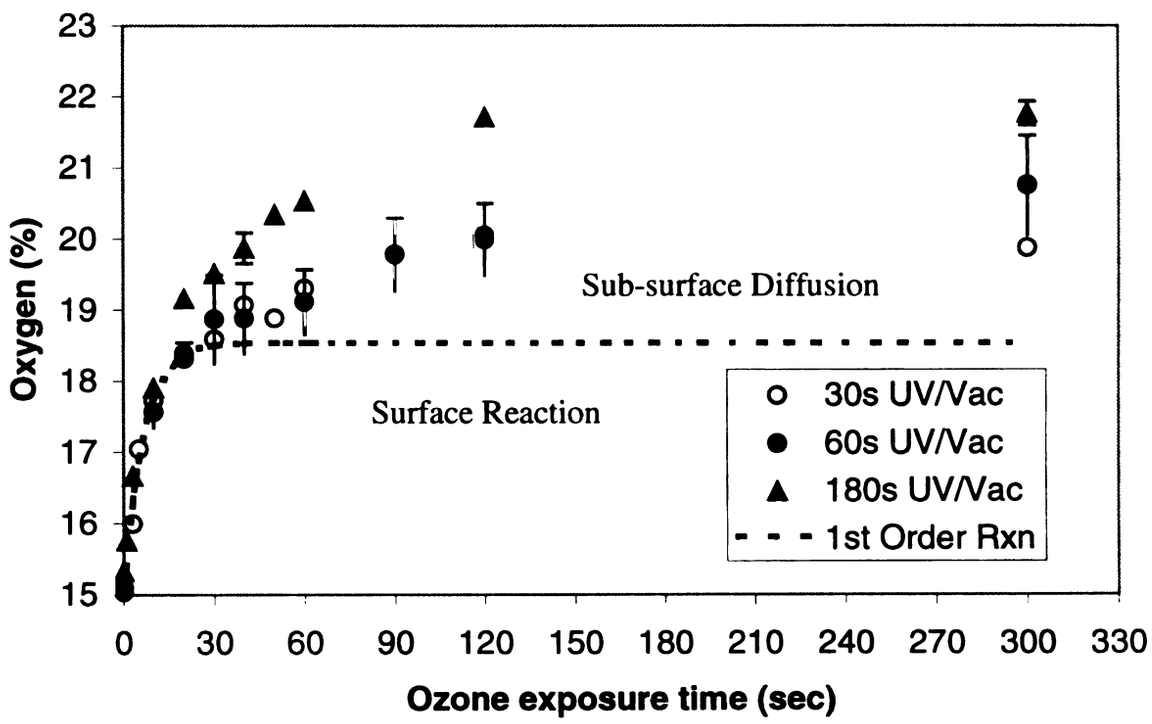

Figure 4.5 UV/Vacuum treated polycarbonate post oxidized with 700 ppm ozone.

4.5 Silver Nitrate Derivatization

XPS is a fairly surface sensitive analytical technique, yet the sampling depth averages over multiple monolayers of the material, making it difficult to attribute any properties to the top monolayer. Angle resolved XPS (AR-XPS) can provide some depth information by using shallow take-off angles to reduce the effective sampling depth. All XPS data shown here was obtained at a 45° take-off angle. AR-XPS was performed at 22° and 78° on UV treated samples, but did not show any significant differences in composition as a function of sampling depth. This may be likely if the chemical changes occur in the material to depths greater than 100 Å.

The C1s spectra of UV treated PC shows an increase in the carboxylate peak which follows the same trend as the overall oxygen ratio. To differentiate between the surface reaction occurring in the top few monolayers and the reactions occurring in the sub-surface monolayers to the XPS sampling depth of 75 to 100 Å, UV treated surfaces were derivitized with silver nitrate. Derivatization techniques have been used in XPS analysis to differentiate between different functional groups [1-3]. Silver nitrate was used to react with the carboxylate groups on the surface [1] to give silver carboxylate as shown in Figure 4.6. The silver on the surface can provide a high cross-section tag for XPS analysis. The assumption in this derivatization experiment is that the probability of formation of carboxylate groups in the first 100 Å due to UV oxidation is uniform and that the silver nitrate in liquid phase does not penetrate into the bulk of the sample and limits the reaction to the top monolayer. The silver atom is large compared to oxygen and has much lower mobility in the liquid phase compared to an aggressive gas phase oxidant such as ozone. Silver nitrate solutions were made in ethanol, a poor solvent for

polycarbonate. UV treated samples were dipped in 2% w/w ethanolic $AgNO_3$ solution for times ranging from 1 to 30 minutes. Silver concentrations on the surface were found to be invariant after 3-4 minutes of reaction. All derivatization data reported in this section was obtained from samples dipped in ethanolic silver nitrate for 5 minutes. Figure 4.7 shows the results of the silver nitrate derivatization experiments. The absolute concentration of silver and carboxylate concentration obtained from C1s curve fit are plotted for a 60 sec UVV treated polycarbonate exposed to ozone up to 300 seconds. The carboxylate concentration follows the general trend seen in the total oxygen concentration and statistically significant increases are seen till 120 seconds ozone exposure. The silver concentration increases rapidly to ca. 0.5% for a 30 second ozone exposure and remains constant thereafter even with increasing carboxylate functionality. The difference in the maximum measured absolute concentrations for silver (0.5%) and carboxylate (2.5%) validates the assumption that the silver ions do not diffuse into the sub-surface to react with all available carboxylate groups and selectively provides information about the top monolayers of the surface. The other important observation is that all samples with more than 30 second ozone exposure do not show increases in the silver concentration indicating that the surface layers are oxidized by ozone in the first 30 seconds and all subsequent increases in oxygen content are the result of ozone diffusion and reaction into the material. It is also important to note that the surface reaction limit of 30 seconds is identical to the exposure for which the oxygen uptake in Figure 4.5 diverges for samples with different levels of UVV irradiation and the surface saturation indicated by the simple kinetic model used to fit the initial oxygen uptake profile.

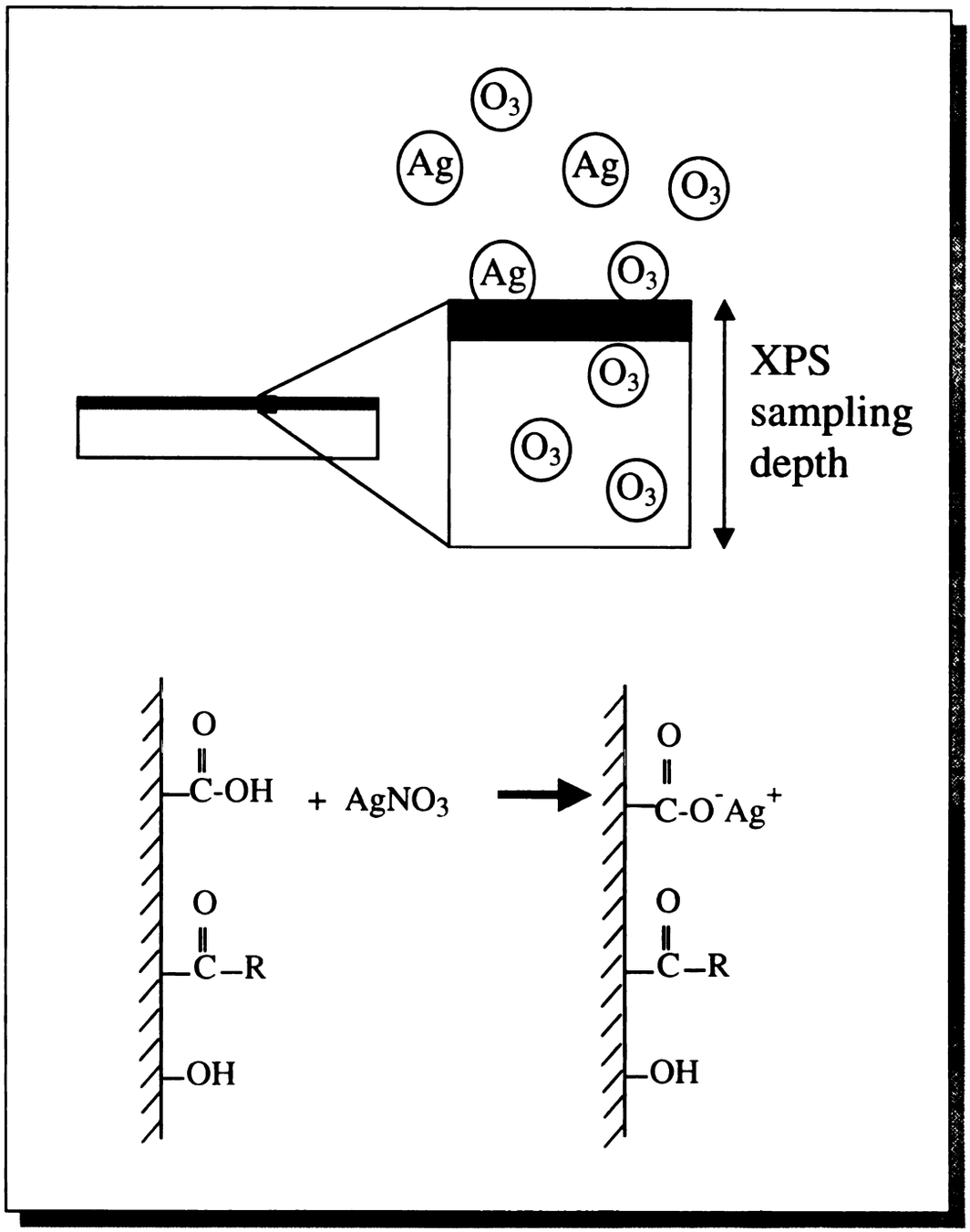

Figure 4.6 Reaction mechanism of silver nitrate with carboxylate groups on UV treated polycarbonate surface. Silver, unlike ozone, is limited to reactions on the top few monolayers of the surface.

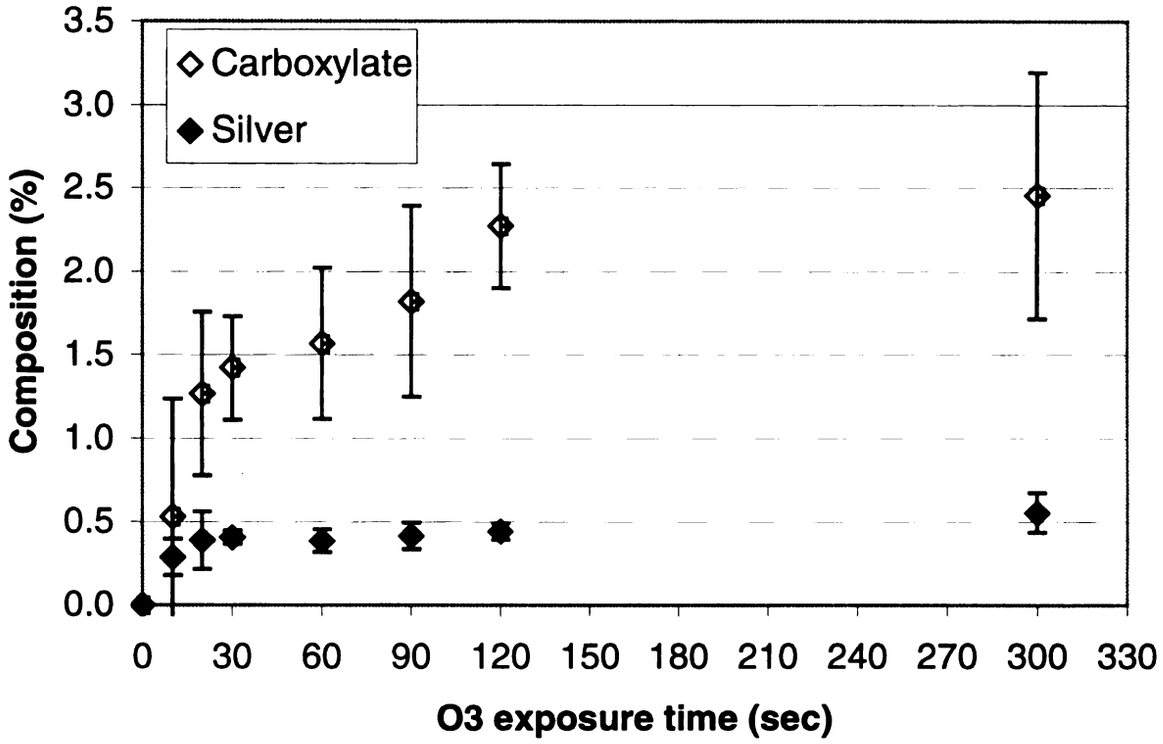

Figure 4.7 Silver and carboxylate concentration in silver nitrate derivatized polycarbonate with 60 sec UVV treatment and post-oxidation with 700 ppm ozone.

4.6 UV Treatment in Inert Atmosphere

The preceeding section described experiments performed in vacuum to separate the effects of irradiation and oxidation. The disadvantage of treating samples in the XPS pre-chamber is that irradiance levels and ozone concentrations are difficult to measure and since the prechamber requires evacuation after any process gas is introduced, exposure times to gases cannot be controlled precisely.

Results similar to UVV treatment can be obtained by irradiating polymers in an inert atmosphere to prevent oxidation. A nitrogen purge was used in the UV treatment chamber to prevent *in-situ* oxidation of samples during irradiation. This was followed by ozone exposure to oxidize the activated surfaces. Experiments in inert atmosphere were designed to compare the properties of *in-situ* and *ex-situ* oxidized polycarbonate.

Figure 4.8 shows the O/C ratio of polycarbonate treated in ozone and nitrogen using the RC747 lamp. UV/Nitrogen treated samples were exposed to 700 ppm ozone for 120 seconds after irradiation. The increase in O/C ratio for UVO treated samples is rapid and reaches a maximum value around 0.5. The UV/Nitrogen treated post-oxidized samples do not show a comparable increase despite the fact that irradiation in nitrogen is typically higher than the irradiation through the UV absorbing ozone atmosphere. The O/C ratio does increase in nitrogen, but only to a value of 0.3, the extent seen in UVV treatment.

The same trend was observed in the physical properties of samples treated in nitrogen and ozone. Figure 4.9 shows the work of adhesion with deionized water for UVO and UV/Nitrogen post-oxidized samples. With UVO treatment the work of adhesion increases sharply while only a slight positive change is observed for samples exposed in nitrogen. The different results of the two types of treatments can be explained

in terms of recombination of radicals. During UVO treatment, any radicals created on the surface can be immediately attacked by ozone adsorbed on the surface, whereas in inert or vacuum environments, the radicals can live long enough to undergo recombination and only a fraction of the original radicals remain on the surface in a state susceptible to ozone attack.

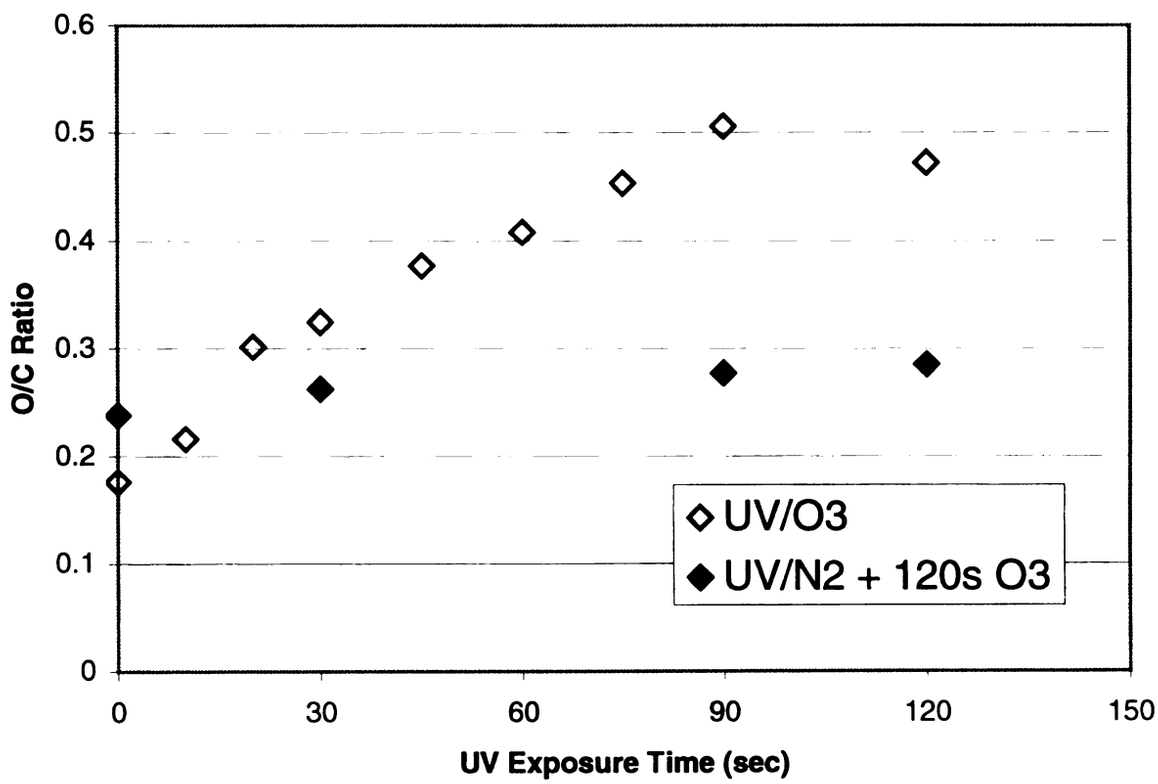

Figure 4.8 O/C Ratio of UVO and UV/N_2 + 120 sec O_3 treated PC

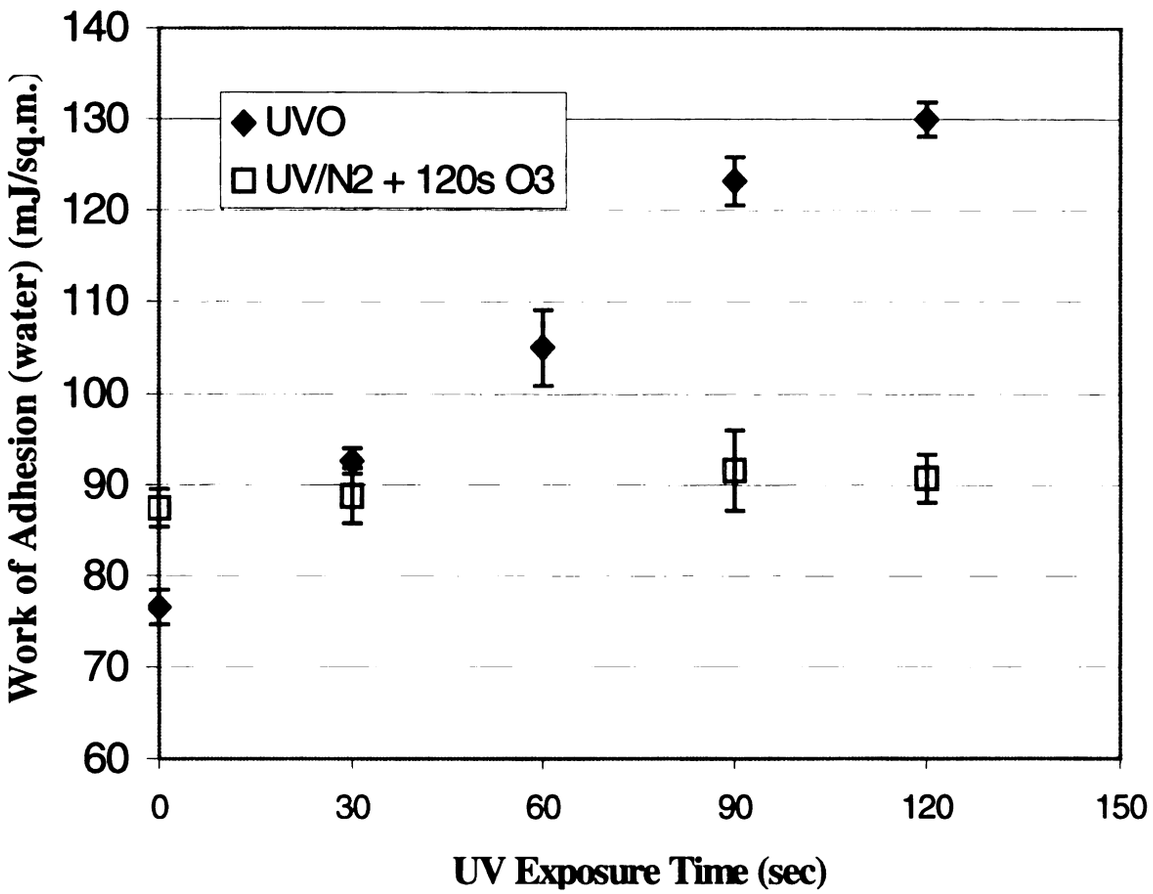

Figure 4.9 Work of adhesion of UVO and UV/N_2 + 120 sec O_3 treated PC

4.7 Washed Films

The formation of low molecular weight (LMW) polymer fragments on the surface after UV oxidation is expected in a polymer such as polycarbonate where both carbonate linkages and hydrocarbon bonds undergo chain scission. The formation of LMW fragments for various polymers has also been reported in literature [4,5]. The LMW fragments are often soluble in water and can be removed by mild rinsing. UVO treated PC was rinsed in deionized water and ethanol to test the presence of LMW fragments and determine the effect of their removal on surface properties.

LMW fragments can increase the wettability in polymers by dissolving in the probe liquid and reducing the overall energy. The presence of labile LMW can also lead to undesirable properties such as the development of a weak boundary layer in the material. Figures 4.10 and 4.11 show the O/C ratio and work of adhesion with deionized water for UVO treated PC (RC747 lamp, 2.6 mW/cm^2 irradiance, 800 ppm ozone) washed with water and ethanol prior to analysis. The removal of LMW fragments from the surface is apparent by the drop in O/C ratio beyond 20 to 30 seconds of treatment. The work of adhesion is reduced after rinsing and ethanol was observed to be slightly more efficient at removing LMW material compared to water.

Table 4.6 shows a comparison between washed UVV and UVO treated samples. The UVV samples were oxidized by post-treatment exposure to ozone. The O/C ratios and C1s curve fit distribution for oxidized UVV samples before and after washing in water are identical. UVO samples treated for the same time show a significant change in the O/C ratio and the C1s curve fit shows a decrease in the carbonyl and carboxylate concentrations that is consistent with the removal of oxidized low molecular weight

material from the treated surface. Similar trends are seen in samples treated for very long times (600 sec UVO). Comparison of the UVV and UVO samples after washing indicates that UVV (or UV/Nitrogen) treatment creates surface sites capable of reacting with ozone, but recombination of radicals in the inert environment lowers the concentration of such sites and the resultant surface has a lower amount of LMW material that can be removed easily. In UVO treated materials the simultaneous presence of ozone and UV decreases the probability of recombination of radicals and leads to extensive formation of oxidation products, which, when exposed to irradiation, can undergo further reactions, ultimately leading to extensive chain scission on the surface and formation of a higher number LMW fragments as indicated in Table 4.6.

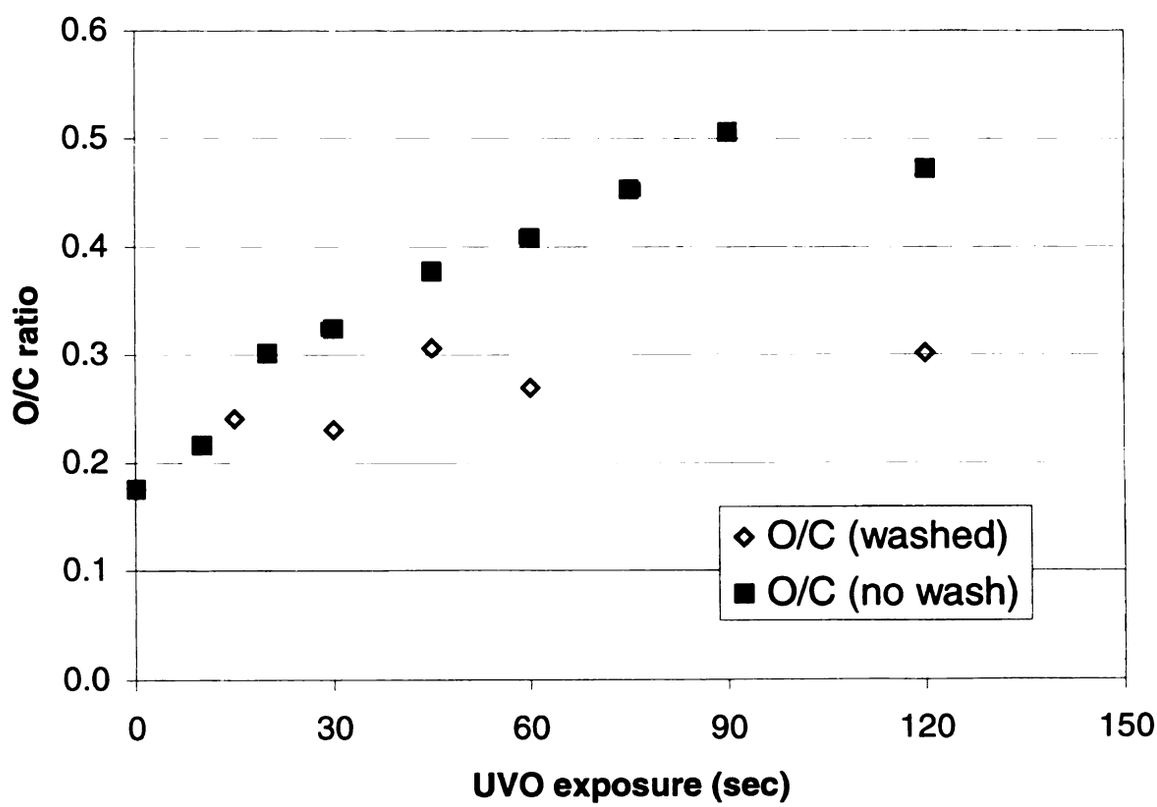

Figure 4.10 O/C ratio for UVO treated PC before and after rinsing with water followed by ethanol.

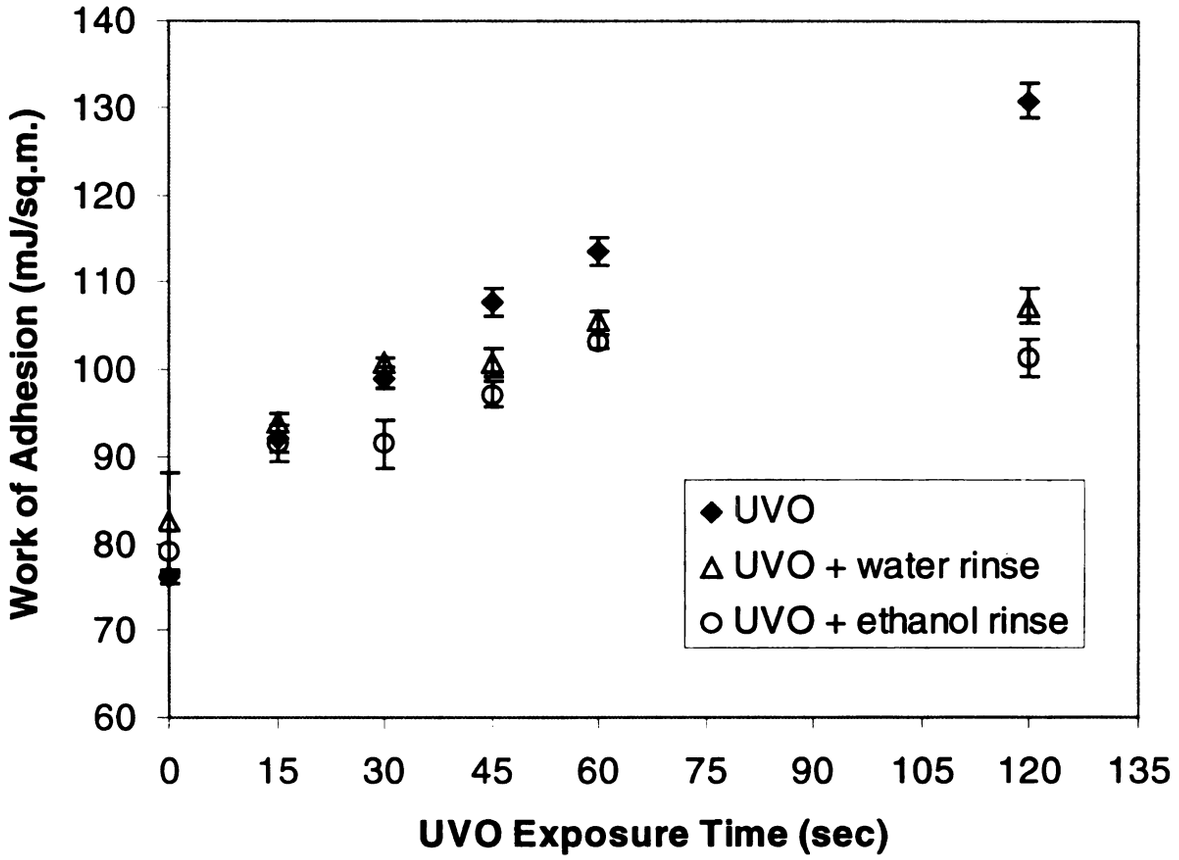

Figure 4.11 Work of adhesion for UVO treated PC after rinsing with water and ethanol.

Table 4.6 Comparison of UVV and UVO treatments after water rinse.

Treatment	C (%)	O (%)	O/C Ratio	Hydro-carbon (%)	Ether/ Hydroxyl (%)	Carbonyl (%)	Carboxyl (%)	Carbonate (%)
60 sec UVV + Ozone	80.7	19.3	0.24	60.2	13.9	1.7	1.7	3.2
60 sec UVV + Ozone + Washed	79.8	20.2	0.25	59.4	14.3	1.9	1.6	2.6
60sec UVO	71.0	29.0	0.41	43.4	13.4	5.9	6.4	1.9
60 sec UVO + Washed	78.5	21.5	0.27	57.0	13.1	3.6	3.1	1.8
600 sec UVO	64.5	32.6	0.50	28.8	13.8	7.5	13.3	1.0
600 sec UVO + Washed	83.0	16.5	0.20	62.7	12.2	3.7	3.5	0.9

4.8 Analysis of Adhesion Test Fracture Surfaces

Tensile and shear adhesion tests performed on UV treated polycarbonate, (see Chapter 3) did not show statistically significant changes in adhesive bond strength or modulus after UV treatment in spite of the higher surface energy and work of adhesion. The formation of an adhesive bond between two materials is a complicated process that depends on many factors including the mechanical properties of the surfaces, morphology, microstructure, and thermodynamic favorability. A strong thermodynamic driving force alone is not sufficient to guarantee strong adhesive bonds.

The failure of adhesive bonds in UV treated polycarbonate was investigated by fracture surface analysis using XPS. Tensile and shear adhesion samples were prepared using epoxy adhesive (Araldite® 2011) to bond an aluminum stub to the UV treated films. During testing, failure of the bond consistently occurs near the polycarbonate–epoxy interface based on visual examination. The two fracture surfaces thus generated are henceforth referred to as 'polycarbonate-side' and the 'adhesive-side' fracture surface. Determination of the locus of failure is an important step in analyzing the failure of adhesive bonds and both fracture surfaces were analyzed by XPS. Analysis of the polycarbonate-side fracture surface showed a surface resembling untreated polycarbonate even in UV treated samples. The analysis of the adhesive-side fracture surface provided more information. Figure 4.12 shows the C1s spectra for the cured epoxy adhesive and fracture surfaces for various UV treated samples.

The adhesive used was an amine cured epoxy that provides a unique nitrogen peak, which is absent in polycarbonate. Table 4.7 shows the atomic composition of cured epoxy adhesive and the adhesive-side fracture surfaces for untreated and UV treated PC

samples. Three samples were analyzed for each condition to ensure accuracy. The cured epoxy has 8.5% nitrogen and 6.1% oxygen on the surface. The adhesive-side fracture surfaces have a much lower nitrogen concentration ranging from 3-4% and a high oxygen concentration between 12-15%. The composition of the fracture surface was identical within experimental error for untreated PC, 30 and 120 sec UVO treated PC, and 120 sec UVO treated PC washed with water to remove low molecular weight material prior to bonding. The composition of the adhesive-side fracture surface is consistent with the presence of a thin layer of polycarbonate on top of the epoxy adhesive. The unique nitrogen tag atom on the epoxy allows further analysis by using the C/N ratio of the pure epoxy to apportion part of the carbon signal from the fracture surfaces to carbon atoms in the epoxy molecule. Using this methodology, the amount of C1s signal attributable to epoxy was calculated and is shown in Table 4.7. The remainder of the carbon signal on the fracture surfaces was attributed to polycarbonate.

The results show that the adhesive-side fracture surface, within the XPS sampling depth, is composed of 50-60% polycarbonate for all samples irrespective of surface treatment or removal of LMW material by washing. The percentage of polycarbonate may be slightly overestimated if the polycarbonate is present in the form of a continuous film on the adhesive surface because of a higher bias towards the top surface layers. Of more importance is the fact that UV treatment does not change the amount of polycarbonate removed. To determine if the material removed is indeed polycarbonate, weighted spectral subtraction of the epoxy C1s spectra from the fracture surface C1s spectra was performed.

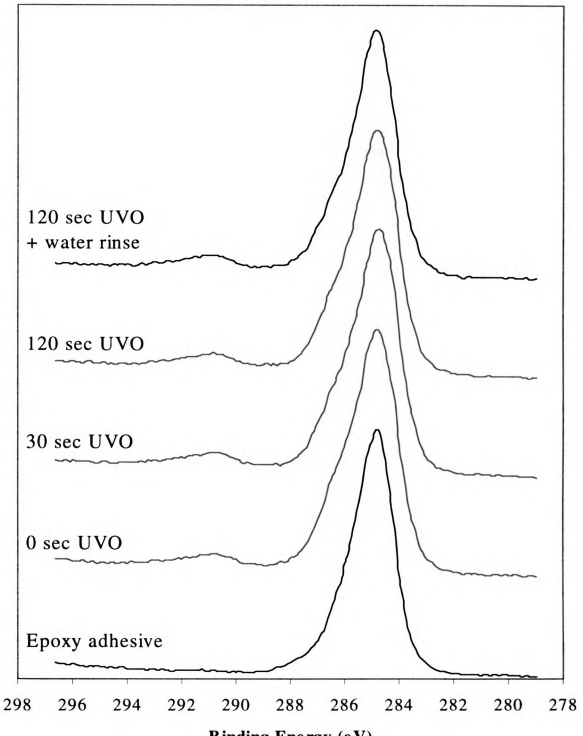

Figure 4.12 C1s spectra of epoxy adhesive and fracture surfaces (adhesive side) for 0 sec UVO, 30 sec UVO, 120 sec UVO, and 120 sec UVO + water rinsed PC.

Table 4.7 Atomic composition and analysis of adhesion test fracture surfaces (adhesive side) for UVO treated polycarbonate - epoxy bonds.

	C (%)	N (%)	O (%)	C/N Ratio	Epoxy (%)	PC (%)
Epoxy	85.4 ± 0.3	8.5 ± 0.2	6.1 ± 0.3	10.1 ± 0.2	100	0
0 sec UVO PC – Epoxy Failure Surface	82.0 ± 3.1	3.2 ± 0.8	14.8 ± 2.4	27.2 ± 8.1	39 ± 11	61 ± 11
30 sec UVO PC – Epoxy Failure Surface	83.1 ± 1.1	3.6 ± 0.9	13.3 ± 0.6	23.8 ± 5.3	44 ± 11	56 ± 11
120 sec UVO PC – Epoxy Failure Surface	81.8 ± 2.7	4.0 ± 1.0	14.3 ± 1.9	21.5 ± 5.6	49 ± 14	51 ± 14
120 sec UVO + water rinsed PC – Epoxy Failure Surface	84.9 ± 2	3.0 ± 0.7	12.1 ± 1.3	29.4 ± 8.1	36 ± 8	64 ± 8

The results of spectral subtraction are shown in Figure 4.13. The resultant spectra are very similar to polycarbonate with a pronounced shoulder indicating the ether/hydroxyl peak and the presence of the characteristic carbonate peak at 291 eV. Deconvolution of the C1s spectra showed a carbon distribution similar to that of polycarbonate.

The results of the fracture surface analysis are indicative of failure occurring approximately within the top 30-60 Å of the polycarbonate surface irrespective of whether the low molecular weight polymer formed by UVO oxidation is removed prior to bonding. Failures such as these are indicative of a weak boundary layer within the substrate or very high interfacial adhesion which propagates the crack into the relatively weaker substrate. This type of cohesive failure in the substrate also explains the invariance of adhesive bond strength after surface treatment. The results from nanoindentation tests show that the modulus of the polycarbonate in the top 500 nm of the surface increases after UVO treatment, but this increase in modulus may either be too small to effect a change in the macroscopic adhesive bond failure or of no consequence if bond failure is caused by a weak boundary layer near the surface.

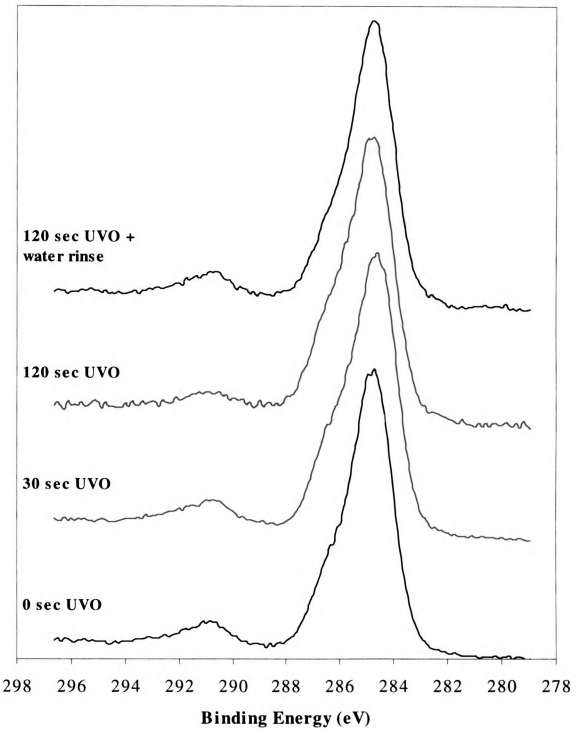

Figure 4.13 C1s spectral profile of adhesive fracture surfaces after subtraction of epoxy C1s signal for 0 sec UVO, 30 sec UVO, 120 sec UVO, and 120 sec UVO + water rinsed PC.

4.9 Summary

Polycarbonate surfaces were analyzed using XPS to characterize the chemical changes occurring on the surface during UV oxidation. The O/C ratios in UVO treated PC were found to depend on the irradiation received by the sample and, like the surface energy, showed no dependence on the irradiance levels or exposure time. Study of the functional groups created on the surface during UVO treatment show that the oxidation process occurs by reactions of ozone, and possibly the by-products of ozone dissociation, with the carbonate groups as well as the hydrocarbon bonds in the bisphenol-A structure.

When *in-situ* oxidation by ozone is prevented by irradiating samples in vacuum or inert gas atmosphere, active sites are created on the polycarbonate surface. The active sites thus generated are unreactive in air and do not show any uptake of oxygen even after many days of aging in ambient conditions. However, the surfaces retain their activity and readily undergo oxidation when exposed to ozone. The increase in oxygen content of these samples is beyond that expected from unirradiated, passive polymer samples exposed to ozone.

The rate of oxidation of activated surfaces, determined by measuring the increase in oxygen content as a function of ozone exposure, showed two distinct processes: i) a fast, initial incorporation of oxygen into the surface that is independent of the amount of irradiation received by the surface, and ii) a slower region of growth which shows direct dependence on the level of irradiation provided to the sample during treatment in a non-oxidative environment. The initial rapid uptake is attributed to the reaction of ozone with active sites in the top few monolayers of the material. Once the surface is depleted of active sites, further oxidation involves the slow diffusion of ozone into the sub-surface

layers to oxidize active sites in the polymer. The validity of this model was tested by derivatization experiments with silver nitrate which allowed differentiation between the oxygen signal contribution from the surface and sub-surface layers of the polymer.

The formation of water soluble low molecular weight oxidized material on the surface during UV treatment was observed. Differences in the amount of LMW material formed on *in-situ* and *ex-situ* oxidized samples provided indication of the different behavior of the polymer when irradiated in inert and oxidizing environments. Irradiation in non-oxidizing environments increases the possibility of radical recombination, or rearrangement, to form a smaller number of stable surface active sites. Irradiation in oxidizing environments enhances the total extent of oxidation because of aggressive reactions between the oxidizer and radicals created on the surface, but the higher extent of reaction can lead to extensive chain scission and formation of LMW fragments for longer treatment times.

Fracture surface analysis was used to determine the locus of failure in adhesion test samples. Fracture surfaces of the epoxy adhesive and polycarbonate substrates were analyzed and results obtained using spectral subtraction techniques showed the removal of approximately 30-60 Å of polycarbonate material by the epoxy adhesive. The cohesive failure in the substrate may be indicative of a weak boundary layer within the polycarbonate surface or a very high level of interfacial adhesion between the epoxy and polycarbonate which forces the locus of failure into the relatively weaker polycarbonate.

References

1. Briggs, D.; Seah, M.P. *Practical Surface Analysis Volume 1*, 2nd ed., pp. 450-454, Wiley, New York, 1983.

2. Dickie, R.A.; Hammond, J.S.; deVries, J.E.; Holubka, J.W. *Anal. Chem.*, Vol. 54, pp. 2045-2049, 1982.

3. Everhart, D.S.; Reilley, C.N. *Anal. Chem.*, Vol. 53, pp. 665-676, 1981.

4. Walzak, M.J.; Flynn, S.; Foerch, R.; Hill, J.M.; Karbashewski, E.; Lin, A.; Strobel, M. *Polymer Surface Modification; Relevance to Adhesion*, K.L. Mittal (Ed.), pp. 253-272, 1995.

5. Strobel, M.; Lyons, C.S. , *J. Adhesion Sci. Technol.*, Vol. 17, No. 1, pp. 15-23, 2003.

CHAPTER FIVE

UV TREATMENT OF POLYMERS

One of the advantages of the UV treatment process is its applicability to a wide range of materials. Surface modification of polymers such as polyethylene (PE) and polypropylene (PP) has always generated interest in the plastics industry because of the widespread use and poor adhesive performance of these materials. In recent years, the growing use of composites has drawn attention to surface treatments for thermosetting composite matrices such as epoxy. Rubbers and thermoplastic polyolefins (TPOs), which typically use hazardous chlorination treatments to enhance wettability, can also benefit greatly from UV surface treatment. The previous chapters described the results of UV modification of polycarbonate. In this chapter, the results of UV modification of several other polymers will be discussed in brief.

5.1 Epoxy

A diglycidal ether of bisphenol A (DGEBA) epoxy resin (Shell, Epon 828) cured with a polyoxypropylene triamine (Huntsman, Jeffamine T403) was used in this study. The structures of the two components are shown in Figure 5.1. The epoxide equivalent weight of the resin is 188 and the amine hydrogen equivalent weight of the curing agent is 81. The cured epoxy has some structural similarity with polycarbonate because of the bisphenol-A unit in the repeat unit. The resin and curing agent were mixed at 100:45 weight ratio and cured at 85°C for 2 hours in an open Teflon® mold followed by postcuring at 150°C for 2 hours. The cured epoxy was cut with a diamond blade saw and

washed with detergent and deionized water to remove traces of cutting lubricants from the surface. The epoxy surface exposed to air during cure was used as the test surface. The polymer was UVO treated using the RC 747 lamp at various irradiance values and contact angles were measured with five liquids, as described in Chapter 2, to determine the surface energy.

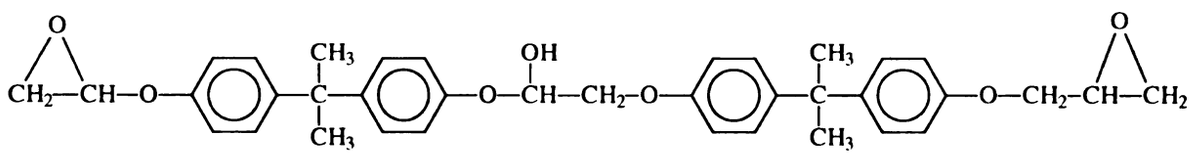

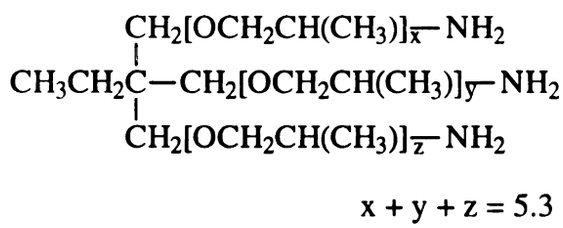

$x + y + z = 5.3$

Figure 5.1 Chemical structures of Epon 828 (top) and Jeffamine T403 (bottom).

Figure 5.2 shows the work of adhesion of the UVO treated surfaces with water as a function of total irradiation. The work of adhesion increases after treatment to an asymptotic value of 130-140 mJ/m^2. Samples were treated at various combinations of irradiance and time, but, as in the case of polycarbonate, the work of adhesion does not show any independent influence of the irradiance or time and only depends on the total irradiation. The change in the work of adhesion is caused by the incorporation of oxygen on the surface. XPS analysis shows an increase in the surface O/C ratio from 0.18 to 0.53 after 320 mJ/cm^2 UVO irradiation. The detailed XPS results are given in Table 5.1.

Analysis of the spectra shows significant increases in the hydroxyl, carbonyl and carboxylate functionality after UVO treatment while the concentration of carbon in hydrocarbon and ether bonds decreases suggesting chain scission and oxidation of the ether linkages and aromatic/aliphatic structures in the epoxy [1]. Although ethers and hydroxyls cannot be distinguished from the C1s spectra alone, the O1s peak clearly shows an increase in the hydroxyl concentration on the surface implying the decrease in the ether/hydroxyl peak in the C1s spectra must be because of a decrease in the ether concentration.

The addition of oxygen functional groups on the surface leads to an increase in the surface energy as shown in Figures 5.3 and 5.4. Increases in surface polarity (polar-dispersive model) and the Lewis base component (acid-base model) are appreciable and are the main contributors to the total increase in surface energy.

Table 5.1 Surface chemical composition of UVO treated epoxy.

	C (%)	N (%)	O (%)	O/C	Hydrocarbon (%) (C1s peak)	Ether/Hydroxyl (%) (C1s peak)	Carbonyl (%) (C1s peak)	Carboxylate (%) (C1s peak)	Hydroxyl (%) (O1s peak, 531 eV)
Untreated	82.4	2.4	15.2	0.18	49.9	27.9	4.6	0.0	1.4
60s UVO	70.6	2.9	26.5	0.38	39.2	17.8	7.2	6.3	11.3
120s UVO	63.4	3.3	33.4	0.53	23.7	19.8	9.6	10.3	11.2

Values expressed as percentages of total surface.

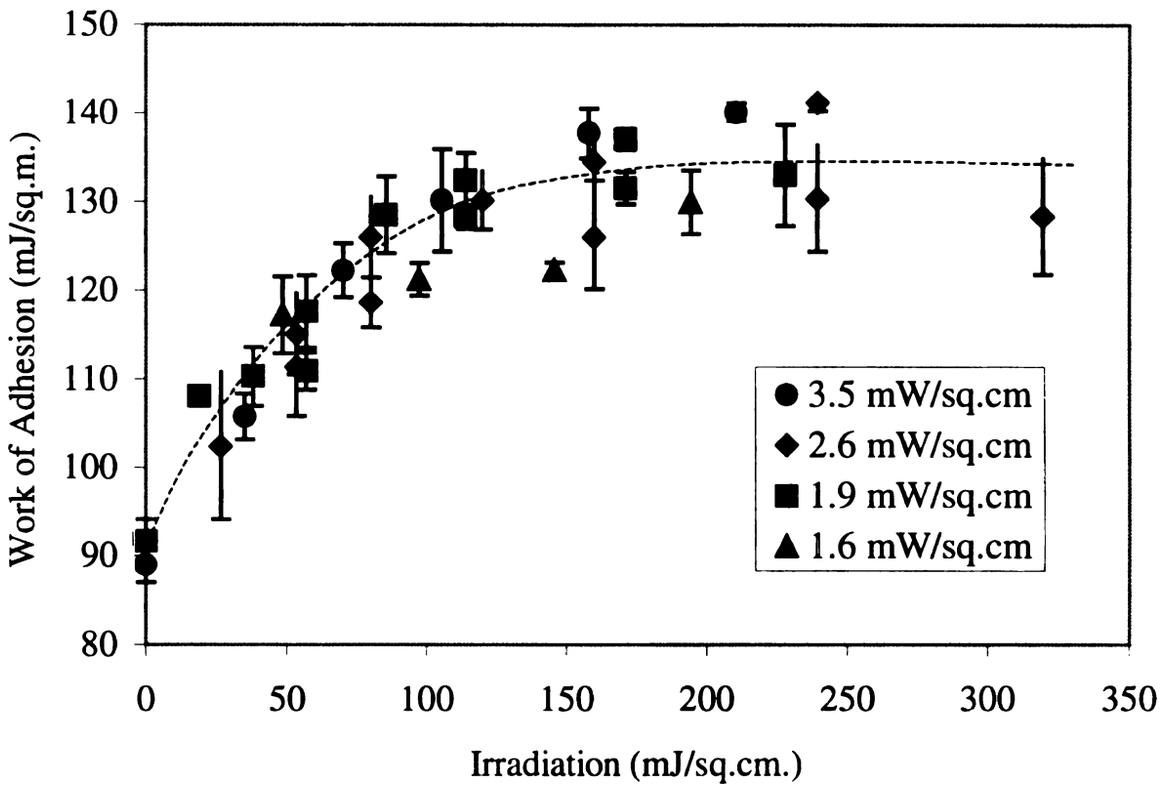

Figure 5.2 Work of adhesion of UVO treated epoxy with deionized water as a function of irradiation. Data obtained at various combinations of irradiance and exposure time.

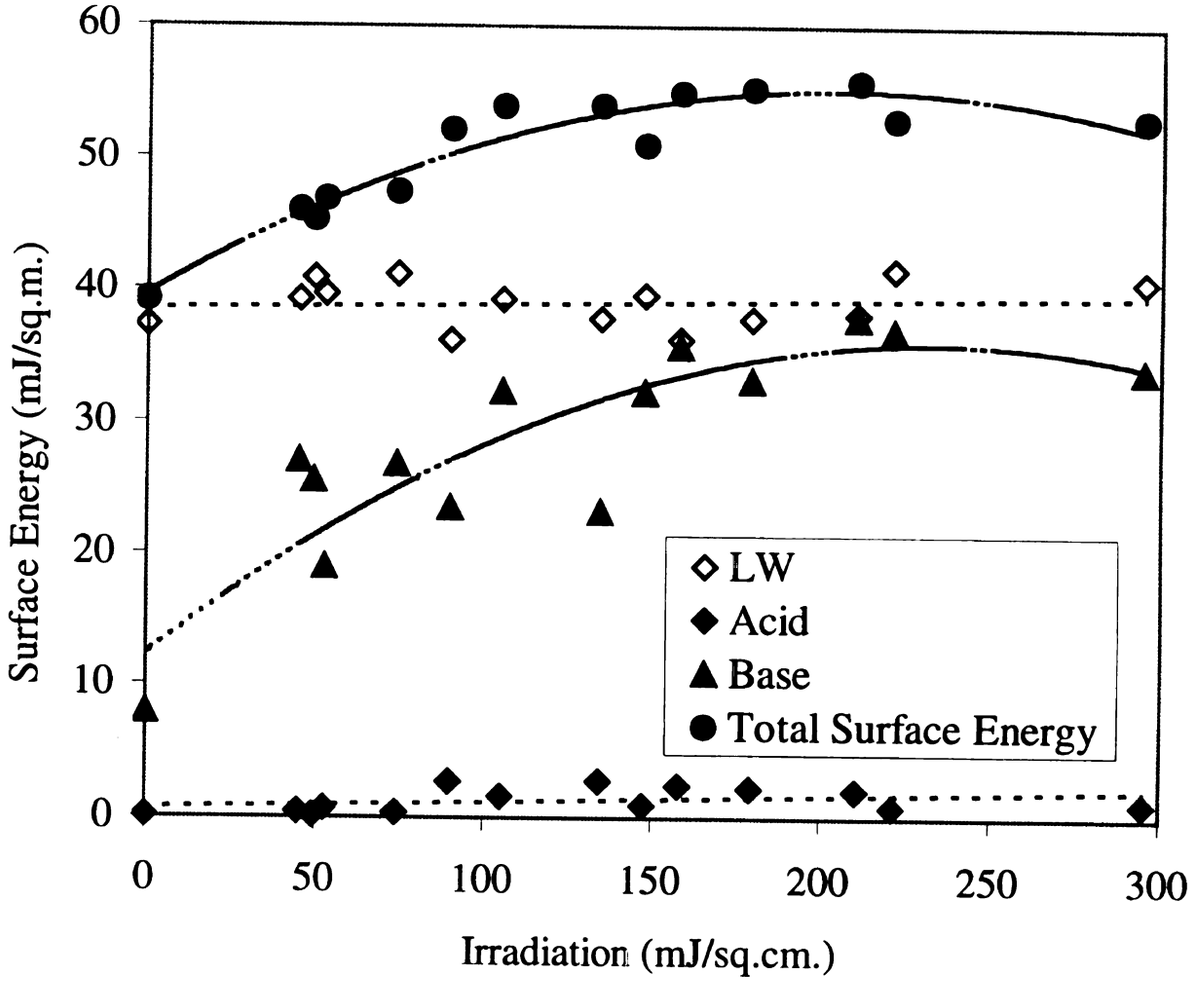

Figure 5.3 Acid-Base surface energy of UVO treated epoxy at various combinations of irradiance and exposure time.

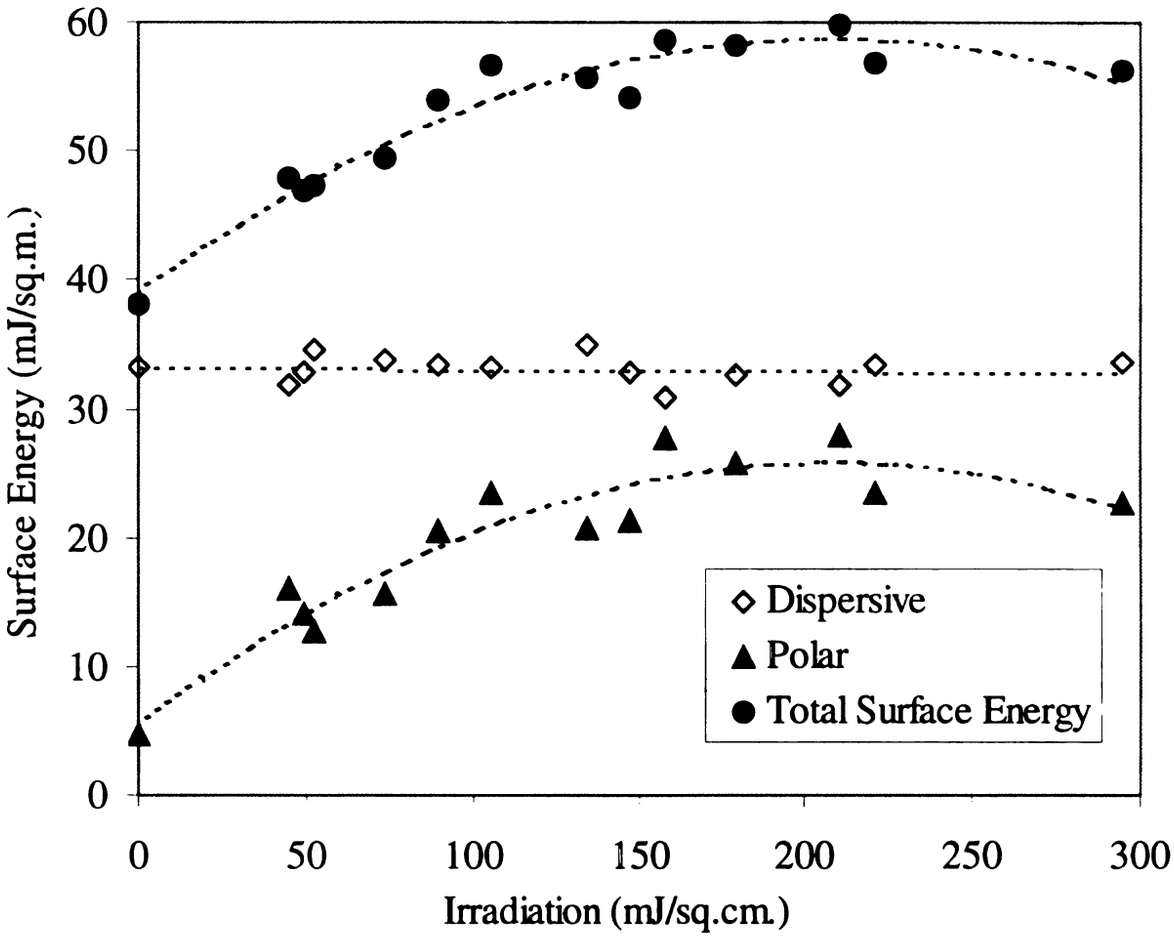

Figure 5.4 Polar-Dispersive surface energy of UVO treated epoxy at various combinations of irradiance and exposure time.

5.2 Crosslinked Tire Rubber Compound

A polydiene rubber compound was obtained in the form of sheets from Goodyear Tire Co. The exact composition of the rubber, used in tire manufacture, is unknown but typically tire rubber compounds are blends of natural and butadiene based synthetic rubbers with high carbon black loadings, UV stabilizers, and anti-oxidants to retard photodegradation and oxidative aging of the material [2]. The untreated elastomer is highly hydrophobic with a water contact angle over 120°. The surface of the rubber sheets has a rough texture which may cause hydrophobic contact angles to be higher, and hydrophilic angles to be lower, than that measured on a chemically equivalent smooth surface [3]. UVO treatment of the material yields a highly hydrophilic surface with a contact angle of 20° and a corresponding increase in the work of adhesion with water from approximately 30 mJ/m^2 to 140 mJ/m^2.

Rubber samples were treated using the RC 747 lamp at different irradiances and times, but the work of adhesion was found to be independent of both and only varies with total irradiation as shown in Figure 5.5. The rate of change in the work of adhesion for rubber is very high because of the high susceptibility of the unsaturated butadiene segments in the elastomer backbone to photooxidation in the presence of ozone.

The presence of carbon black in rubber leads to heating of the surface as the material is exposed to radiation, especially the infrared radiation emanating from the UV lamp. The effect of surface temperature on the observed properties was studied using the RC 500 lamp. Surface temperatures were measured by an infrared pyrometer using an emissivity value of 0.95 for the polymer. Table 5.2 shows the temperature rise in the surface of a rubber sample placed 20 mm away from the UV lamp.

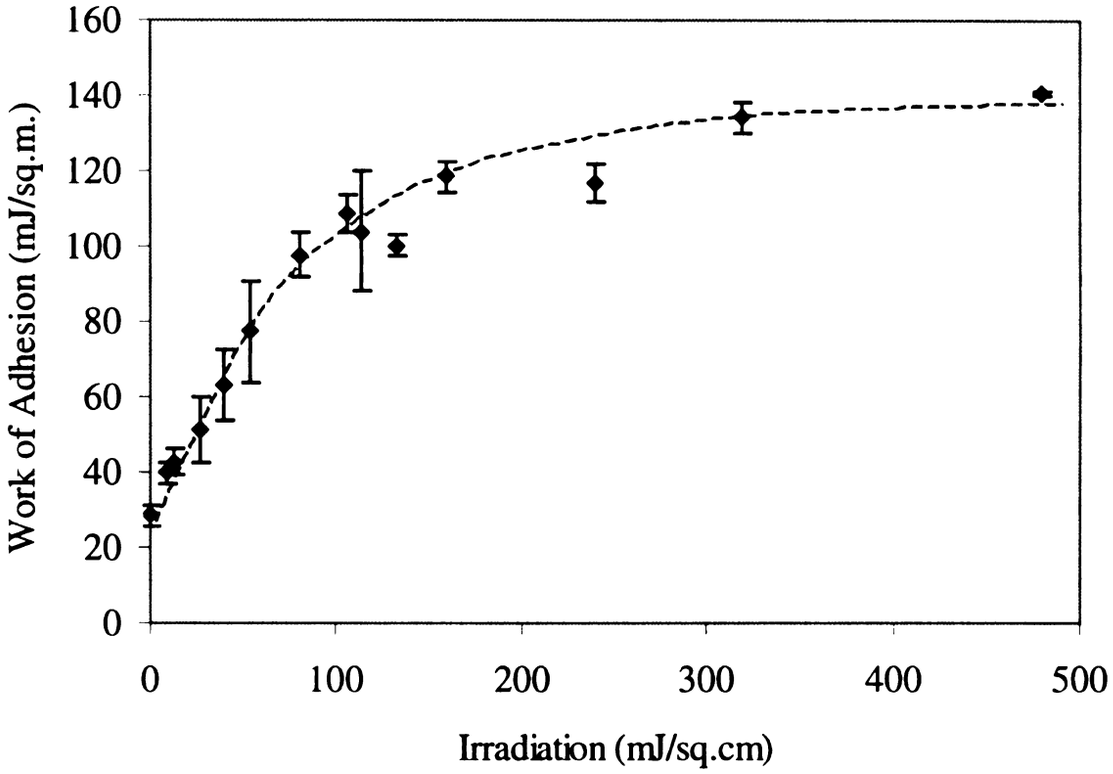

Figure 5.5 Work of adhesion of UVO treated crosslinked tire rubber compound with deionized water as a function of irradiation. Data obtained at various combinations of irradiance and exposure time.

Table 5.2 Temperature of crosslinked tire rubber compound surface after UV exposure in RC 500 lamp.

Exposure Time (RC 500 lamp, 20 mm)	Temperature (°C)
0 sec	24 ± 1
30 sec	79 ± 2
60 sec	107 ± 3
120 sec	139 ± 12
240 sec	158 ± 5

The surface temperature can be a very important variable in the treatment of low T_g polymers such as elastomers because the high energy polar functional groups introduced on the surface by oxidation experience a thermodynamic driving force to reorient below the surface in an effort to reduce the overall surface energy of the material. This reorientation can occur more easily in polymers above the Tg due to enhanced chain mobility caused by an increase in the free volume. The effect of reorientation was studied in rubber by comparison of contact angles in samples allowed to reach high temperatures and samples whose surface temperature was maintained below 75°C by intermittent UV exposure to allow cooling of the surface. The intermittent exposure cycle used for lowering the rubber surface temperature when exposed to the RC 500 lamp was: 30 seconds on, 30 seconds off. Only the 'on' segments are used to calculate the total UV exposure time. Table 5.3 shows the strong effect of temperature on the rubber contact angle. A similar effect of temperature was observed in the surface composition and wettability of UVO treated polyethylene (section 5.5) and Bexloy® (section 5.6).

Table 5.3 Effect of temperature on UVO treated crosslinked tire rubber compound.

Treatment	Exposure Cycle	Maximum Temp. (°C)	Contact Angle (deg)
Untreated	--	24 ± 1	120 ± 5
120 sec Ozone	Continuous Ozonation	24 ± 1	120 ± 6
120 sec UVO	Continuous UVO (120 Hz)	139 ± 12	64 ± 29
120 sec UVO	Intermittent UVO (120 Hz) 30 sec On + 30 sec Off	69 ± 5	20 ± 4

5.3 Poly(ethylene terephthalate)

The polyethylene terephthalate (PET) polyester (Melinex®, Dupont Teijin Films) was obtained in the form of biaxially oriented sheets of 125 micron thickness. The chemical structure of PET is shown in Figure 5.6.

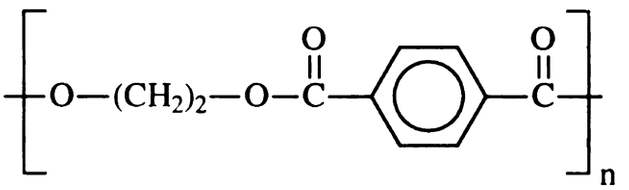

Figure 5.6 Chemical structure of PET.

Samples were UVO treated using the RC 747 lamp at different irradiances and times. Figure 5.7 shows the work of adhesion with water for PET at various values of irradiation. The work of adhesion was found to be independent of both irradiance and time, and only varies with the total irradiation.

Table 5.4 describes the chemical changes on the PET surface before and after UVO treatment. The untreated PET has a O/C ratio of ca. 0.33 which increases to ca. 0.44 after 120 seconds of UVO exposure. Details of the C1s spectrum for the untreated PET shows approximately 48% hydrocarbon, 15% ether/hydroxyl, and 10% carboxylate carbon atoms on the surface. The errors associated with the above concentrations are approximately 10%. Following UVO treatment, there is a 11-12% decrease in carbon atoms with hydrocarbon bonds and a slight increase in the carboxylate carbon content indicating oxidation of the polymer.

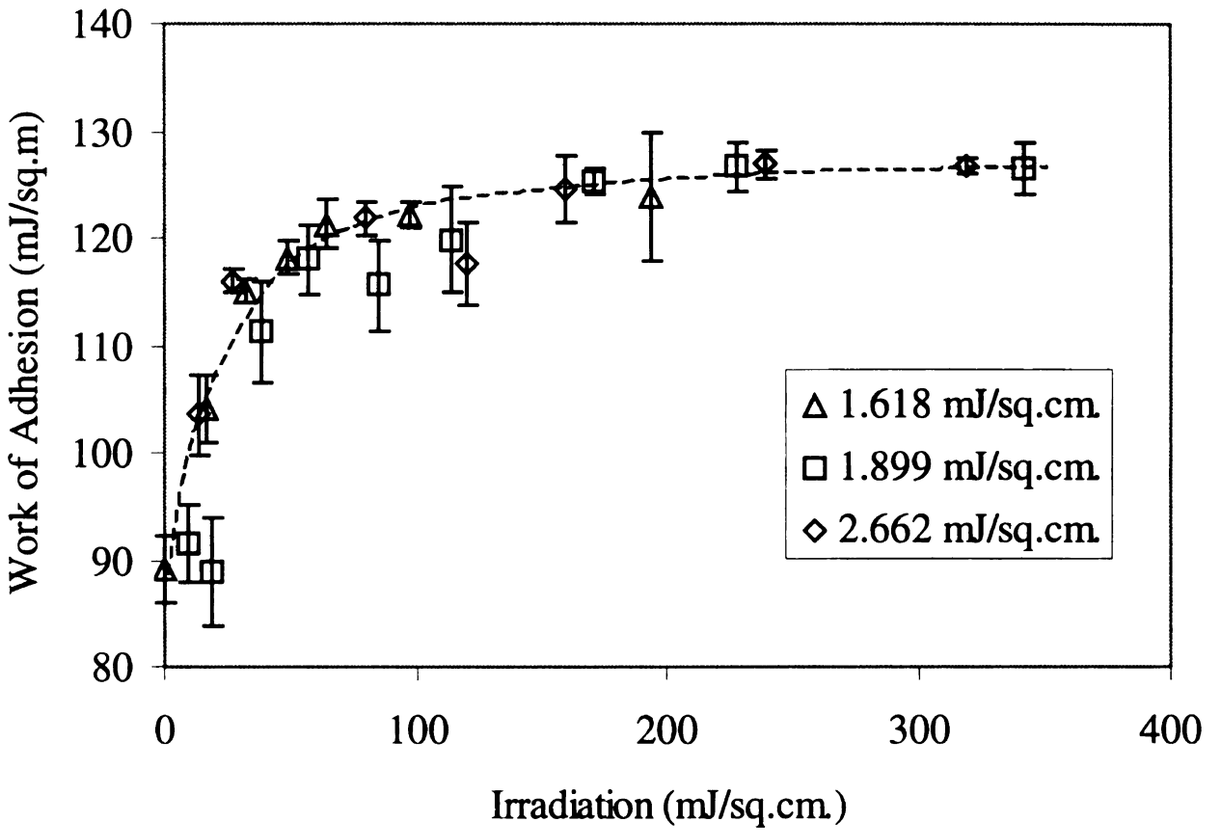

Figure 5.7 Work of adhesion of UVO treated PET with deionized water as a function of irradiation. Data obtained at various combinations of irradiance and exposure time.

Table 5.4 Surface chemistry and atomic composition of UVO treated PET surface

	C (%)	O (%)	O/C Ratio	C-C (%)	Ether/ Hydroxyl (%)	Carbonyl (%)	Carboyxlate (%)
Untreated	74.3	24.5	0.33	48.4	14.9	0.0	10.0
60 sec UVO	69.6	28.8	0.41	39.6	15.7	0.0	13.2
120 sec UVO	68.1	29.9	0.44	36.6	15.7	1.1	13.4

5.4 Poly(tetrafluoro ethylene)

Polytetrafluoroethylene (PTFE, Teflon®) is an inert polymer with very high resistance to thermal and photodegradation, oxidation, and chemical attack because of the stable bonds between carbon and the highly electronegative fluorine atom. Figure 5.8 shows the chemical structure of PTFE. The UV radiation available from xenon lamps is of insufficient energy to cause $\sigma \rightarrow \sigma^*$ transitions in C-F bonds. Surface modification of fluorinated polymers is very difficult and often involves changing the topography of the surface to enhance adhesion by means of increasing contributions from mechanical interlocking processes. Aggressive treatments such as plasma etching and oxidation are more often needed to modify PTFE.

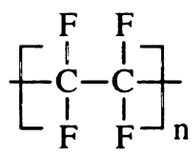

Figure 5.8 Chemical structure of PTFE.

The strong carbon-fluorine bond has very low absorption in the wavelength range available from xenon lamps and no change in surface energy is expected after UVO treatment. PTFE samples were UVO treated using the RC747 lamp and approximately 700 ppm ozone. The contact angles before treatment were approximately 110° and did not change even after extended UV exposure as shown in Figure 5.9.

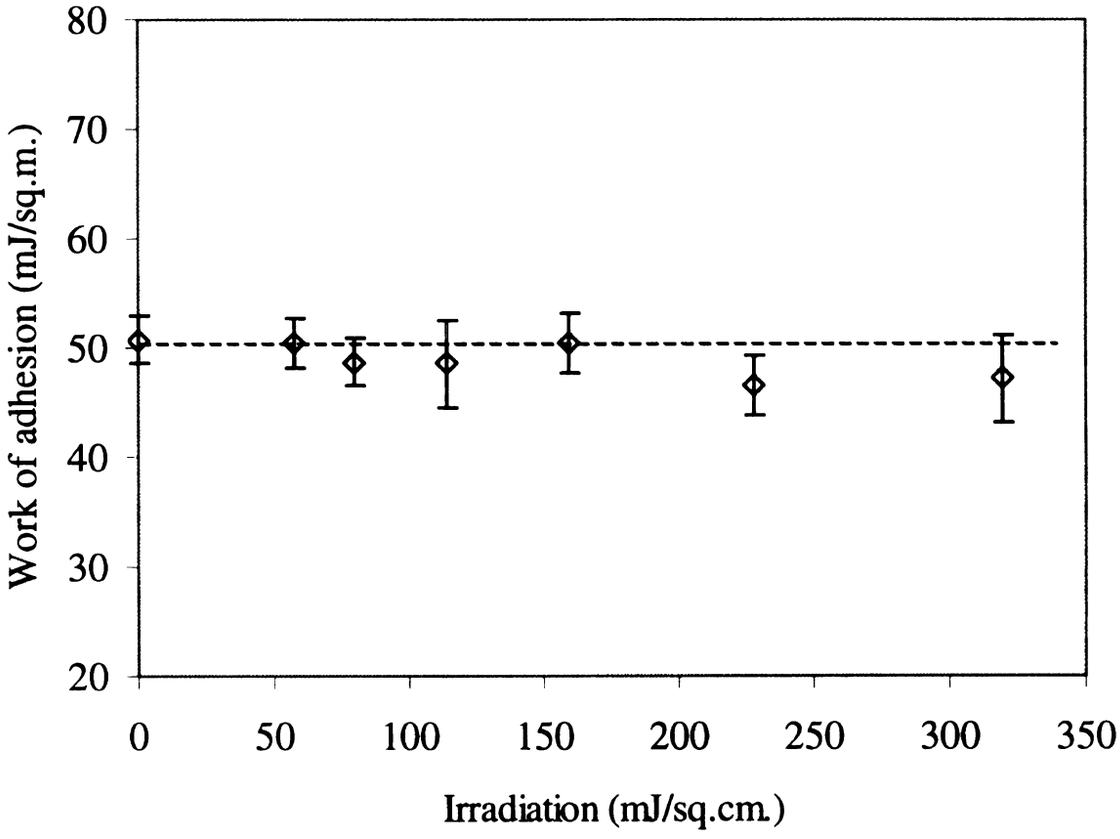

Figure 5.9 Work of adhesion of UVO treated PTFE with deionized water as a function of irradiation.

5.5 Polyolefins

Polyolefins represent one of the major groups of polymers used in the consumer goods industry. Polyethylene (PE), polypropylene (PP), and polypropylene based thermoplastic polyolefin elastomers (TPO) are the commercially important polymers in this class. Polyolefins have simple structures comprising of C-H bonds that are very stable under UV irradiation. The stability of C-H bonds is a result of the high energy required for $\sigma \rightarrow \sigma^*$ transitions. Typically this energy is available only in wavelengths below 160 nm. UV irradiation with a xenon lamp should theoretically not have any effect on saturated polyolefins. However, saturated polyolefins have been the subject of many studies [4-13] which show that it is possible to oxidize and modify these materials. The consensus is that oxidation in these materials is sensitized by internal and processing impurities. Internal impurities include main chain unsaturation, catalyst residues from the manufacturing process, and carbonyl groups formed by adventitious oxidation. Processing impurities can include hydroperoxides, carbonyl groups, and transition metal ions from polymer processing equipment [1]. UV irradiation forms free radicals at these impurity sites and further reactions of the polymer with the free radicals leads to chain scission, crosslinking, and oxidation. Three types of polymers, an ultra high molecular weight polyethylene (UHMWPE), PP, and TPO were studied.

UHMWPE samples were abraded with 360 and 600 grit wet sandpaper for 5 mins to remove any contaminated surface layers and washed with water prior to irradiation using the RC500 lamp. Initial experiments showed the UHMWPE surfaces to be very difficult to treat. Table 5.5 shows the results of contact angle measurements on UHMWPE after UVO treatment. The contact angles of untreated UHMWPE did not

show any appreciable statistically significant change. The surface temperature of the PE was measured to be approximately 100°C after 120 seconds of UV exposure. The Tg of polyethylene is –78°C, which, as mentioned in the previous section, can lead to surface reorientation at high temperatures. Samples were treated at low temperatures by intermittent irradiation for 15 seconds followed by a dark cooling period of 60 seconds. The maximum temperatures recorded for the intermittently irradiated samples was approximately 40°C. The low temperature treatment enhances the wettability of the polymer. The adhesive bond strength of the treated surfaces with epoxy adhesive (Araldite 2011) is shown in Figure 5.10. Increases in the adhesive bond strength up to 300% were measured for UVO treated UHMWPE.

Polypropylene was obtained in the form of powder (KE020, Montell) and injection molded into plaques. A reactor grade TPO based on polypropylene and ethylene-propylene rubber (Equistar) was also studied. The two materials behave very similarly, and contact angles of the untreated material range from 90°-100° and UVO treatment does not change the contact angles significantly. However, adhesion tests show a large increase in the adhesive bond strength of these materials. Table 5.6 shows the XPS analysis of UVO treated PP and TPO. The O/C ratio of both PP and TPO increases following UVO treatment and the oxygen incorporated into the surface is mainly in the form of ethers which are relatively non-polar and hence do not contribute to an increase in surface energy. The irradiation of saturated polyolefins can lead to the formation of extensive crosslinks in the polymer [5,6,9]. The increase in the adhesive bond strength of UVO treated materials is thus most likely a result of surface crosslinking which increases the modulus of the surface. In the case of TPO, some silicon is measured and this is likely

from a process additive blooming to the surface from the bulk. After UVO treatment, the silicon content increases suggesting an increase in the bloom caused by heating of the substrate during treatment. In spite of the silicon bloom, adhesive strength increases by 400-500% in the case of TPO as shown in Figure 5.11.

Table 5.5. Water contact angles of Ultra-High Molecular Weight Polyethylene after UVO treatments with and without thermal management.

Treatment	Contact Angle (Temp ≈ 100°C)	Contact Angle (Temp ≈ 40°C)
Untreated	100 ± 8	100 ± 8
30 sec UVO	97 ± 4	--
60 sec UVO	94 ± 3	89 ± 2
120 s UVO	88 ± 2	67 ± 6

Table 5.6 Surface chemistry of PP and TPO after UVO treatment.

Material	C (%)	O(%)	Si(%)	O/C	Si/C
Untreated PP	97.3	2.7	--	0.03	--
120 sec UVO PP	87.0	13.0	--	0.15	--
Untreated TPO	91.9	6.3	1.9	0.06	0.02
120 sec UVO TPO	82.2	14.0	3.8	0.17	0.05

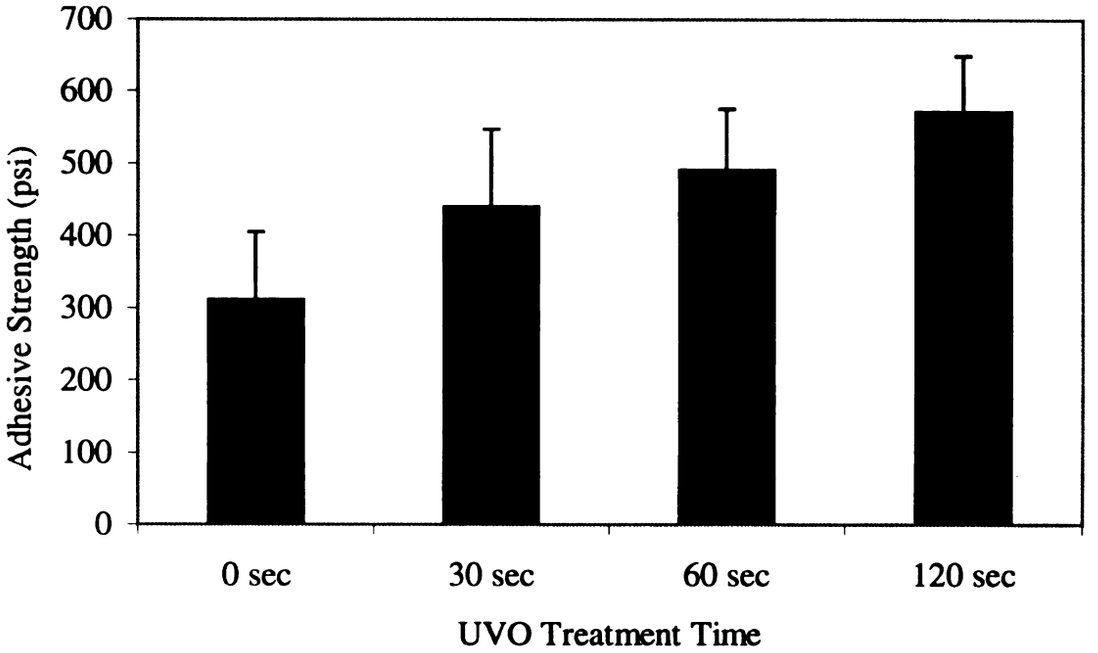

Figure 5.10 Stub pull adhesive bond strength of UVO treated UHMWPE.

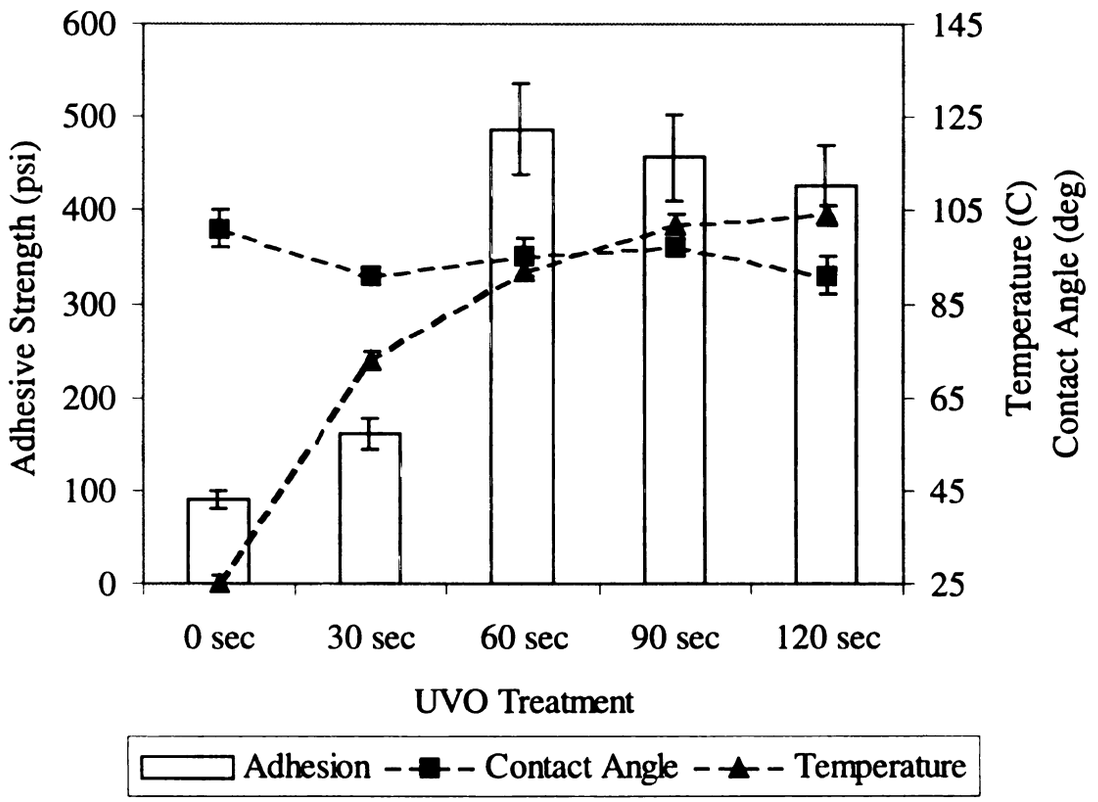

Figure 5.11 Adhesive strength, contact angles and surface temperature of UVO treated TPO showing no significant change in contact angles despite the increase in adhesive bond strength.

5.6 Ionomers (Bexloy®W)

Bexloy®W (DuPont) is a glass filled composite based on Surlyn®, an ionomer of ethylene methacrylic acid copolymers. The ionomer is made by neutralizing part of the methacrylic acid with metal ions such as sodium. The polymer structure has three regions: amorphous polymer, crystalline polymer, and ionic clusters which act as crosslinks in the material. The polymer has a low glass transition temperature (Tg) and increasing the temperature of the polymer causes the domains to lose structure and undergo reorientation. The Tg of the Bexloy®W used was 50°C.

UVO treated Bexloy®W sheets were analyzed by XPS and contact angle measurements[1]. Samples were treated under continuous and intermittent UV exposure. Continuous exposure caused the polymer surface temperature to exceed the Tg whereas intermittent exposure cycles with 30 second exposure and 30 second dark cooling period was sufficient to limit the surface temperature to below 50°C.. The results are shown in Figure 5.12. The O/C ratio and wettability increases with UVO exposure as long as the temperature was maintained below the Tg. When the temperature was allowed to exceed the Tg, and immediate decrease in the O/C ratio and wettability was observed. The time of irradiation was found to have no effect on this reorientation as samples treated for longer times at temperatures below 50°C did not show any reorientation.

[1] Experiments performed by Dr. Per A. Askeland, Composite Materials & Structures Center, Michigan State University.

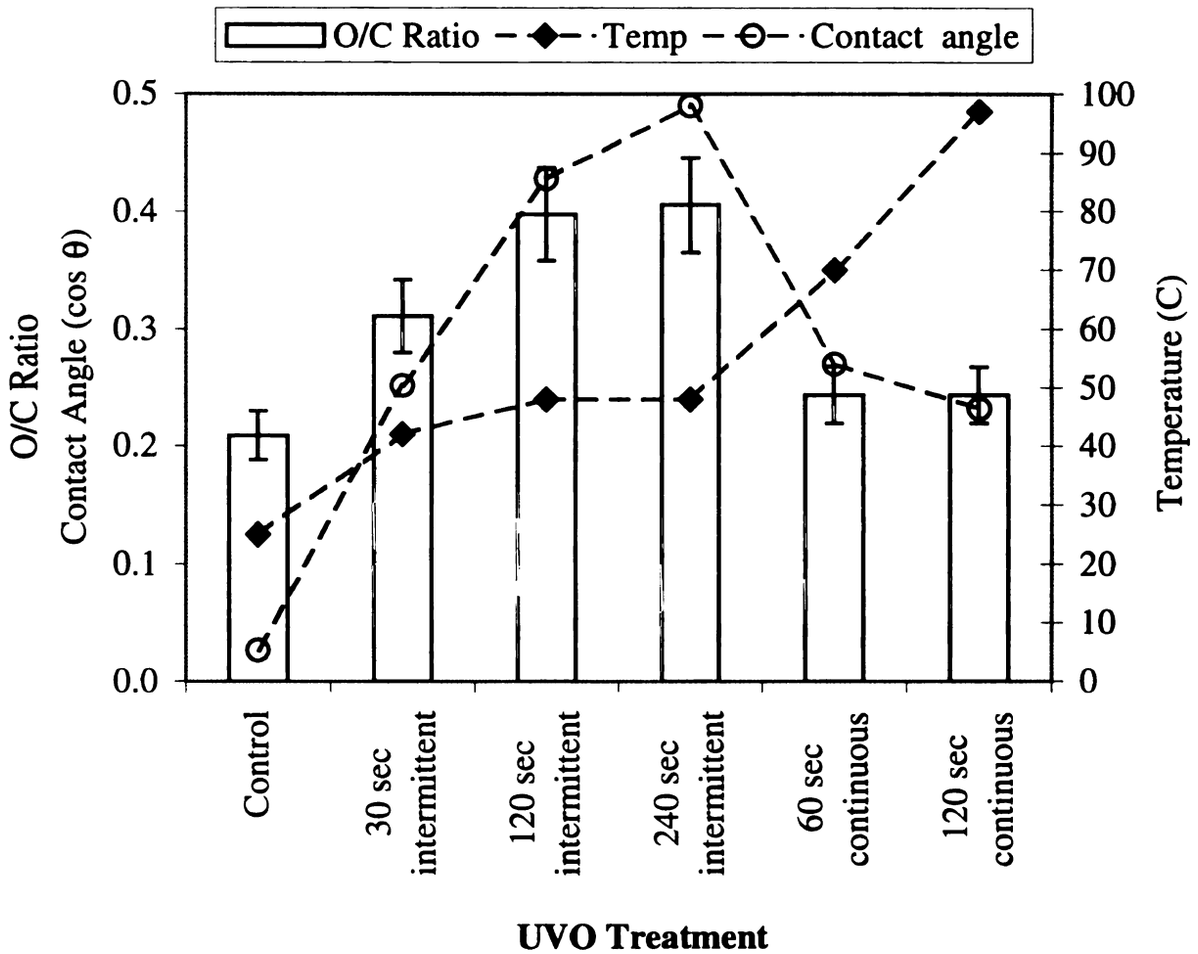

Figure 5.12 O/C ratio, contact angles and surface temperature of UVO treated Bexloy®W showing surface reorientation effect above the Tg (50°C).

5.7 Summary

The surface modification of some common polymers with UVO treatment was described in this chapter. For most materials, sharp increases in the surface oxygen, wettability, and adhesive strength are observed. The properties of epoxy, PET, and rubber were studied in detail and the wettability was found to depend entirely on the amount of irradiation given to the sample. In the case of rubber, a strong effect of temperature on the surface properties was also observed. The rise in surface temperature caused by exposure to UV and IR radiation from the lamp was observed to cause reorientation of the oxidized polar groups. The effect of this regeneration is readily observed by the decrease in wettability. This regeneration of the low energy surface was also observed very clearly in thermoplastics like polyethylene and Bexloy®W polymers above their glass transition temperatures.

The adhesive strength of surfaces depends on many factors other than surface energetic favorability. In polymers like PP and TPO, the wettability of the surface does not change after UVO treatment. However, the adhesive strength increases by 400% to 500% of the untreated material. This is believed to be an effect of the crosslinking of the surface and near-surface polymer leading to the formation of high modulus material at the interphase which can enhance adhesion.

Almost all materials treated with UVO show beneficial changes in properties except fluorocarbon based polymers. The fluorocarbon bond is very strong and UV radiation in the range provided by xenon lamps is not energetic to cause excitations in the C-F bond. Teflon did not show any changes in the surface properties even after long exposures to UVO. With the help of the phenomenological data obtained for various

types of polymers, the following chapter will attempt to identify trends in various UV treatment process and model the changes in a way that can be easily applied in industry to understand and predict the properties of UVO treated materials.

References

1. Rabek, J.F. *Mechanisms of Photophysical Processes and Photochemical Reactions in Polymers*, John Wiley, New York, 1987.

2. Brydson, J.A.; *Plastics Materials*, 5th ed., London, 1989.

3. Adamson, A.W. *Physical Chemistry of Surfaces*, 5th ed., Wiley Interscience, New York, 1990.

4. Dasgupta, S. *Journal of Applied Polymer Science*, Vol. 41, pp. 233-248, 1990.

5. Qu, B.; Ranby, B. *Journal of Applied Polymer Science*, Vol. 49, pp. 1799-1807, 1993.

6. Ranby, B. *Polymer Engineering and Science*, Vol. 38, No. 8, pp. 1229 –1243, 1998.

7. Wilken, R.; Hollander, A.; Behnisch, J. *Macromolecules*, Vol. 31, pp. 7613-7617, 1998.

8. Strobel, M.; Jones, V.; Lyons, C.S.; Ulsh, M.; Kushner, M.J.; Dorai, R.; Branch, M.C. *Plasmas and Polymers*, Vol. 8, No. 1, pp. 61-95, 2003.

9. Yu, J.R.; Chen, Z.L.; Zhu, J.; Liu, Z.F.; Wang, Q.R. *Intern. Polymer Processing*, XIV, 4, pp. 331-335, 1999.

10. Pasternak, M. *Journal of Applied Polymer Science*, Vol. 57, pp. 1211-1216, 1995.

11. Macmanus, L.F.; Walzak, M.J.; Mcintyre, N.S. *Journal of Polymer Science: Part A: Polymer Chemistry*, Vol. 37, pp. 2489-2501, 1999.

12. Gijsman, P.; Sampers, J. *Polymer Degradation and Stability*, Vol. 58, pp. 55-59, 1997.

13. Gijsman, P.; Meijers, G.; Vitarelli, G. *Polymer Degradation and Stability*, Vol. 65, pp. 433-441, 1999.

CHAPTER SIX

DISCUSSIONS AND PROCESS MODEL

In the preceeding chapters, the effects of UV modification on the surface properties of various polymers have been discussed. This chapter will provide an overview of the process and discussions about the effects of different process variables, followed by a proposed process model that can be used as a predictive tool for estimating surface properties of UV modified polymers.

6.1 Process Variables

The main variables which can be controlled in the UV treatment process are: spectral output of the UV lamp, lamp pulse frequency, irradiance, exposure time, temperature, humidity, and ozone concentration. The effect and importance of these variables are discussed below.

6.1.1 Spectral Output

Pulsed xenon flashlamps were used in this study because of the strong spectral output of these lamps in the UV-C region, which provides radiation at 185 nm and above. Analysis of polymers UVO treated through a Pyrex® window acting as a 280 nm high pass filter showed no appreciable change in the surface properties. This is because of two reasons: i) the ozone absorption maximum (λ_{max}) is at 254 nm and in the absence of this wavelength, photodissociation of ozone does not occur, and ii) most engineering and commodity polymers are designed to withstand ground level exposure to solar irradiation

and consequently do not have chromophores with very high absorption coefficients above 300 nm, or are modified to enhance stability at those wavelengths [1]. The presence of continuous radiation in the 185 nm – 280 nm is thus essential for UV treatment. Considering the ultimate goal of developing the UV treatment process to modify a vast range of polymers, which may have widely different UV absorption bands, the use of lamps with continuous spectral output, as opposed to line output, is also essential. In this respect, xenon flashlamps are preferred over mercury lamps because of their broader output especially at wavelengths below 254 nm.

Excimer lamps and lasers also suffer the handicap of narrow spectral outputs which may be able to excite a specific chromophore in a polymer but may have no effect on a slightly different chromophore. The absorption profiles of most organic bonds become virtually continuous in the VUV region (below 185 nm) because of the close spacing of the excited energy levels [2], and conceptually, surfaces can be UV oxidized more efficiently under VUV irradiation, but the drawback of using VUV radiation is the strong absorption by oxygen which necessitates exposure in vacuum. In a commercial process, the use of vacuum is a severely limiting factor, not only in terms of complicated equipment, but also in terms of low throughputs and the necessity of batch operations as opposed to continuous operations. The use of xenon flashlamps with strong output between 185 and 280 nm makes it possible to treat the widest range of polymers in ambient conditions and makes the process more adaptable to continuous processing in manufacturing environments.

6.1.2 Irradiance

The effect of irradiance on the changes observed in surface properties for a wide range of polymers has been previously described in detail in Chapters 3, 4, and 5. For all the polymers evaluated in this study, it was possible to achieve identical surface properties even when the irradiance (power) was varied by a factor of five as long as the total energy incident on the surface (irradiation) was equal. In terms of irradiation of the surface, this implies a trade-off between the irradiance and time. Samples exposed to long exposures at low power, and short exposures at high power, were found to have equivalent surface properties. Thus it can be concluded that irradiance itself is not a controlling process variable in the UV treatment of surfaces.

However, such a broad conclusion can only be made for the surface of the material and does not describe the changes occuring within the material. For a polymer following Beer's law of absorption [1], which states that the intensity of radiation I, at a depth of b from the surface in a material with absorptivity ε, concentration c, and incident intensity I_o, is given by $I = I_o\ 10^{-ecb}$, the irradiance at any depth is dependent on the incident irradiance. If the modification is a function of irradiation, then a change in irradiance will affect the depth of penetration of the radiation, and possibly the depth of modification. Equivalent irradiation at low irradiance (low power) should then be expected to have lesser penetration into the material compared to irradiation at high irradiance (high power). Thus, the trade-off between power and time could affect the depth of treatment and possibly the properties of the bulk material. It is important to reflect on the use of the term 'treatment' in the context of changes occuring below the polymer surface. The modification of a polymer by UV and ozone encompasses a variety

of processes including photolysis, photorearrangement, photooxidation, and crosslinking. Moreover, the concentrations of quenching species like oxygen and ozone in the bulk polymer are very different from that on the surface and can affect the rates of free radical recombination in the bulk polymer. The balance between these multiple parallel processes can change with depth and affect what is conveniently termed the 'treatment' of the bulk polymer. Although the effective depth of penetration of the photons in the polymer is known, the effect of that irradiation on the polymer can be very different from what is observed on the surface. Due to the difficulties involved in measuring properties at spatial resolution of monolayers, the effect on the depth of treatment has not yet been measured. The evolution of properties in the bulk polymer as a function of depth in the near surface polymer is one of the areas which needs to be investigated in the future.

Another assumption in this study concerns the measurement of irradiance. UV irradiance at 254 nm was measured with a 10 nm bandpass filter. The spectral irradiance over the entire UV-C spectrum ranging from 185 – 280 nm was not measured due to the unavailability of a NIST calibrated standard lamp. The irradiance at 254 nm is a narrow band measurement and characterization of the UV treatment process based on irradiance involves the implicit assumption that the complete spectral profile of the lamp is similar at all irradiances within the measured range. Measurement of irradiance in such a manner also makes it imperative to state that the results obtained in this study are only verified for pulsed xenon flashlamps operating at 120 Hz frequency and whether other types of UV sources yield the same results must be verified experimentally.

6.1.3 Exposure Time

As in the case of irradiance, the overall UV exposure time is not a controlling variable and the exposure time is important only in the determination of the total irradiation incident on the surface for a chosen value of irradiance. Other time factors which may be important are the time required for the process gas (ozone) to reach a surface newly introduced in the treatment environment. The amount of ozone required in the surface oxidation process is very small and a monolayer of ozone gas adsorbed on the surface is adequate to oxidize the top surface layer of the material. No dependence on the exposure time was observed at the irradiance levels used in this study (i.e. for exposures on the order of seconds.) This is likely the result of the rate of formation of a physisorbed monolayer of a gas at standard pressure and temperature which typically occurs within a fraction of a second.

6.1.4 Ozone Concentration

The actual ozone concentration used in UVO treatment did not have a pronounced effect on the surface properties, although at very low concentrations (less than 200 ppm), the variability in data was observed to increase. This was studied in detail for polycarbonate, but the effect was observed in elastomers as well, and is believed to be due to the inefficiencies in the treatment chamber used in this study. For many samples treated at low ozone concentrations, some areas of the sample showed high wettability while other areas had properties similar to the untreated material. This type of non-uniform surface can be caused by channeling of the gas flow where there is incomplete mixing between the incoming stream of process gas and the existing gas in the chamber,

causing local areas of starvation where no ozone is present. At higher concentrations, these inefficiencies are alleviated to some degree by the excess amount of ozone as well as increased diffusion throughout the chamber. Thus, we can conclude that ozone is necessary for UV oxidation of polymers, but the concentration of ozone near the sample surface is far in excess of the ozone necessary for the surface reaction, hence the concentration does not have any effect on the degree to which the surface can be treated when ozone concentrations on the order of a few hundred ppm are used and would not be a rate limiting factor.

The ozone concentration can, however, affect the UVO treatment in other ways. It has been demonstrated earlier that the extent of surface modification is dependent on the total irradiation and the wavelengths necessary for UV oxidation range from 185 nm to 300 nm. A concentration dependence can arise indirectly in the process at very high ozone concentrations because ozone has a strong absorption maximum centered at 254 nm and ranging in width from 200 to 300 nm as shown in Figure 2.6. This wide absorption in the UVC region can cause attenuation of irradiance which has already been shown to be the main variable in the UV treatment process. In this study the attenuation by ozone was accounted for by measuring the irradiance under actual processing conditions, including passage of the UV radiation through a layer of ozone at the typical concentrations used in UVO treatment.

6.1.5 Temperature

The surface temperature during UV treatment can have a pronounced effect on the extent of surface modification for polymers above their glass transition temperature (Tg). Studies on rubber, Bexloy®, and polyethylene suggest that extensive surface restructuring, including thermodynamically driven reorientation of the polar functional groups away from the surface in order to reduce the total surface energy [12], can occur in the polymer as the surface temperature increases during treatment. This effect is not seen in polymers treated below their Tg because of the reduced chain mobility.

The increase in the surface temperature during UV treatment can occur because of various reasons. UV lamps can have significant output in the infrared (IR) region. IR radiation is absorbed by the polymers resulting in vibrational excitation to higher levels. The relaxation from the excited vibrational states to the ground state is accompanied by release of thermal energy. Similarly, UV radiation causes electronic excitations in molecules and the relaxation processes from the excited state often include intermediate vibrational relaxations (leading to the phenomena of fluorescence and phosphorescence) which ultimately leads to the release of thermal energy[3]. In addition heat generation by radiation, the exothermic oxidation reactions occurring on the surface can also contribute to the increase in temperature. Thermal management strategies have been shown to work well for such polymers. The use of water filters, or dichoric reflectors on UV lamps can reduce the amount of IR radiation reaching the surface. Similarly, lamp design can be modified to reduce the fraction of IR emission from the lamps. A more practical approach is to remove the generated heat from the polymer surface during treatment. One of the approaches adopted in this study is the use of intermittent exposure. Samples were

irradiated for short times and allowed a dark cooling period to maintain low surface temperatures and the process was repeated till the desired irradiation was achieved.

The most striking results were obtained in Bexloy® which has a Tg of ca. 50°C. With temperatures maintained below the Tg by the use of intermittent exposures, both the O/C ratio measured by XPS, and the wettability measured by contact angles, increases with UVO treatment. When no thermal management is present, and the surface temperature is allowed to exceed the Tg, the polymer loses its ionic crosslinks and undergoes extensive reorientation, resulting in a decrease in the O/C ratio and wettability. The influence of temperature on the measured O/C ratio, which is an average of the composition over a sampling depth of 75-100 Å, illustrates that restructuring can occur well below the top monolayer of the material.

6.1.6 Pulse Frequency

The experimental work described so far was performed on xenon flashlamps operating at a pulse frequency of 120 Hz. The UV lamps used also have the capability to be operated at different frequencies. The RC740 lamp operates at 10 Hz while the RC747 lamp has a variable frequency module allowing operation at 3Hz and 120 Hz. The advantage of using a pulsed lamp is the dark period available for cooling of the surface between two UV pulses. Table 6.1 shows the average cooling time, pulse widths, and pulse energy for different operating frequencies. It can be readily observed that as the pulse frequency increases, the cooling time available between two pulses, as well as the average energy output per pulse, decreases as the reciprocal of the frequency. The considerations of low sample surface temperatures have been discussed in the previous

section. To keep the temperatures low, and yet have high enough irradiance to treat surfaces in as short a time as possible, a balance must be reached between the energy given to the surface per pulse and the cooling time available between two such pulses.

Table 6.1 Cooling time and energy per pulse for a 2.6 mW pulsed UV output.

Pulse Frequency	Pulse Width	Cooling Time/Pulse	Energy/Pulse
3 Hz	150 μs	333.1 ms	887 μJ/pulse
10 Hz	150 μs	99.9 ms	266 μJ/pulse
120 Hz	150 μs	8.2 ms	22 μJ/pulse

It was found from observation that increasing the cooling time between pulses was not as effective a thermal management strategy as reduction of the energy per pulse. The reason for this is that the radiation is absorbed by the polymer to some depth and this absorption depth increases with increasing intensity of the pulses. At low frequencies, the high intensity pulses can cause liberation of more thermal energy, and at greater depths, compared to high frequency, low intensity pulses. In poor thermal conductors such as polymers, the high intensity pulses give rise to thermal gradients and the low thermal conductivity can cause higher transient temperatures on the surface than low intensity pulses. The greater cooling time between low frequency pulses was found to be insufficient compensation for the amount of heat generated in polymers. Surface temperatures of polymers treated at 3Hz pulse frequency were invariably found to be higher than the temperatures recorded for equivalent irradiation at 120 Hz. In fact, at 3

Hz, the heating effect of the UV lamp is so strong that even thermally stable, high temperature polymers such as silicone rubber were found to char and combust after 4 -5 minutes of UVO exposure. Thus, for polymers, higher frequencies with low intensity pulses are more suitable than low frequency high intensity pulses.

6.1.7 Humidity

The effect of humidity was not determined in this study, although some experiments were performed to successfully demonstrate the possibility of treating polymers through a film of water. The interaction of UV with water has been well reported in literature [4,5]. UV radiation leads to the formation of hydroxyl and hydroperoxy radicals in water which have the ability to react with chemical waste compounds as well as polymer substrates. This chemistry is widely used in water purification and remediation systems and similar reactions can occur in water in the gas phase. The influence of humidity is one of the UV treatment process variables that needs to be studied in greater detail in the future.

6.2 Process Model

The UV oxidation process involves far too many different sub-processes and pathways to describe the changes occurring in a wide range of materials with a unique universal model. The oxidation of each polymer follows different pathways and unless all the intermediate reaction mechanisms are known and characterized, analytical descriptions are bound to fall short. In addition, the polymers studied here are commercial polymers, many of which are compounded with stabilizers, anti-oxidants,

and processing additives. These low molecular weight additives often migrate to the surface and create a chemistry which is almost always different from that expected from a pure material. The surfaces of polymers processed at high temperatures can also be oxidized to a certain extent. Processing conditions can also affect the surface morphology and a polymer processed at two different conditions can have very different surface properties, be it due to changes in crystalline structure, molecular weight, or composition. Unfortunately, such 'real world' materials are the rule rather than the exception in most industrial applications and the description of a process to modify these materials must take into account the inherent variability of the surface. It is fair to say that for a commercial polymer we often only have a general idea of the composition, structure, and processes occurring on the surface. To describe the effect of a surface treatment process on such materials, an empirical approach is the most direct route.

In that respect, UVO treatment has many similarities to long term photodegradation and weathering in polymers. Some investigators in the field of polymer degradation have developed the concept of polymer sensitivity curves to describe the susceptibility of a polymer to long term photodegradation. Allan et al. proposed an approach to model the UV degradation of the bulk properties of a polymer with different loadings of photostabilizers [6]. The model is based on the determination of a "wavelength sensitivity spectrum" over a range of solar wavelengths to model the degradation of polystyrene with benzotriazole, benzophenone, and triazine UV stabilizing additives. Their approach was to model the change in any property (P) of the bulk polymer in terms of the incident irradiance and an empirically determined sensitivity (S). The Allan model is described by Equations 6.1 to 6.4.

$$\frac{\Delta P(\lambda,x)}{t} = I(\lambda,x)S(\lambda) \tag{6.1}$$

where $I(\lambda,x)$ is the irradiance in the sample at wavelength λ and depth x, and $S(\lambda)$ is the wavelength sensitivity spectrum. The depth of penetration of the radiation is modeled for a solid obeying Beer's law such that $I = I_o\, 10^{-\varepsilon c x}$.

$$\frac{\Delta P(\lambda, x)}{t} = I_o 10^{-\varepsilon c x} S(\lambda) \tag{6.2}$$

Integrating Equation 6.2 over the over depth x = 0 to d, gives

$$\frac{\Delta P(\lambda)}{t} = I_o \frac{1-10^{-\varepsilon c d}}{\varepsilon c} S(\lambda) \tag{6.3}$$

The total degradation rate in the polymer is determined by numerical integration over all wavelengths using experimentally determined source spectra, absorbance spectra, and sensitivity spectra.

$$\frac{\Delta P}{t} = \int I_o \frac{1-10^{-\varepsilon c d}}{\varepsilon c} S(\lambda) d\lambda \tag{6.4}$$

The wavelength sensitivity spectrum was determined by measuring the degradation of the property using a series of Schott glass cut-off filters. Differences in property degradation between samples exposed behind different pairs of cut-off filters were ascribed to the radiation in that band of wavelengths by assuming that the sensitivity is constant over the measured irradiance band between the two filters. The irradiance bandpass between two filters spanned almost 100 nm at 10% transmittance in their study. A similar approach has been followed to model the UV surface treatment process.

6.2.1 UVO Surface Treatment Model for Xenon Flashlamps

Investigation of the various process parameters described in section 6.1 show that for UV treatment, the only dependence of the evolution of surface properties in the presence of excess ozone is on the irradiation, H, received by the sample. The spectral band mainly responsible for the photooxidation reactions has also been determined to range from 185 - 280 nm. Given the ca. 100 nm bandwidth of the radiation of interest, irradiance measurement at 254 nm was used as a one-point measurement for the entire spectral band. The use of irradiance measurement at 254 nm can be used in a manner similar to the irradiance bandpass measured by Allan for a pair of Schott glass filters. The most general relationship for the rate of change in an arbitrary property of the polymer surface can be expressed as

$$\frac{\Delta P(H,\lambda,x)}{t} = I(\lambda,x)S(H,\lambda) \tag{6.5}$$

where P is the change in the measured property, t is the exposure time, x is the distance from the surface, S is a depth dependent spectral sensitivity function, I is the irradiance, and H is the total irradiation given by the product of irradiance and time. Due to the limitation of using a single spectral bandpass, an assumption can be made that the empirical sensitivity of the polymer is constant over the entire range from 185 – 280 nm provided future comparisons with this model are made with lamps having a similar spectral output (i.e. xenon arc flashlamps). Equation 6.5 can then be simplified to

$$\Delta P(H,x) = H(x)S(H) \tag{6.6}$$

To describe the surface treatment of polymers, the above equation only needs to be evaluated for depth x = 0

$$\Delta P(H) = \Delta H \cdot S(H) \tag{6.7}$$

For a differential change in a surface property caused by a differential increase in irradiation, the sensitivity function, S(H), can be expressed as

$$S(H) = \frac{d(\Delta P(H))}{dH} \tag{6.8}$$

The change in the property can be obtained by integration of Equation 6.8 over the irradiation range to give

$$(\Delta P)_{H2-H1} = \int_{H1}^{H2} S(H)dH \tag{6.9}$$

The sensitivity function can be empirically determined for a particular polymer, and the integral of the sensitivity function gives the net change in the measured property, P, from the reference value.

6.2.2 Determination of Sensitivity Functions

Work of adhesion sensitivity functions for five ambient temperature UVO treated polymers (PC, PET, Rubber, PTFE, and Epoxy) were calculated using data obtained from contact angle measurements with water. The change in the work of adhesion (Wa) for all polymers, except PTFE, increases rapidly with irradiation and then reaches an asymptotic value at high values of irradiation. The rate of change of Wa decays exponentially as the susceptible surface sites on the polymer are oxidized. Wa was plotted as a function of the irradiation, H, and the resulting plots were analyzed using a curve fitting software (CurveExpert 1.34 for Windows). Details of the curve fit are given in Appendix B. From observation of the trends in the surface properties (work of adhesion and O/C ratio) of the polymers, as well as the derivatives of the work of adhesion curves, the use of an exponential decay function to describe the trends is strongly indicated. The Wa vs H

curves for the polymers were fit to a three parameter exponential association function of the form y=a(b-exp(-cx)) as shown in Equation 6.10.

$$W_a = a\left(b - e^{-cH}\right) \tag{6.10}$$

where a, b, and c are empirical correlation constants, the work of adhesion has units of (mJ/m^2), and irradiation has units of (mJ/cm^2). This function should only be applied within the range of irradiances measured and does not extrapolate beyond the measured values. This type of function was fit to the data for four polymers which showed a change in the work of adhesion. The work of adhesion sensitivity function S(H) for the polymers is calculated by differentiating Equation 6.8 to give

$$S(H) = \frac{dW_a}{dH} = ac\left(e^{-cH}\right) \tag{6.11}$$

For polymers like PTFE that do not absorb radiation in the specified range, the exponential association function does not apply and the data is fit with a linear function of the form Wa = aH + b, which gives a sensitivity function of S(H) = a. Other polymers may not necessarily fit this shape in which case numerical differentiation can be performed. Wa sensitivity curves were generated using the empirical constants a and c over the measured irradiation range. Table 6.2 lists the empirical correlation constants for the five polymers. The corresponding sensitivity functions are illustrated in Figure 6.1.

Table 6.2 Correlation constants for the work of adhesion sensitivity functions for PC, PET, Epoxy, Rubber, and PTFE.

Polymer	Work of Adhesion S(H) =	*a*	*b*	*c*
PC	(*a***c*) exp(-*c*H)	72.6	1.97	0.0107
PET	(*a***c*) exp(-*c*H)	37.7	3.31	0.0292
Epoxy	(*a***c*) exp(-*c*H)	45.2	3.00	0.0155
Rubber	(*a***c*) exp(-*c*H)	107.2	1.27	0.0107
PTFE#	*a*	0	--	--

PTFE does not absorb in the tested UV range, hence no modification is possible.

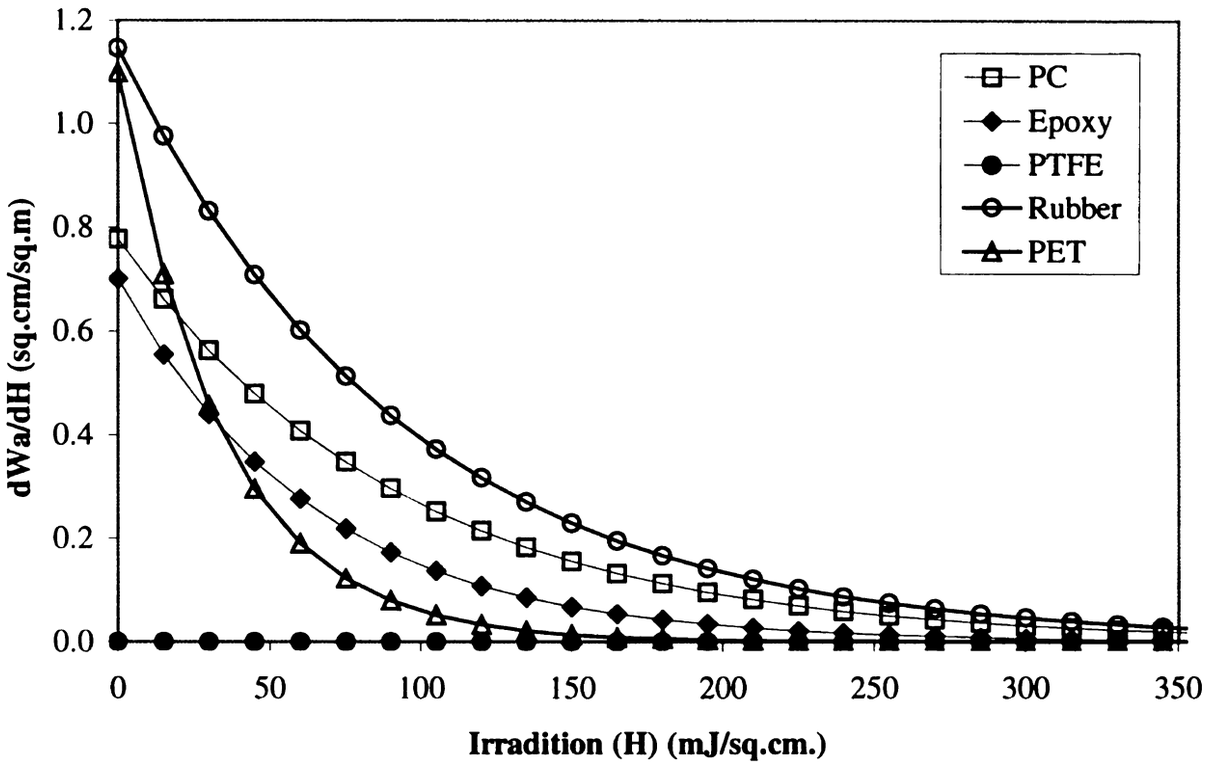

Figure 6.1 Work of adhesion sensitivity curves for UVO treated polycarbonate (PC), epoxy, polytetrafluoroethylene (PTFE), crosslinked tire rubber compound, and polyethylene terephthalate (PET) showing the rate of property change as a function of irradiation.

6.2.3 Relation to Physical Properties

Examination of the empirical correlation constants *a*, *b*, and *c* shows that *b* is simply a scaling parameter related to the reference value of the work of adhesion of the untreated polymer, thus a higher value of *b* indicates a higher starting value of the work of adhesion of the polymer. The parameter *c* defines the rate of exponential decay of the sensitivity function. The parameter *a* is related to the extent to which changes in the work of adhesion occur, but has no effect on the rate of decay.

Assuming the changes in the work of adhesion are a combined result of photooxidation and ozonation of the photolysis products on the polymer surface, the rate of decay of the sensitivity, *c*, must be related to the rate of depletion and, by inference, the susceptibility, of chromophores in the polymer to UV oxidation (absorptivity), as well as susceptibility to oxidative attack by ozone. The extent of modification, affected primarily by the parameter *a*, can be related to the relative population of susceptible sites on the surface.

The parameter *a* describes the populations of susceptible sites on the polymer which can be oxidized by UVO exposure. A higher value of *a* can indicate a chemical structure with high frequency of susceptible sites, or a polymer microstructure which causes a large number of susceptible bonds to be exposed on the surface. An estimate of the relative populations of reactive sites on the surface of different polymers for the purpose of comparison can be obtained by determining the fractional number of susceptible bonds in the polymer. A first approximation for the relative density of susceptible bonds can be obtained by normalizing the number of bonds or sites expected to react during UV oxidation with respect to the molecular weight of the repeat unit of the

polymer. This can provide a very rough estimate for rapid qualitative comparisons. The utility of this approach is limited because the number of sites are normalized in terms of the molecular weight and the effects of surface microstructure and configuration are not considered. A more rigorous calculation should take into account the fractional area or volume of the surface covered by susceptible bonds, the physical configuration of the polymer chains, steric shielding effects, and any other factors which may affect the density of surface sites capable of reacting in UVO exposure conditions. The fractional volume of susceptible sites can be calculated using the additive group contributions approach of Bondi and Van Krevelen [7] to determine the Van der Waals volume of the polymer. This is a more reliable method than comparison based on mass. The two methods are compared below.

Approximation of 'a' by number of sites per unit mass.

Assuming the diene rubber to be pure polybutadiene, there is one unsaturated bond in the repeat unit of molecular weight 54 Daltons, giving a reactive site population density of 1/54 = 1.85 sites/100 Daltons. Similarly, the polycarbonate can be assumed to have 4 sites sensitive to direct UVO attack – the two carbonate linkages and the two methyl groups in the Bisphenol A unit. The reactive site population density for PC is 4/254 = 1.57 sites/100 Daltons. PET has a repeat unit of molecular weight of 192 and has two aromatic ester chromophores which are expected to react, giving a site density of 1.04 sites/100 Daltons. The epoxy is a two part system of DGEBA (MW = 582) and Jeffamine T 403 (MW = 470) in 100:45 weight ratio. The average molecular weight of the epoxy "repeat unit" is (582*1)+(470*0.45) = 793.5 Daltons. The epoxy resin has 10

potential sites in the backbone capable of reacting if the C-N crosslinks are considered reactive, and the curing agent has three ether groups. The three amine groups in the curing agent are not counted to avoid double counting. The average number of sites for epoxy are (10*1)+(3*0.45) = 11.3 sites/unit and the site density is 11.3/793 = 1.43 sites/100 Daltons. These values are provided only to aid qualitative comparisons and should not be used for any quantitative purposes for the reasons outlined previously.

Approximation of 'a' by Van der Waals volume from group contribution methods.

The concept of additive group contributions is based on the assumption that a physical property of a molecule is in some way determined by a sum of contributions made by the structural and functional groups in the molecule. In a polymer, the contributions from various sub-groups in the repeat unit can be added to approximate the properties of the polymer. The Van der Waals volume of a molecule is defined as the space occupied by the molecule, which is impenetrable to other molecules having normal thermal energies. The Van der Waals volume of a molecule is assumed to be the volume of several interpenetrating spheres. The radii of the spheres corresponds to the atomic radii of the elements involved and the distance between their centers correspond to bond lengths. Van Krevelen has tabulated the group increments to Van der Waals volumes determined by Bondi, Slonimskii, and Askadskii, along with group increments for amorphous, crystalline and semi-crystalline polymers [7]. The molar volumes of polymers in the rubbery state (V_r), glassy state (V_g), crystalline state (V_c), and semi-crystalline state (V_{sc}) have all been related to the Van der Waals volume as shown in Table 6.3.

Table 6.3 Ratio of amorphous, glassy, crystalline, and semi-crystalline molar volumes of polymers to Van der Waals volumes by group contribution [REF].

Ratio at 298 K	Mean Values
V_r/V_w	1.6
V_g/V_w	1.6
V_c/V_w	1.435
V_{sc}/V_w	$1.6 - 0.165x_c$

* x_c = crystalline mole fraction.

Since the ratios of the molar volumes of polymers in different physical states to the Van der Waals volume are constant, calculation of the volume fraction of the polymer repeat unit susceptible to UVO oxidation is independent of the physical state of the polymer and scales directly with the Van der Waals volume except in certain extreme cases such as a highly crystalline polymer subjected to a big temperature change spanning a strong transition. Moreover, many polymers are semi-crystalline and the crystalline fraction of the surface is not always known, so the Van der Waals volume is the simplest way to calculate volume fractions of susceptible groups without requiring extensive *a priori* characterization of the polymer.

Van der Waals molar volumes for the entire repeat unit and the molar volumes of the susceptible groups in the repeat unit were calculated for PC, Polybutadiene, PET, and Epoxy (Epon 828 + Jeffamine T403). Susceptible groups were chosen on the basis of absorption of UV in the 185 - 280 nm range as well as possibility of oxidative and free radical attack based on photodegradation mechanisms from literature. The details of the

calculations are provided in Appendix C. Since the Van der Waals volume is calculated assuming a series of spheres, an approximation of the projected surface area of the susceptible groups can be given by

$$A = \left(\frac{3}{4}V\right)^{2/3} \pi^{1/3} \tag{6.12}$$

where V is the total or fractional volume, and A is the total or fractional area of the molecule or repeat unit.

The results of the Van der Waals fractional volume and fractional area of susceptible sites on the surface are compared with the experimentally determined values of the parameter *a* for the four polymers in Figure 6.2. The results of the approximate estimation of *a* by mass normalization are also shown for comparison. It can be readily observed that the Van der Waals fractional volume and fractional area are excellent predictors of the value of the parameter *a* provided the susceptible groups are chosen properly.

Parameter *c* describes the susceptibility of the above mentioned surface sites to photo-oxidation and photolysis. PC has the highest stability to UV radiation because the Photo-Fries rearrangement products (hydroxybenzophenones) of the polymer are very good UV stabilizers, resulting in shielding of the rest of the polymer from further UV degradation [8]. The epoxy resin has aromatic ethers and hydroxyl groups in the structure which are not very strong absorbers at higher wavelengths and the curing agent has a high percentage of hydrocarbon content which is also not expected to be very sensitive to UV degradation, hence the susceptibility of epoxy is considered to be moderate. PET is reported to be extremely sensitive to photodegradation because of the high absorption

coefficient of the aromatic ether group. Studies on PET have shown that even short UV exposures can cause significant yellowing and cracking in PET [9], hence the PET should be rated as having very high susceptibility. Virgin rubber (polybutadiene) is also highly susceptible to ozone and UV attack because of the strong absorption coefficient of the π bond in the polymer backbone and should ideally have a value of c that is comparable with PET.

It can be seen from Table 6.2 that the value of c agrees well with this qualitative comparison for all polymers, except rubber, which shows a much reduced susceptibility to UV oxidation than expected. This apparently anomalous behavior of rubber may be due to two possible reasons: i) surface restructuring of the rubber due to entropic and thermal effects, and ii) the effect of UV stabilisers and anti-oxidant additives. The Tg of polybutadiene is approximately –98°C and at room temperature the increase in free volume of the polymer allows a high degree of chain mobility. Even though bonds in the polymer may absorb strongly and get oxidized, the polar groups experience a thermodynamic driving force to rotate away from the surface and present a fresh low energy surface, which, from a macroscopic view of the surface, is equivalent to a bond having low absorptivity. Evidence of this mechanism was provided in Table 5.3 where the rubber shows an increased rate of overall surface oxidation when temperatures are lowered by intermittent treatment. The second reason for this behavior is the high loading of carbon black, which acts as a physical screen for photons, and anti-oxidant additives in the compound which are designed to retard the oxidation process by quenching and scavenging free radicals. The low value of c, compared to the expected behavior, can be explained in terms of an apparent stabilizing effect due to surface reorientation and

restructuring, and a real stabilizing effect due to additives. However, the net change in the work of adhesion of rubber is the highest of all four polymers indicating that even though the rate of oxidation may be retarded by restructuring and stabilization, the ultimate extent of oxidation described by parameter a remains unaffected and can be reached at higher levels of irradiation.

A modelistic determination of c is difficult because several processes govern the decay of the sensitivity function. The molar absorptivities of various chromophores are widely tabulated in literature, but the precise mechanisms of oxidation and the corresponding rate constants are often not known. In addition, the influence of stabilizing additives in the polymer needs to be studied in detail. Lastly, the effect of free volume also needs to be accounted for polymers above the Tg. Empirical group contribution models for temperature dependent molar volume changes may be of use in such cases. But the biggest stumbling block is the insufficient quantitaive characterization of the individual oxidative processes which are responsible for the majority of the changes occurring on the surface.

The three parameters discussed in this section are summarized below in terms of the physical properties of the polymer which can possibly affect them:

$a = f$ (population of sites, microstructure, chain configuration, steric effects)

$c = f$ (absorptivity, oxidation rates, free volume, chain flexibility, stabilizers & additives)

$b = f$ (initial properties of the surface)

The trends in the three empirical parameters and their correlation to the physical properties of the polymer are given in Table 6.4.

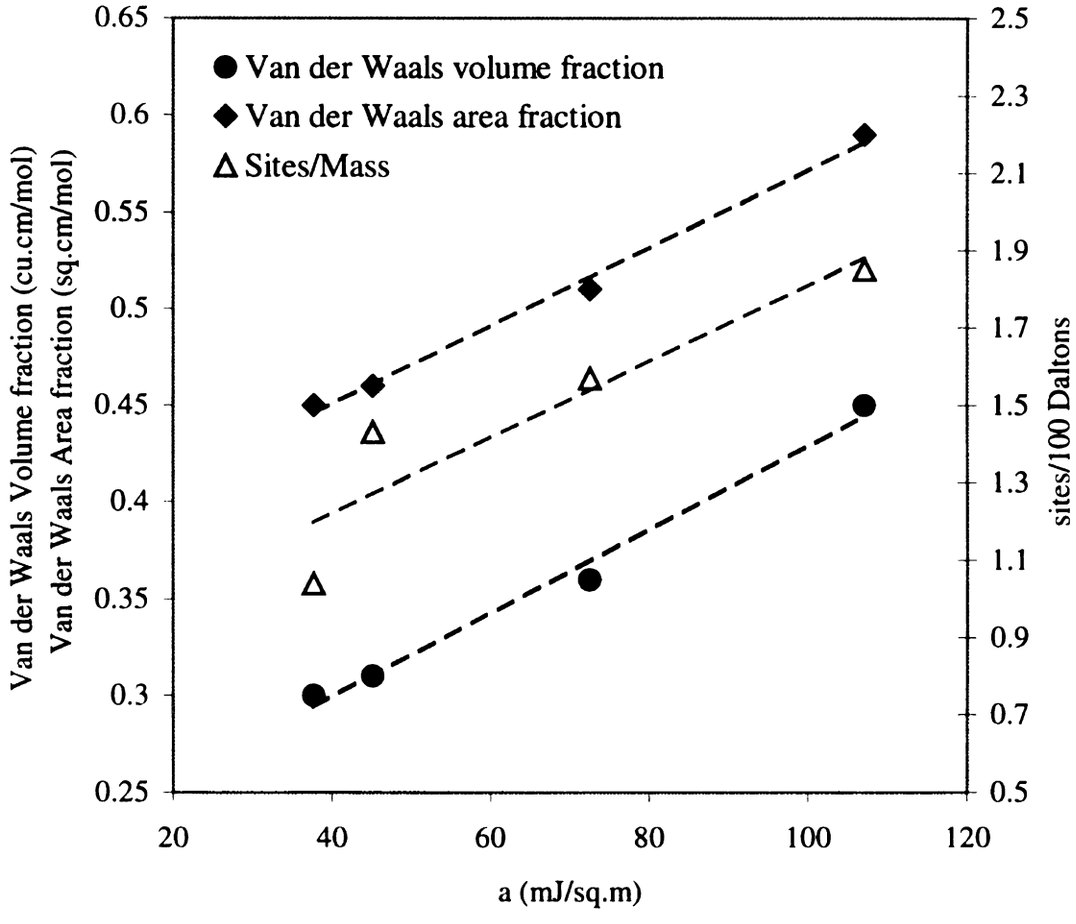

Figure 6.2 Comparison of the Van der Waals fractional volume and fractional area of susceptible sites in PC, PET, Crosslinked Tire Rubber Compound, and Epoxy with the parameter *a* calculated from curve fit to the work of adhesion data. Data for rapid estimation of *a* by counting number of sites per mass is also shown for comparison.

Table 6.4 Correlation between empirical parameters and physical properties of UVO treated PET, Epoxy, PC, and crosslinked tire rubber compound.

Polymer	Dimensionless Scaling Factor		Maximum possible change in Work of Adhesion		Rate of change of Work of Adhesion	
	Baseline Wa (mJ/m^2)	*b*	Fractional volume of susceptible sites*	*a* (mJ/m^2)	Susceptibility of sites	*c* (cm^2/mJ)
PET	91	3.31	0.30	37.7	High	0.0292
Epoxy	91	3.00	0.31	45.2	Moderate	0.0155
PC	69	1.97	0.36	72.6	Low	0.0107
Rubber	28	1.27	0.45	107.2	High#	0.0107

* from group contributions to Van der Waals volume [7].
# expected for rubber with no UV stabilizers or anti-oxidants.

6.2.4 Extention to Bulk Polymer

In the previous section a model was presented to describe the oxidation of polymers by UVO treatment. The model is applicable only to the evolution of surface properties because the effect of UV irradiation on the bulk polymer is ignored. However, photolytic reactions can occur in the polymer up to the depth of penetration of the radiation. The penetration depth of deep UV radiation in many polymers is estimated by Rabek to be around 300-400 nm [1]. To describe the changes occurring in the near surface polymer, hereafter referred to as 'bulk polymer' for convenience, a general form of Equation 6.5 can be written using Beer's law

$$\Delta P(H,x) = H_0 e^{-\varepsilon c x} \cdot S(H,x) \tag{6.12}$$

where H_o is the product of exposure time (t) and surface irradiance (I_o), and S(H,x) describes an overall sensitivity function which varies with depth. It was assumed in modelling the surface reaction that excess oxygen or ozone is available at the surface. In the polymer bulk, this does not hold true and the chemical changes in the bulk will be severely limited by the concentration of the oxidizing species. The variation of the sensitivity (S) with depth (x) can be considered to be a function of the availability of oxygen or ozone at that depth by defining a term $R(c_o)$ to describe the reaction rate dependence on the concentration of the oxidizing species. This dependence can be built into the model as

$$S(H,x) = S(H)R(c_O)c_O(x) \tag{6.13}$$

where $c_o(x)$ is the concentration of the oxidizing species at depth x in the polymer.

In this study the ozone concentration was reduced to approximately 10 ppm, the lower limit of detection of the ozone measurement experimental setup, and no change in

the rate of surface modification was observed. However, when no ozone or oxygen is present, no changes in the surface properties are evident. Thus the reaction rate dependence on the ozone concentration must be rate determining at some value of ozone concentration between 0 and 10 ppm. In the future, a detailed study of the rate of surface modification at very low ozone concentrations can provide information about $R(c_o)$.

The concentration gradient of the oxidizing species in the polymer, $c_o(x)$, is more easily accessible. The concentration profile of ozone can be modeled analytically using well established gas diffusion models. The diffusion of gases in polymeric solids is well described by Fick's second law [10, 11]. The concentration depth profiles for one dimensional diffusion can be obtained from solutions to

$$\frac{\partial c_O}{\partial t} = D\left(\frac{\partial^2 c_O}{\partial x^2}\right) \tag{6.14}$$

where D is the diffusion coefficient. A more pertinent approach The overall modification of the depth dependent material property in the bulk polymer can be expressed as

$$\frac{\Delta P(H,x)}{t} = I_O e^{-\varepsilon c x} \cdot S(H) \cdot R(c_O) \cdot c_O(x) \tag{6.15}$$

The biggest hurdle in this approach is the determination of property changes in the top layers of the surface with good spatial resolution. Analytical techniques like XPS can characterize surfaces over average depths of 7-10 nm, monolayers can be characterized by techniques like SIMS, but depth profiling of bulk polymer properties remains a challenge.

6.3 Application to Unknown Polymers

One of the motivating factors for developing a process model for UVO surface treatment is the ability to predict *a priori* the properties of UV modified polymers. From the results described in the previous sections, it can be seen that for a polymer that absorbs radiation in the spectral output available from pulsed xenon lamps, and undergoes oxidation, the change in the work of adhesion can be expressed in terms of the empirical parameters, a and c. This is not limited to the work of adhesion and can be used for any property that evolves due to UV oxidation, although the values of the empirical parameters for different properties are likely to vary. A knowledge of these two constants can fully describe the evolution of the property under investigation as a function of irradiaton.

The parameter a has been shown to vary with the Van der Waals fractional volume for four polymers belonging to different classes: elastomers, thermosets, amorphous thermoplastic, and semi-crystalline thermoplastics. This relationship between a and the molar volume fraction must be verified over a larger range for more polymers. It is unlikely for the trend to be linear over large ranges of the fractional volume of susceptible sites. It is also possible that various types of polymers may follow diverging patterns. If a verified relationship between the fractional volume of susceptible sites and a is available, an estimation of a for an untested polymer can be made using group contribution models. The parameter c refers to the susceptibility of the material to UV oxidation and hence must be experimentally determined, but it can be reasonably estimated for homologous polymers if they have similar chromophores and structures.

An alternate, empirical approach can also be used to measure *a* if the *c* for a homologous polymer is known and assumed to be equal to that of the untested polymer. Two measurements of the work of adhesion can be obtained; one for the untreated surface and one for the surface treated to saturation. The difference between $Wa_{(saturated)} - Wa_{(untreated)}$ is the experimentally determined *a*. The value of *b* can be calculated as $b = 1+(Wa/a)$ and the profile for the evolution of the work of adhesion as a function of irradiance can be generated for all intermediate values. The value of *c* can be adjusted by measurements at two or more intermediate points and successive iterations can converge on the true value of *c*.

6.4 Summary

The variables in the UV treatment process have been systematically studied. It was found that radiation in the 185 - 280 nm band is necessary for the application of the process to a broad range of polymers. Radiation in this band is capable of *in-situ* production of ozone. Although ozone is necessary for the process to work efficiently, within the range of concentrations measurable by our equipment (>10 ppm) , no effect of the ozone concentration was observed. The variable with the largest effect on the process is the irradiance and the surface properties were found to have a direct relationship with the irradiant energy incident on the surface. Temperature of the substrate can affect properties, especially above the glass transition temperature in polymers, by providing a driving force for surface reorientation. Temperature was also affected by the pulse frequency of the lamps. At lower frequencies, the pulses are more intense and lead to higher surface temperatures than those reached by high frequency, low intensity pulses.

This is most likely a limitation posed by the poor thermal conductivity of polymers. However, lower frequencies also provide more dark cooling time for the surface. The lamps used in this study could be operated at 3 Hz, 10 Hz, and 120 Hz. Among these lamps 120 Hz was the most effective frequency for treatment of polymers. UV treatment with lamps operating at intermediate frequencies may provide interesting results. The effect of humidity is also an avenue which needs to be explored. Preliminary work shows that it is possible to treat polymers effectively through thin layers of water. The presence of hydroxyl and hydroperoxy radicals created in water by UV irradiation can yield very different products compared to direct attack by ozone and oxygen radicals.

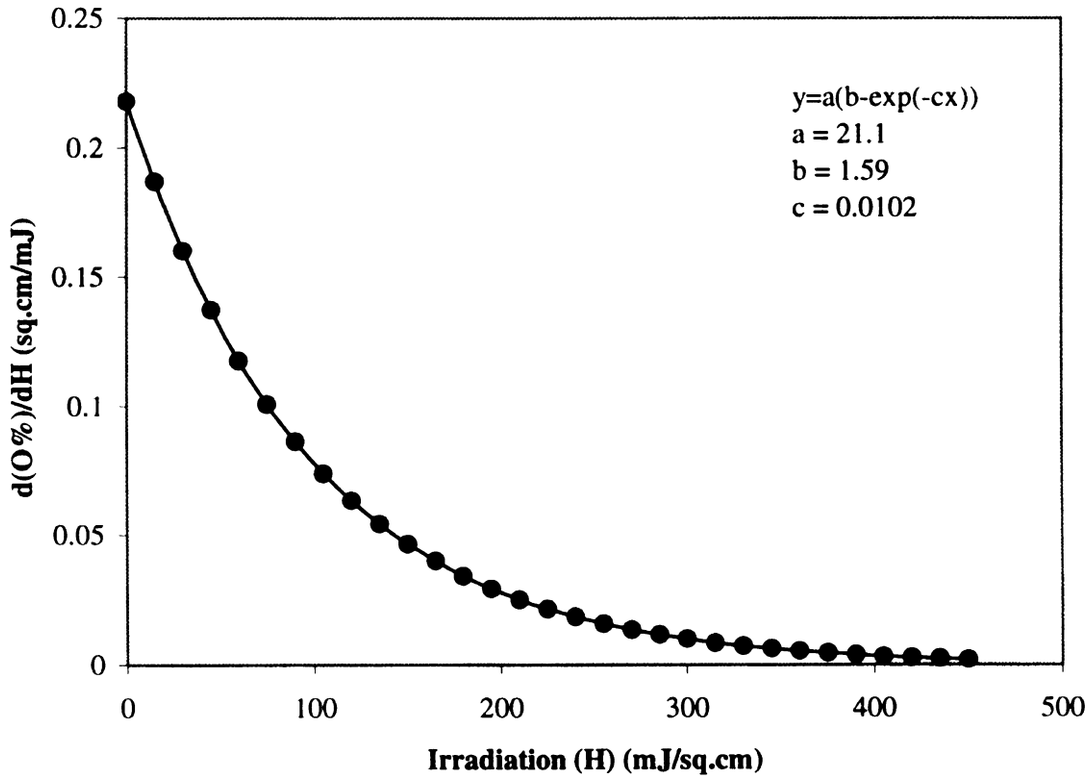

Figure 6.3 Sensitivity function for surface oxygen content in UVO treated PC.

An empirical process model has been proposed to describe the UVO treatment process. The model is analogous to the wavelength sensitivity spectrum approach used to model long term bulk photodegradation of polymers. The model describes the evolution of surface properties after UV irradiation in ozone for pulsed xenon lamps. Sensitivity functions for work of adhesion with water were determined for five polymers: PC, PET, Epoxy, Rubber, and PTFE. The functions were fit with a three parameter exponential association model. The parameters correlate with physical properties of the polymer: the parameter *a* provides information about the density of reactive sites on the polymer, *b* is a parameter that describes the initial properties of the polymer, and *c* provides information about the general reactivity of the polymer sites to photo-oxidation and other photoinduced reactions. Sensitivity functions can be determined for other surface properties as well. Figure 6.3 shows the oxygen content sensitivity function for polycarbonate. It is observed that the *c* value for the O/C ratio of UVO treated polycarbonate (c = 0.0102 O%/mJ) has very good agreement with that for the Work of Adhesion (c = 0.0107 cm^2/mJ) although the two properties are unique and measured over different sampling depths. Sensitivity functions for other polymers can be developed in the future to create a database of parameters which can be applied to predict the properties of new UVO modified polymers, blends, copolymers, and composites.

To use this model in a predictive capacity for previously untested polymers, at this stage, prediction of extrapolated parametric values may not be reasonable except over a very narrow range for specific homologous polymers. The initial verification for untested polymers can be performed by measurements at four to five points ranging from H=0 to H = ∞ (saturation of the surface property) and the value of *a* can be determined

from this data. The value of c can be determined by iteratively fitting the profile at intermediate measurements. With the generation of more data for a wider variety of polymers and homologues, predictive accessment of the properties can be accomplished with increasing reliability.

References

1. Rabek, J.F. *Mechanisms of Photophysical Processes and Photochemical Reactions in Polymers*, John Wiley, New York, 1987.

2. Hollander, A.; Klemberg-Sapieha, J.; Wertheimer, M.; *J. Polymer Science Part A: Polymer Chemistry*, Vol. 23, pp. 2013-2025, 1995.

3. Atkins, P.W.; Friedman, R.S. *Molecular Quantum Mechanics*, Third Ed., Oxford University Press, Oxford, 1997.

4. Gonzalez, M.; Martire, D.O. *Water Sci. Tech.* Vol. 35, No.4, pp. 49-55, 1997.

5. Hashem, T.M.; Zirlewagen, M.; Braun, A.M. *Wat. Sci. Tech.*, Vol. 35, No. 4, pp. 41-48, 1997.

6. Allan D.S.; Maecker, N.L.; Priddy, D.B.; Schrock, N.J. *Macromolecules*, Vol. 27, pp. 7621-7629, 1994.

7. VanKrevelen, D.W. *Properties of Polymers*, 3rd ed., Elsevier, Amsterdam, 1990.

8. Pickett, J.E. *Permanence of UV Absorbers in Plastics and Coatings*, Handbook of Polymer Degradation, Second Edition, S. H. Hamid ed., Marcel Dekker, New York, 1998.

9. Praschak, D.; Bahners, T.; Schollmeyer, E. *Appl. Phys. A*, Vol. 66, pp. 69-75, 1998.

10. Bird, R.B.; Stewart, W.E.; Lightfoot, E.N. *Transport Phenomena*, Wiley, New York, 1960.

11. Poulsen, L.; Zebger, I.; Klinger, M.; Eldrup, M.; Sommer-Larsen, P.; Ogilby P.R. *Macromolecules*, vol. 36, pp. 7189-7198, 2003.

12. Naito, T.; Horie K.; Mita, I. *Macromolecules*, vol. 24, pp. 2907-2911, 1991.

CHAPTER SEVEN

MARKET AND ECONOMIC ANALYSIS

Adapted from a report submitted by Alekh Bhurke[1] and Matthew Jenson[2] towards completion of an independent project in Management of Technology & Innovation (MT&I Program, ML890) administered by the Case Center for Computer-Aided Engineering and Manufacturing at Michigan State University, December 1997.

7.1 Abstract

With the automotive industry using more polymers in the manufacture of components, there is a need for proven surface treatment technologies that will provide enhanced performance at reasonable costs. Growing concerns over the environmental impact of existing processes and the advent of ISO 14000 standards have also contributed to the need for development of environmentally friendly processes. The manufacturing industry is looking to incorporate new surface treatment technologies for several reasons:

- Commercial applications involving painting and adhesive bonding of low energy polymers are increasing.
- Existing surface pretreatment techniques are labor intensive, time intensive, hazardous, or present environmental problems.
- There is a push to develop and transition to environmentally benign manufacturing processes due to the increasing environmental awareness in society.

[1] Department of Chemical Engineering & Materials Science, Michigan State University, MI 48824, USA
[2] School of Supply Chain & Management, Michigan State University, MI 48824, USA

Based on our research, the UV surface treatment developed by Michigan State University shows great promise – provided an actual, pilot scale process is developed to mimic real manufacturing environments. Not only is there a great need in the automotive industry for this process, but there are also markets in the biomedical industry which require modern surface treatment technologies. A basic cost analysis indicates the UV surface treatment is a viable alternative to existing processes and information obtained from communications with leaders in the automotive industry (General Motors and Ford Motor Co.) shows a willingness to consider this process if certain conditions and qualifications are met.

7.2 Introduction

Polymers usually have low surface energies, making the material difficult to wet and presents problems with adhesion of paints and other materials. Various surface treatments are available in industry to improve the wettability and adhesion of such materials. The more common surface treatments used for this purpose are flame treatment, plasma treatment, corona discharge, acid etching, solvent washes, halogenation, etc. The disadvantages of these treatments are that they are typically expensive, labor intensive and present several environmental and safety concerns. The release of volatile organic compounds (VOCs) into the atmosphere via these processes is also a growing concern in today's world. An alternative process for surface treatment using ultraviolet (UV) light has thus been studied. This process is economical, easy to incorporate into a manufacturing environment, presents minimal safety concerns, and is environmentally benign.

Ultraviolet light in the 180 - 280 nm wavelength (UVC region) is known to interact with atmospheric oxygen to produce ozone and nascent oxygen, both of which are strong oxidizing agents. Exposure of a material to UVC radiation for short times in the presence of oxygen or ozone leads to oxidation of the surface. Surfaces thus oxidized have higher surface energies leading to lower contact angles and higher wettability. The by-products of such a process are usually small molecules like water and oxides of carbon.

With growing concern over environmental impact and the advent of ISO 14000 standards, there is a need for development of an environmentally friendly process. In the UV treatment process, no volatile or particulate emissions are produced and no wet chemicals are used, making the process viable for use in future manufacturing environments. A brief comparison of the various surface treatment processes used in industry with the UV treatment process is made in the following section.

7.3 Surface Treatment Processes

7.3.1 Chemical/Solvent Wash

In many current painting and bonding processes, a chemical wash is used in which the surface to be painted or bonded is cleaned with solvents, coated with primers and adhesion promoters, and finally coated with multiple layers of paints. This method is neither economical nor environmentally sound because it uses primers which are typically organic solvent based, and the solvents used are known to cause volatile organic compound (VOC) emissions. Water based paints and primers are typically difficult to use in polymer applications because of the difficulties involved in spreading them on low

energy polymer surfaces. This process is suited to continuous flow manufacturing and generally inexpensive. Within the auto industry, chemical, detergent and solvent washes are the norm. Solvent washes are primarily used to clean surfaces not to modify the surface chemistry. With the danger of VOC emissions, the chemical wash process must take place in a controlled environment.

7.3.2 Flame Treatment

Flame treatment is performed by passing a hydrogen flame (temperatures higher than 3000°F) rapidly over a surface. The adhesive characteristics of the surface are enhanced by a combination of two factors: an increase in surface energy by oxidation and the degradation of weak boundary layers or contaminants. The flame creates oxygen radicals in the air which attack the polymer and form polar groups on the surface. The substantial oxidation and increase in polarity enhances the attraction between the substrate and the paint, adhesive, or ink being applied. The hydrogen flame head is typically placed 0.25 inch from the product's surface which allows throughput speeds of up to twenty inches per second. The treated surface may remain stable for several weeks. Flame treatment is not particularly suitable for three dimensional objects and the use of combustion of fuel as the primary source of energy has obvious environmental consequences.

7.3.3 Plasma Treatment

Plasma treatment exposes a material to gaseous oxygen, nitrogen, argon, or any other gas that is energized or excited to a plasma state in a vacuum chamber. The plasma

can be high temperature (energized by electrical discharge) or cold (energized by radio frequency). The components of the gas mixture can be chosen to seed certain functional groups on the surface, and during the 0.5 to 10 minute exposure to the gas plasma, the surface undergoes chemical, morphological and topographical changes that can improve adhesion. As with the flame treatment, the surface is also cleaned in the process and organic compounds or contaminants are removed from the surface. The plasma treatment can be time limited or permanent depending on the material. An advantage over flame treatment is that the entire surface of three-dimensional objects can be treated, but the requirements of a controlled atmosphere and vacuum are disadvantages.

7.3.4 Corona Treatment

Corona discharge, also known as 'non-vacuum plasma', is commonly used to pretreat polymers in web type applications. Treatment occurs when high voltage (10,000 volts) is applied to an electrode positioned a short distance from the substrate. The air gap is ionized and this corona of ionized air oxidizes the surface, resulting in a polymer surface which is better suited for printing or laminating and has better adhesive properties. Corona treatments are less likely to mar or damage treated surfaces than other treatment processes. The corona treatment is environmentally friendly because the use of volatile solvents and potentially hazardous process gases is eliminated. Corona is well suited to continuous manufacturing environments but not suited to treat complex surface geometries as well as other methods. Typical cycle-times for treating three dimensional objects like car bumpers with corona is 30 seconds. A concern with corona treatment is the build up of static charges that could cause explosions in a paint booth if the static

electricity is not removed. The high-voltage of the corona discharge is another safety concern. The only environmental concern with corona treatments is the production of large amounts of ozone.

7.3.5 Ultraviolet Treatment

UV treatment consists of exposing the substrate to UV radiation. The UV energy converts oxygen in the air to ozone and nascent oxygen, and these reactive species have the ability to oxidize organic material on the surface. The ozone also activates the surface material – making it more reactive with the ozone. Materials are generally placed within a few centimeters from the UV source. UV treatment combines the benefits of low temperature with the convenience of operating at ambient pressures and temperatures. Basic precautions must be taken when using UV surface treatments to not expose the skin or eyes to the UV light. The ozone produced in UV treatment is typically several orders of magnitude lower than that produced in corona treatment and the only environmental issue is the removal of this low level of ozone. In summary, the UV process has the following favorable characteristics:

- Environmentally benign (no harmful by products)
- Inexpensive (low capital and operating costs)
- Fast (treatment times on order of 1-2 minutes)
- Non-contact process
- Ability to treat complex geometries
- Easily integrated into the manufacturing environment

The process under investigation and analysis is the modification of an existing process. Surfaces can be cleaned and oxidized by exposing them to UV radiation of appropriate wavelength in ambient atmospheres. The resulting oxidized surface has beneficial chemistry for adhesive bonding, painting, printing, or metallization. The UV process has the potential to be less expensive than chemical and solvent washes modification, it is able to treat three dimensional parts, large surface areas, and it is environmentally friendly. The initial research study has identified UV oxidation and surface activation as a viable surface treatment process that can be used in a manufacturing environment. The goal of the technical research at Michigan State University is the development of a model to reduce UV treatment times and increase the reliability of the process, making it an attractive process for use in manufacturing environments.

7.3.6 Surface Treatment Process Comparison Matrix[3]

Using information obtained from literature searches and position papers, a matrix (Table 7.1) was constructed to compare the available surface treatment techniques. The ratings are subjective opinions of the authors and based on a scale of 1 (best) to 5 (worst). With the UV surface treatment under consideration, treatment times and cost are both rated "2" but with further development, it is believed these two areas will improve.[4]

Corona and UV seem to be the two most viable surface treatment technologies for the future. As an improvement over baseline treatments, plasma has gained popularity and market share in European markets but not in the United States because of the

[3] All opinions presented reflect the state of the industry in 1997.
[4] State of the UV treatment process as evaluated by the authors in 1997.

unsuitability to continuous manufacturing. The United States markets are now looking at the other surface treatment technologies – bypassing the original alternative surface treatments such as plasma. Solvent washes, even though popular today, are subject to future competition from environmentally friendly techniques. With further research and experience, UV treatment times and costs will be reduced – making UV one of the more attractive surface treatments for the future.

Table 7.1 Surface treatment process comparison matrix.*

Technology	Performance	Ability to treat 3D Geometries	Controlled Environments	Treatment Times	Stability of Treatment	Cost	Environmental Impact	Suitability in Production	Overall Rating	Ranking
Chemical Wash	3	1	4	2	1	1	5	1	18	4
Flame	2	5	2	1	1	2	2	1	16	3
Corona	1	2	1	1	1	2	1	1	10	1
Plasma	1	1	5	3	1	3	2	4	20	5
UV	1	1	2	2#	1	2#	1	1	11	2

*Subjective scale from 1–5 based on 1997 data. Lower is better.
Properties targeted for improvement.

7.4 Surface Treatment Cost Comparisons

The qualitative cost comparison made in the previous section was based on information received from surface modification equipment manufacturers. Since comparisons are made between a wide variety of existing surface treatments, all on a different scale, it is important to find a good basis for detailed cost-benefit analysis. To avoid any inconsistencies in the analysis, a simple approach was adopted. The costs associated with each method of treatment were normalized on the basis of costs incurred to treat a square inch of a surface. Only the cost of operating the equipment for a unit of time was considered and the amount of surface area treated in this unit time was calculated. This serves the advantage of providing a base value for cost comparison. These values, calculated for various processes, can then be used to estimate the approximate costs that would be incurred given a certain performance requirement or application for a given treatment method. The downstream and labor costs were ignored on the assumption that the UV surface treatment technique will parallel other existing technologies in terms of these associated parameters. Another reason to adopt this approach is the fact that these associated costs differ widely depending on the type of process used. For example, the costs associated with using robotic arms or any automated process would be very different from a manual batch operation and thus cannot be taken into account when comparing the cost of the technology itself. It was observed from some examples obtained during our communications with equipment manufacturers and users, that the associated costs could be several orders of magnitude higher than the cost of the treatment. The essential information would thus be lost if associated costs were included.

The cost comparison was done for a hypothetical production-line application of treating car bumpers at the rate of 200 bumpers per hour. The area of the bumpers needing surface treatment was assumed to be 5 feet x 1 feet. Five surface treatment systems: plasma, corona, UV lab scale, UV pilot scale, and UV production scale were evaluated. The cost data for plasma, corona and UV laboratory scale equipment was obtained through communication with existing commercial product vendors. The cost data for UV pilot scale and UV production scale equipment was taken from the best engineering estimates obtained from manufacturers and users of the technologies involved.

The results of the cost analysis for the five surface treatment processes are given in Tables 7.2 to 7.6. The capital and operating costs were used to define a normalized cost for treatment of a unit area of the surface. These base costs were extended to a production line treating car bumpers at the rate of 200 bumpers per hour with 5 sq. ft. area per bumper. The normalized annual costs for each of the processes for this application are given in Table 7.7.

From the above analysis it can be seen that, as expected, the UV treatment process, at the laboratory scale, cannot be very competitive with other production scale processes. However, the forecasts for the UV-Pilot and UV-Production scale cost estimates, based on information gathered from UV equipment suppliers, show that the normalized operating and capital costs decrease sharply at larger scales The low capital and working costs of a production scale UV treatment process makes it a particularly attractive choice and is cost-competitive with the established treatment processes such as corona and plasma treatment.

Table 7.2 Cost analysis of plasma treatment process.

Capital Costs			
Equipment	Life (hours)	Total Cost	Cost/hour
Plasma Unit Cost	87600	$800,000	$9.13
Total Capital Investment		$800,000	$9.13
Operating Costs			
Description	Hours	Cost	Cost/hour
Maintainance (5% Annually)	1	$4.57	$4.57
Total Operating Costs		$4.57	$4.57
Total Costs			
Total cost per hour of operation			$13.70
Surface area treated per hour (sq. inch)			144,000
Cost per 10 square feet of treated area			$0.14
Annual Cost			$120,000
Area Treated Annually (sq. inch)			876,000

Table 7.3 Cost analysis of corona treatment process.

Capital Costs			
Equipment	Life (hours)	Total Cost	Cost/hour
Corona Unit Cost	35040	$150,000	$4.28
Total Capital Investment		$150,000	$4.28
Operating Costs			
Description	Hours	Cost	Cost/hour
Electricity (10 kWh)	1	$1.00	$1.00
Maintainance (10% Annually)	1	$1.71	$1.71
Total Operating Costs		$1.00	$2.71
Total Costs			
Total cost per hour of operation			$6.99
Surface Area Treated per hour. (sq. inch)			86,400
Cost per 10 square feet of Treated Area			$0.12
Annual Cost			$61,260
Area Treated Annually (sq. inch)			525,600

Table 7.4 Cost analysis of UV laboratory scale treatment process.

Capital Costs			
Equipment	Life (hours)	Total Cost	Cost/hour
UV Lamp	1000	$500	$0.50
Power Supply	35040	$9,500	$0.27
Ozone Generator	35040	$500	$0.01
Air Supply Unit	35040	$600	$0.02
Total Capital Investment		$11,100	$0.80
Operating Costs			
Description	Hours	Cost	Cost/hour
Electricity (1 kWh)	1	$0.10	$0.10
Total Operating Costs		$0.10	$0.10
Total Costs			
Total cost per hour of operation			$0.90
Surface Area Treated per hour. (sq. inch)			300
Cost per 10 square feet of Treated Area			$4.33
Annual Cost			$7,906
Area Treated Annually (sq. inch)			1,825

Lamp area = 5 in. x 2 in., treatment time = 120 seconds.

Table 7.5 Cost analysis of UV pilot scale treatment process.

Capital Costs			
Equipment	Life (hours)	Total Cost	Cost/hour
UV Lamp	1000	$500	$0.50
Power Supply	35040	$26,500	$0.76
Ozone Generator	35040	$500	$0.01
Air Supply Unit	35040	$600	$0.02
Total Capital Investment		$28,100	$1.29
Operating Costs			
Description	Hours	Cost	Cost/hour
Electricity (2 kWh)	1	$0.20	$0.20
Total Operating Costs		$0.20	$0.20
Total Costs			
Total cost per hour of operation			$1.49
Surface Area Treated per hour. (sq. inch)			1,200
Cost per 10 square feet of Treated Area			$1.79
Annual Cost			$13,032
Area Treated Annually (sq. inch)			7,300

Lamp area = 20 in. x 2 in., treatment time = 120 seconds.

Table 7.6 Cost analysis of UV production scale treatment process.

Capital Costs			
Equipment	Life (hours)	Total Cost	Cost/hour
UV Lamp	1000	$400	$0.40
Power Supply	35040	$50,000	$1.43
Ozone Generator	35040	$500	$0.01
Air Supply Unit	35040	$600	$0.02
Total Capital Investment		$51,500	$1.86
Operating Costs			
Description	Hours	Cost	Cost/hour
Electricity (10 kWh)	1	$1.00	$1.00
Total Operating Costs		$1.00	$1.00
Total Costs			
Total cost per hour of operation			$2.86
Surface Area Treated per hour. (sq. inch)			43,200
Cost per 10 square feet of Treated Area			$0.10
Annual Cost			$25,039
Area Treated Annually (sq. inch)			262,800

Lamp area = 60 in. x 12 in., treatment time = 60 seconds.

Table 7.7 Summary of cost analysis based on a production facility treating 200 bumpers (5 ft. x 1 ft.) per hour.

Treatment	Area treated per hour (sq. in/hour)	Cost of treatment (per 10 sq.ft.)	Annual cost for treating 200 bumpers/hour
Plasma	144,000	$ 0.14	$ 120,000
Corona	86,400	$ 0.12	$ 102,100
UV (Lab Scale)	300	$ 4.33	$ 3,794,880
UV (Pilot Scale)	1,200	$ 1.79	$ 1,563,840
UV (Production)	43,200	$ 0.10	$ 83,463

7.5 Potential Markets

Based on our market surveys, in addition to the known market in the automobile industry, the biomedical industry represents the most developed opportunity for UV surface treatment. To be successful in the biomedical industry a process or technology must be efficient and reliable. In this industry reliability is a matter of life and death; customers depend on a product that performs flawlessly every time. The technology must deliver uniform results each time. The demands on product performance are paramount in the biomedical industry. With increased pressure on margins, a cost-effective solution is needed to allow the products to perform at the level required. In general the biomedical industry is more concerned about environmental consequences than other industries. This industry requires technologies and processes with the following characteristics: no use of CFC's or solvents, clean operation, and low energy process. With several different types

of products and seemingly endless applications, this industry requires an innovative process that can treat many different types of materials. The industry requires perfect quality and an innovative approach – all characteristics of a UV surface treatment.

Several companies have developed surface treatment applications for the medical device industry. All types of surface treatments are used: corona, gas plasma, flame, and UV for curing applications. Our research showed over 40 surface treatment companies are competing in the biomedical industry. Devices treated include catheters, angioplasty balloons, intraocular lenses, sensors, pacemakers, filter membranes, assay trays, filter housings, and syringe hubs. Surface treatments utilized in the biomedical industry are typically used to:

- increase adhesive bond strengths
- improve lubricity and biocompatibility
- increase plastic to metal adhesion
- ultra-cleaning and surface modification for better wetting characteristics
- activate surfaces of sensors
- enhance other surface characteristics such as microbial resistance and cell adhesion.

The biomedical industry is known as an industry that embraces innovation provided the innovation delivers some sort of perceived benefit; often measured in terms of the number of new biomedical products and growth. There is a high level of product awareness and customer acceptance. While there are several firms competing in this industry, innovative products and processes providing an improvement over current technology have the best chances of success.

7.5.1 Industry Comparison Matrix

Based on the information obtained through surveys, an industry comparison matrix was constructed. Table 7.8 shows the comparison between the automobile and biomedical industry.

Table 7.8 Comparison between the automobile and biomedical industry.

	Automobile	Biomedical
Current Process	Chemical	Plasma, Corona, UV
Awareness	Low	High
Process Flow	Continuous	Batch & Continuous
Investment in New Technology	Low	High
Relationship Power	Manufacturer	Shared
Life Cycle	Long	Short
Environmental Concerns	Moderate	Important
Primary Concern	Cost	Performance
Growth Potential	Low	High
Industry	Traditional	Innovative

7.5.2 Marketing Considerations

Before the UV surface treatment technology can be marketed or licensed, several issues must be considered. At this point, the process is only a lab scale process and no real product exists. For this process to create any sort of return for Michigan State University, a product must first be developed. According to the information received through the surveys of engineers and managers at Ford Motor Company and General Motors, the process must meet certain threshold requirements before it can be considered a viable product. The following information must be obtained before this process is considered a 'real' alternative:

- Demonstrate consistent performance on varying substrates.
- The process must be reliable, durable and duplicable.
- A reasonable estimate of costs in a production environment must be developed.
- The process must work in a continuous flow environment.
- Some sort of validation and quality control must exist to verify results.
- The affect on throughput must be minor.
- Suppliers must be motivated to use such processes and technology.

Both automotive manufacturers contacted indicated that the supplier base is an integral part of any solution. In most situations the components arrive at a manufacturing facility already processed or treated. The supply base would need to adopt and develop the UV treatment process to their current manufacturing environments. Granting companies like Ford and General Motors exclusive rights, will not ensure the adoption of

this process. The intellectual property agreements must be drafted to allow MSU and the supply base to develop an actual working product that incorporates the UV surface treatment process. With such arrangements, MSU could partner with a supplier or an alliance of suppliers to develop this new technology into an actual product that could be marketed to automobile manufacturers.

7.6 Recommendations and Implementation Plan

The UV surface treatment developed by Professor Lawrence Drzal at Michigan State University and preliminary laboratory results indicate that the process will generate interest in both the automotive industry and the biomedical industry. Based on the information received from industry, the process would not yet be considered a viable technology. In its current state, the process has little value to the interested parties. The process must be proven on a larger scale and an actual product must be developed. In an effort to push this technology into the marketplace, the following steps are recommended:

- Patent the process ($40,000).
- Develop pilot facility focused on refining the process (outside funding).
- Receive waiver of exclusive rights.
- Market process at industry trade fairs ($5000).
- Seek out a partner to develop actual product – perhaps an alliance of suppliers as defined by GM and Ford.
- Reach out to the biomedical industry.

Since the process has the potential to be less costly than current processes, delivers improved performance, and is environmentally friendly process, the UV surface treatment process has value in the marketplace if it can be developed into a product. With the increasing use of polymers, the process has the potential to be used on every automobile. Furthermore, the process could be used by the biomedical industry, representing another sizable market. With over 6,000,000 passenger vehicles produced in the United States last year and potentially five areas of the vehicle subject to a UV surface treatment, there was the potential of 30,000,000 UV surface treatments in 1996 - not including biomedical applications. The real value would be determined by the licensing arrangement and the fee structure agreed between the parties. For the process to be valuable, the automotive suppliers would be required to pay an up-front or per use licensing fee.

With the size of the markets under consideration, the UV surface treatment process does have potential as a revenue generating technology for Michigan State University, but the exact value is difficult to determine. At this point, an actual product needs to be developed which can either be sold or licensed.

7.7 Summary

Research is under way at Michigan State University to determine if a few seconds of UV light treatment in air can clean and oxidize polymer, plastic, and polymer composite surfaces with no environmentally hazardous by products. It has been shown that there are beneficial chemical and physical effects on adhesion of paint and adhesives to polymer and plastic surfaces resulting from short, high intensity exposure to ultraviolet (UV) light

in air. This study has shown that UV oxidation and surface activation is a viable surface treatment process which can be used in a manufacturing environment. At this juncture in the research project, it has been demonstrated that the UV treatment process is:

- A new, alternative, environmentally benign, surface pretreatment process for treating the majority of polymer, plastic and polymer composite surfaces using ultraviolet light.
- The non-contact process is adaptable to treat flat or convoluted external surfaces and has the potential to require exposures on the order of a few seconds to produce significant increases in wettability and adhesion of paints and adhesives to treated surfaces.
- The UV process is environmentally benign since it does not create VOCs or suspended airborne particulates.
- A process comparison and cost analysis of the UV process indicates that this new technology is strongly competitive with existing processes (flame, corona and plasma). It is at least equal to current technologies in terms of cost and effectiveness of cleaning and pretreating surface for painting and adhesive bonding.
- The UV process is a low cost (ca. $0.01 per square foot) and high speed process.
- MSU has been granted two US patents based on the results from this research and several other applications are pending.

References

1. Bhurke, A.S.; Jensen, M.; *UV Treatment – A Low Cost, Environmentally Friendly Surface Treatment Technique*, ML890 Report, Case Center for Computer-Aided Engineering and Manufacturing, Michigan State University, USA. (1997)

CHAPTER EIGHT

CONCLUSIONS AND RECOMMENDATIONS

8.1 Conclusions

A wide range of polymers including thermosets, elastomers, amorphous, semi-crystalline, and crystalline thermoplastics were successfully modified by UV treatment. One of the many advantages of UV surface treatment is the ability to use it to modify surfaces under ambient conditions. UV irradiation consisting of wavelengths in the 185 nm – 280 nm (UVC) band can oxidize polymers in air by producing ozone. The combined effect of UV activation of the surface and oxidative attack by ozone creates high energy polar functional groups on polymer surfaces, increasing the surface energy and thereby providing the thermodynamic driving force required for good wettability and adhesion.

The investigation into the mechanisms of surface treatment of polymers by UV radiation was characterized by wettability, surface energy, and surface chemistry measurements. UV exposure in ozone and air was found to impart a strongly hydrophilic nature to most polymer surfaces that have absorption in the range of wavelengths provided by xenon arc lamps. With the exception of high purity saturated polyolefins and fluorocarbon polymers which do not have absorption in the UVC band, this process can be used for oxidative treatment of a wide variety of materials. Even in the case of polyolefins which do not have significant absorptivity above 185 nm, the presence of internal and process impurities can lead to the formation of radicals which can be oxidized or crosslinked, thereby improving the adhesive properties of the polymers.

polym
indep
proce
polyr
and t
be va
found
advar
treatn

T
surfac
expos
pheny
photoc
PC ar
polym
interm
by ozo
this ox
increas
respon

The use of supplemental ozone to maintain high local ozone concentrations on the polymer surface during treatment was helpful in ensuring a steady state process independent of mass transfer limitations. Under these conditions, the most important process parameter is the UV irradiance (power). The changes in surface energy of the polymer are strongly dependent on the total irradiation (energy) incident on the surface and the process is virtually independent of the exposure time provided the irradiance can be varied. Short exposures at high irradiances and long exposures at low irradiances were found to yield identical surface properties. This gives UV treatment a significant advantage over competitive processes in manufacturing environments where short treatment times are necessary.

The molecular properties of UV treated bisphenol-A based polycarbonate (PC) surfaces studied with ATR-FTIR, and UV spectroscopic techniques show that UV exposure leads to the photo-Fries rearrangement of the bisphenol-A carbonate to form phenyl salicylate and di-hydroxy benzophenone. This is consistent with mechanisms of photodegradation of PC reported in literature. The photo-Fries rearrangement products of PC are strong UV stabilizers and in the normal course of weathering, stabilize the polymer from further degradation. However, in the case of UVO treatment, the intermediate and final products of UV degradation on the surface can undergo oxidation by ozone to form hydroxyl, carbonyl, and carboxylate functional groups. The net result of this oxidation is the formation of conjugate bases on the surface which is seen as a strong increase in the basic component of the surface energy. This increase in surface polarity is responsible for the enhanced wettability of UV modified surfaces.

EPR spectroscopy of UV exposed PC showed a strong paramagnetic response from the material after UVA and UVO treatments. This is believed to arise from trapped free radicals, or radical ions in the polymer. The majority of the paramagnetic sites were found to be near the surface of the polymer and they can be effectively quenched or undergo reactions with an amine cured epoxy adhesive.

The mechanical properties of the UVO modified PC probed by nanoindentation tests showed an increase in the modulus in the top 500 nm, which can be attributed to crosslinking of the irradiated polymer by processes similar to those seen in thermally oxidized and aged PC. Despite the increase in surface modulus, adhesion tests showed no change in the adhesive bond strength with epoxy and polyurethane adhesives. It was determined from fracture surface analysis that the PC-epoxy interphase failure occurs within the PC substrate and material equivalent to approximately 30-60 Å of PC is removed by the epoxy adhesive. The cohesive failure in the PC may be indicative of a weak boundary layer or a very high level of interfacial adhesion between the epoxy and PC which forces the locus of failure into the relatively weaker PC.

The surface chemistry, probed by XPS, shows that the correlation of measured O/C ratios with the surface energy of the polymer is very good and both properties vary predictably with the total irradiation received by the sample and have no dependence on the irradiance or exposure time. The functional groups created on the surface during UVO treatment show that the oxidation process occurs by reactions of ozone, and possibly the by-products of ozone dissociation, with the carbonate groups as well as hydrocarbon bonds in the bisphenol-A structure.

When *in-situ* oxidation by ozone is prevented by irradiating samples in vacuum or inert atmospheres, active sites are created on the PC surface, but these active sites are unreactive in air and the polymer do not exhibit any uptake of oxygen even after many days of aging in ambient conditions following irradiation. However, the surfaces retain their activity and readily undergo oxidation when exposed to ozone. The increase in oxygen content of these samples is beyond that expected from unirradiated, passive polymer samples exposed to ozone alone.

The rate of oxidation of activated surfaces, determined by measuring the increase in oxygen content as a function of ozone exposure, showed two distinct processes: i) a fast, initial incorporation of oxygen into the surface that is independent of the amount of irradiation received by the surface, and ii) a slower region of growth which shows dependence on the level of irradiation provided to the sample during treatment in a non-oxidative environment. The initial rapid uptake is attributed to the reaction of ozone with active sites in the top few monolayers of the material. Once the surface is depleted of active sites, further oxidation involves the slow diffusion of ozone into the sub-surface layers to oxidize active sites in the polymer. This was demonstrated by derivatization experiments with silver nitrate which allowed differentiation between the contributions to the total oxygen signal from the surface and sub-surface layers of the polymer.

Formation of water soluble low molecular weight oxidized material on the surface after UV treatment was also observed. Differences in the amount of LMW material formed on *in-situ* and *ex-situ* oxidized samples provided indication of the different behavior of the polymer when irradiated in inert and oxidizing environments. Irradiation in non-oxidizing environments increases the possibility of radical recombination, or

rearrangement, to form a smaller number of stable surface active sites. Irradiation in oxidizing environments enhances the total extent of oxidation because of aggressive reactions between the oxidizer and radicals created on the surface, but the higher extent of reaction can lead to extensive chain scission and formation of LMW fragments.

For most materials, sharp increases in the surface oxygen, wettability, and adhesive strength are observed following UVO treatment. The properties of epoxy, polyethylene terephthalate (PET), and polydiene rubber were studied in detail and trends similar to polycarbonate were observed. The wettability was found to depend entirely on the amount of irradiation given to the samples. In the case of rubber, a strong effect of temperature on the surface properties was also observed. The rise in surface temperature caused by exposure to UV and IR radiation from the lamp is believed to cause reorientation of the oxidized polar groups. The regeneration of low energy surface was also observed in thermoplastics like polyethylene and Bexloy®W polymers when treated above their glass transition temperatures (Tg). This is believed to be an effect of the higher free volume and increased chain mobility in polymers above the Tg. In polymers like PP and TPO, the wettability of the surface does not change after UVO treatment because the inherent stability of the hydrocarbon bonds to radiation above 185 nm prevents extensive chain scission and oxidation. However, impurities such as carbonyl groups, main chain unsaturation, and metal atoms present in commercial polyolefins sensitize the polymer by creating free radicals which can attack other polymer chains and ultimately cause cross-linking in the polymer. The adhesive bond strength of polyolefinic materials (PP, TPO) with epoxy adhesives increases by 400% to 500% compared to the untreated polymers because of photo-induced crosslinking which increases the modulus

of the polymer. Almost all materials treated with UVO show beneficial changes in properties except fluorocarbon based polymers such as Teflon®.

The variables in the UV treatment process were systematically studied. It was found that radiation in the 185 nm to 280 nm band is necessary for the application of the process to a broad range of polymers. Although ozone is necessary for the process to work efficiently, within the range of concentrations measurable by our equipment (>10 ppm), no effect of the ozone concentration was observed. For all polymers investigated, the surface properties were found to have a direct relationship with the irradiant energy incident on the surface. Temperature of the substrate can affect properties, especially above the glass transition temperature in polymers, by providing a driving force for surface reorientation. Surface temperature of the material can be affected by the pulse frequency of the lamps for a given power output. At lower frequencies, the high intensity pulses lead to higher surface temperatures than those reached by high frequency, low intensity pulses. However, lower frequencies also provide more dark cooling time for the surface. The lamps used in this study could be operated at 3 Hz, 10 Hz, and 120 Hz. Among these lamps 120 Hz was the most effective frequency for treatment of polymers. UV treatment with lamps operating at intermediate frequencies may provide interesting results.

A process model has been proposed to describe the UVO treatment process. The model describes the evolution of surface properties after UV irradiation in ozone for pulsed xenon lamps. A sensitivity function approach was employed to describe the evolution of any property of the surface as a function of the irradiation. Sensitivity functions for work of adhesion with water were determined for PC, PET, epoxy, and

polydiene rubber. The functions were fit with a three parameter exponential association model. The parameters correlate with physical properties of the polymer: the parameter *a* provides information about the density of reactive sites on the polymer, *b* is a dimensionless scaling parameter that describes the initial properties of the polymer, and *c* provides information about the general susceptibility of the polymer sites to photo-oxidation and other photoinduced reactions. A good correlation between *a* for the four tested polymers and the Van der Waals volume fraction of reactive sites on the surface was obtained. Sensitivity functions can be determined for other surface properties as well. Sensitivity functions for other polymers can be developed in the future to create a database of parameters which can be applied to predict the properties of new UVO modified polymers, blends, copolymers, and composites.

To use this model in a predictive capacity for previously untested polymers, at this stage, prediction of extrapolated parametric values may not be reasonable except over a very narrow range for specific homologous polymers. However, rapid initial verification for untested polymers can be performed by measurements at three to four irradiation values ranging from $H = 0$ to $H = \infty$ (saturation of the surface property) and the value of *a* can determined from this data. The value of *c* can be determined by fitting the generated profile at intermediate measurements. With the generation of more data for a wider variety of polymers and homologues, predictive assessment of the properties can be accomplished with increasing reliability.

8.2 Recommendations for Future Work

The UV oxidation surface treatment process in polymers was studied with the objective of formulating a process model that would be applicable to a wide range of polymers. The effect of irradiation on the surface properties is measured and well understood, but the effect of irradiation on the polymer below the surface, more specifically the near surface polymer, needs to be investigated because adhesion and other interfacial phenomena are rarely limited to a two dimensional interface, and are more often controlled by the formation of three dimensional interphases. The degradation of properties below the first few monolayers can negate the enhancement of properties in the top monolayers if, for example, the degradation leads to the formation of a weak boundary layer. Bulk polymer degradation phenomena are reported in literature, but these are usually applicable to long term weathering for UVA and UVB (solar) wavelengths. Specifically, it would be interesting to model the behavior of polymers in the top 500 nm of the surface. Assuming the same mechanisms observed on the surface also occur in the sub-surface polymer, the information required for this would be the depth profiles of ozone concentration in the polymer and the rate dependence of UV induced oxidation on the ozone concentration. The former can be based on models used to determine the diffusion of oxygen in polymers. The experimental verification can be accomplished by measurements on well characterized thin films. The determination of reaction rate dependence on ozone concentration is more challenging because of difficulties in accurately measuring low values of ozone concentration and the variety of parallel reactions occurring in the polymer. In this study no reaction limitation due to ozone concentration was observed at ozone concentrations as low as 10 ppm. However, a more

sensitive ozone sampling setup or treatment at low pressures may be able to yield this information. The diffusion of ozone in the polymer on the short time-scales used in UV treatment may not be significant, but the influence of pre-diffused oxygen must also be considered. Molecular oxygen plays two important roles in this process. Oxygen can quench the polymer from the excited state, and it can also prevent the recombination of free radicals formed by photolysis of the polymer by reacting with them to form peroxy radicals which can undergo further reactions. On the polymer surface, the presence of ozone and atomic oxygen, both strong oxidizers, can mask the contribution of oxygen in these processes. In the bulk polymer, these mechanisms may be quite different.

The proposed process model for surface oxidation is described in terms of three parameters and the physical properties expected to contribute to the two material dependent parameters *a* and *c* are given in Table 8.1.

Table 8.1 Process model parameters and relation to physical properties.

Parameter	Physical Properties
a	Population of reactive sites Microstructure Chain configuration Steric effects
c	Absorption coefficient Oxidation rates Free volume (temperature) Chain flexibility Stabilization (internal and external) Anti-oxidant additives

The effect of the population of reactive sites has been demonstrated, but the effects of differing microstructures and chain configurations of the polymer on the population of sites exposed to UV oxidation can be studied further. Specifically, the effect of crystallinity on the rate of oxidation for semi-crystalline polymers could be interesting. The parameter *c*, related to the reactivity of the surface can be easily characterized in terms of the UV absorptivity, but it is also strongly dependent on the rate of oxidative attack by ozone and the reorientation of reacted surfaces at temperatures above the Tg of the polymer. The free volume of the polymer determines the rate at which reorientation or isomerism can occur within the polymer, and it is perhaps the key variable to characterize the constant *c* for polymers above the Tg at treatment temperatures. The effect of internal (photo-rearrangement products) and external (additive) UV stabilizers and anti-oxidants can be modeled as functions decreasing the absorptivity of the polymer.

The verification and extension of the process model for other polymers also needs to be performed. A detailed study of polymers belonging to a homologous series, or binary random copolymers with different ratios of monomers, can be used to measure the effect of changes in populations and reactivity of surface sites on the rate and extent of UV surface oxidation. The effect of free volume or temperature ($T_{treatment}$ - Tg) on surface reorientation can also be studied on copolymers which exhibit variation in the Tg as a function of composition. Alternatively UV treatment can be performed at different temperatures. The latter approach to measuring the effect of temperature presents challenges such as the accurate measurement of transient surface temperatures on the polymers as they undergo UV oxidation.

APPENDIX A

SURFACE ENERGY CALCULATIONS

Results of contact angle measurements with five liquids were used to determine the surface energy of the solid using polar-dispersive (Equation A.1) and acid-base (Equation A.2) models.

$$\gamma_L(1+\cos\theta) = 2\left(\sqrt{\gamma_S^d \gamma_L^d} + \sqrt{\gamma_S^p \gamma_L^p}\right) \tag{A.1}$$

$$\gamma_L(1+\cos\theta) = 2\left(\sqrt{\gamma_S^{LW} \gamma_L^{LW}} + \sqrt{\gamma_S^+ \gamma_L^-} + \sqrt{\gamma_S^- \gamma_L^+}\right) \tag{A.2}$$

Polar-dispersive model analysis was performed by finding the linear regression fit to five data points obtained by plotting $\gamma_L(1+\cos\theta)/2(\gamma_L^d)^{1/2}$ against $(\gamma_L^p/\gamma_L^d)^{1/2}$ for each liquid. The slope of the linear fit is given by $(\gamma_S^p)^{1/2}$ and the intercept is $(\gamma_S^d)^{1/2}$.

The analysis for acid-base model was performed using the sum of least squares to reduce the five three-dimensional equations to three three-dimensional equations. The following procedure was used for data reduction. Equation A.3 shows the general form Equation A.2 for each liquid (*Li*, *i*=1 to 5) and the three unknown variables γ_s^{LW}, γ_S^+, and γ_S^-. The liquid values of surface tension are known and the five linear simultaneous equations will be henceforth expressed as shown in Equation A.4.

$$\gamma_{Li}^{LW}\left(\sqrt{\gamma_S^{LW}}\right) + \gamma_{Li}^-\left(\sqrt{\gamma_S^+}\right) + \gamma_{Li}^+\left(\sqrt{\gamma_S^-}\right) - \left(\frac{\gamma_{Li}(1+\cos\theta)}{2}\right) = 0 \tag{A.3}$$

$$a_i.x + b_i.y + c_i.z - P_i = 0, \qquad i = 1 \text{ to } n \tag{A.4}$$

The sum of least squares approach is used to find the values of variables x, y, and z to minimize the RHS of equation A.4. This is accomplished by taking partial derivatives of

the summation of the square of equation A.4 (Equation A.5) with respect to variables x, y, and z (Equations A.6, A.7, A.8).

$$\Sigma(a_i.x + b_i.y + c_i.z - P_i)^2 = +\delta \qquad i = 1 \text{ to } n \qquad (A.5)$$

$$\Sigma\, a_i\,(a_i.x_1 + b_i.x_2 + c_i.x_3 - P_i) = 0 \qquad i = 1 \text{ to } n \qquad (A.6)$$

$$\Sigma\, b_i\,(a_i.x_1 + b_i.x_2 + c_i.x_3 - P_i) = 0 \qquad i = 1 \text{ to } n \qquad (A.7)$$

$$\Sigma\, c_i\,(a_i.x_1 + b_i.x_2 + c_i.x_3 - P_i) = 0 \qquad i = 1 \text{ to } n \qquad (A.8)$$

Equations A.6 – A.8 can be solved simultaneously to obtain the values of the three variables corresponding to the Lifshitz-van der Waals, acid, and base components of the solid surface energy.

APPENDIX B

SENSITIVITY CURVE FITS

1. Polycarbonate

Exponential Association (3): y=a(b-exp(-cx))

Coefficient Data:

a = 72.607165

b = 1.9687052

c = 0.010709325

Standard Error: 4.1877087

Correlation Coefficient: 0.9752584

Comments: The fit converged to a tolerance of 1e-006 in 8 iterations. No weighting used.

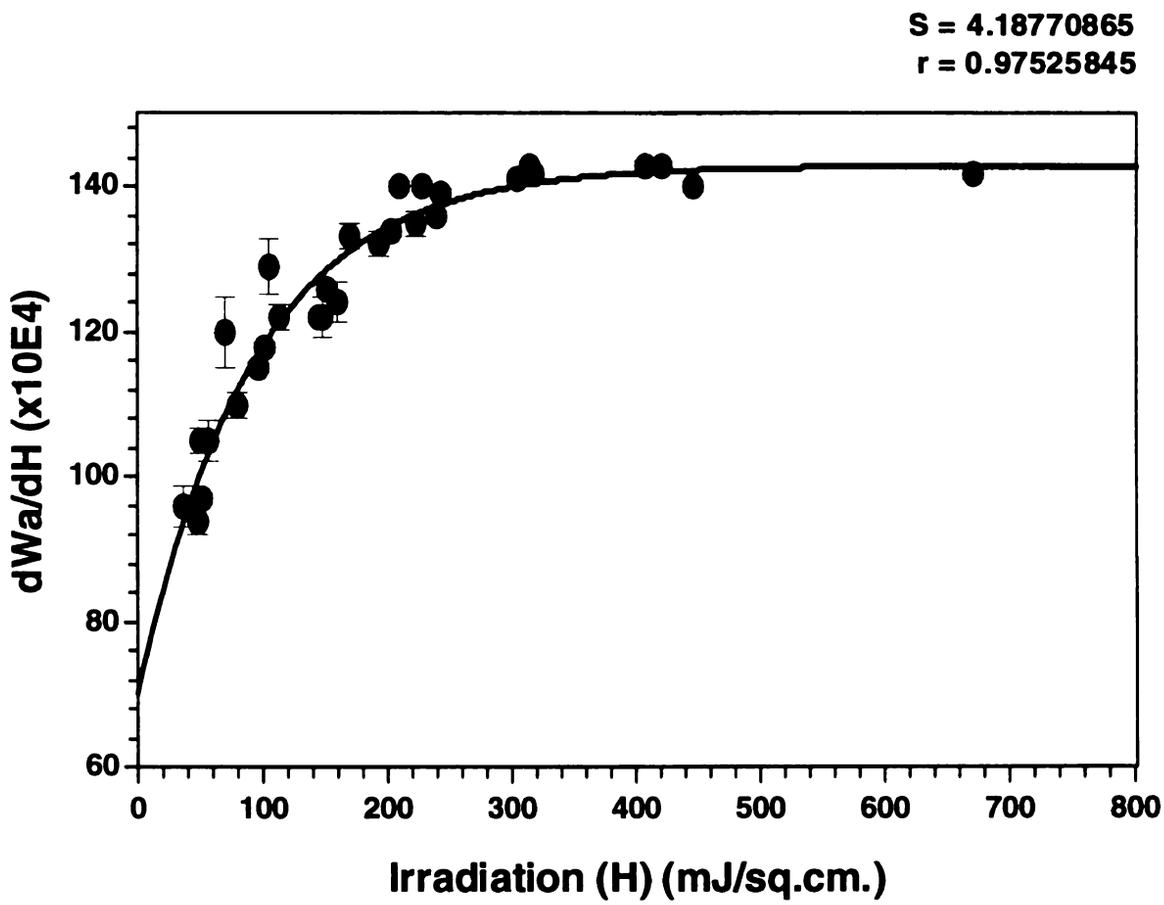

Figure B.1 Curve fit for work of adhesion of PC.

2. Epoxy

Exponential Association (3): y=a(b-exp(-cx))

Coefficient Data:

a = 45.179984

b = 2.9992781

c = 0.015529191

Standard Error: 4.5793659

Correlation Coefficient: 0.9295959

Comments: The fit converged to a tolerance of 1e-006 in 8 iterations. No weighting used.

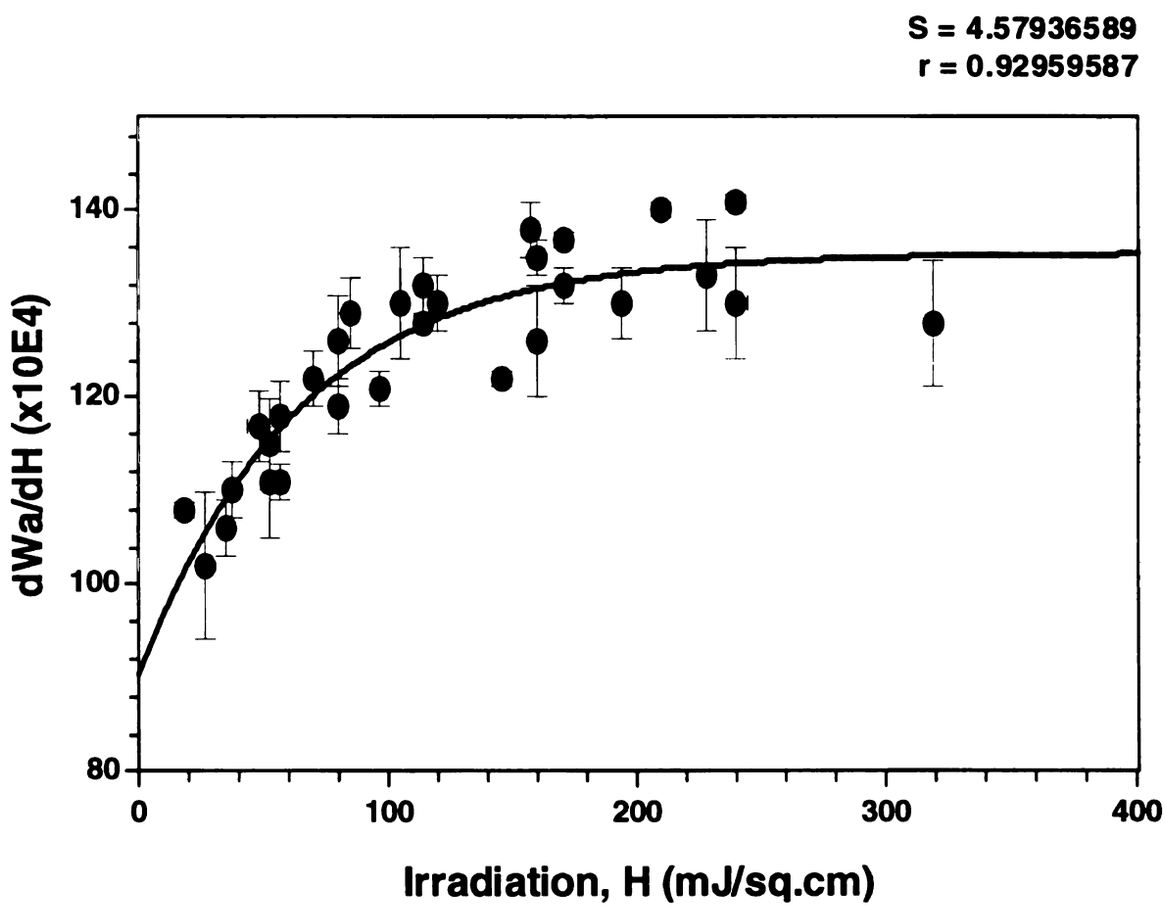

Figure B.2 Curve fit for work of adhesion of epoxy.

3. PET

Exponential Association (3): y=a(b-exp(-cx))

Coefficient Data:

a = 37.703992

b = 3.3117358

c = 0.029163071

Standard Error: 4.8290926

Correlation Coefficient: 0.9248849

Comments: The fit converged to a tolerance of 1e-006 in 9 iterations. No weighting used.

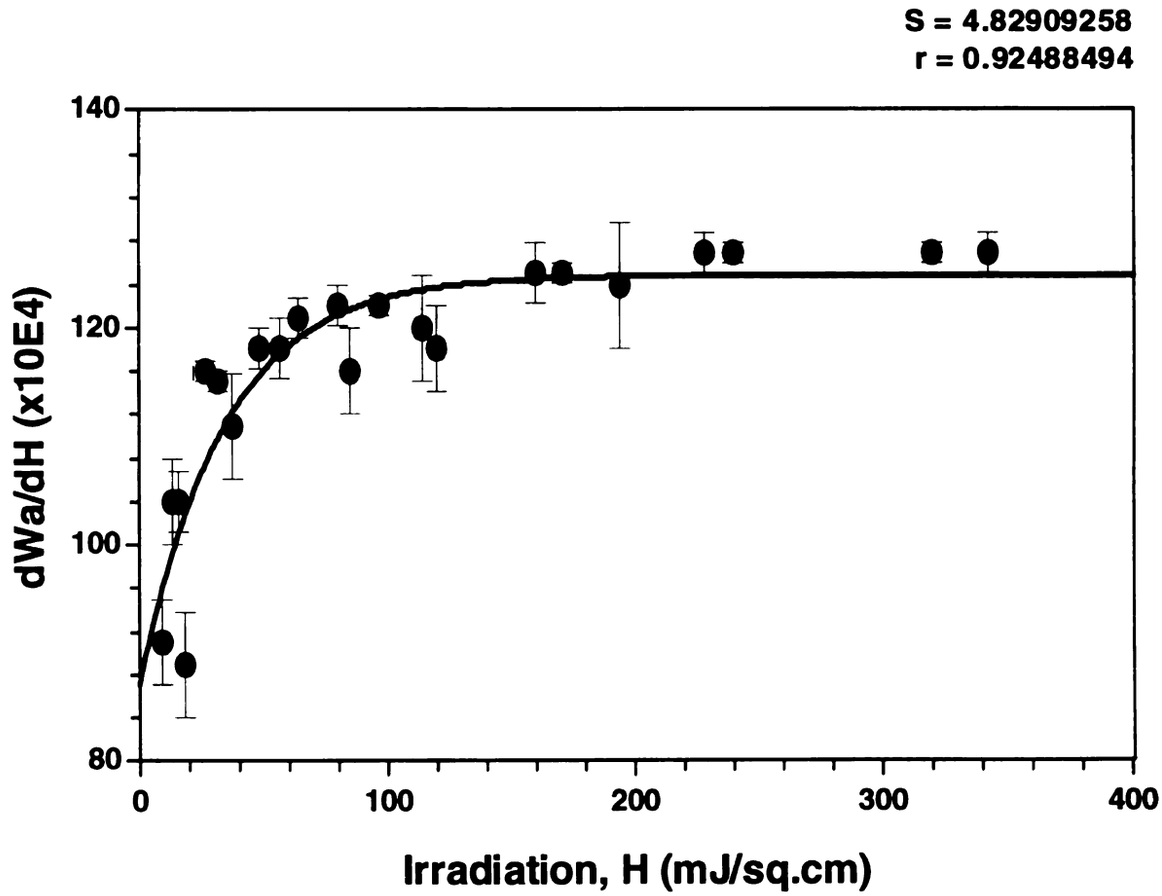

Figure B.3 Curve fit for work of adhesion of PET.

4. Crosslinked Rubber Compound

Exponential Association (3): y=a(b-exp(-cx))

Coefficient Data:

a = 107.18317

b = 1.2668587

c = 0.010698666

Standard Error: 6.0723686

Correlation Coefficient: 0.9884397

Comments: The fit converged to a tolerance of 1e-006 in 11 iterations. No weighting used.

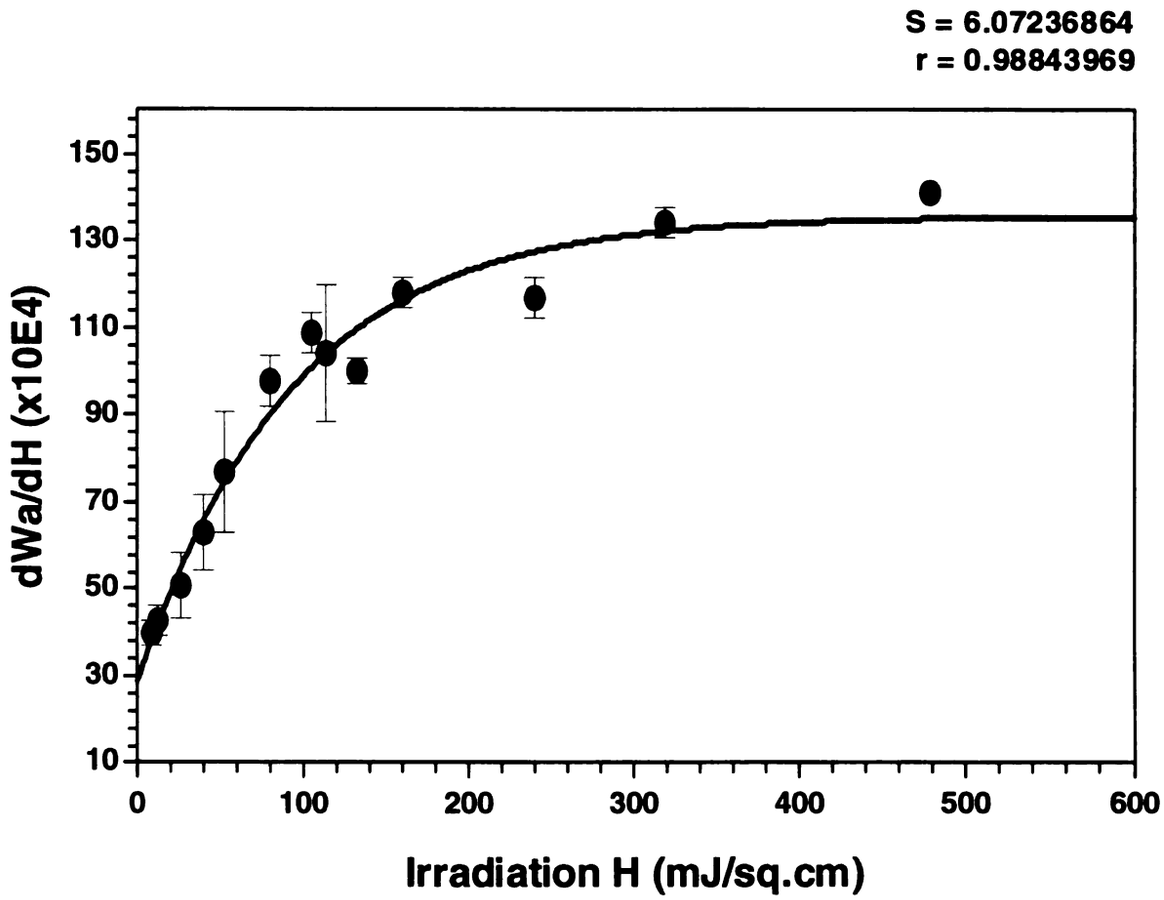

Figure B.4 Curve fit for work of adhesion of crosslinked rubber compound.

APPENDIX C

CALCULATION OF POLYMER VOLUMES

1. Polycarbonate

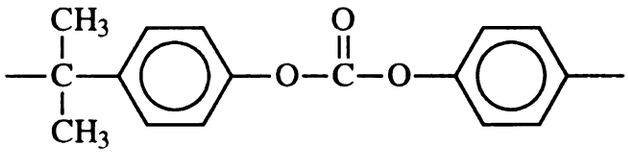

Table C.1 Reactive volume fraction of polycarbonate from group contribution theory.

Structural Group	Groups per Repeat Unit	Volume per Group (cc/mole)	Reactive Site (Yes/No)	Reactive Volume (cc/mole)	Net Volume (cc/mole)
	2	43.3	N	--	86.6
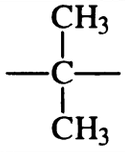	1	30.7	Y	30.7	30.7
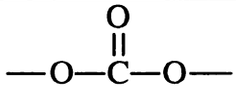	1	18.9	Y	18.9	18.9
Total Volume				49.6	136.2
Reactive Volume Fraction = 0.36					

2. Polybutadiene

$CH_2—CH=CH—CH_2$

Table C.2 Reactive volume fraction of polybutadiene from group contribution theory.

Structural Group	Groups per Repeat Unit	Volume per Group (cc/mole)	Reactive Site (Yes/No)	Reactive Volume (cc/mole)	Net Volume (cc/mole)
$—CH_2—$	2	10.23	N	--	20.46
CH=CH	1	16.9	Y	16.9	16.9
Total Volume				16.9	37.36
Reactive Volume Fraction = 0.45					

3. Poly(ethylene terephthalate)

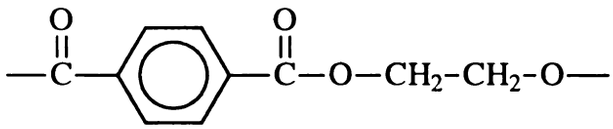

Table C.3 Reactive volume fraction of PET from group contribution theory.

Structural Group	Groups per Repeat Unit	Volume per Group (cc/mole)	Reactive Site (Yes/No)	Reactive Volume (cc/mole)	Net Volume (cc/mole)
	1	43.3	N	--	43.3
$-CH_2-$	2	14.03	N	--	28.06
$-\overset{O}{\overset{\|\|}{C}}-O-$	2	15.2	Y	30.4	30.4
Total Volume				30.4	101.76
Reactive Volume Fraction = 0.30					

4. Epoxy (Epon 828 + Jeffamine T403)

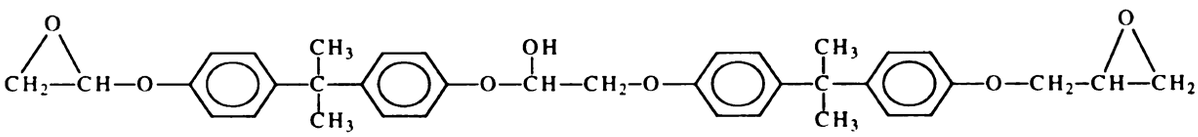

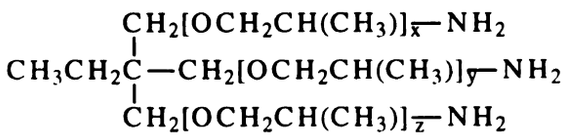

$x + y + z = 5.3$

Table C.4 Reactive volume fraction of epoxy (Epon 828 + Jeffamine T403) from group contribution theory.

Structural Group	Groups per Repeat Unit	Volume per Group (cc/mole)	Reactive Site (Yes/No)	Reactive Volume (cc/mole)	Net Volume (cc/mole)
Epon 828 Resin					
	4	43.3	N	--	173.2
$-\overset{CH_3}{\underset{CH_3}{C}}-$	2	30.7	Y	61.4	61.4
$-CH_2-$	4	10.23	N	--	40.92
$-\overset{OH}{CH}-$	3	14.8	Y	44.4	44.4
$-O-$	4	5	Y	20	20
Total Volume (Epon 828 Resin)				125.8	339.92
Jeffamine T403					
CH_3-	1	13.67	N	--	13.67
$-CH_2-$	9.3	10.23	N	--	95.14
$-\overset{\vert}{\underset{\vert}{C}}-$	1	3.3	N	--	3.3
$-O-$	5.3	5	Y	26.5	26.5
$-\overset{CH_3}{CH}-$	5.3	20.45	N	--	108.38
$-N\begin{matrix}/\\ \backslash\end{matrix}$	3	4.3	Y	12.9	12.9
Total Volume (Jeffamine T403)				39.4	259.89
Mixture (100:45 wt. ratio)					
1 mol Epon 828 (Mol wt. 598)				125.8	339.92
0.62 mol Jeffamine T403 (Mol wt. 432)				24.42	161.13
Total Volume of Mixture				150.22	501.05
Reactive Volume Fraction = 0.30					